
01 Oct 1958

An investigation of high-strength, deformed steel bars for concrete reinforcement part II

Sidney A. Guralnick

George Winter

Follow this and additional works at: <https://scholarsmine.mst.edu/ccfss-library>

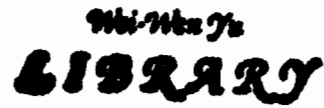


Part of the [Structural Engineering Commons](#)

Recommended Citation

Guralnick, Sidney A. and Winter, George, "An investigation of high-strength, deformed steel bars for concrete reinforcement part II" (1958). *Center for Cold-Formed Steel Structures Library*. 58.
<https://scholarsmine.mst.edu/ccfss-library/58>

This Technical Report is brought to you for free and open access by Scholars' Mine. It has been accepted for inclusion in Center for Cold-Formed Steel Structures Library by an authorized administrator of Scholars' Mine. This work is protected by U. S. Copyright Law. Unauthorized use including reproduction for redistribution requires the permission of the copyright holder. For more information, please contact scholarsmine@mst.edu.



DEPARTMENT OF STRUCTURAL ENGINEERING
SCHOOL OF CIVIL ENGINEERING
CORNELL UNIVERSITY

AN INVESTIGATION OF HIGH-STRENGTH, DEFORMED
STEEL BARS FOR CONCRETE REINFORCEMENT

PART II

by

Sidney A. Guralnick

Project Director

George Winter

A research project sponsored jointly by
The Reinforced Concrete Research Council and
The United States Bureau of Public Roads

October 1958

TABLE OF CONTENTS

	Page
LIST OF TABLES	1
LIST OF FIGURES	11
A. INTRODUCTION	
1. Objectives	2
2. Scope	3
3. Project Personnel	3
4. Acknowledgements	4
5. Notation	4
B. EXPERIMENTAL PROGRAM	
6. Description of Test Program and Beam Specimens	6
7. Materials	8
a. Cement	
b. Aggregate	
c. Concrete mix	
d. Reinforcing steel	
8. Testing Techniques and Procedures	10
C. TEST RESULTS	
9. Test Data	10
a. Properties of concrete	
b. Properties of reinforcing steel	
c. Beam Tests	
10. Behaviour of Beams Under Load	13
a. Beams with plain webs	
b. Beams with web reinforcement	
D. ANALYSIS OF BEAM TEST RESULTS	
11. Diagonal-Tension Cracking and Stirrup Stresses	16
12. Shear Failures	22
13. Flexural Failures	24
14. Load-deflection Characteristics	26
15. Flexural Crack Formation	29
16. Comparison of Ultimate Loads of Beams Failing in Shear with Design "Safe" Loads Using Provisions of A.C.I. Code No. 318-56, Chapter 8	31
E. SUMMARY AND CONCLUSIONS, by S. A. Guralnick and George Winter	33
F. REFERENCES	41
G. APPENDIX, Curves for Steel Stress & Moment versus Crack Widths for all Beams of this Project and Original Program	100

List of Tables

1. Properties of Beam Specimens
2. Gradation of Aggregates
3. Composition of Alloy Steel
4. Average Dimensions of Longitudinal Reinforcing Bars
5. Test Results: Properties of Concrete
6. Test Results: Average Mechanical Properties of Reinforcing Steel
7. Beam Test Results
8. Comparison of Test Results with Ultimate Flexural Strength Values
Calculated according to Provisions of Appendix to ACI Building Code
No. 318-56
9. Comparison of Test Results with Theoretical Ultimate Flexural Strength
Values
10. Comparison of Test Results with Theoretical Ultimate Shear Strength
Values
11. Deflection, at "Service Load" of all Beams Tested in Parts I and II
of this Investigation which Failed in Flexure
12. Crack Data at One-half Ultimate Load
13. Crack Data, at "Service Load", of all Beams Tested in Parts I and II
of this Investigation which Failed in Flexure
14. Comparison of Shear-Strength of Beams which Failed in Diagonal-
Tension with ACI Building Code Values for Allowable Loads
15. Comparison of Test Results with Theoretical Initial-Diagonal-Tension-
Crack Shear for all Beams Tested in Parts I and II of This Investigation

List of Figures

1. Arrangement of Reinforcement for Series I Beams with Plain Webs
2. Arrangement of Reinforcement for Series II Beams with Plain Webs
3. Arrangement of Reinforcement for Series III Beams with Plain Webs
4. Arrangement of Reinforcement for Series II Beams with Reinforced Webs
5. Arrangement of Reinforcement for Series III Beams with Reinforced Webs
6. Photograph of Concentrated-Load Test Setup in Process of Assembly Showing Strain Gage Instrumentation
7. Typical Stress-Strain Curves for the Two Types of Concrete Used in Beam Specimens
8. Typical Stress-Strain Curves for High-Strength Steel Reinforcing Bar Material Used in Beam Specimens
9. (a) and (b). Photographs of Beams with Plain Webs After Failure
10. Photographs of Beams with Reinforced Webs After Failure
11. (a) thru (j). Moment-Deflection Curves for Beams of Parts I and II of this Investigation
12. (a) Typical Moment-Deflection Curve for Beams with Web Reinforcing which Failed in Flexure
(b) Typical Moment-Deflection Curve for Beams without Web Reinforcing which Failed in Shear
13. (a) Typical Curves for Steel Stress and Moment versus Crack Widths for Beams without Web Reinforcing
(b) Typical Curves for Steel Stress and Moment versus Crack Widths for Beams with Web Reinforcing
14. (a) thru (d). Comparison of Moment versus Width of Negative Tension Crack Curves for Beams having "Bunched" and Beams having "Distributed" Negative Tension Reinforcing
15. (a) Typical Applied Moment - Longitudinal Steel Strain Curves for Beams without Web Reinforcing which Failed in Diagonal-Tension
(b) Typical Applied Moment - Longitudinal Steel Strain Curves for Beams with Web Reinforcing which Failed in Flexure
16. (a) thru (d). Stirrup Strain Distribution at Each Stage of Applied Load

17. (a) thru (d). Measured Stirrup Stress versus Computed Stirrup Stress Curves
18. Comparison of Actual Deflections with Calculated Values for all Beams Failing in Flexure
19. Comparison of Failure Moment with Calculated Ultimate Flexural Moment

AN INVESTIGATION OF HIGH-STRENGTH, DEFORMED
STEEL BARS FOR CONCRETE REINFORCEMENT

A. INTRODUCTION

The previous phase of this investigation of high-strength steel for concrete reinforcement is described in Report No. TSR-4730-7146, which was released in July, 1957. This previous testing program was designed to provide information on the following topics, among others:

(a) The shear (primarily) and flexural (secondarily) strength of restrained Tee-beams reinforced with steel of approximately 80 ksi yield point for main reinforcement and with standard steel for web reinforcement.

(b) The formation of diagonal tension cracks and flexural cracks and the width of flexure and shear cracks at various loads and particularly at "design loads" (say, half the ultimate loads).

(c) Deflections at "design load" of beams of this kind.

(d) The validity of the Illinois shear investigations in regard to their applicability to high strength reinforcement.

(e) Extension of the range of information on shear failures by a substantial number of tests with variables (such as r , p , a/d) outside the Illinois range.

It is believed that adequate information on these points has been furnished by these tests.

At the same time a number of important phenomena have been observed during these tests which appeared to warrant further investigation before definite design recommendations could be made for the use of high-strength reinforcement. Firstly, it was observed that in some cases negative flexural cracks through the flange of the Tee-section were so large at "design" load as to be considered objectionable for construction practice. Secondly, it was noticed that diagonal-tension cracks in the web of the Tee-section at "design" loads were also large and numerous enough to be considered

objectionable. Thirdly, it was found that the use of the usual method of calculation for ultimate flexural strength which does not include explicit strain relations for the steel and concrete leads, in many cases, to a rather large underestimate of the actual flexural strength of doubly-reinforced Tee-beams with high strength steel.

Lastly, no beams without web reinforcement were tested. To complete the information on the shear strength of Tee-beams with high-strength reinforcement, and to test the applicability of various theories of shear strength of unreinforced webs additional test data seem desirable.

1. Objectives

(a) To investigate the effect on negative flexural cracking of relocating and distributing the negative tensile reinforcement in the flange of the Tee-beam. (It was strongly suspected that distributing the negative tensile reinforcement across the flange of the Tee-section would tend to exert more control on flexural cracking than the original "bunched" arrangements.)

(b) To investigate in more detail the formation and growth of diagonal-tension cracks using both data from the original program and from the new program.

(c) To determine the shear strength of restrained Tee-beams with high-strength steel reinforcement, but without web reinforcement, and to compare it with existing shear-strength theories as well as with present code provisions for such strength.

(d) To compare actual beam deflections at service loads (as defined by the Appendix to A.C.I. 318-56) with values calculated by existing design formulas or simple modifications thereof.

(e) To compare the flexural failure loads of beams of the present program and of the original program with flexural strength calculations based on explicit strain relations.

2. Scope

Ten restrained Tee-beams were tested to destruction. Six beams were loaded by concentrated forces and the remaining four were loaded by means of a series of closely-spaced hydraulic rams to simulate the effect of a uniformly-distributed load.

Two concrete strengths were used having nominal values of approximately 3000 and 5000 psi. cylinder compression strength. All longitudinal reinforcement was of alloy steel having a nominal yield strength of 80,000 psi. All web reinforcement was of intermediate grade plain carbon steel having a nominal minimum yield strength of 40,000 psi. All steel reinforcing bars used in the project were deformed bars conforming to ASTM Standard A305. Six beams had plain webs and the remaining four had reinforced webs.

Experimental data included crack width measurements, beam deflections, strains in longitudinal and web reinforcement, and bar end slip.

3. Project Personnel

The project was carried out in the Structural Research Laboratory of the Department of Structural Engineering at Thurston Hall, Cornell University.

The work was supervised by Dr. George Winter, Head, Department of Structural Engineering as Project Director. Principal Investigator was Dr. S. A. Guralnick, Assistant Professor of Civil Engineering. Other personnel engaged in the project included Messers Wei Wen Yu, W. J. Lauck and W. C. Hansell, Research Assistants and Mr. E. Pittman, Laboratory Mechanician. Mr. Wei Wen Yu merits special commendation for his careful and conscientious work in all phases of laboratory and computing work connected with this project.

4. Acknowledgements

This project was sponsored jointly by the Reinforced Concrete Research Council and the United States Bureau of Public Roads. A task committee appointed by the Reinforced Concrete Research Council, to provide general supervision of the investigation was constituted as follows: Dr. E. Hognestad, Chairman, Messrs. O. W. Irwin, R. C. Reese and C. A. Willson, members.

Mr. Perkins and Mr. Nichols of the University Sand and Gravel Corp. of Ithaca, New York, have contributed greatly to the progress of the project by carefully stockpiling and batching aggregate for the project and by making available a truck-mounted mixer whenever it was needed.

The author is deeply grateful to these persons and to his many friends and colleagues of the College of Engineering whose suggestions and encouragement proved so helpful in the conduct of this project.

5. Notation

- A_s = Area of tension reinforcement
- A'_s = Area of compression reinforcement
- a = Shear span or distance from plane of nearest concentrated load to plane of support
- b = Overall width of flange of Tee-beam
- b' = Width of web of Tee-beam
- C = Total internal compressive force in the concrete
- c = Length of arm of internal couple of flexural resisting moment, or distance between C and T .
- d = The effective depth, or distance between outermost compression fiber of beam and the centroid of the tension reinforcement
- d' = Distance between outermost compression fiber of beam and the centroid of the compression reinforcement
- E_c = Secant modulus of concrete*
- E_s = Modulus of elasticity of steel*
- E_t = Initial tangent modulus of concrete*

* In these cases a prime (') or double prime (") mark over a letter indicates that the quantity so designated is the result of calculation, not of test measurement.

- f'_c = Cylinder compressive strength of concrete
- f_c = Compressive flexural stress in concrete
- f_r = Tensile modulus of rupture for concrete
- f_s = Stress in longitudinal reinforcing steel
- f_v = Stress in vertical stirrups
- f_y = Yield stress of reinforcing steel
- I = Moment of inertia
- I_g = Gross moment of inertia of whole concrete cross section
- I_e = Effective moment of inertia of a reinforced concrete beam
- I_r = Moment of inertia of cracked or "transformed" rectangular cross-section
- I_t = Moment of inertia of cracked or "transformed" Tee cross-section
- h = Overall depth of beam section
- j = Ratio of depth of neutral axis to effective depth
- k_1, k_2, k_3 = Parameters describing shape and size of flexural compression stress block
- L = Total length of beam
- M = Bending Moment
- M_f = Calculated ultimate flexural resisting moment
- M_{f6} = Calculated ultimate flexural resisting moment assuming that steel stress is limited to 60,000 psi and concrete stress to $.85f'_c$
- M_s = Calculated ultimate shear moment
- M_{sl} = "Service Load" moment = $M_{f6}/1.8$
- M_u = Maximum applied moment at failure in test beam*
- n = E_s/E_c , the modular ratio
- p = The longitudinal tension steel percentage as defined in the text
- p' = The longitudinal compression steel percentage as defined in the text
- Q_g = First statical moment of gross concrete area above neutral axis about same
- r = The web steel percentage referred to the stem of the Tee-section

* A bar (-) over the letter indicates the quantity includes the dead load as well as the applied load.

- T = Total force in the tensile reinforcement
- t = Thickness of flange of Tee-beam
- V = Shearing force
- v = Shearing stress
- V_c = Maximum shearing force occurring in beam at the appearance of the first diagonal-tension crack
- v_c = Shearing stress corresponding to V_c
- V_u = Maximum shearing force occurring in test beam at failure**
- V_{al} = Maximum shearing force allowable in beam under the provisions of Chapter 8, A.C.I. Building Code No. 318-56
- W = Total force applied to test specimen as indicated by dial of testing machine, or "machine load"
- W_c = Machine load at the appearance of the first diagonal-tension crack
- W_u = Machine load at failure of test specimen

Greek Letters

- δ = Actual deflection of test beam measured at a point just below the interior load in the case of restrained beams, or at the beam centerline in the case of simple beams*

B. EXPERIMENTAL PROGRAM

6. Description of Test Program and Beam Specimens

The experimental program consisted of the testing to destruction of ten restrained Tee-beams. Six beams were loaded by two concentrated forces, and the remaining four were loaded by means of a series of closely spaced hydraulic rams to simulate the effect of a uniformly-distributed load. The beams were designed on the basis of the following considerations:

(a) All beams were identical in overall dimensions with those of the original program. The reinforcement ratios were also practically identical to corresponding beams of the original program; however, in four specimens the negative reinforcement was rearranged and distributed across the flange of the Tee-section.

* In these cases a prime (') or double prime (") mark over a letter indicates that the quantity so designated is the result of calculation, not test measurement.

** A bar (-) over the letter indicates the quantity contains the dead load as well as the applied load.

(b) To duplicate the conditions of the original program,* all specimens were designed for sharp-yielding steel of 80 ksi yield strength for main reinforcement and for standard, intermediate grade steel for web reinforcement. Two concrete strengths were used, a low strength concrete of about 3000 psi and a high strength of about 5000 psi.

(c) Six specimens had plain webs and high longitudinal steel ratios. Three of these specimens were made of 3000 psi concrete and the other three of 5000 psi concrete. These beams are designed to fail in shear. These six specimens are duplicates of specimens IA-1, IC-1, IIA-1, IIC-1, IIIA-1 and IIIC-1** of the original program except that they did not have web reinforcing. Beams IIIA-1 and IIIC-1 were tested under uniform load, the others under point loading.

(d) The four remaining specimens were duplicates of specimens IIB-1, IIC-1, IID-1 and IIID-1** of the original program except that the negative reinforcement was distributed across the width of the flange of the Tee-section. In addition, electrical resistance strain gages were mounted on stirrups in the high-shear region in each beam in order to obtain information on possible correlation between diagonal-tension crack widths and stirrup strains. Beams IIB-1, and IID-1 were tested under uniform load, the others under point loading.

(e) In all beams, electrical resistance strain gages were located on the reinforcing steel at the regions of maximum moment in order to obtain moment vs. strain relations during most stages of the loading history.

(f) Loading arrangements were identical in all respects to those used in the previous program.

* The term "original program" will hereinafter refer to Part I of the investigation as described in Report No. TSR 4730-7146, released in July, 1957.

** Beams of this program are numbered to correspond with comparable beams of the original program except that the suffix "m" (meaning "modified") is appended to their designation number to distinguish them from the original beams.

Properties of the beam specimens appear in Table 1. Figures 1, 2, 3, 4, and 5 give the physical details for each series of beams including bar sizes and placement, stirrup spacing, position of loads and reactions, and bar strain gage locations.

7. Materials

a. Cement

Cement was purchased in two lots and stored in a dry place for not longer than two months before use. Type I, Lehigh brand Portland Cement was used in all specimens.

b. Aggregate

Aggregate for the 3000 psi. concrete was supplied by the Ithaca-Rumsey Sand and Gravel Corp. from local sources. The grading of these aggregates (termed "Ithaca") is given in Table 2. The maximum size of the gravel was 5/8 inch and the fineness modulus of the sand was 2.71. The specific gravity of the gravel was 2.64 and that of the sand 2.67.

Aggregate for the 5000 psi. concrete was supplied in two lots by the Eastern Rock Products Corp. from their pits at Boonville, New York. The grading of these aggregates (termed "Boonville") is also given in Table 2. The maximum size of the gravel was 7/8 inch and the fineness modulus of the sand was 2.87. Specific gravity of the gravel was 2.68 and that of the sand was 2.65.

Mineralogic composition of the "Ithaca" and "Boonville" aggregates is given in Tables 3 and 4 of the original report.

c. Concrete Mix

Two mixes were used having the following proportions:

(1) For 3000 psi. concrete with "Ithaca" aggregate

sand, SSD	1700 lbs./cu. yd.
gravel, dry	1610 lbs./cu. yd.
cement (type I)	5 bags/cu. yd.
water (total)	35 gals/cu. yd.

(2) For 5000 psi concrete with "Boonville" aggregate

sand, SSD	1600 lbs./cu. yd.
gravel, dry	1600 lbs./cu. yd.
cement (type I)	7 bags/cu. yd.
water (total)	35 gals/cu. yd.

Aggregates were batched by weight at the ready-mix plant and delivered to the laboratory in a truck-mounted, six cubic-yard capacity, horizontal, non-tilting mixer. Cement and water were carefully measured and added to the truck mixer at the laboratory. Mixing time was from six to ten minutes. Final proportioning of the water was on the basis of the slump test. Slump for all mixes was maintained at 2-1/2 to 3 inches. Two to four beams were poured from each batch of concrete. Nine control cylinders and four modulus of rupture beams were taken from each batch of concrete during pouring. Cylinder compressive strengths and modulus of rupture values are reported in Table 5.

d. Reinforcing Steel

Longitudinal reinforcement was made of alloy steel deformed bars supplied by the Inland Steel Co. The composition of this steel is given in Table 3. A large number of tensile coupons were taken from bars in each size range and tested to rupture. Spacing, width and height of deformation were measured on each of the test coupons. The results of the deformation measurements appear in Table 4.

Web reinforcement was, wherever used, made of #4 standard, intermediate grade steel reinforcing bar with a nominal yield strength of 40,000 psi. Stirrups were fabricated from this material in the laboratory on a Di-Accro* bar bender. Tensile coupons were also taken from the web reinforcement material and tested to rupture.

Mechanical properties are reported in Table 6.

* Trade name of the O'Neil-Irwin Manufacturing Company.

8. Testing Techniques and Procedures

All of the beams tested in this program were fabricated, cast, cured and tested exactly according to the procedures outlined in Sections 8 and 10 of the original report. The testing equipment employed was the same as that described in Section 9 of the original report.

C. TEST RESULTS

9. Test Data

a. Properties of Concrete

Table 5 gives cylinder compression strength and modulus of rupture data for the concrete used in the various groups of beams. Also, the initial tangent modulus, E_t , and the secant modulus, E_s , for a stress equal to one-half the ultimate compressive strength are reported. Figure 7 shows typical stress-strain curves for the two types of concrete used in the project.

Empirical equations which relate the tangent modulus and the secant modulus to compressive strength have been proposed by Jensen (7) and by Gaston, Siess, and Newmark (6) and are respectively:

$$E'_t = \frac{30 \times 10^6 f'_c}{5E'_c + 10,000} \quad (1)$$

$$E'_c = 1.8 \times 10^6 + 460 f'_c \quad (2)$$

Values of E'_t and E'_c computed according to the above equation are also given in Table 5. The comparison between calculated and actual values of the two concrete moduli given in Table 5 indicates good agreement between test results and calculated values in two cases and only fair agreement in the remaining two cases. Equations (1) and (2) are used in a subsequent section of this report, dealing with beam deflections, for the purpose of computing the flexural rigidity of reinforced concrete beams.

b. Properties of Reinforcing Steel

The average mechanical properties of one-third of the total number of bars in each size group are given in Table 6. The maximum standard deviation of sample data was found to be in no case greater than 2% of the arithmetic mean and the extreme range of sample data in no case exceeded $\pm 5\%$ of the arithmetic mean. Thus it was considered reasonable to assume that the actual value of any mechanical property for any given bar did not differ from the tabulated mean value by more than 5% in either direction. Since the anticipated difference between actual values and the average was so small, it was not considered necessary to test a coupon cut from each bar.

A typical stress-strain curve for each size group of high strength steel bar used in the beam specimens is shown in Fig. 8. Two reasons may account for the differences in mechanical properties of the main bars apparent in this figure and in Table 6. Firstly, the high-strength steel bars were supplied in three batches; the #5 and #6 bars in one batch, the #7 bars in the second and the #10 bars in the third batch. Table 3 indicates the distinct difference in composition between the steel supplied for the #5, #6 and #7 bars and that supplied for the #10 bars. Secondly, the #5 bars may have undergone some extra cold-working during rolling over that encountered by the larger-size bars; thus accounting for the high yield stress exhibited by the #5 bars. The effect of cold-working on the mechanical properties of the high-strength steel bars supplied for the project is treated in section 11 of the original report.

Although it was anticipated that the high-strength, alloy steel supplied by Inland Steel Company for the project would have a rather long "yield-plateau",* Fig. 8 shows that this was not the case. A long "yield-plateau" is considered a desirable feature in a structural steel because of the warning, through excessive deflections and cracking, given by structures

* This term means the horizontal portion of the stress-strain diagram which occurs just after yielding but before work-hardening starts.

made with such steel when stressed to dangerous levels. Also, the alloy steel supplied for the project had a lower percent elongation than was expected from the specifications for such steels* given in the American Society for Metals Handbook, reference (8). Except for the #10 bars, the alloy steel bars supplied for the project were of the "gradual-yielding" type and their "yield stresses" were determined by the 0.2% offset method.

c. Beam Tests

Results of tests on all beam specimens are summarized in Table 7. This table gives the machine load and maximum shear at the formation of the first diagonal tension crack; the machine load, maximum shear, maximum positive and negative moments at failure; the type of failure, deflection, maximum tensile steel strain, maximum compression steel strain, and maximum stirrup steel strain at a load, at, or just before, failure occurred.

Diagonal-tension cracking was assessed by visual observation. The diagonal-tension cracking load was taken as the load at which a decidedly inclined crack first intersected the level of the mid-depth of the beam at an angle of approximately forty-five degrees.

Failure load was taken as the maximum load carried by the beam. In all cases, loading was continued beyond the maximum load until the specimen was destroyed.

Failures occurred in one of two modes: diagonal-tension failure (abbreviated -- D.T.) or flexural-tension failure (abbreviated -- F.T.). These modes are defined for the purposes of this investigation as follows:

(1) Diagonal-tension failure is a failure characterized by total destruction of the load-carrying capacity of the beam through the prolongation of a diagonal-tension crack from the bottom to the top of the beam resulting in a sudden rupture.

* i.e. for SAE No. 5150 or 9255 steels

(2) Flexural-tension failure is a failure by yielding of the reinforcement in the tension zone at a region of maximum moment after considerable deflections have taken place and before crushing of the compression concrete has occurred. Final destruction of the beam is through crushing of the compression concrete after the tension steel has yielded and usually occurs at a load only slightly higher than that causing the yielding in the tension steel. For beams reinforced with a "gradual-yielding" steel, as was the case in this project, the term "yield-point" is defined as the stress at which a specified inelastic strain is attained (e.g. as in the 0.2% offset method) and the term "yielding" is used to denote the portion of the steel stress-strain diagram after the "yield-point" has been reached. In beams reinforced with this type of steel, the beam may continue to accept significant increases in load after the "yield-stress" has been reached in the tension steel and it loses its carrying capacity only after the compression concrete fails by crushing.

Table 9-A of the original report gives a summary of the characteristics of the various modes of failure and it was used to assign a definite failure mode to the test specimens of this project.

10. Behaviour of Beams Under Load

Figures 9(a) through 16(d) illustrate the behaviour under load of the test specimens. Figures 9(a), 9(b) and 10 are photographs of all the beam specimens after failure and show the crack pattern and the location of the areas where failure occurred. The moment versus deflection curves for all beams of this project and corresponding beams of the original program are given in figures 11(a) through (j). In each of these figures, curves are plotted for beams having the same longitudinal reinforcement and nominal concrete strength but with varying amounts of web reinforcement and, in some cases, different arrangements of negative tension reinforcing. In all

cases, data for the moment-deflection curves was recorded from dial gages placed at the point of maximum positive moment.

At low loads little or no cracking was evident in the test beams. As the test loads increased, flexural cracks in the positive and negative moment tension zones appeared and increased in width, length and number with increasing loads. In most instances, the first appearance of flexural cracks occurred at a load which corresponded to a computed tensile stress in the beam of the order of magnitude of the modulus of rupture of the concrete. Diagonal-tension cracks usually did not appear until a load of at least twice the initial flexural cracking load was imposed on the beam. The first diagonal-tension cracks appeared invariably in the beam web in the area between the interior support and the point of contraflexure. As loads were increased, the diagonal-tension cracks in this area increased in width, length and number and new diagonal-tension cracks appeared at other high-shear locations in the beam.

a. Beams with Plain Webs

Six of the ten beams tested had plain webs and all six failed in diagonal-tension. Failure occurred in these beams when one of the large inclined web cracks extended itself from the bottom to the top of the beam progressing entirely through the flange of the Tee. This type of failure was quite sudden and it occurred, with one exception, at a load about twenty to thirty percent higher than the load causing the first diagonal-tension crack to appear (c.f. table 7). Beam IIC-1^m was the exception; in this case the beam failed immediately after diagonal-tension cracking appeared (c.f. Fig. 9b).

The crack or cracks causing failure were quite pronounced and may be easily seen in the photographs shown in Fig. 9(a) and 9(b). These cracks usually started in the web near the interior support at a load of about two to three times that causing the first flexural cracks to form. In all cases

the diagonal-tension cracks formed independently of any existing flexural cracks. In some cases the crack causing failure remained relatively straight along its entire length (see beam IA-1^m, Fig. 9(a)). In other cases this crack remained fairly straight only until it reached the flange. On reaching the flange, it turned to a horizontal plane and ran along the plane of intersection between the flange and web for a short distance, finally turning upward into the flange at a point between the point of contraflexure and the interior load (see beams IC-1^m and IIA-1^m, Fig. 9(a)).

The curves of Fig. 15(a) show a reversal in direction of strain (from compression to tension) in the compression steel occurring at a load of about two-thirds the ultimate load. This strain reversal which was typical for all six beams usually took place at the same load which caused one or more diagonal-tension cracks to intersect the level of the compression reinforcing. Such changes in direction of strain have also been found in rectangular beams in the shear investigations of Viest, Moody, Hognestad and Elstner (1), and were interpreted by them as evidence of a "redistribution of stress" in the high shear region.*

b. Beams with Web Reinforcement

All four beams of the testing program which were provided with web reinforcing failed in flexural tension. In these beams the first diagonal-tension cracks usually formed at the head of an existing negative-moment flexural crack rather than independently of the flexural cracks as was the case with the beams having plain webs. The diagonal-tension cracks which did form were more numerous, narrower and shorter than those in the plain-web beams. In these four beams the diagonal-tension cracks did not penetrate the flange of the Tee-beam during any stage of loading preceding failure. In beam IID-1^m, however, a diagonal-tension crack penetrated

* The hypothesis that "redistribution of stress" occurs before a diagonal-tension or shear-compression failure can take place is essential to certain of the theories advanced by the researchers mentioned above.

the compression flange after beam failure occurred. This propagation of a diagonal-tension crack into the flange appears to have been strictly a secondary effect and not a cause of failure.

Flexural cracks were numerous and quite evenly distributed in both the negative and positive-moment regions of the beam by the time the failure load was reached. The first flexural cracks appeared in the positive-moment tension zone at a load of about ten percent of ultimate; cracking in the negative moment tension zone (i.e. in the flange of the Tee over the interior support) usually did not appear until a load of about twenty percent of ultimate was reached. Positive flexural cracks extended into the flange of the Tee, before failure, in only one of the four beams (see beam IIB-1^m, Fig. 10). Failure was quite gradual with warning of distress through large deflections, much flexural-tension and diagonal-tension cracking and through spalling and cracking in the compression concrete at the failure location. Final destruction of the beam was through crushing of the compression concrete in a region of maximum moment.

D. ANALYSIS OF BEAM TEST RESULTS

11. Diagonal-Tension Cracking and Stirrup Stress

As was mentioned in the original report, the shear, V_c , at which the first diagonal-tension crack forms appears to be rather an unpredictable quantity. No reasonable correlation was found between test data and the equation:

$$v_c = \frac{V_c}{7/8 bd} = 0.12 \left(1 - 0.1 \frac{M}{V_d} \right) f'_c \left(1 - \frac{f'_c}{10,000} \right) \quad (3)$$

which was given in reference (1). It appears that V_c may be influenced by the "pure shear" strength of the concrete and by the presence and amount of web reinforcing as well as by the other parameters included in Eq. 3. Also, it must be noted that simple expressions such as:

$$v = \frac{V}{b_j d} \quad (4)$$

or,

$$v = \frac{V Q}{I b} \quad (5)$$

are not valid for computing stresses in beams or portions of beams in which the M/Vd ratio is much below 3.0 (see reference (10) and (11) for discussion), since in such cases diaphragm rather than beam action occurs.

Instead of adopting a strictly empirical approach to the question of predicting the shear at first diagonal-tension cracking, it appeared interesting to determine what correlation, if any, could be found between test data and values predicted by using the elementary relation for shear stress in a beam as given by Eq. 5. In order to use Eq. 5 one must be able to determine in some way the strength of plain concrete subjected to a "pure" shear state of stress (i.e. v_c). In reference (10) it is shown that a reasonable estimate of v_c can be obtained from the equation:

$$v'_c = \frac{\frac{f_r}{2} \frac{f'_c}{2}}{\frac{f_r}{2} + \frac{f'_c}{2}} \quad (6)$$

The use of a relation such as Eq. 6 is necessitated by the difficulty, if not impossibility, of testing a specimen of plain concrete in "pure" shear. Using Eqs. 5 and 6 then, one obtains the following simple formula for predicting the shear, V'_c , at which the first diagonal-tension crack will form in a beam:

$$v'_c = \frac{I_g b}{Q_g} v'_c = \frac{I_g b}{Q_g} \cdot \frac{f_r}{f_r + 2f'_c} \quad (7)$$

In this equation the terms I_g and Q_g refer to the section properties of the gross concrete cross-section not including reinforcing steel.

The test data and the results of calculations based on Eq. 7 for all beams of Parts I and II of this investigation appear in table 15. It will be noted that for the beams of Part I the column headed \bar{V}_c is different from that appearing in table 9 of the original report. This change was made necessary by an error found in a conversion factor used in making the original calculations for that column of figures.* The column headed \bar{V}_c/V_c' in table 15 indicates that the best agreement between test and theory is to be found amongst the series-II specimens. This is as it should be because in all the other specimens the M/Vd ratio in the high-shear portion of the beam at the interior support was approximately 1.5 or less; thus diaphragm rather than beam action was to be anticipated. In the series-II beams, however, the M/Vd ratio at the interior support was approximately 3.0; therefore, the elementary equations for beam stresses are valid and reasonable agreement between test results and theory may be expected. It may be observed that in most cases the theory is conservative. Much more work, especially of a statistical nature, remains to be done about the question of initial-diagonal-tension cracking before any general conclusions can be reached. Tentatively, however, one may conclude from the results of this investigation that for beams in which the M/Vd ratio is 3.0 or larger, Eq. 7 gives a reasonably reliable estimate of the shear at the appearance of the first diagonal-tension crack.

Strain gages were placed on the web steel in the high-shear regions of all beams having vertical stirrups. The results of the stirrup strain measurements are plotted in Figs. 16a, b, c, and d. The strain in each stirrup provided with a gage is plotted for each increment of load. The location of each stirrup and each strain gage as well as the major cracks in

* Fortunately this error was not repeated in other calculations in the original program and all other tabular data reported therein agree perfectly with the results of an independent recheck.

the high-shear region are also shown. One may observe from these figures that the crack pattern very strongly influences measured stirrup strain. That is, those strain gages directly crossed by a crack record the highest strains, while those gages located fairly far from cracks record the lowest strains. It may also be observed that in all cases very low strains were recorded in stirrups adjacent to the interior support and the interior load points. This is to be expected, of course, because of the restraint on web cracking caused by the large compressive stresses at these points induced by the concentrated forces. This is experimental confirmation of a suspicion long held by the author, among others, that stirrups in the immediate neighborhood of a concentrated load or reaction may hardly be called upon to bear the portion of the full shear assigned to them by the application of the simple "truss-analogy" theory.

Since the "truss-analogy" is such a widely-accepted design method, a comparison between measured stirrup stress and stirrup stress computed according to this design method appeared in order. Figs. 17a, b, c and d, representing data from beams IIB-1^m, IID-1^m, IIIB-1^m, and IIID-1^m respectively, show graphs of measured stirrup stress versus stirrup stress computed according to the equation:

$$f'_v = \frac{s V}{A_v j d} \quad (8)$$

In this equation V is the total shear force acting on the section under consideration (i.e. the stirrups alone are assumed to carry the total shear). In addition, a graph of the width of the largest diagonal-tension crack versus shear has been plotted in each of the above figures. This last graph may also be read against a scale of computed stirrup stress as well as against shear. The forty-five degree line appearing in each

figure is, of course, the graph of the equation:

$$f_v = f'_v$$

In the first two figures, which represent data from series-II beams, curves are plotted from the data of the stirrup having maximum strains, from the averages of the data taken from the two stirrups having the highest strains and from the averages of data from all stirrups provided with gages. Since the shear diagram in the region between the interior support and the interior load was horizontal and the stirrups were evenly spaced in these beams, at any load each stirrup had the same computed tensile stress, f'_v . This stress, f'_v , was, of course, directly proportional to the shear, V , according to Eq. 8. Data from the uniformly loaded series-III beams is represented in Figs. 17c and d. The curves appearing in these figures are plotted from the data of the stirrup having maximum strain and from the stirrup having the second highest strain. The spacing of stirrups in these series-III* beams was so arranged that the computed stresses in each stirrup were approximately equal.

In each of Figs. 17a through d it may be observed that measured stirrup stresses are very low until the initial-diagonal-tension-cracking load is reached. As soon as this load is imposed on the beam, measured stirrup stresses increase very sharply and in most cases the f_v vs. f'_v curves eventually attain an almost constant slope of approximately forty-five degrees to the horizontal. In three of the four beams, the f_v vs. f'_v curves all lie below and to the right of the forty-five degree line; thus indicating that the stirrups were not carrying the total external shear imposed on the beam (as was assumed in making the f'_v - calculation). This means that the

* Beams were loaded by a series of closely spaced hydraulic rams to simulate "uniformly distributed" loading.

concrete and/or the longitudinal steel also resisted part of the shear imposed on the beam. Sachnowski (12) assumes that the shear not taken by the stirrups is resisted by the longitudinal reinforcing (presumably in dowel action). Dr. Royston Jones (13) has presented some interesting experimental evidence indicating that both the longitudinal steel and the concrete resist the extra shear not taken by the stirrups. In Fig. 27a which represents data taken from beam IIB-1^m, the f_v vs. f'_v curves for the stirrup recording maximum strain and the stirrup recording the second highest strain lie above and to the left of the forty-five degree line. At first glance this would lead one to the startling conclusion that the stirrup in question is resisting more shear than the total external shear being imposed on the beam. This apparent anomaly occurred because an unsymmetrical diagonal-tension crack pattern developed in this beam which did not occur in the others. In this beam a crack appearing on one side of the beam at say eighteen inches from the support would appear on the other side at perhaps fourteen or fifteen inches from the support. Since only one leg of the stirrup was provided with a strain gage, doubling the reading to account for the stress in the other leg would, of course, give an erroneous value for the total stress carried by the stirrup. Therefore, the two graphs in question should be interpreted as exhibiting a stress-concentration occurring in one leg of the particular stirrup due to the occurrence of an unsymmetrical diagonal-tension crack pattern. The curve for the averages of all stirrup stress data for this beam is, as anticipated, below and to the right of the forty-five degree line.

The curves giving widths of largest diagonal-tension crack versus shear and computed stirrup stress indicate that in all cases the width of the largest crack did not exceed 0.011 ins.* at one-half the ultimate load.

* A width of 0.01 inches is often used as an upper limit for permissible crack widths in reinforced concrete structures.

As a matter of fact in three of the four beams with web reinforcement, the maximum crack width recorded during the entire loading history did not exceed 0.01 ins. In all cases the width of the largest crack appears to vary almost linearly with shear and thus with computed stirrup stress. There is insufficient data however, to make any general remarks about this phenomenon. One thing appears obvious from this investigation, though: if all the shear is assigned to the stirrups and computed stirrup stress at design load (using Eq. 8) is limited to about 20,000 psi, diagonal-tension cracks, if any appear, will very probably be narrower than the maximum tolerable limit of 0.01 ins.

12. Shear Failures

Comparison of Test Results with Existing Theories

Results from tests on the six beams with plain webs which failed in diagonal-tension have been compared with the shear strength theories proposed by Messers. Viest, Moody, Hognestad and Elstner (1), and by Messers. Laupa, Siess and Newmark (2). The former theory contains the assumption that the shear-span to depth ratio has an effect on ultimate shear strength and is thus limited to beams subjected to concentrated loads. The latter theory does not contain any explicit assumptions as to the effect of the shear-span to depth ratio on ultimate shear strength and appears to be applicable both to beams subjected to concentrated loads and to beams subjected to uniformly-distributed loads.

The major equations used in this project to calculate the ultimate shear moment, M_s , from the Viest, Moody, Hognestad, Elstner report for restrained beams with plain webs are (in their original notation):

$$M_s = N p f_s b d^2 (Z - k_2 \frac{N p f_s}{k_1 k_3 f_c}) \quad (9)$$

in which: $N = 1 + \frac{M_b}{M_a} \cdot \frac{d}{d'}$ (10)

$$Z = 1 - \frac{N-1}{N} \cdot \frac{d''}{d} \quad (11)$$

$$f_s = \frac{3 \frac{M}{Vd} - 0.45}{3 \frac{M}{Vd} + 0.55} \left[6.9 \times 10^4 E_s \left(-1 + \sqrt{1 + \frac{1450}{N_p E_s / k_1 k_3 f'_c}} \right) \right] \quad (12)$$

The major equations used to calculate the ultimate shear moment, M_s^1 , from the Laupa, Siess, Newmark for beams with tension and compression reinforcement are (in their original notation):

$$M_s^1 = b d^2 f'_c (k + n p') (0.57 - \frac{4.5 f'_c}{10^5}) \quad (13)$$

in which $k = \sqrt{[n(p + p')]^2 + 2n(p + p' - p't)} - n(p + p')$ (14)

$$n = 5 + \frac{10,000}{f'_c} \quad (15)$$

In all shear calculations the concrete cross-sectional area, bd , was taken as the stem width times the distance from the outermost compression fiber to the centroid of the tension steel.

Table 10 gives a comparison of the test data with the ultimate shear strengths predicted by the above two theories. For all cases in which shear failure occurred, the ratios of computed shear moments to failure moments are given. The last two columns in table 10 indicate that there is quite good agreement between the test data and the results of calculations based on the Viest-Moody-Hognestad-Elstner theory, but relatively poor agreement between the test data and the results of calculations based on the Laupa-Siess-Newmark theory. The latter theory tends to seriously overestimate the shear strength of the beams in question.

As in the original project it may be noted again that apparently no increase in shear strength was gained by the Tee-section over a similarly reinforced equal-depth rectangular section having a breadth equal to the stem width of the Tee-section. On the contrary, according to the Laupa, Siess, Newmark theory at least, the plain web Tee-beam may even be somewhat weaker in shear than the corresponding rectangular beam (this apparent anomaly in which a beam having more material in its compression zone may

actually be weaker in shear strength than a beam having less material in said zone is discussed in reference (10)). Also, as was mentioned in the original report, the relatively high stress levels in the longitudinal tensile steel of the beams in this project did not appear to influence their shear strength in any discernible way.

13. Flexural Failures

Comparison of Test Results with Existing Theories

The four beams in this project provided with web reinforcing were designed to fail in flexure. The ultimate moments in these beams as well as the ultimate moments for all beams in the original program which failed in flexure are compared with theoretical ultimate flexural moments in table 9. Strain gage readings from the compression reinforcing bars in beams in both this project and the original project indicated that little, if any, stress was being transferred to the compression steel (c. f. Fig. 15b). Consequently, the effect of compression steel on flexural properties was neglected in all calculations of flexural strength.

The equations for flexural strength calculations are:

$$M_f = p b d^2 f_y \left(1 - \frac{k_2}{k_1 k_3} p \frac{f_y}{f'_c} \right) \quad (16)$$

in which: $\frac{k_2}{k_1 k_3} = \frac{1600 + 0.46 f'_c - (f'_c)^2 / 80,000}{3900 + 0.35 f'_c}$

The latter equation was taken from "Concrete Stress Distribution in Ultimate Strength Design" by Hognestad, Hanson and McHenry (14). The ratios of calculated moment, M_f , to actual ultimate moment, \bar{M}_u , given in table 9 indicate that the theoretical approach used herein is quite conservative. It should be noticed, however, that agreement between test and theory is better for some beams with higher reinforcement ratios, p , than for beams with lower ratios. This phenomenon is probably due to the fact that in lightly-reinforced beams concrete compressive stresses are so low during most of the loading history that the tensile steel may still be able to

pick up additional stress even after the "yield-point" is reached before the stress level in the concrete becomes high enough to cause crushing. Thus, the actual ultimate strength of such beams is in excess of that predicted by formulas based on the premise that failure occurs when the stress in the steel reaches the "yield-stress". This extra flexural strength of beams with low p has also been observed by Jensen (7), Lash (16) and may be inferred from the experimental points plotted in Fig. 3 of Whitney's original paper on Ultimate Strength Design (15).

As in the previous report, it is believed that the excess strength of these beams as compared to predictions of ultimate strength theory is caused by the fact that these steels had little or no yield plateau and entered strain hardening immediately upon reaching their (offset) yield strength. (See Fig. 8). Correspondingly, failure through concrete crushing occurred when the steel was in the strain hardening range and at a stress higher than the yield strength. This is confirmed by the strain measurements made on the tension reinforcement (see Table 8). This behavior is not new. It has been observed in Europe with steels of similar stress-strain diagrams. At its 1957 (?) meeting the European Committee for Reinforced Concrete, Commission on Steel, under the chairmanship of Professor George Wästlund, stated: "For beams with low percentages of such steel the observed failure moments, for short-time tests, are always on the average 5 to 20% higher than the moments calculated on the basis of the 0.2% offset yield strength." This statement refers to European cold stretched or cold twisted steel, which also lacks a yield plateau and goes directly into strain hardening.

A comparison of test results with ultimate moments computed according to the Appendix to ACI Code 318-56 is given in table 8. The provisions of this part of the code require that the steel stress used in computation of ultimate flexural moment be limited to 60,000 psi and the maximum concrete

compressive stress be limited to $0.85 f'_c$. The column headed \bar{M}_u/M_{f6} in table 8 indicates that the ACI Code approach in all cases results in a very large underestimation of the actual failure moment. This underestimation, of course, occurs mainly because of the use of the unrealistic value of 60,000 psi for the maximum steel stress at failure.

14. Load-deflection Characteristics

Figs. 11(a) thru 11(j) give the moment versus deflection curves for all beams tested in this program. These same figures also include moment-deflection curves from beams of the original program which had the same longitudinal reinforcement and nominal concrete strength. The only differences between any three beams whose moment-deflection curves appear on the same sheet are the amount of web reinforcing and, in some cases, the arrangement of the negative tension reinforcing. Fig. 12(a) is a typical moment-deflection curve for one of the four beams of this project with web reinforcing which failed in flexure and Fig. 12(b) is a typical moment-deflection curve for one of the six beams of this project without web reinforcing which failed in shear.

A line representing moment versus deflection based on the gross concrete section and E'_t and one based on the cracked transformed section and E'_c are superimposed on the moment-deflection diagrams of Figs. 12(a) and 12(b). It may be observed in both cases typified by these figures that at low loads the test curve of moment versus deflection is quite steep and follows the $E'_t I_g$ line. As the load increases the test curves tend to flatten out and approach and perhaps even cross the $E'_c I_e$ line. It is interesting to observe that the curve of Fig. 12(b) is really only a "blown-up" picture of the lower portion of a curve such as the one shown in Fig. 12(a). Thus the curve of Fig. 12(b) represents only a small fragment of the full moment-deflection curve of the beam if it did not have a weakness in shear and were allowed to reach its full flexural capacity.

One of the major objectives of this program is to compare actual beam deflections at service loads (as defined by the appendix to A.C.I. Code 318-56) with values calculated by existing design formulas or simple modifications thereof. The "service-load" moment, M_{S1} , is defined herein to be $1/1.8$ times the calculated ultimate flexural resisting moment, M_{f6} , assuming that steel stress is limited to 60,000 psi and concrete stress to $0.85 f'_c$. The failure moments \bar{M}_u , of those beams which were designed to fail in shear in this and in the original program were so low compared to M_{f6} (in some cases \bar{M}_u was even less than M_{S1}), that these beams were quite unrealistic in design by comparison with those to be encountered in construction practice. Consequently, as suggested to the writers by Mr. J. DiStasio, it appears unwarranted to attempt an analysis of the load-deflection characteristics of such beams. For this reason all further remarks will pertain only to those beams which failed in flexure.

At a load which imposed a moment equal to M_{S1} on the test beam, in all cases it was observed that flexural cracking was very much in evidence. Therefore, it is apparently quite reasonable to base deflections on the cracked, "transformed" section rather than on the gross concrete section. Deflection calculations at a load which produced the "service-load" moment were undertaken for all beams of this project and of the original program. These calculations were based on the following assumptions:

- (a) The modulus of elasticity E'_c , of concrete may be calculated according to the equation:

$$E'_c = 1.8 \times 10^6 + 460 f'_c \quad (2)$$

- (b) The influence of compression reinforcing on section properties may be neglected; since strain measurements consistently indicated that little or no contribution was made by this steel to the resisting moment of the beam.
- (c) The influence of concrete in the tension zone on section properties may be neglected.
- (d) The moment of inertia about the neutral axis of any

cross-section is taken to be the sum of the moments of inertia of the compression concrete area and "n" times the tensile steel area about said neutral axis.

- (e) Since differences between the moment of inertia, I_r , of sections in the negative-moment region and the moment of inertia I_t , of sections in the positive moment region for beams of the testing program were quite small (of the order of five to ten percent of the larger value) an average value of moment of inertia, I_e , is taken as applicable to the whole beam to reduce complications in the calculations. This average moment of inertia is:

$$I_e = \frac{I_r + I_t}{2} \quad (18)$$

- (f) The modular ratio, n , used in the calculation of moments of inertia is taken to be the modulus of elasticity of the steel, E_s , divided by the modulus of elasticity of the concrete, E'_c , given by Eq. 2 above.

Deflection calculations, using the product of E'_c and I_e as the "flexural rigidity" term, were carried out in the usual way (i.e. by the "moment-area" or "conjugate beam" method) for all beams of this and the original program which failed in flexure. These calculations were made for a load which imposed a maximum positive moment equal to the "service-load" moment, M_{sl} , on the beam. The results of these calculations together with pertinent test data appear in Table - 11. The extreme right-hand column in Table - 11 gives the ratios of calculated deflections to measured deflections. A graphical picture of the ratios of calculated deflections to measured deflections is given in Fig. 18.

The grouping of points about the forty-five degree line in Fig. 18 indicates rather good agreement between test and theoretical values in all but four cases. In three of these four cases the theory overestimates deflection and is thus on the conservative side. The one instance in which the theory underestimates deflection occurs in the case of beam IIIB-1. It may be observed from Fig. 11h that the moment-deflection curve for this beam does not follow the trends of the other two beams in this series. It seems reasonable to infer from curves of Fig. 11h that beam IIIB-1 had some

unexplained weakness or that there was a defect in the deflection measuring apparatus which was not apparent during the conduct of the test. In any case since there was only one such case of the theory underestimating the deflection significantly, it may be concluded that the method of calculating deflections employed herein yields reasonable agreement between test and theory and that significant errors, if any occur, are to be mainly expected on the conservative side.

15. Flexural Crack Formation

In the original program it was found that negative flexural cracks were few in number but often they were wide enough at design loads to be considered objectionable. It was conjectured in the report of the original program that this poor negative flexural crack pattern was due to the fact that the negative tensile reinforcing bars were bunched together over the stem of the Tee section. Consequently, one objective of this program was to investigate the effect on negative flexural cracking of relocating and distributing the negative tensile reinforcement in the flange of the Tee beam. Accordingly four beams were tested which were made as nearly identical as possible with beams of the original program with the exception that the negative tensile reinforcement was distributed across the flange of the Tee-section. These four beams corresponded to beams of the original program which were designed to fail in flexure in order to allow a well-developed crack pattern to form before failure occurred.

Table-13 gives crack data at the "service load" for all beams tested in parts I and II of this investigation which failed in flexure. It is quite apparent from table - 13 that negative crack widths at service loads for the part - II beams represent a considerable improvement over those occurring in corresponding part - I beams. The curves appearing in Figs. 14(a) through 14(d) also show the improved cracking characteristics of the part - II beams over the corresponding part - I beams. Crack widths at

service loads for part - II beams varied from approximately one-third to one-half of those in corresponding part - I beams and the average widths at "service loads" in no case exceeded a value of 0.007 inches. Thus it has been shown that while flexural cracking may be quite pronounced at "service loads" in beams reinforced with high-strength steel, it is nevertheless possible to insure adequate crack control by careful attention to proper bar location and placement.

Table - 12 gives crack data at one-half ultimate load for beams tested in part - II of this project. This table may be compared directly with table - 13 of the original program since they both give data at one-half ultimate load. Again it may be observed that the part - II beams with distributed negative tensile reinforcing had improved negative flexural crack characteristics over the part - I beams all of which had "bunched" negative tensile reinforcing. Even at loads which imposed a moment equal to one-half the ultimate the maximum average negative flexural crack widths of the part - II beams having distributed negative tensile reinforcing in no case exceeded 0.011 inches. In corresponding part - I beams with bunched reinforcing, the maximum average negative flexural crack widths varied from 0.016 to 0.030 inches.

Fig. 13a gives typical curves for steel stress and moment versus crack widths for beams without web reinforcing and Fig. 13b gives similar curves for beams with web reinforcing. In both figures it is apparent that flexural crack widths increase in rough proportion to steel stresses; however, the rate of increase in width of negative flexural crack is almost double that of the positive flexural cracks. Since in all beams top and bottom steel was identical, it is thus demonstrated that the smaller the ratio of surrounding tensile concrete area to steel perimeter, the narrower are the widths of flexural cracks. In cases where it is not possible to reduce the ratio of surrounding tensile concrete area to

steel perimeter in order to achieve better crack control, it has been shown that distributing the tensile steel area in such a way that each bar has about the same amount of concrete area on each side also has very beneficial effects on crack control.

16. Comparison of Ultimate Loads of Beams Failing in Shear with Design Safe Loads Using Provisions of A.C.I. Code No. 318-56, Chapter 8.

All beams of this project which failed in shear were reviewed according to the provisions of Chapter 8 of the current A.C.I. building code. The results of these calculations appear in Table - 14 along with other data, such as concrete strength, type failure, and maximum shear at failure. The ratio* of the maximum shear at failure, V_u , to the maximum allowable shear, V_{al} , is given for all beams which failed in shear. These "Safety Factors" range in value from 2.76 to 5.94. The higher values occur in beams having high-strength concrete. This is so because of the cutoff provision which limits the maximum shearing stress to 90 psi. As in the original program, the very highest values of the ratio of maximum shear at failure to maximum allowable shear occur in the case of the uniformly-loaded beams. The next highest values appear in the case of the series - I beams and the lowest "Safety Factors" are evident for the series - II beams. The higher shear strengths of the uniformly-loaded beams and the series - I beams was to be anticipated because of their relatively low M/Vd (approx. 1.5) ratios in comparison with those of the series - II beams (M/Vd for series - II beams is approx. 3.0). The former beams were acting more like diaphragms than beams as was explained earlier in section - II.

In view of these results it appears likely that beams with M/Vd ratios of about 2.0 or less can, in general, be expected to have higher shear

* This ratio is herein designated as the "Safety Factor"

strengths than beams with M/Vd ratios which are in excess of 2.0. Since there is no allowance for extra shear strength for beams in the diaphragm category in the present A.C.I. building code, the beams of this program exhibiting such extra strength would of course, have a high "Safety Factor."

Certain conclusions, paralleling those made in the original report, may be drawn:

- (a) A beam having high-strength steel longitudinal reinforcing and a plain web designed under the provisions of the present A.C.I. building code is amply safe in shear if concretes of the usual practical strengths are used.
- (b) Evidence from parts I and II of this investigation indicates that beams with M/Vd ratios of about 2.0 or less can, in general, be expected to have higher shear strengths than beams whose M/Vd ratios are in excess of 2.0.
- (c) As was mentioned in the original report, beams reinforced with high-strength steel can be made shallower and narrower than equivalent conventionally-reinforced beams but the shear provisions of the present A.C.I. building code may be so stringent as to prevent the realization of the full economies possible with the use of high-strength steel.

E. SUMMARY AND CONCLUSIONS, by S. A. Guralnick and George Winter.

The conclusions given below refer to the entire investigation which consisted of Parts I and II. Part I was reported on separately (Report No. TSR 4730-7146 of July 1957) and consisted of 24 web-reinforced restrained T-beams reinforced with high strength steel. Undamaged portions of eight of these beams were retested as simple beams, making a total of 32 beams tested. Part II consisted of 10 restrained T-beams, six of them with plain webs and four with web reinforcements. The details of the test data on these ten beams are given in the body of the present Report (No. TSR 4730-7146, Part II) which also contains an Appendix giving detailed crack data on all beams of both Parts.

The following, detailed conclusions can be drawn from the combined evidence of Parts I and II:

(1) Flexural Strength

(a) Of the 42 beams of the combined two programs, 16 failed exclusively or primarily in flexure. Comparison of the experimental ultimate moments \bar{M}_u with the theoretical moments M_F computed by ultimate theory, using k_2/k_1k_3 from Ref. 14 shows that the average value of M_F/\bar{M}_u is 1.22, the range being from 1.04 to 1.42.

It is concluded that the excess flexural strength by test over that predicted by ultimate theory on the basis of a flat yield plateau was caused by the fact that little or no such plateau was present in these steels. In this respect these steels behaved more like cold-twisted than like "natural" steels. The fact that the excess strength was larger for the low steel ratios fits this explanation. For low p the concrete strain which occurs simultaneously with the steel yield strain is small, permitting the steel to go considerably into the work hardening range before failure occurs by concrete crushing.

(b) The Appendix to the 1956 ACI Code limits the useable yield strength of high strength steels to 60 ksi. whereas the actual yield points of these steels ranged from 83.7 to 103.1 ksi., the majority being between 84 and 92 ksi. If M_{f6} is the ultimate moment computed by 1956 Code on the basis of 60 ksi, the values of \bar{M}_u/M_{f6} ranged from 1.46 to 2.12. This shows that from the viewpoint of strength alone the limitation to 60 ksi is excessively conservative. For appropriate observations on crack development at steel stresses in excess of those corresponding to 60 ksi., see below.

(c) Strain measurements showed that the compression reinforcement was not acting to any significant degree to resist bending moments, regardless of whether measurements were taken at the maximum positive moment location (i.e. where the flange is in compression) or over the continuous support (where the beam acts as rectangular). It must be concluded that an ultimate theory which assumes that the compression reinforcement yields at flexural failure, regardless of distance from neutral axis, is not tenable.

(2) Shear Strength

(a) If, for the 30 beams which failed in shear or a combination of shear and flexure, the ultimate shear forces V_u are compared with the allowable shear forces V_{a1} computed on the basis of the 1956 ACI Code, one obtains: (i) for the beams with f'_c smaller than 3900 psi an average value of $V_u/V_{a1} = 4.0$, with a range from 2.76 to 5.95; (ii) for the beams with f'_c larger than 3900 psi an average value of $V_u/V_{a1} = 5.3$, with a range from 3.30 to 7.19.

From this it is concluded (i) that the use of high-strength steels in connection with present provisions for diagonal tension results in adequate safety in regard to shear failure; (ii) that the present provisions which do not recognize any increase in shear strength for concrete in excess of 3000 psi are excessively conservative when applied to these test results, (iii) that the excessive spread in "safety factors" which results from the application of the ACI Code provisions to these tests provides a further indication

that the present Code method does not represent a sound design basis.

(b) In regard to more recent shear strength theories, comparison with the Viest-Moody-Hognestad_Elstner theory shows reasonably good agreement for point-loaded beams with web reinforcement (deviations of computed from measured shear strength ranging from - 32 to + 49%) and satisfactory agreement for beams with plain webs (- 17 to + 4%). For these point-loaded beams the Laupa-Siess-Newmark theory shows more, and more unconservative, scattering for beams with web reinforcement (- 18 to + 110%) and is unsatisfactory and unconservative for beams with plain webs (+ 74 to + 123%). For uniformly loaded beams the former theory has not been developed. The latter, with one exception (+ 74%) is in reasonable agreement with test results (- 18 to + 35%). It is concluded, however, that these newer approaches, though a definite improvement as compared to the Code method, do not represent the final answer to the problem of shear strength.

(c) Since no shear strength tests with analogous beams with standard strength longitudinal reinforcement have been made, the question whether the high steel stresses adversely affected the shear strength of these beams cannot be decided directly. Assuming that the two shear theories of (b), above, have at least indicative validity for these tests, study of Table 11 of the first Report, and of Table 10 of the present Report reveal that by far the preponderant majority of deviations of test strength from computed value is significantly on the unconservative side. This may be regarded as a possible indication that the high steel stresses may, indeed, have reduced the shear strength to some extent. (In judging the possible validity of this supposition the large scatter of theory vs. test should be taken into account as well as the fact that, purposely, many parameters of the specimens of this investigation were outside the range of those tests on which the above two theories have been based; see p. 4, pt. 6 of first Report.)

(d) From the limited data obtained by stirrup strain gaging it appears that the stirrups, after diagonal tension cracking, carry from 70 to 85% of the total shear, at crack locations. Stirrup stresses considerably exceeding this value were measured in unusual cases but were found to be due to skew cracks which happened to cross one leg of the stirrup but not the other. Stirrup stresses were found to be sharply influenced by crack pattern, the measured stirrup stresses being highest when a diagonal tension crack happened to cross a stirrup at a gage location.

(e) Stirrups in the immediate vicinity of concentrated loads or reactions carry much smaller shears than elsewhere (for the same V-value), due to the vertical compression stresses which reduce diagonal tension and cracking.

(f) In all shear calculations the concrete area was taken as the stem width times the effective depth. The comparison, above, of test data with existing theory seems to indicate no gain in shear strength of a T-beam as compared to that of the corresponding rectangular beam.

(3) Deflections.

(a) According to a suggestion made by the late Mr. DiStasio, deflections have been evaluated only for those 16 beams which failed in flexure. This seems advisable because those beams which were designed to fail in shear, particularly those with web reinforcing, showed sufficiently heavy diagonal cracking at service loads to be unrepresentative of practical beams which are designed to fail in flexure rather than in shear. Deflections were evaluated at the "service-load" moments according to the Appendix, ACI Code 1956 which are defined as $1/1.8$ times the ultimate flexural moment calculated on the basis of a steel "yield point" of 60 ksi.

(b) It was found that best correlation with short-time deflections at service load was obtained by using for E the secant modulus

$$E'_c = 1.8 \times 10^6 + 460 f'_c$$

and for the moment of inertia the value for the transformed, cracked section,

excluding the effect of compression reinforcement (in view of 1, c. above). For the restrained beams the arithmetic mean was taken of I for the T-beam section and of I for the rectangular beam section, in view of the negative moments. For the simple beams the I of the T-beam was used.

(c) On this basis the average ratio of computed to measured deflection was 1.01 with deviations for 13 of the 16 beams confined approximately to the range of $\pm 15\%$, the remaining three beams having deviations not exceeding $\pm 30\%$.

(d) The above method has been developed to allow a satisfactory estimate to be made of short-time deflections. It is not suggested that this represents a sufficiently complete answer to a very complex problem. An extensive investigation, not connected with this project, of short and long-time deflections of r/c beams, including tests on creep deflections, of high-strength steel reinforced T-beams, is now under way at Cornell University.

(4) Crack Development

(a) Crack data have been evaluated at two characteristic loads: (i) at "service loads" as defined by the Appendix to the 1956 ACI Code (see 4, a, above), i.e. based on a presumptive yield point of 60 ksi., and (ii) at one-half the experimental ultimate load. Service load crack observations, (i) above, are given in Table 13 of the present Report and permit judgement in regard to crack magnitude for steel stresses at design loads of the order of 30 ksi. Observations at one-half the ultimate load, (ii) above, are given in Table 13 of the First Report and Table 12 of the present Report. They permit judgement on the degree of cracking which would be obtained if the present Code limitation of 60 ksi were relaxed. The present evaluation is limited to those beams which failed in flexure (as listed in Table 13 of present Report) since the crack formation of those beams which were designed to fail in shear is unrepresentative of actual conditions. "Re-test" beams were excluded since some cracking had taken place in the first testing of these beams. Hence all data refer to restrained beams, the re-test beams having been the only simple beams in this program. - For the record, complete

crack data on all beams of both programs are presented graphically in the Appendix to this Report, enabling additional crack studies to be made, if desired.

(b) Flexural Cracking.

(i) Positive Moment Cracks. Inspection of Table 13 shows that average width of positive moment cracks at "service loads", i.e., at a steel stress of the order of 30 ksi, ranged from $3/1000$ to $5/1000$ in. with the exception of Beam IIIB-2 which will be discussed separately. The average of the widths of the two widest cracks ranged from $5/1000$ to $10/1000$ in. It is seen that these crack widths are not excessive if $1/100$ in. is regarded as an acceptable value. If, under low-corrosive conditions, $1.5/100$ in. is taken as an acceptable maximum crack width, inspection of Table 13 of the First Report and Table 12 of the present Report shows for the beams which failed in flexure that steel stresses of 50 ksi under service conditions (corresponding to a yield point of about 90 ksi) would still result in acceptable positive crack width. - The exception to this situation is Beam IIIB-2 which is seen to have significantly wider cracks than any of the other. This beam failed in a combination of flexural tension and shear compression, and was originally designed to fail in shear. This observation emphasizes the fact that adequate shear strength is beneficial to crack control, even as regards positive moment cracks.

(ii) Negative Moment Cracks. In the beams of the First Report tension reinforcement over the continuous support had been "bunched" within the width of the web. In the corresponding beams of the present Report it had been spread out uniformly over the width of the flange. Inspection of the relevant data reveals that the "bunched" reinforcement resulted in the formation of only one or two negative cracks of excessive width, at "service load" as well as at one-half of ultimate load (of the order of $2/100$ in. and more). Spreading the reinforcement over the entire width of the flange resulted in a much larger number of negative cracks and a reduction of the average crack width

to as low as one-third of the previous value. Study of the appropriate graphs in the Appendix reveals that, with reinforcement spread out, maximum negative cracks at service loads were below 1/100 in. and at a steel stress of about 50 ksi. (corresponding to a yield point of about 90 ksi.) did not exceed 1.5/100 in.

(Since in both arrangements the reinforcement was the same, the ratio "concrete tension area/ total bar perimeter" which is thought to be roughly proportional to crack width, was, formally speaking, the same. This shows that mechanical application of such a rule may be misleading. Actually, with the "bunched" reinforcement this ratio was "infinitely large" in the flange projections where no longitudinal steel was located. Therefore, widely spaced cracks of great width probably originated there and then spread toward the reinforced central zone.)

(c) Diagonal Tension Cracking.

(i) The shear force at which the first diagonal tension crack appears can be estimated with reasonable reliability from the equation

$$V_c' = \frac{I_g b}{Q_g} \cdot \frac{f_r f_c'}{f_r + 2f_c'}$$

for beams in which M/Vd is 3 or larger. (For symbols see "Notation.") This equation emphasizes that in order to analyze shear behavior it is apparently necessary, in addition to f_c' , to have some knowledge of the tension strength of the concrete, expressed here indirectly in terms of the modulus of rupture f_r (see Ref. 10, soon to be published in J. Struct. Div. ASCE).

(ii) Width of maximum diagonal tension crack at "service load" as per 1956 ACI Code Appendix was below 1/100 in. except for beams IID-1 and IIIB-2, in which they were 1.8/100 and 1.4/100 in. respectively. Both these beams failed in a combination of flexural and shear failure, emphasizing again that an ample reserve of shear strength over flexural strength is essential to good crack control. In regard to diagonal tension cracks at one-half the ultimate flex-

ural load, of the eight beams of the first Report which failed in flexure, four showed diagonal cracks far in excess of 1.5/100 in., i.e. beams IIB-1, IID-1, IIIA-1, and IIIB-2. Of these beams IID-1 and IIIB-2 had been mentioned before as having failed in a combination of flexure and shear. It is worth noticing that two of these four beams were duplicated in the second phase with the "bunched" negative reinforcement replaced by distributed reinforcement (beams IIB-1^m and IID-1^m). In both cases the width of diagonal cracks at one-half of ultimate load was sharply reduced and was below 1.5/100 in. It is to be concluded that for adequately web reinforced beams diagonal tension crack widths are below permissible limits for steel stresses of the main reinforcement of the order of 30 ksi. Moreover, with special attention to detailing of both the web and the main reinforcement these cracks can also be kept below permissible limits for flexural steel stresses as high as 50 ksi (corresponding to a yield stress of 90 ksi.).

(iii) In the four beams where strain gages were placed on stirrups, no definite relationship between maximum measured stirrup stress and maximum diagonal tension crack width is apparent (Figs. 17 a through d). It is remarkable, though, that if the total external shear is assigned to the stirrups, then a computed stirrup stress of 40 ksi corresponded to a maximum diagonal crack width of about 1/100 in. in all four beams. It was these same four beams which had the distributed negative tension reinforcement (see above).

F. REFERENCES

1. Elstner, Moody, Viest, and Hognestad, "Shear Strength of Reinforced Concrete Beams", Parts 1, 2, 3, and 4, Journal of the American Concrete Institute, Vol. 26, December 1954, January, February, and March 1955.
2. Laupa, Siess, and Newmark, "Strength in Shear of Reinforced Concrete Beams", University of Illinois Engineering Experiment Station Bulletin, No. 428, 1955, Urbana, Illinois.
3. Blakey, F. A., "A Theory of Deflection of Reinforced Concrete Beams Under Short Term Loads", Magazine of Concrete Research, No. 7, August, 1951, Great Britain.
4. Guralnick, S. A., "A Study on the Deflections of Reinforced Concrete Beams", A thesis presented to the Graduate School of Cornell University in partial fulfillment of the requirements for the degree of Master of Science, February, 1955, Ithaca, N. Y.
5. Portland Cement Association Publication, "Deflection of Reinforced Concrete Members", Portland Cement Association, 1947.
6. Gaston, Siess, and Newmark, "An Investigation of the Load-deformation Characteristics of Reinforced Concrete Beams up to the Point of Failure", University of Illinois, Civil Engineering Studies Structural Research Series, No. 40, December, 1951, Urbana, Illinois.
7. Jensen, Vernon P., "Ultimate Strength of Reinforced Concrete Beams as Related to the Plasticity Ratio of Concrete", University of Illinois Engineering Experiment Station Bulletin, No. 345, 1943, Urbana, Illinois.
8. Handbook of the American Society For Metals.
9. Building Code of the American Concrete Institute, No. 318-56.
10. Guralnick, S. A., "Some Basic Aspects of the Problem of Shear Strength of Reinforced Concrete Beams", A thesis presented to the Graduate School of Cornell University in partial fulfillment of the requirements for the degree of Ph.D., February, 1958, Ithaca, N. Y.
11. Chow, Conway, & Winter, "Stresses in Deep Beams", Transactions American Society of Civil Engineers, Vol. 118, 1953.
12. Sachnowski, K. W., Stahlbeton-Konstruktionen, Veb Verlag Technik, 1956, Berlin, Germany.
13. Jones, Royston, "The Ultimate Strength of Reinforced Concrete Beams in Shear", Magazine of Concrete Research, No. 23, August 1956, Great Britain; Discussion: No. 25, March 1957.

14. Hognestad, Hanson and McHenry, "Concrete Stress Distribution in Ultimate Strength Design", Journal of the American Concrete Institute, Vol. 27, No. 4, December, 1955.
15. Whitney, C. S., "Application of Plastic Theory to the Design of Modern Reinforced Concrete Structures," Journal of the Boston Society of Civil Engineers, Vol. 35, No. 1, January 1948, Boston Mass.
16. Lash, S. D., "Ultimate Strength and Cracking Resistance of Lightly Reinforced Beams", Journal of the American Concrete Institute, Vol. 24, No. 6, February 1953.

TABLE 1
Properties of Beam Specimens

For all beams: $b' = 7.0$ in., $b = 23.0$ in., $t = 4.0$ in., $h = 15.25$ in.												
BEAM	LENGTH	d	$d-d'$	a/d	f'_c	f_r	f_y	LONG. REINF.	$A_s = A'_s$	WEB REINF.	r	AGE AT TEST
	(ft.)	(ins.)	(ins.)		(psi)	(psi)	(ksi)		(in ²)		(%)	(days)
IA-1 ^m	17.0	12.55	10.09	2.87	3898	390	92.2	2-#7 2-#6	2.08			31
IC-1 ^m	17.0	12.46	9.92	2.89	4862	455	83.7	2-#7 2-#10	3.73			32
IIA-1 ^m	19.0	12.55	10.09	5.74	3898	390	92.2	2-#7 2-#6	2.08			28
IIB-1 ^m	17.0	12.63	11.07	5.70	3237	366	103.1	4-#5	1.24	#4@3½	1.63	28
IIC-1 ^m	19.0	12.46	9.92	5.78	4862	455	83.7	2-#7 2-#10	3.73			29
IIO-1 ^m	17.0	12.55	10.89	5.74	4493	461	92.2	2-#7 2-#6	2.08	#4@3½	1.63	29
IIIA-1 ^m	20.0	12.55	10.09		4019	428	92.2	2-#7 2-#6	2.08			27
IIIB-1 ^m	20.0	12.63	11.07		3237	366	103.1	4-#5	1.24	#4 var.	varies	28
IIIC-1 ^m	20.0	12.46	9.92		4862	455	83.7	2-#7 2-#10	3.73			28
IIID-1 ^m	20.0	12.55	10.89		4493	461	92.2	2-#7 2-#6	2.08	#4 var.	varies	27

TABLE 2
GRADING OF AGGREGATES
(Aggregates stockpiled in two lots)

SIEVE SIZE	Cumulative Percent Retained			
	"Ithaca" Aggregates		"Boonville" Aggregates	
	SAND	GRAVEL	SAND	GRAVEL
1 "	0	0	0	0
3/4 "	0	0	0	14.30
1/2 "	0	43.0	0	37.50
3/8 "	0	80.0	0	56.80
1/4 "	0	97.0	0	84.20
NO. 4	1.15	99.9	0.70	97.60
8	14.55	100.0	11.65	99.95
16	32.05	100.0	33.25	100.00
30	52.85	100.0	58.90	100.00
50	77.05	100.0	86.70	100.00
100	93.65	100.0	95.90	100.00

Fineness Modulus 2.71 2.87

TABLE 3
COMPOSITION OF ALLOY STEEL

ALLOYING ELEMENT	PERCENT BY WEIGHT			
	*5 BAR	*6 BAR	*7 BAR	*10 BAR
CARBON	0.54	0.54	0.58	0.59
MANGANESE	0.90	0.90	0.96	0.85
PHOSPHOROUS	0.014	0.014	0.014	0.028
SULFUR	0.027	0.027	0.022	0.022
SILICON	0.24	0.24	0.26	1.92
CHROMIUM	0.81	0.81	0.78	0.18

SAE - DESIGNATION OF *5, *6 & *7 BAR MATERIAL IS CHROMIUM - ALLOY STEEL No. 5150 WITH NORMALIZING TEMPERATURE OF 1650°F.

SAE - DESIGNATION OF *10 BAR MATERIAL IS SILICON - MANGANESE ALLOY STEEL No. 9255 WITH NORMALIZING TEMPERATURE OF 1650°F.

TABLE - 4

AVERAGE DIMENSIONS OF LONGITUDINAL REINFORCING BARS

Dimensions measured as specified in ASTM Standard No. A305-56T, are averages for ten bars taken at random from each size group. Transverse deformations in all bars were in a spiral pattern (Inland Steel Co. Standard).

BAR SIZE	DIAMETER (INS)	AREA (IN) ²	PERIMETER (INS)	UNIT WEIGHT (lbs/ft)	DEFORMATIONS		
					SPACING (INS)	HEIGHT (INS)	GAP (INS)
*5	0.629	0.310	1.975	1.055	0.347	0.041	0.098
6	0.752	0.444	2.361	1.508	0.404	0.031	0.107
*7	0.896	0.630	2.815	2.143	0.435	0.035**	0.109
*10	1.275	1.277	4.006	4.343	0.574	0.073	0.113

* SPECIFIED MINIMUM IS 0.038 ins.

** SPECIFIED MINIMUM IS 0.044 ins.

TABLE - 5

TEST RESULTS: PROPERTIES OF CONCRETE AT 28 DAYS

POUR NUMBER	USED IN BEAM NUMBER	AVERAGE TEST VALUES				CALCULATED VALUES		E_t'/E_t	E_c'/E_c
		f_c' (psi)	f_r (psi)	Initial/Tangent Modulus, E_t (10^6 psi)	Secant Modulus at $f_c = \frac{f_c'}{2}$, E_c (10^6 psi)	E_t' (10^6 psi)	E_c' (10^6 psi)		
1	IA-1" IIA-1"	3898	390	3.29	2.76	3.97	3.58	1.21	1.30
2	IIIA-1"	4019	428	3.53	2.92	4.01	3.65	1.14	1.25
3	IC-1" IIC-1" IIIC-1"	4862	455	5.25	4.05	4.25	4.04	0.81	1.00
4	IID-1" IIID-1"	4493	461	4.62	4.08	4.15	3.87	0.90	0.95
5	IIB-1" IIIB-1"	3237	366	3.19	2.78	3.71	3.29	1.16	1.18

47

TABLE - 6

TEST RESULTS: AVERAGE MECHANICAL PROPERTIES
OF REINFORCING STEEL

Mechanical properties are averages for coupons taken from one-third of the total number of bars in each size group. Maximum standard deviation of sample data was in no case greater than 2% of average value.

BAR SIZE	YIELD STRESS (psi)	ULTIMATE STRESS (psi)	PERCENT ELONGATION (%)
WEB REINFORCING:			
#4	54,400	84,700	18.2
LONGITUDINAL REINFORCING:			
#5	103,100 *	146,800	9.0
#6	100,200 *	148,700	17.4
#7	84,200 *	139,600	19.6
#10	83,200	137,300	14.10

*OBTAINED BY THE 0.2% OFFSET METHOD

TABLE - 7
BEAM TEST RESULTS

MAIN SPECIMENS

BEAM	Diagonal Tension Cracking		Failure				Type Failure [*]	Deformation at Load approaching Failure Load			
	Machine Load, W_c (kips)	Maximum Shear, V_c (kips)	Machine Load, W_u (kips)	Maximum Shear, \bar{V}_u (kips)	Max. pos. Moment, $+\bar{M}_u$ (in-kips)	Max. Neg. Moment, $-\bar{M}_u$ (in-kips)		Deflection at point of max. pos. Mom. (ins)	Maximum Measured Strains		
									Tension Steel (10^{-6} in/in)	Compression Steel ^{**} (10^{-6} in/in)	Stirrup Steel (10^{-6} in/in)
IA-1 ^m	31.6	21.4	48.7	31.4	543	554	D. T.	0.150	710	+690	-
IC-1 ^m	40	26.3	54.8	34.9	607	618	D. T.	0.115	400	+850	-
IIA-1 ^m	35	16.7	41.0	19.1	649	642	D. T.	0.144	890	-170	-
IIB-1 ^m	30	14.7	126.5	53.3	1880	1873	F. T.	0.785	8680	-980	1910
IIC-1 ^m	50	22.7	50.0	22.7	779	772	D. T.	0.104	480	-30	-
IID-1 ^m	30	14.7	188.0	77.9	2766	2759	F. T.	0.740	3640	-200	1510
IIIA-1 ^m	54	25.3	72.9	33.4	835	661	D. T.	0.372	1120	+280	-
IIIB-1 ^m	54	25.3	167.4	74.1	1874	1474	F. T.	1.368	6240	-310	1170
IIIC-1 ^m	72	33.0	90.0	40.8	1023	808	D. T.	0.241	660	+160	-
IIID-1 ^m	54	25.3	245.7	107.8	2736	2149	F. T.	1.719	7700	+460	1770

* D.T. = Diagonal-tension failure; F.T. = Flexure-tension failure

** A negative sign (-) in this column indicates Compression and a positive one (+) indicate tension

TABLE - 8

COMPARISON OF TEST RESULTS WITH ULTIMATE FLEXURAL STRENGTH VALUES CALCULATED ACCORDING TO APPENDIX, ACI CODE 318-56

BEAM	TEST DATA		CALCULATION RESULTS			
	MAX. MOMENT AT FAILURE, \bar{M}_u (IN - KIPS)	TYPE FAILURE	M_{fg}^* (IN - KIPS)	$M_{sl} = \frac{M_{fg}}{1.8}$ (IN - KIPS)	\bar{M}_u / M_{fg}	\bar{M}_u / M_{sl}
IB - 1	1240	D.T. & F.T.	790	439	1.570	2.825
IIB - 1	1549	F.T.	790	439	1.961	3.530
IID - 1	2467	D.T. & F.T.	1388	771	1.777	3.199
IIIA - 1	2171	F.T.	1329	738	1.634	2.941
IIIB - 1	1617	F.T.	803	446	2.014	3.626
IIIB - 2	1557	S.C. & F.T.	825	458	1.887	3.400
IIIC - 1	3439	D.T. & F.T.	2350	1306	1.463	2.633
IIID - 1	2706	F.T.	1384	769	1.955	3.519
IA - 1 ^R	2102	F.T.	1318	732	1.595	2.872
IB - 1 ^R	1472	F.T.	790	439	1.863	3.353
IC - 1 ^R	3272	S.C. & F.T.	2330	1294	1.404	2.527
ID - 1 ^R	2219	F.T.	1378	766	1.610	2.898
IIB - 1 ^m	1880	F.T.	887	493	2.120	3.816
IID - 1 ^m	2766	F.T.	1463	813	1.891	3.404
IIIB - 1 ^m	1874	F.T.	887	493	2.113	3.803
IIID - 1 ^m	2736	F.T.	1463	813	1.870	3.366

* BASED ON A FICTITIOUS YIELD STRESS OF 60,000 psi

TABLE - 9

COMPARISON OF TEST RESULTS WITH THEORETICAL
ULTIMATE FLEXURAL STRENGTH VALUES

BEAM	TEST DATA		CALCULATION RESULTS			
	Max. Moment at Failure \bar{M}_u (in-kips)	TYPE Failure	$p = \frac{A_s}{bd}$ (%)	$\frac{k_2}{k_1, k_3}$	M_f (in-kips)	$\frac{M_f}{\bar{M}_u}$
<u>Beams of part I:</u>						
IB-1	1240	D.T. & F.T.	0.44	0.560	1097	0.885
IIB-1	1549	F.T.	0.44	0.560	1097	0.708
IID-1	2467	D.T. & F.T.	0.77	0.645	1984	0.804
IIIA-1	2171	F.T.	0.77	0.588	1881	0.866
IIIB-1	1617	F.T.	0.44	0.588	1115	0.689
IIIB-2	1557	S.C. & F.T.	0.43	0.588	1146	0.736
IIIC-1	3439	D.T. & F.T.	1.38	0.642	3170	0.922
IIID-1	2706	F.T.	0.77	0.642	1978	0.731
IA-1 ^R	2102	F.T.	0.77	0.590	1889	0.899
IB-1 ^R	1472	F.T.	0.44	0.560	1097	0.745
IC-1 ^R	3272	S.C. & F.T.	1.38	0.638	3134	0.958
ID-1 ^R	2219	F.T.	0.77	0.638	1966	0.886
<u>Beams of part II:</u>						
IIB-1 ^m	1880	F.T.	0.43	0.590	1484	0.789
IID-1 ^m	2766	F.T.	0.72	0.630	2183	0.789
IIIB-1 ^m	1874	F.T.	0.43	0.590	1484	0.792
IID-1 ^m	2736	F.T.	0.72	0.630	2183	0.798

TABLE - 10

COMPARISON OF TEST DATA WITH THEORETICAL ULTIMATE SHEAR STRENGTH VALUES

BEAM	TEST DATA			CALCULATION RESULTS			
	Shear Span to Depth Ratio, a/d	Max. Moment at Failure \bar{M}_u (in - kips)	TYPE Failure	Ultimate Shear Strength Moment M_s^* (in - kips)	Ultimate Shear Strength Moment $M_s'^{**}$ (in - kips)	M_s / \bar{M}_u	M_s' / \bar{M}_u
IA - 1 ^m	2.87	554	D.T.	493	962	0.890	1.736
IC - 1 ^m	2.89	618	D.T.	643	1381	1.040	2.235
IIA - 1 ^m	5.74	649	D.T.	539	962	0.831	1.438
IIB - 1 ^m	5.70	1880	F.T.	3105	1867	—	—
IIC - 1 ^m	5.78	779	D.T.	699	1381	0.897	1.772
IID - 1 ^m	5.74	2766	F.T.	3329	2724	—	—
IIIA - 1 ^m	—	835	D.T.	—	976	—	1.169
IIIB - 1 ^m	—	1874	F.T.	—	—	—	—
IIIC - 1 ^m	—	1023	D.T.	—	1381	—	1.350
IIID - 1 ^m	—	2736	F.T.	—	—	—	—

* M_s is calculated according to the Viest-Moody-Hognestad-Elstner theory, reference (1)

** M_s' is calculated according to the Laupa-Siess-Newmark theory, reference (2)

TABLE - 11
DEFLECTION, AT "SERVICE LOAD", OF ALL BEAMS
TESTED IN PARTS I AND II OF THIS INVESTIGATION
WHICH FAILED IN FLEXURE.

BEAM	Service Load Moment, $M_{SL} = \frac{M_{fg}}{1.8}$ (in-kips)	TEST RESULTS		CALCULATED VALUES				Deflection @ Service Load Moment, δ' (ins.)	δ'/δ
		Deflection at Service Load Moment, δ (ins.)	TYPE FAILURE	I_r^* (in ⁴)	I_t^* (in ⁴)	$I_e = \frac{I_r + I_t}{2}$ (in ⁴)	$E_c' I_e$ (10 ³ kip-in ²)		
Beams of Part I:									
IB-1	439	0.150	D.T. & F.T.	863	1167	1015	2964	0.127	0.847
IIB-1	439	0.220	F.T.	863	1167	1015	2964	0.192	0.873
IID-1	771	0.200	D.T. & F.T.	956	1318	1137	4935	0.202	1.010
IIIA-1	738	0.390	F.T.	1151	1656	1404	4549	0.383	0.982
IIIB-1	446	0.480	F.T.	800	1074	937	3036	0.347	0.723
IIIB-2	458	0.330	S.C. & F.T.	854	1136	995	3224	0.335	1.015
IIIC-1	1306	0.330	D.T. & F.T.	1376	2000	1688	7157	0.431	1.306
IIID-1	769	0.370	F.T.	972	1344	1158	4910	0.370	1.000
IA-1 ^R	732	0.145	F.T.	—	1637	1637	5386	0.127	0.876
IB-1 ^R	439	0.120	F.T.	—	1167	1167	3408	0.121	1.008

TABLE - 11 (cont'd.)

BEAM	Service Load Moment, $M_{SL} = \frac{M_{fg}}{1.8}$ (in-kips)	TEST RESULTS		CALCULATED VALUES					δ' / δ
		Deflection @ Service Load Moment, δ (ins.)	TYPE FAILURE	I_r^* (in. ⁴)	I_t^* (in. ⁴)	$I_e = \frac{I_r + I_t}{2}$ (in. ⁴)	$E_c' I_e$ (10 ³ Kip-in ²)	Deflection @ Service Load Moment, δ' (ins.)	
IC-1 ^R	1294	0.165	S.C. & F.T.	—	2147	2147	8738	0.139	0.842
ID-1 ^R	766	0.125	F.T.	—	1387	1387	5645	0.127	1.016
<u>Beams of Part II:</u>									
II B-1 ^m	493	0.172	F.T.	951	1260	1106	3639	0.176	1.023
II D-1 ^m	813	0.170	F.T.	1189	1649	1419	5492	0.192	1.129
III B-1 ^m	493	0.270	F.T.	951	1260	1106	3639	0.320	1.185
III D-1 ^m	813	0.270	F.T.	1189	1649	1419	5492	0.349	1.292

* Moment of inertia of cracked or "transformed" section including tension steel but not including compression steel.

TABLE - 12

CRACK DATA AT ONE-HALF ULTIMATE LOAD

BEAM	$\frac{+ \bar{M}_u}{2}$ (in-kips)	STRESS IN LONG. STEEL $f_s = \frac{+ \bar{M}_u}{2 A_s j d}$ (Ksi)	$\frac{- \bar{M}_u}{2}$ (in-kips)	STRESS IN LONG. STEEL $f_s = \frac{- \bar{M}_u}{2 A_s j d}$ (Ksi)	WIDTH OF CRACKS				NO. OF CRACKS		
					Ave. of ALL POS. FLEXURAL (ins)	Ave. of 2 MAX. POS. FLEXURAL (ins)	Ave. of ALL NEG. FLEXURAL (ins)	MAXIMUM DIAGONAL TENSION (ins)	POSITIVE FLEXURAL	NEGATIVE FLEXURAL	DIAGONAL TENSION
IA-1 ^m	272	11.9	277	12.1	0.003	0.004	0.012	—	4	1	—
IC-1 ^m	304	7.5	309	7.6	—	—	0.001	—	—	1	—
IIA-1 ^m	325	14.2	321	14.1	0.002	0.003	0.016	—	13	1	—
IIB-1 ^m	940	68.6	937	68.4	0.006	0.012	0.010	0.004	23	11	4
IIC-1 ^m	390	9.6	386	9.5	0.002	0.002	—	—	7	—	—
IID-1 ^m	1383	60.6	1380	60.4	0.005	0.010	0.011	0.005	17	10	5
IIIA-1 ^m	418	18.3	331	14.5	0.003	0.005	0.020	—	15	1	—
IIIB-1 ^m	937	68.4	737	53.8	0.006	0.013	0.009	0.004	33	10	2
IIIC-1 ^m	512	12.6	404	9.9	0.002	0.003	0.008	—	11	1	—
IIID-1 ^m	1368	60.0	1075	47.0	0.004	0.009	0.007	0.011	30	8	5

55

TABLE - 13

CRACK DATA AT "SERVICE LOAD" OF ALL BEAMS
TESTED IN PARTS I AND II OF THIS INVESTIGATION
WHICH FAILED IN FLEXURE

BEAM	M_{F6} (in-kips)	$M_{SI} = \frac{M_{F6}}{1.8}$ (in-kips)	WIDTH OF CRACKS				NO. OF CRACKS		
			AVE. OF ALL POS. FLEXURAL (ins)	AVE. OF 2 MAX. POS. FLEXURAL (ins)	AVE. OF ALL NEG. FLEXURAL (ins)	MAXIMUM DIAGONAL TENSION (ins)	POSITIVE FLEXURAL	NEGATIVE FLEXURAL	DIAGONAL TENSION
<u>Beams of part I:</u>									
IB-1	790	439	0.004	0.008	0.021	0.001	10	2	1
IB-1	790	439	0.004	0.007	0.015	—	12	2	—
IID-1	1388	771	0.004	0.006	0.021	0.018	14	2	4
IIIA-1	1329	738	0.004	0.010	0.006	0.009	30	4	5
IIIB-1	803	446	0.005	0.009	0.013	—	18	2	—
IIIB-2	825	458	0.008	0.014	0.020	0.014	16	1	2
IIIC-1	2350	1306	0.003	0.008	0.008	0.007	31	4	5
IIID-1	1384	769	0.003	0.005	0.014	0.001	29	3	1
<u>Beams of part II:</u>									
IB-1 ^m	887	493	0.004	0.007	0.007	—	14	6	—
IID-1 ^m	1463	813	0.004	0.007	0.007	0.003	14	7	1
IIIB-1 ^m	887	493	0.004	0.007	0.007	—	16	2	—
IIID-1 ^m	1463	813	0.003	0.005	0.005	0.001	24	5	1

TABLE - 14

COMPARISON OF SHEAR STRENGTH OF BEAMS WHICH FAILED IN
DIAGONAL-TENSION WITH ACI BUILDING CODE VALUES FOR
ALLOWABLE LOADS

BEAM	LONGITUD. REINFORCING	WEB REINFORCING	EFFECTIVE DEPTH, d (ins)	CONCRETE STRENGTH, f'_c (psi)	TYPE FAILURE	MAXIMUM SHEAR AT FAILURE, \bar{V}_u (kips)	MAXIMUM ALLOWABLE SHEAR, V_{AL}^* (kips)	SAFETY FACTOR $S.F. = \frac{\bar{V}_u}{V_{AL}}$
IA-1 ^m	2-#7 2-#6	—	12.55	3898	D.T.	31.4	6.92	4.538
IC-1 ^m	2-#7 2-#10	—	12.46	4862	D.T.	34.9	6.87	5.080
IIA-1 ^m	2-#7 2-#6	—	12.55	3898	D.T.	19.1	6.92	2.760
IIC-1 ^m	2-#7 2-#10	—	12.46	4862	D.T.	22.7	6.87	3.304
IIIA-1 ^m	2-#7 2-#6	—	12.55	4019	D.T.	33.4	6.92	4.827
IIIC-1 ^m	2-#7 2-#10	—	12.46	4862	D.T.	40.8	6.87	5.939

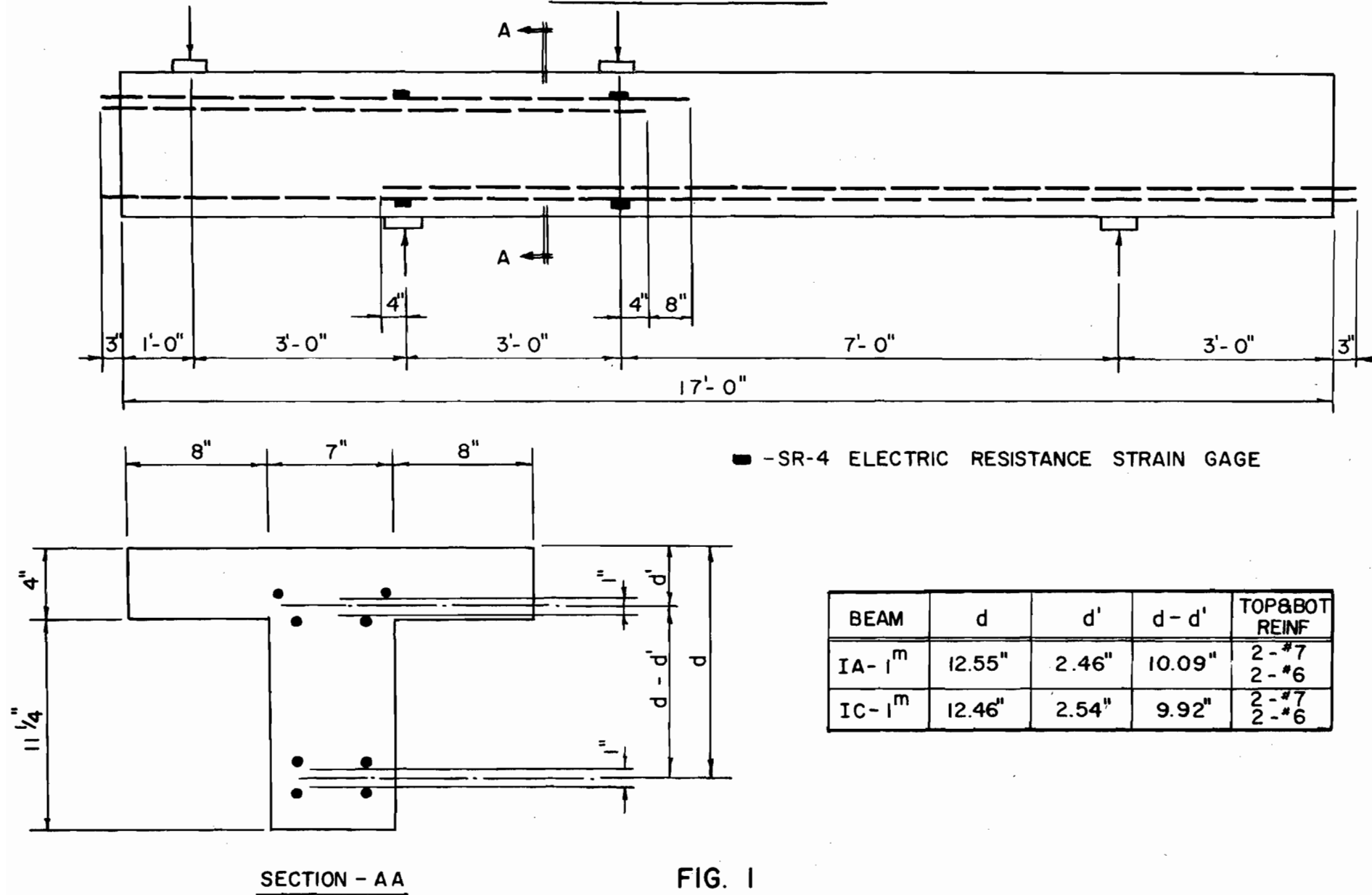
* MAXIMUM ALLOWABLE SHEAR, V_{AL} , IS CALCULATED ACCORDING TO SECTION 305(a) AND CHAPTER 8 OF ACI BUILDING CODE NO. 318-56.

TABLE - 15

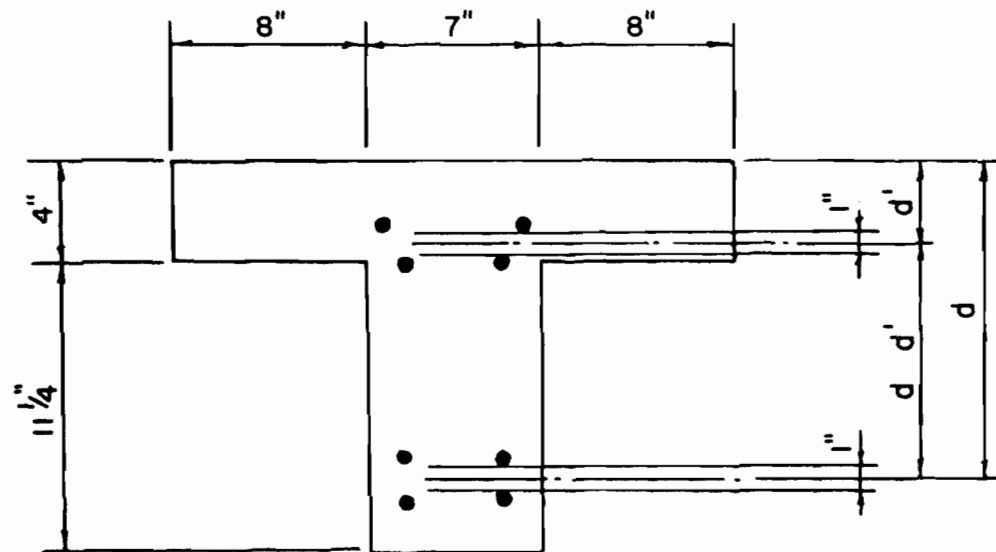
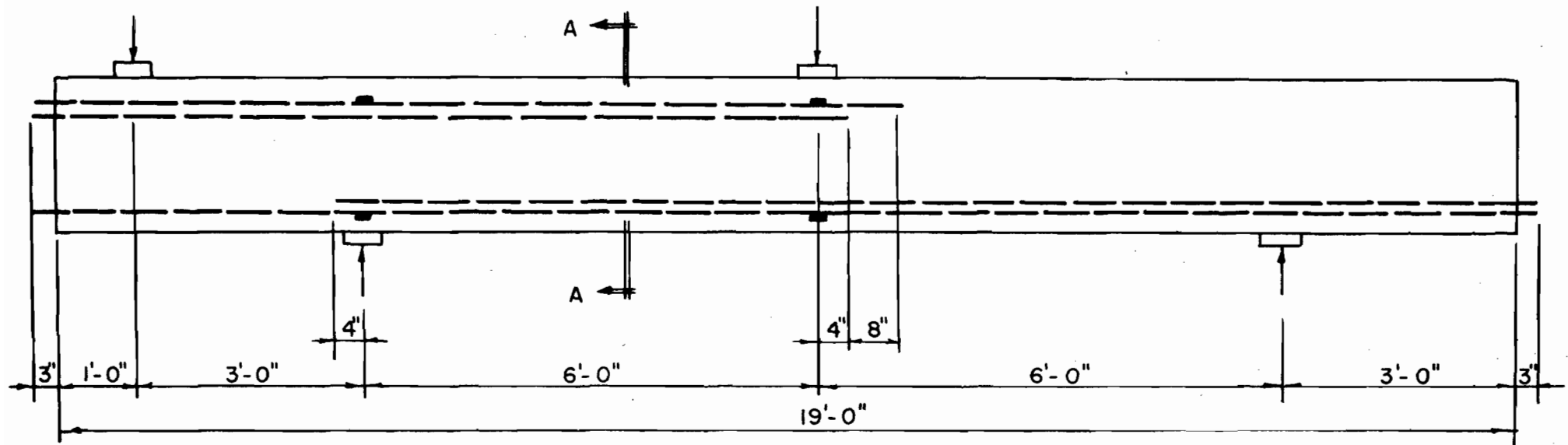
COMPARISON OF TEST RESULTS WITH THEORETICAL INITIAL-DIAGONAL-TENSION-CRACK SHEAR FOR ALL BEAMS TESTED IN PARTS I & II OF THIS INVESTIGATION

BEAM	W_c kips	\bar{V}_c kips	f_c' psi	f_r psi	U_c' psi	V_c' kips	\bar{V}_c/V_c' —
IA-1	20	14.7	3230	315	151	10.9	1.35
-2	20	14.7	2620	330	155	11.2	1.31
IB-1	40	26.3	2440	310	146	10.5	2.50
-2	34.2	22.9	2440	310	146	10.5	2.18
IC-1	40	26.3	4930	470	224	16.2	1.62
-2	50	32.1	4930	470	224	16.2	1.98
ID-1	40	26.3	4930	470	224	16.2	1.62
-2	27	18.7	4930	470	224	16.2	1.15
IIA-1	15	8.7	3230	315	151	10.9	0.80
-2	20	10.7	2620	330	155	11.2	0.96
IIB-1	40	18.7	2440	310	146	10.5	1.78
-2	20	10.7	2440	310	146	10.5	1.02
IIC-1	60	26.7	5520	486	233	16.8	1.59
-2	60	26.7	5520	486	233	16.8	1.59
IID-1	40	18.7	5520	486	233	16.8	1.11
-2	40	18.7	5520	486	233	16.8	1.11
IIIA-1	54	23.3	3130	356	168	12.1	1.93
-2	36	17.5	3130	356	168	12.1	1.45
IIIB-1	90	40.8	3130	356	168	12.1	3.37
-2	36	17.5	3130	356	168	12.1	1.45
IIIC-1	72	33.0	5300	526	251	18.1	1.82
-2	72	33.0	5300	526	251	18.1	1.82
IIID-1	72	33.0	5300	526	251	18.1	1.82
-2	72	33.0	5300	526	251	18.1	1.82
IA-1 ^m	31.6	21.4	3898	390	186	13.4	1.67
IC-1 ^m	40	26.3	4862	455	218	15.7	1.68
IIA-1 ^m	35	16.7	3898	390	186	13.4	1.25
IIB-1 ^m	30	14.7	3237	366	173	12.5	1.18
IIC-1 ^m	50	22.7	4862	455	218	15.7	1.45
IID-1 ^m	30	14.7	4493	461	220	15.9	0.92
IIIA-1 ^m	54	25.3	4019	428	203	14.7	1.72
IIIB-1 ^m	54	25.3	3237	366	173	12.5	2.02
IIIC-1 ^m	72	33.0	4862	455	218	15.7	2.10
IIID-1 ^m	54	25.3	4493	461	220	15.9	1.59

ARRANGEMENT OF REINFORCEMENT FOR SERIES I BEAMS WITH PLAIN WEBS



ARRANGEMENT OF REINFORCEMENT FOR SERIES II BEAMS WITH PLAIN WEBS



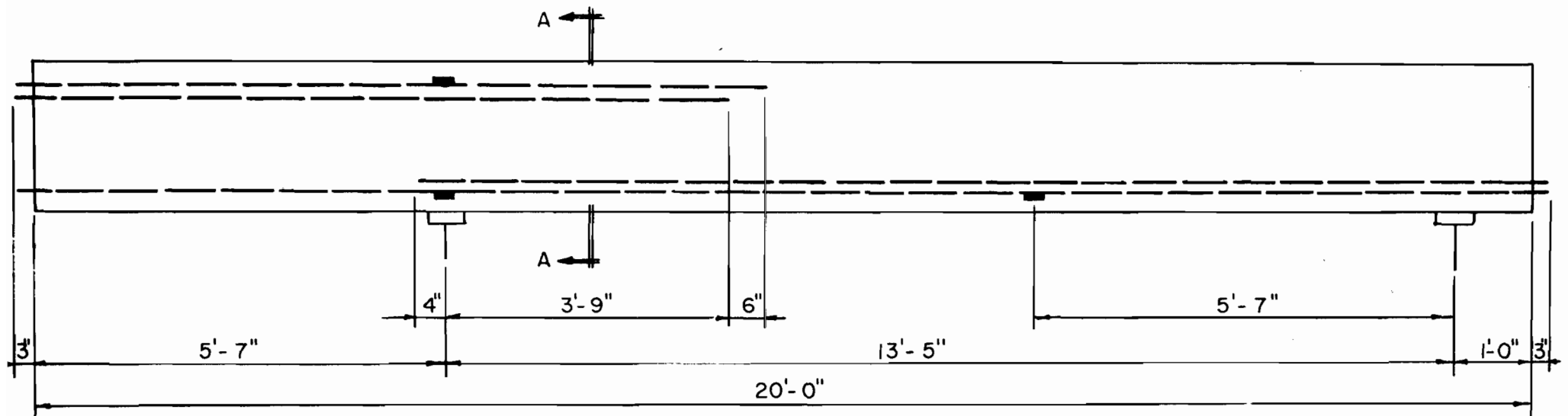
■ — SR-4 ELECTRIC RESISTANCE STRAIN GAGE

BEAM	d	d'	$d - d'$	TOP & BOT REINF
IIA-1 ^m	12.55"	2.46"	10.09"	2-#7 2-#6
IIC-1 ^m	12.46"	2.54"	9.92"	2-#7 2-#10

SECTION - AA

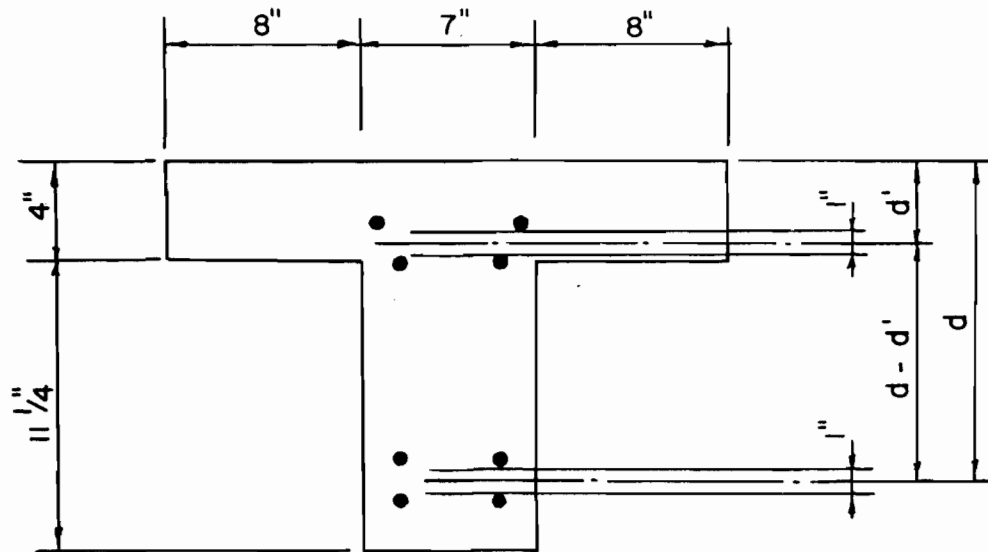
FIG. 2

ARRANGEMENT OF REINFORCEMENT FOR SERIES III BEAMS WITH PLAIN WEBS



19

■ — SR-4 ELECTRIC RESISTANCE STRAIN GAGE

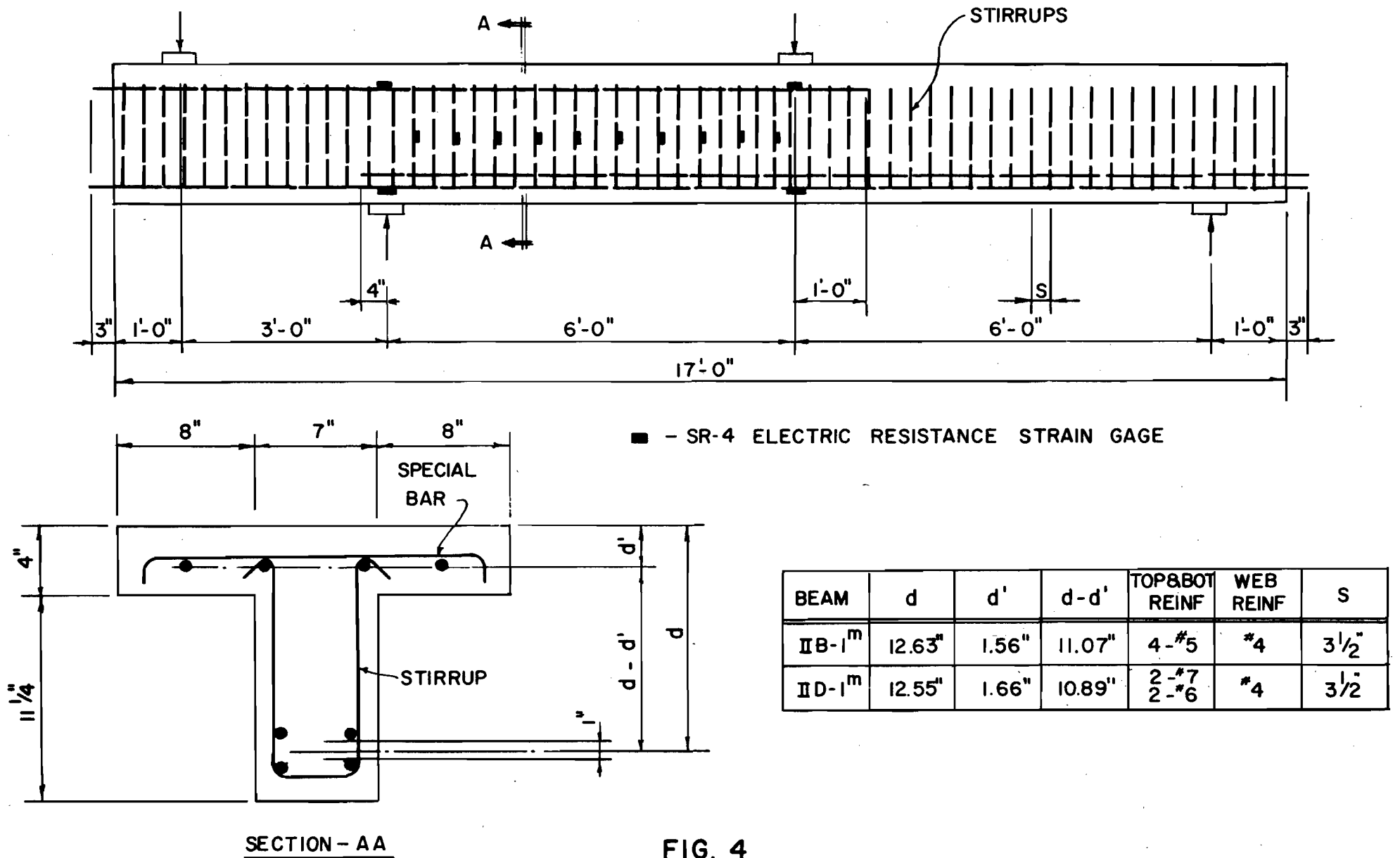


SECTION-AA

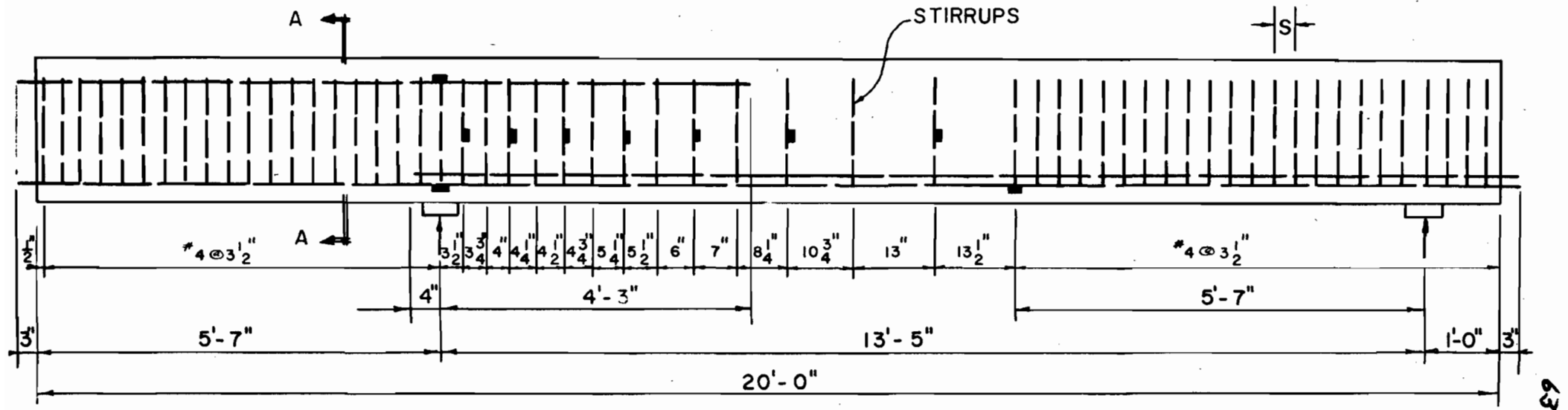
FIG. 3

BEAM	d	d'	d - d'	TOP&BOT REINF
III A - 1 ^m	12.55"	2.46"	10.09"	2 - #7 2 - #6
III C - 1 ^m	12.46"	2.54"	9.92"	2 - #7 2 - #10

ARRANGEMENT OF REINFORCEMENT FOR SERIES II BEAMS WITH REINFORCED WEBS

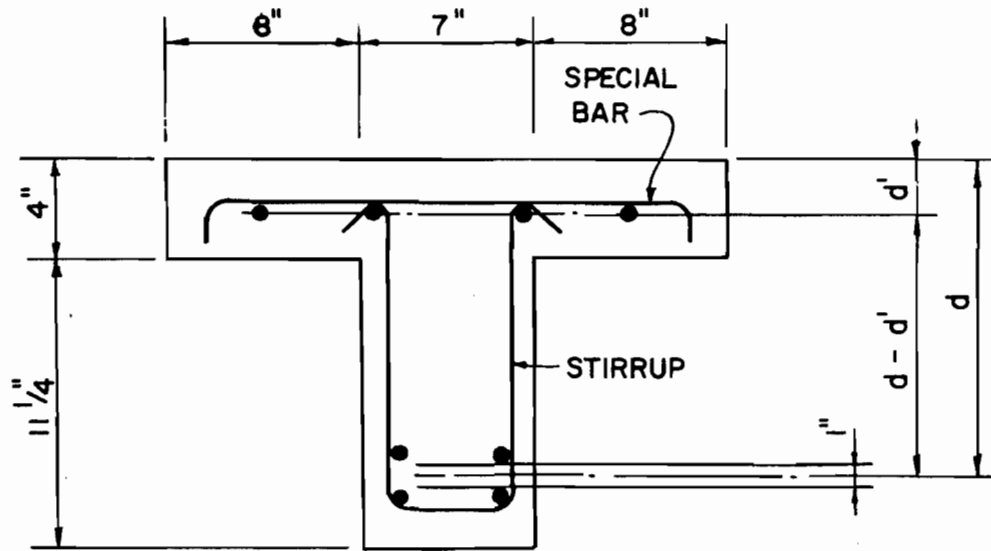


ARRANGEMENT OF REINFORCEMENT FOR SERIES III BEAMS WITH REINFORCED WEBS



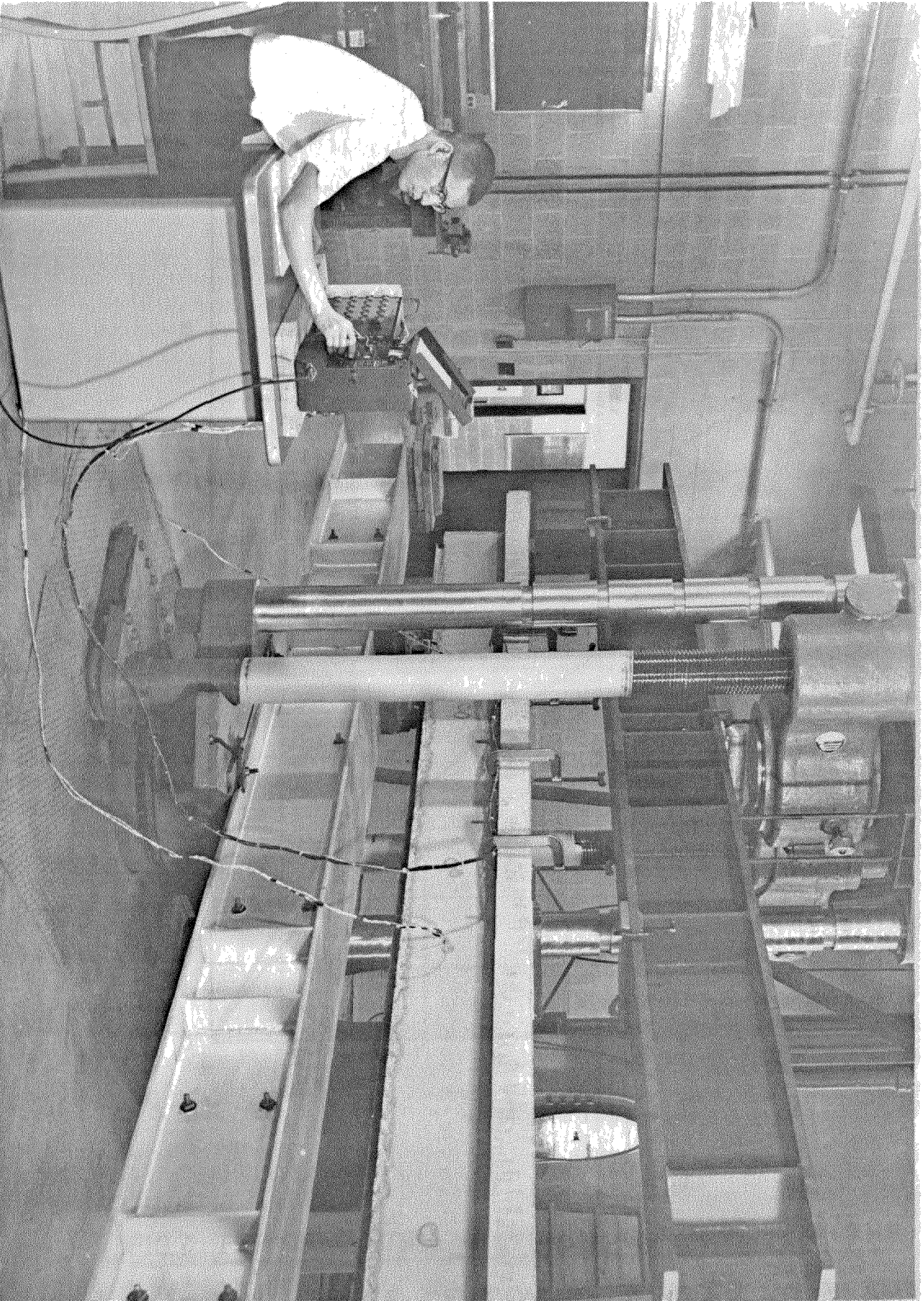
■ — SR-4 ELECTRIC RESISTANCE STRAIN GAGE

BEAM	d	d'	d - d'	TOP & BOT REINF	WEB REINF	S
III B-1 ^m	12.63"	1.56"	11.07"	4 - #5	#4	VARIABLE
III D-1 ^m	12.55"	1.66"	10.89"	2 - #7 2 - #6	#4	VARIABLE



SECTION - A A

FIG. 5



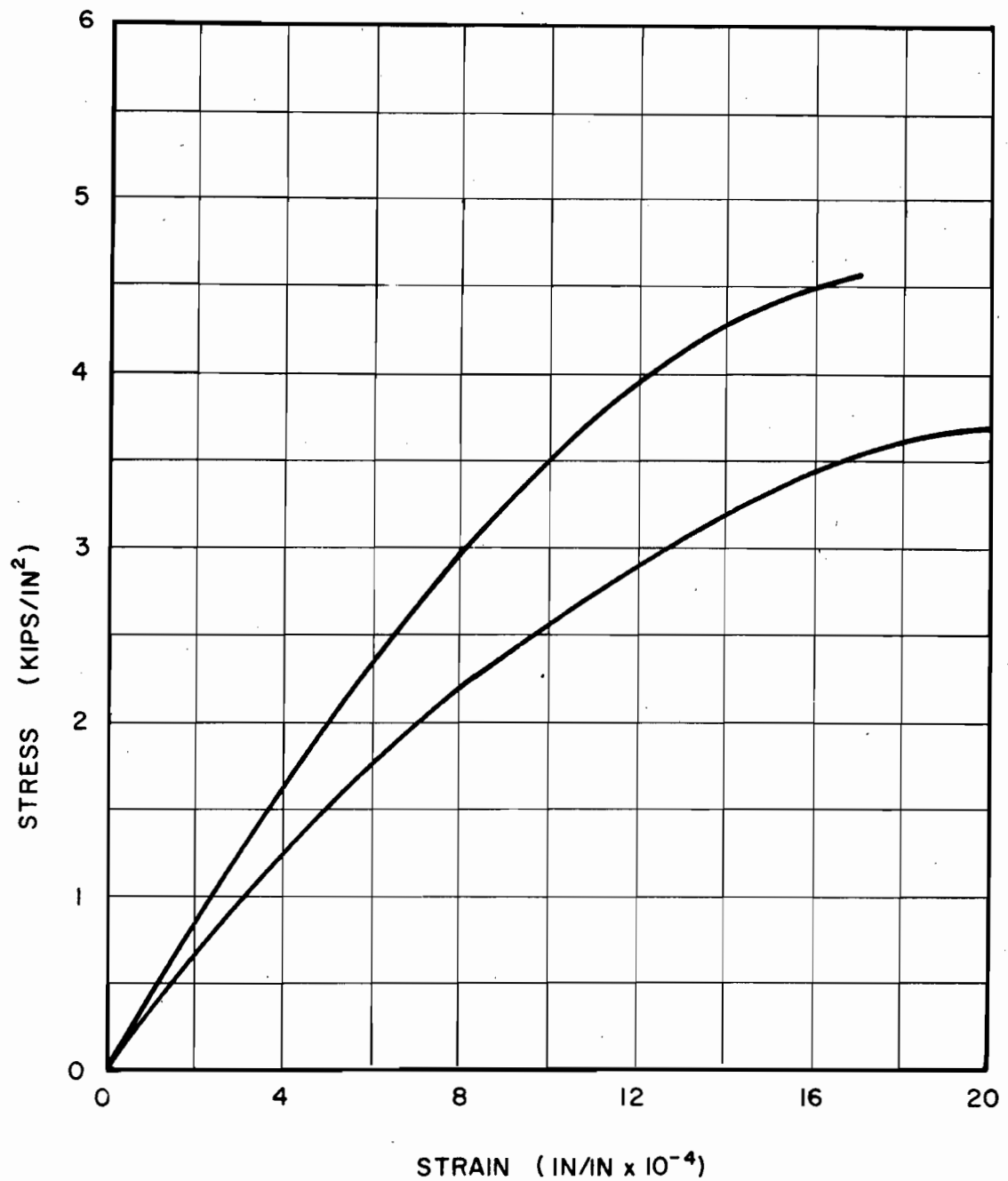


FIG.7 TYPICAL STRESS-STRAIN CURVES FOR THE
TWO TYPES OF CONCRETE USED IN BEAM
SPECIMENS

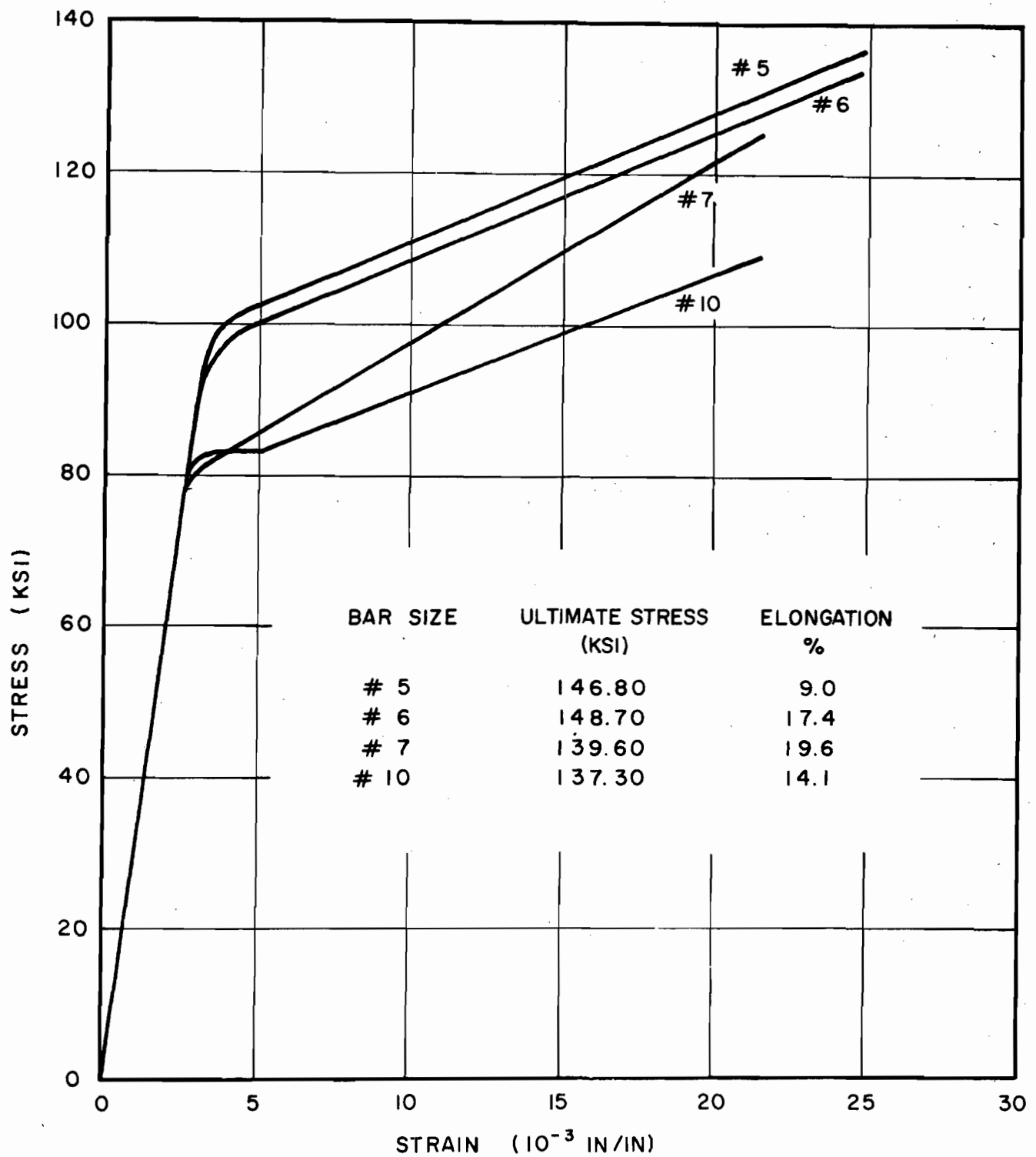


FIG. 8 TYPICAL STRESS-STRAIN CURVES FOR HIGH-STRENGTH STEEL REINFORCING BAR MATERIAL USED IN BEAM SPECIMENS

FIG. 9a PHOTOGRAPHS OF BEAMS WITH PLAIN WEBS
AFTER FAILURE

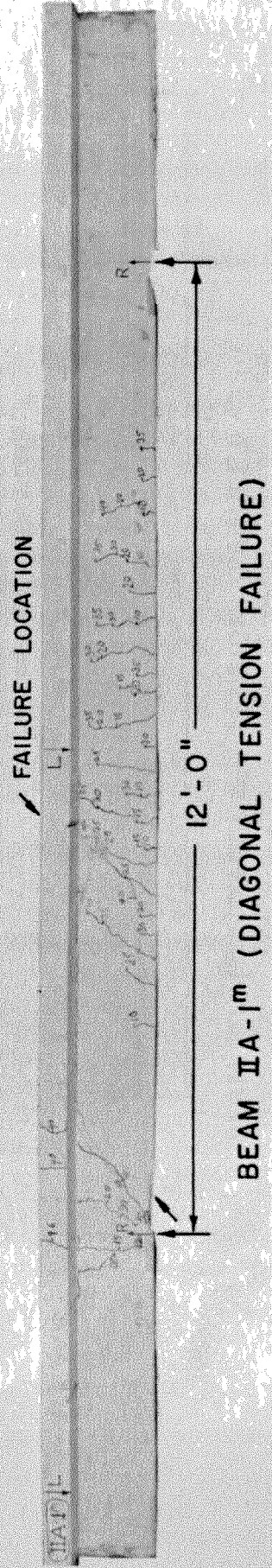
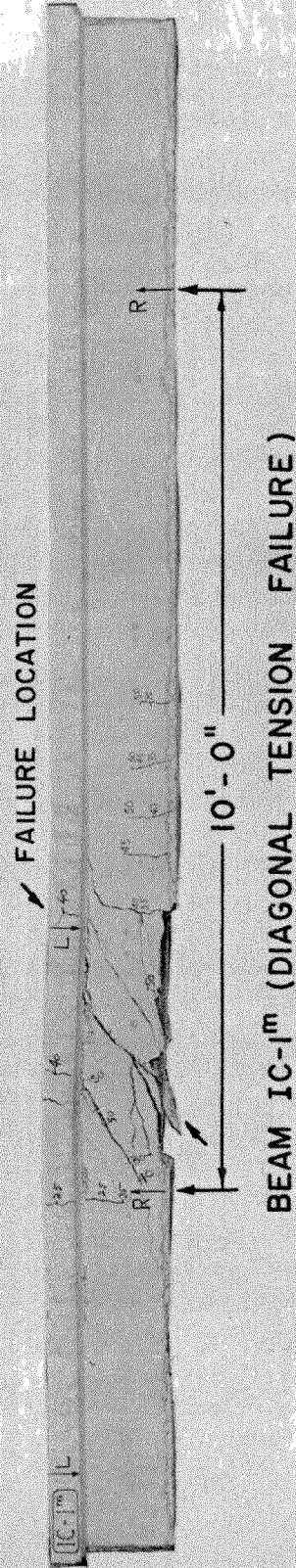
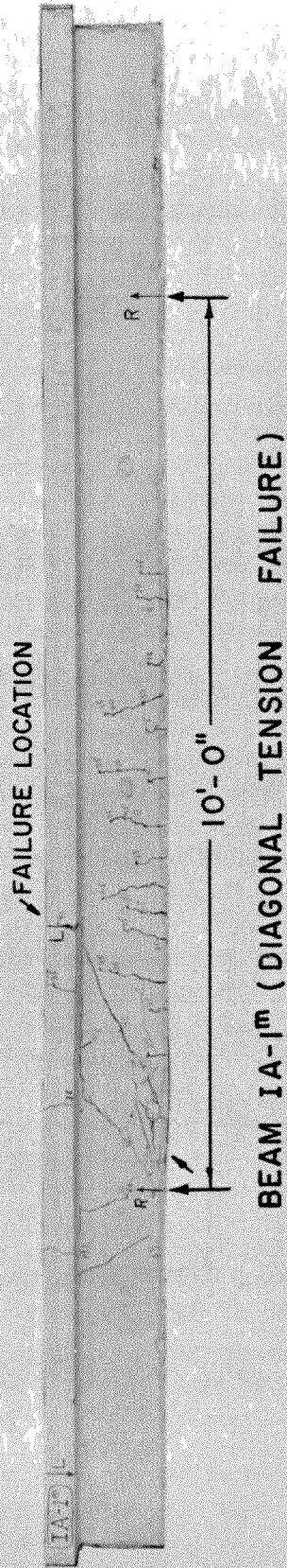
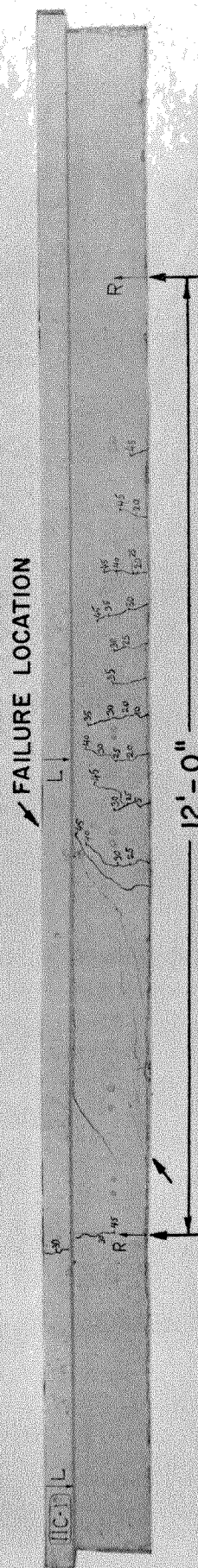
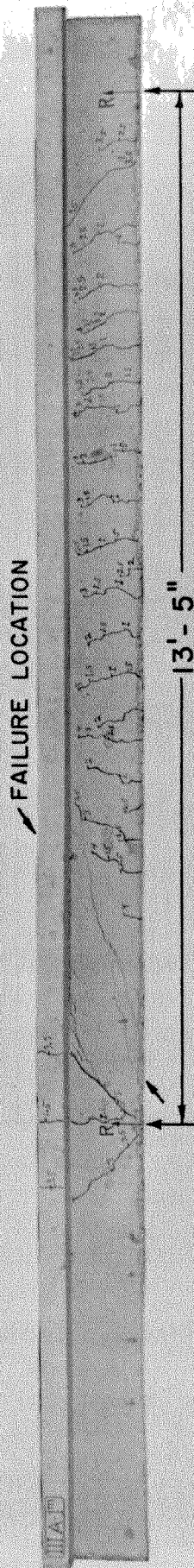


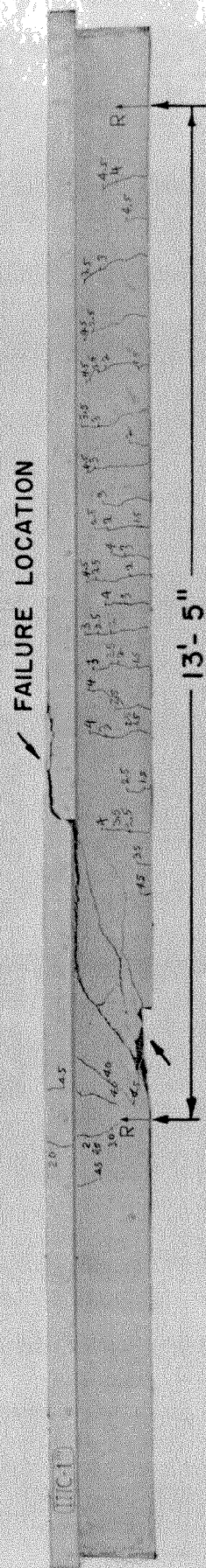
FIG. 9b PHOTOGRAPHS OF BEAMS WITH PLAIN WEBS
AFTER FAILURE



BEAM IC-1^m (DIAGONAL TENSION FAILURE)

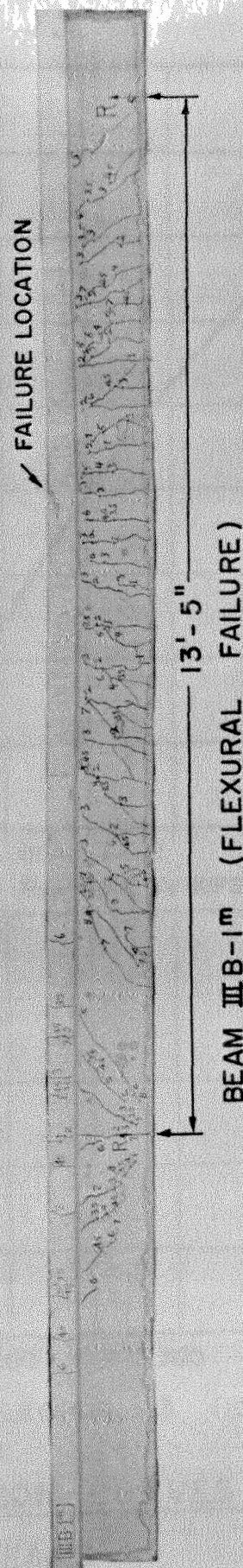
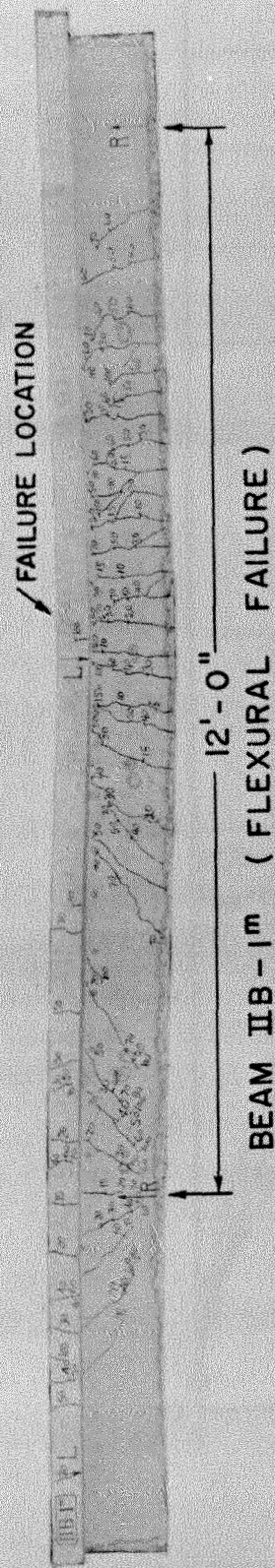


BEAM IIIA-1^m (DIAGONAL TENSION FAILURE)



BEAM IIIC-1^m (DIAGONAL TENSION FAILURE)

FIG. 10 PHOTOGRAPHS OF BEAMS WITH REINFORCED WEBS
AFTER FAILURE



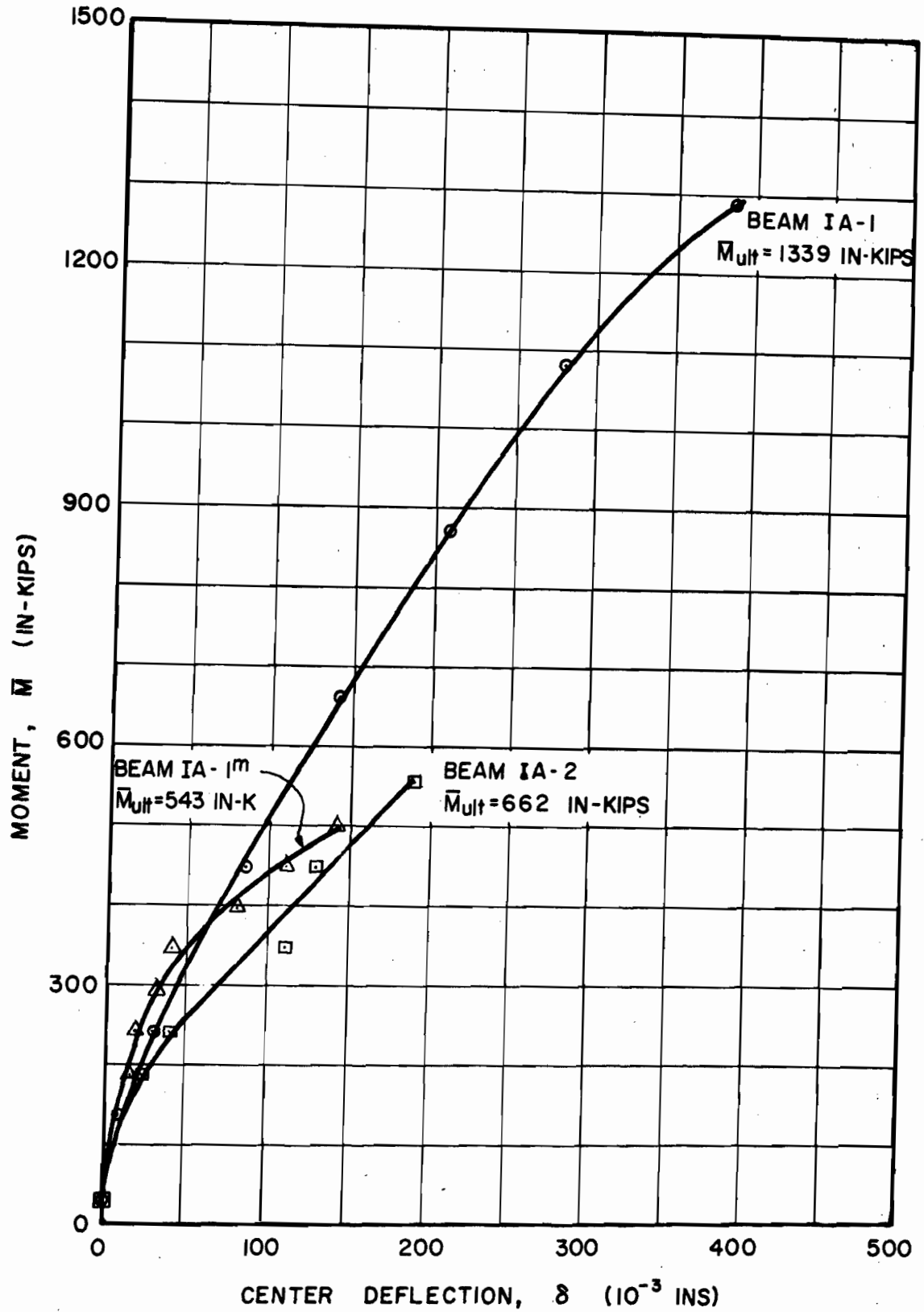


FIG. II a MOMENT-DEFLECTION CURVES FOR SERIES
IA BEAMS

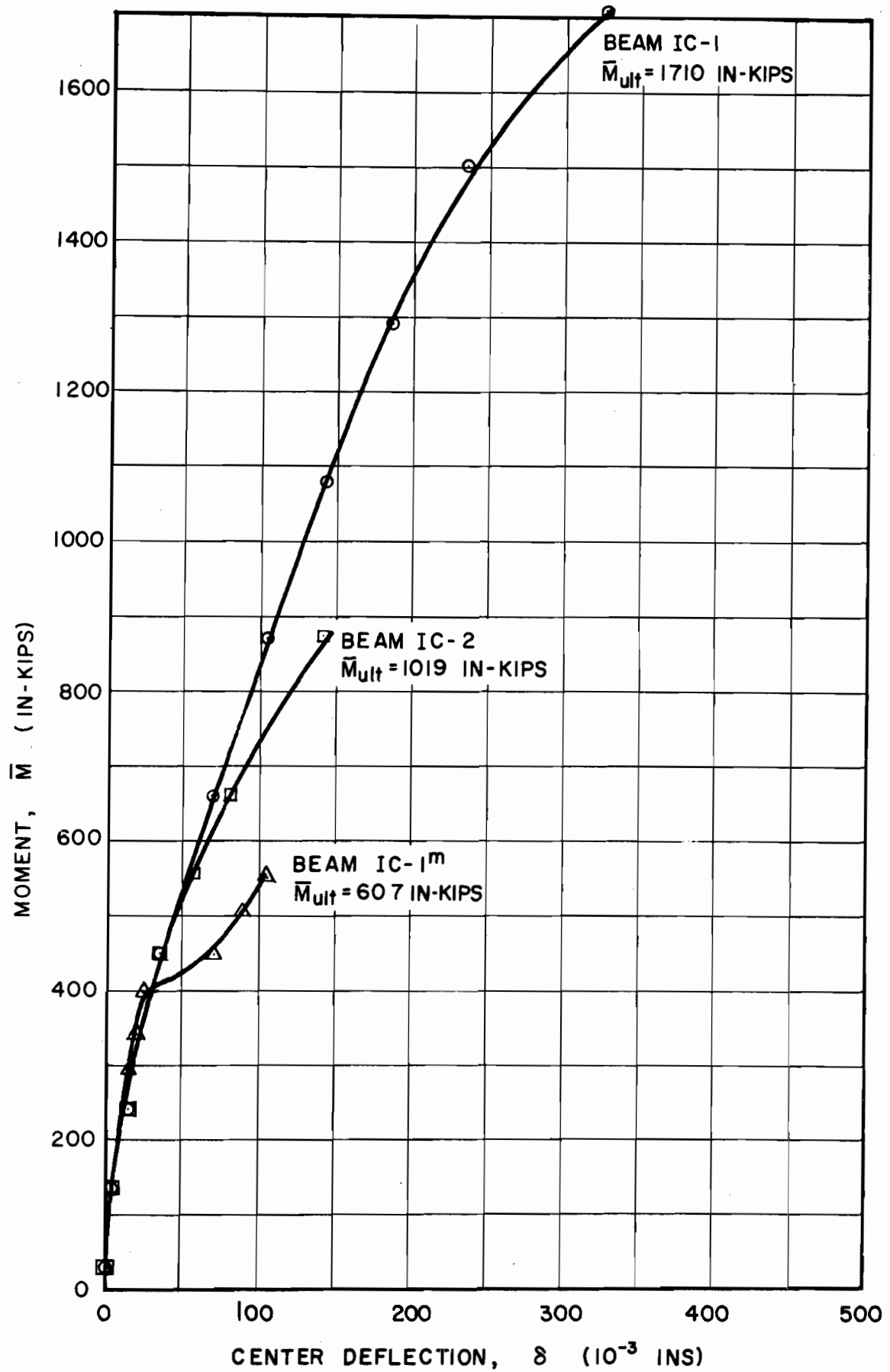


FIG. IIb MOMENT-DEFLECTION CURVES FOR SERIES
IC BEAMS

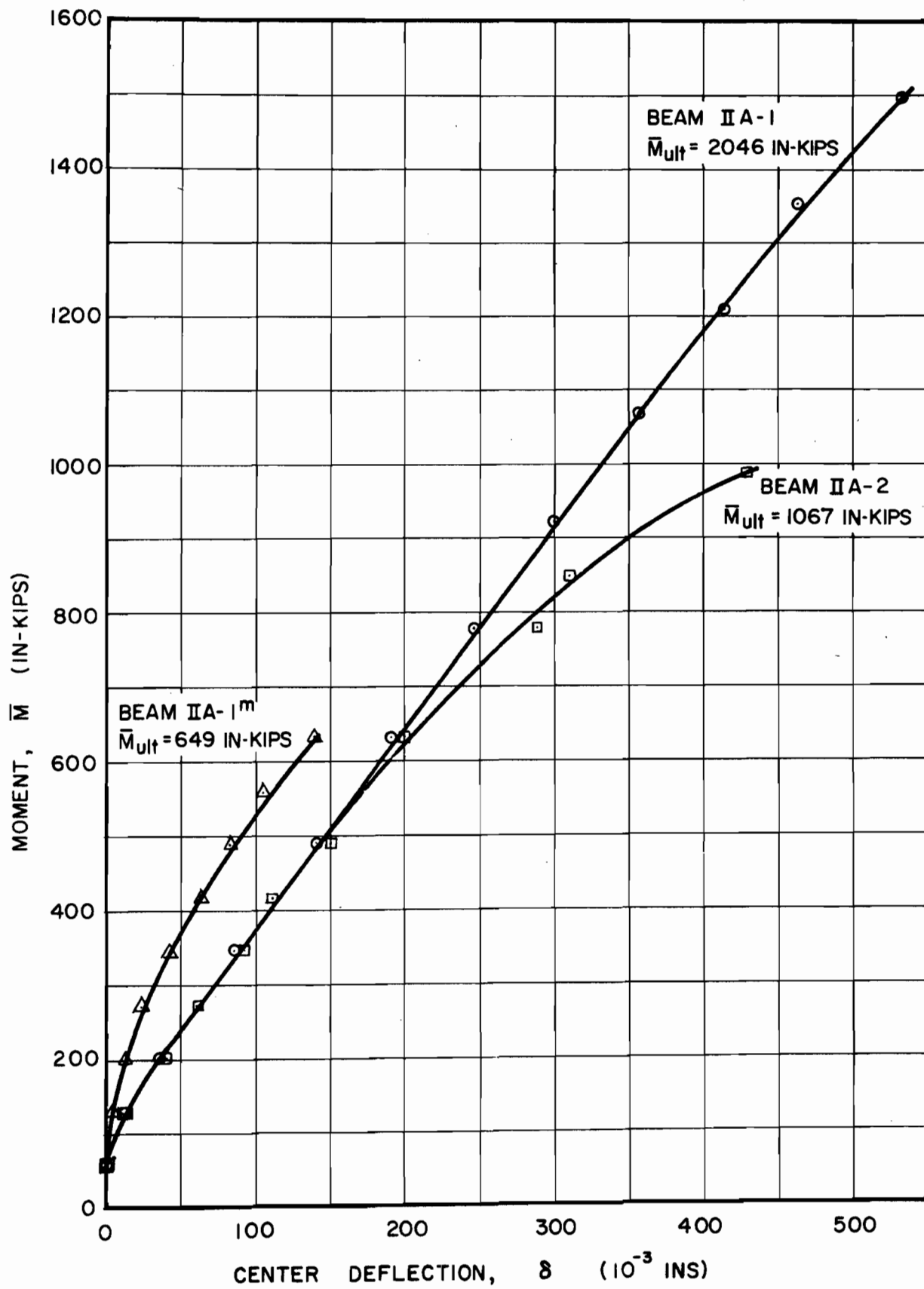


FIG. IIc MOMENT-DEFLECTION CURVES FOR SERIES II A
BEAMS

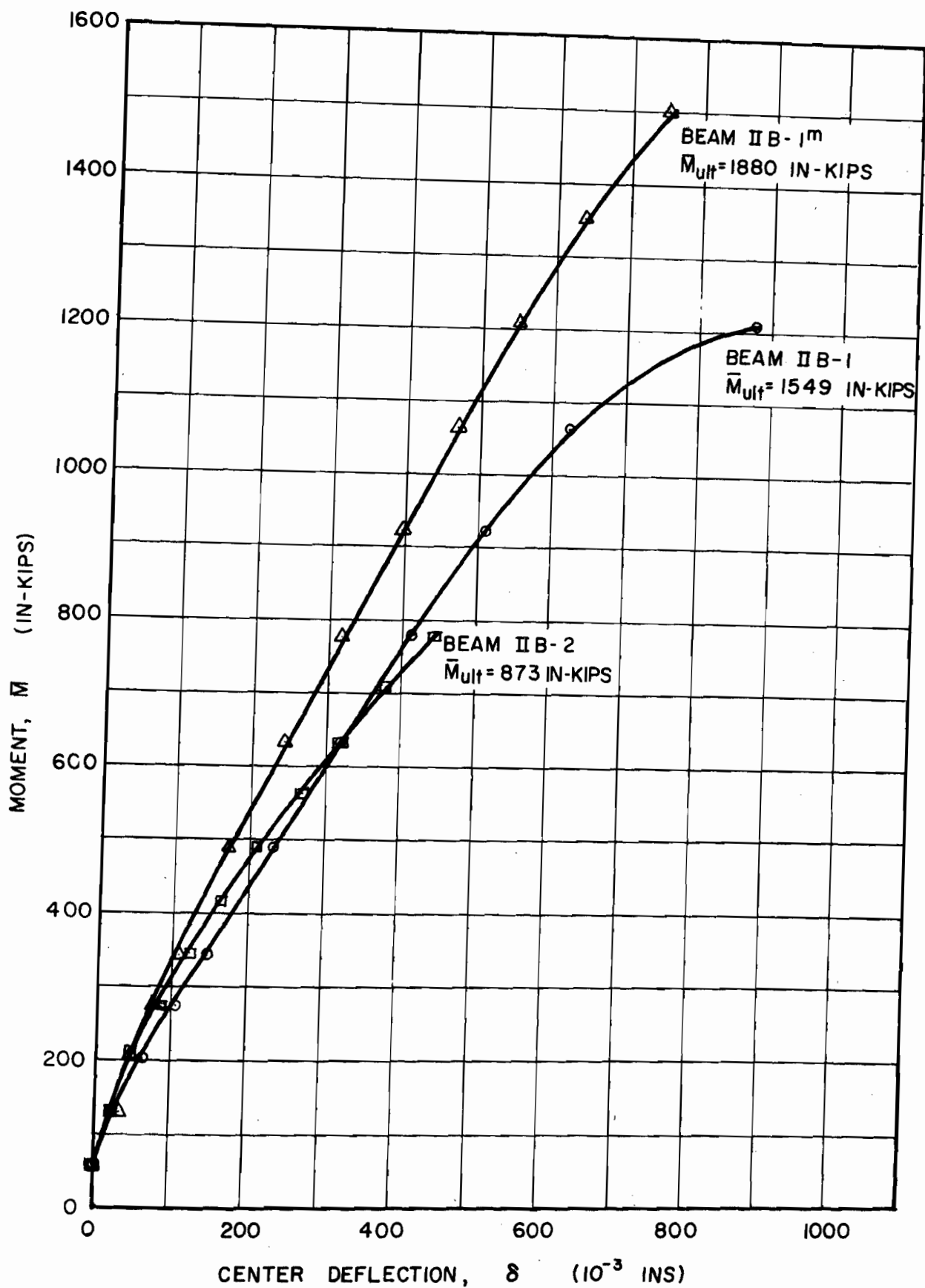


FIG. IId MOMENT-DEFLECTION CURVES FOR SERIES IIB
BEAMS

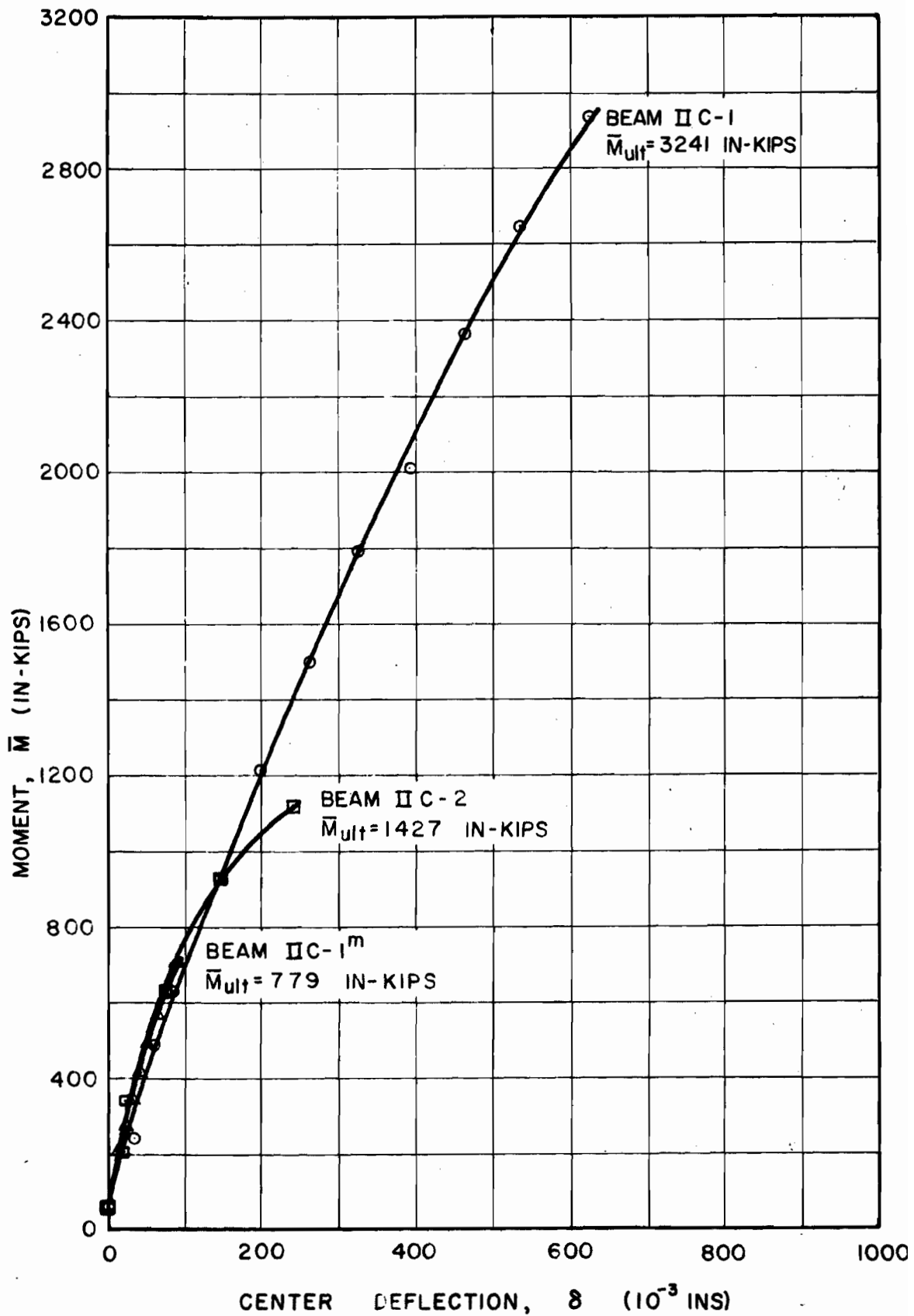


FIG. IIe MOMENT-DEFLECTION CURVES FOR SERIES
IIC BEAMS

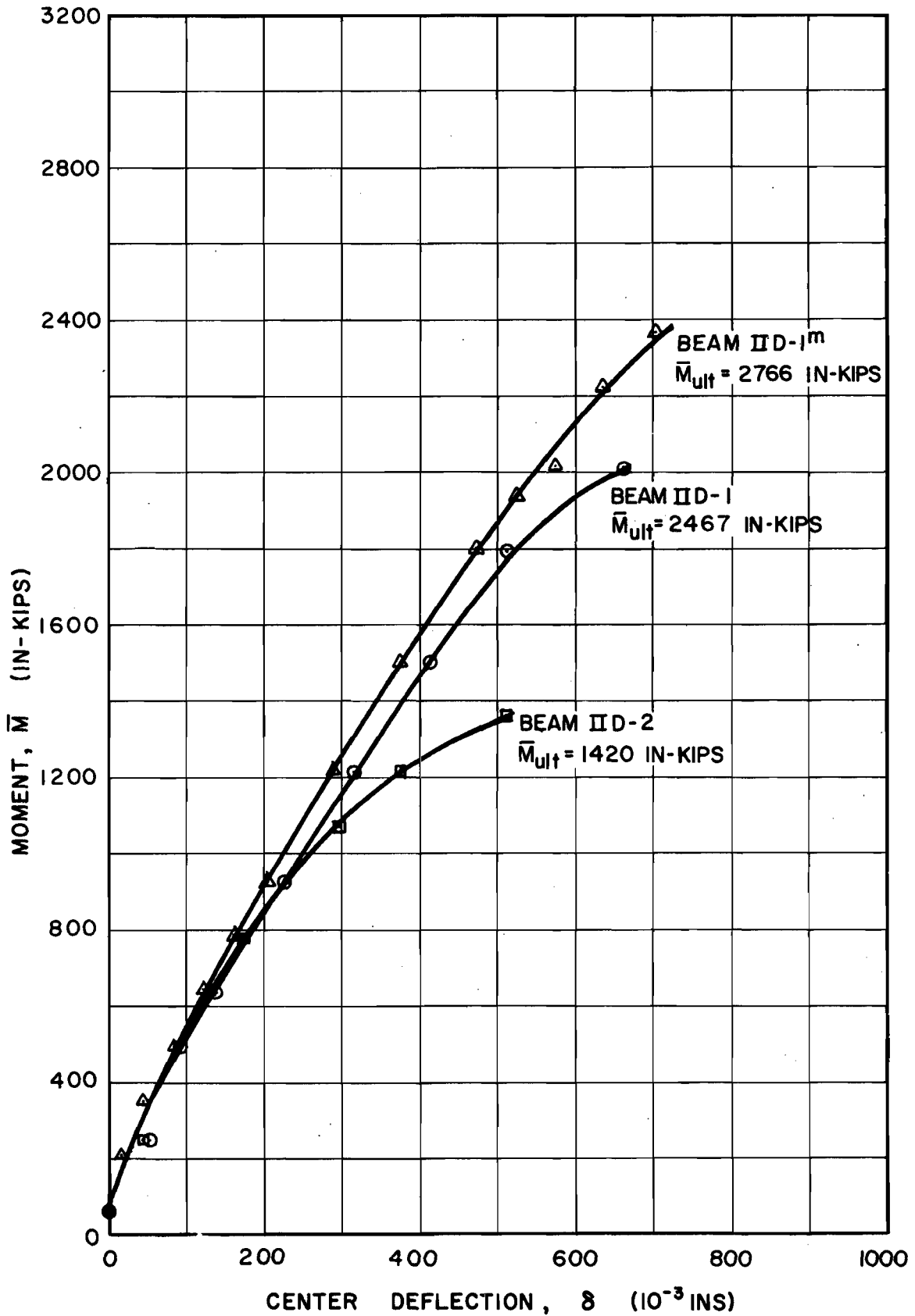


FIG. II f MOMENT-DEFLECTION CURVES FOR SERIES
IID BEAMS

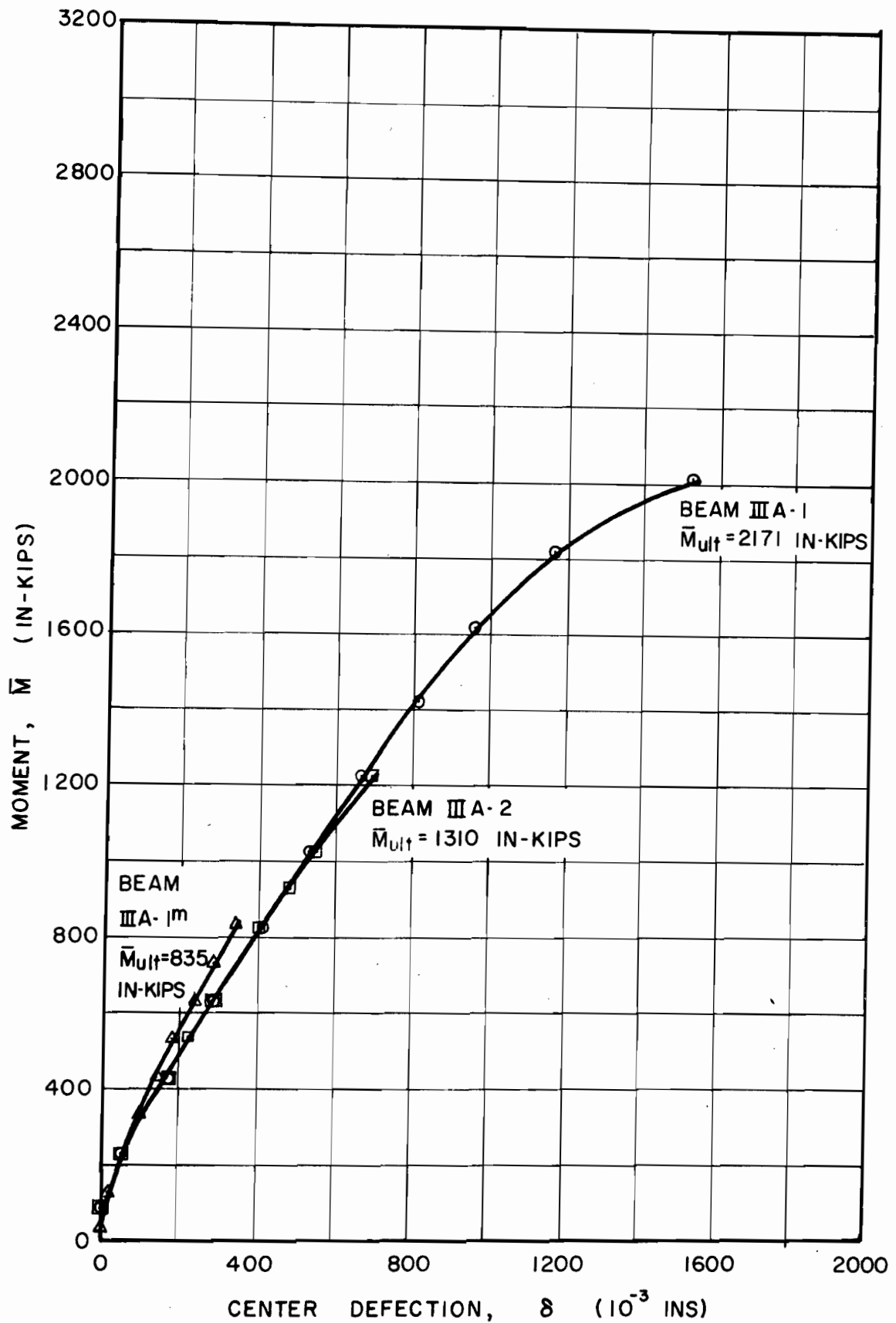


FIG. IIg MOMENT-DEFLECTION CURVES FOR SERIES
III A BEAMS

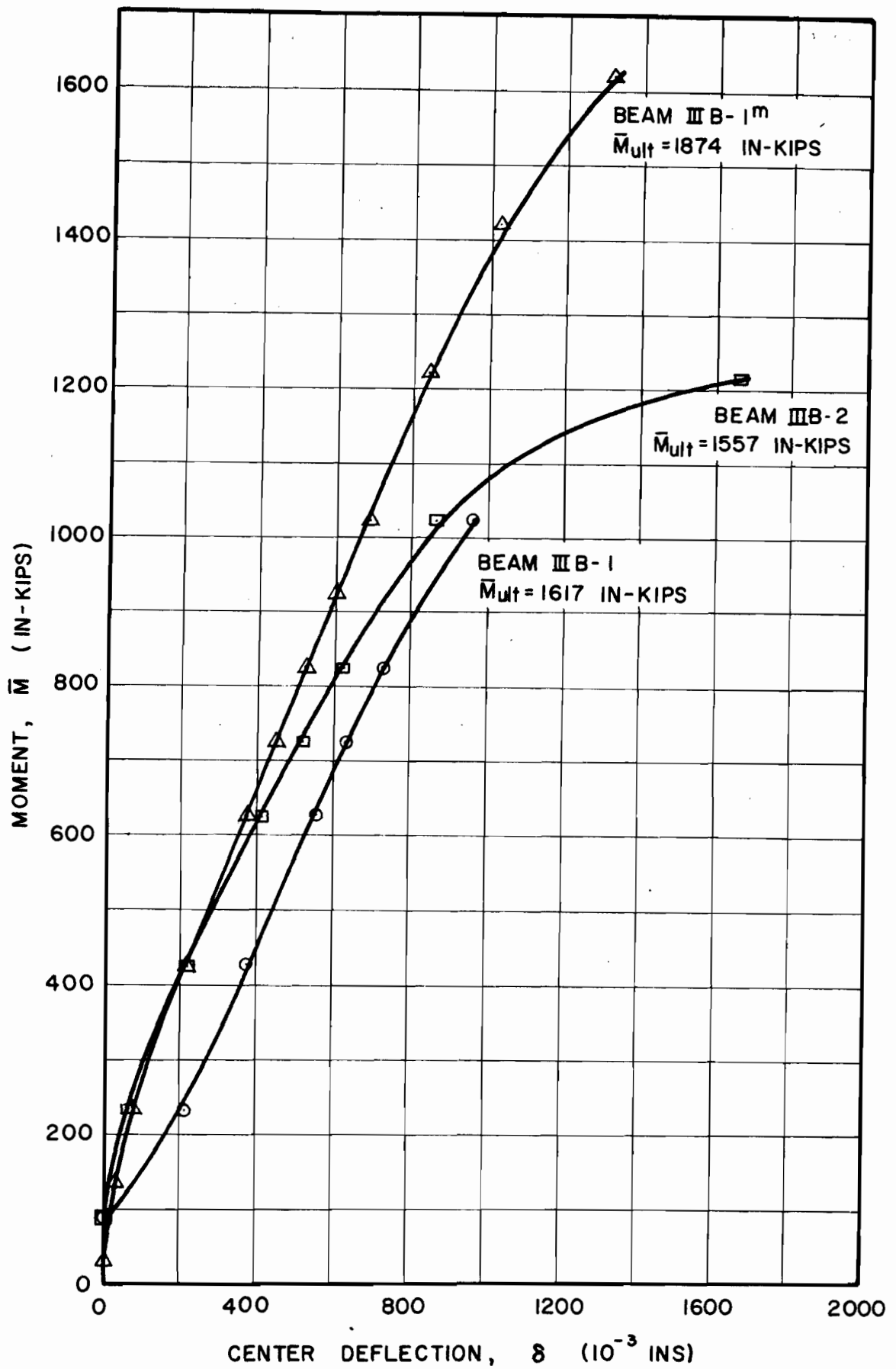


FIG. IIh MOMENT-DEFLECTION CURVES FOR SERIES
III B BEAMS

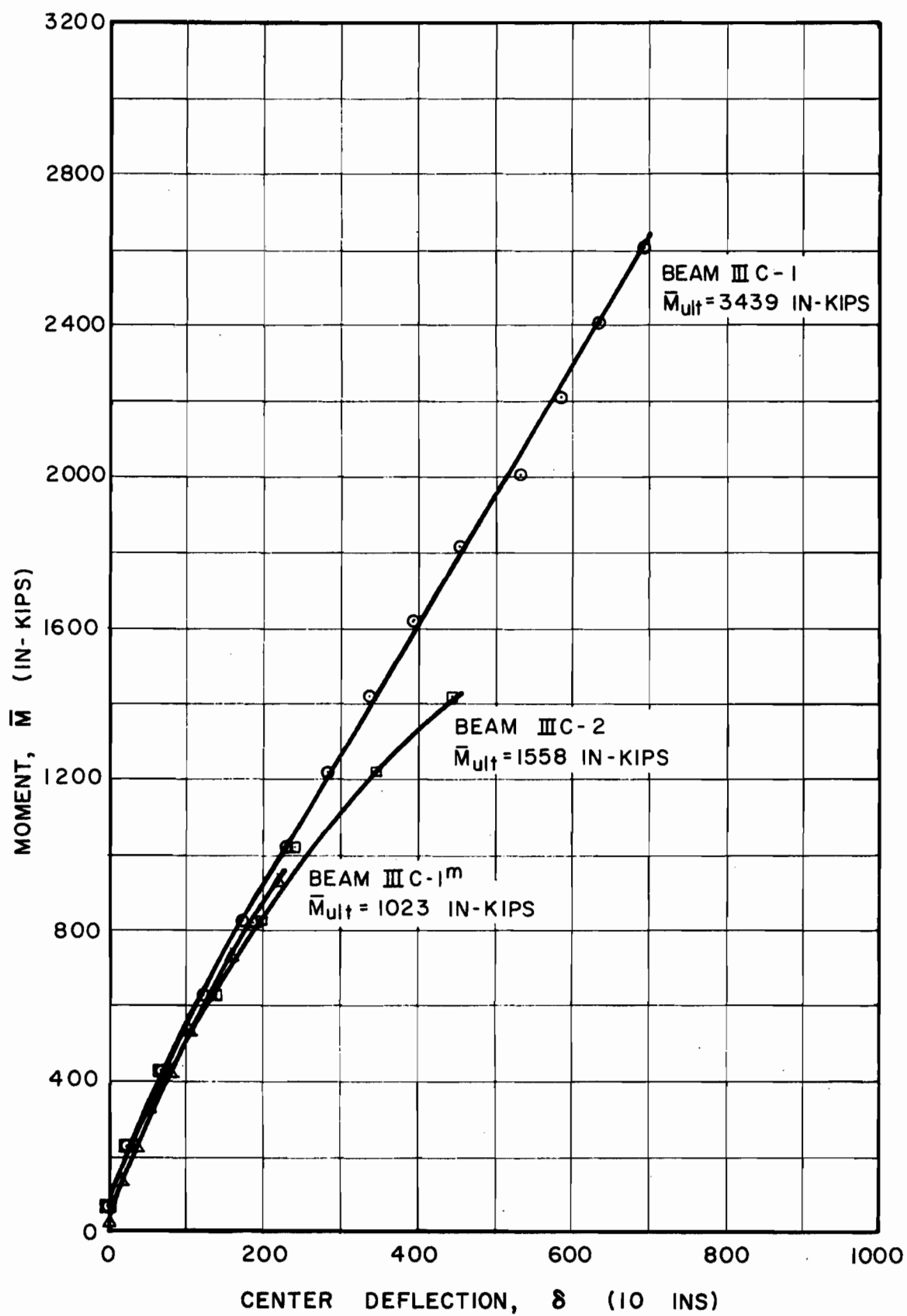


FIG. III MOMENT-DEFLECTION CURVES FOR SERIES
III C BEAMS

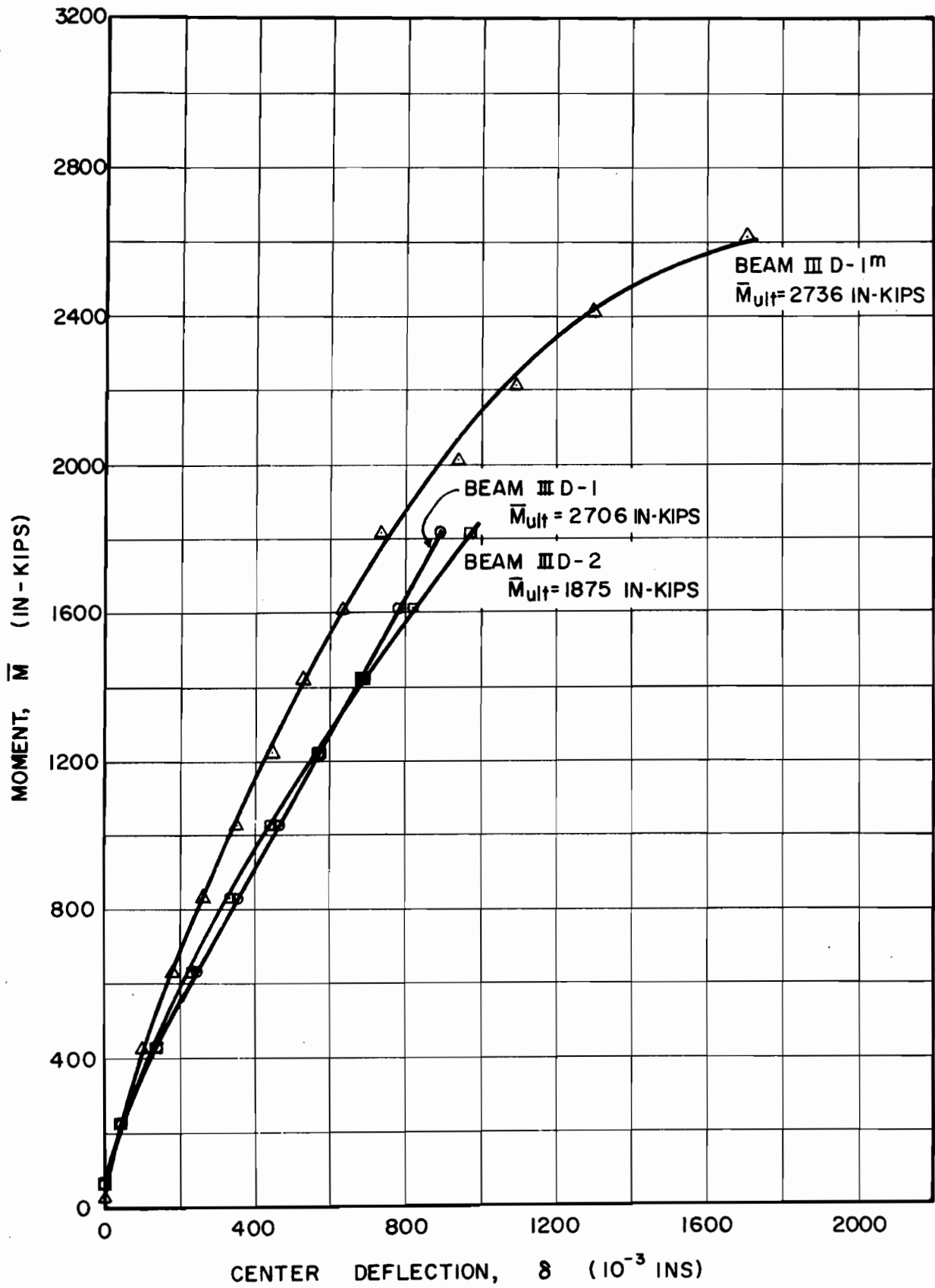


FIG. IIj MOMENT-DEFLECTION CURVES FOR SERIES
III D BEAMS

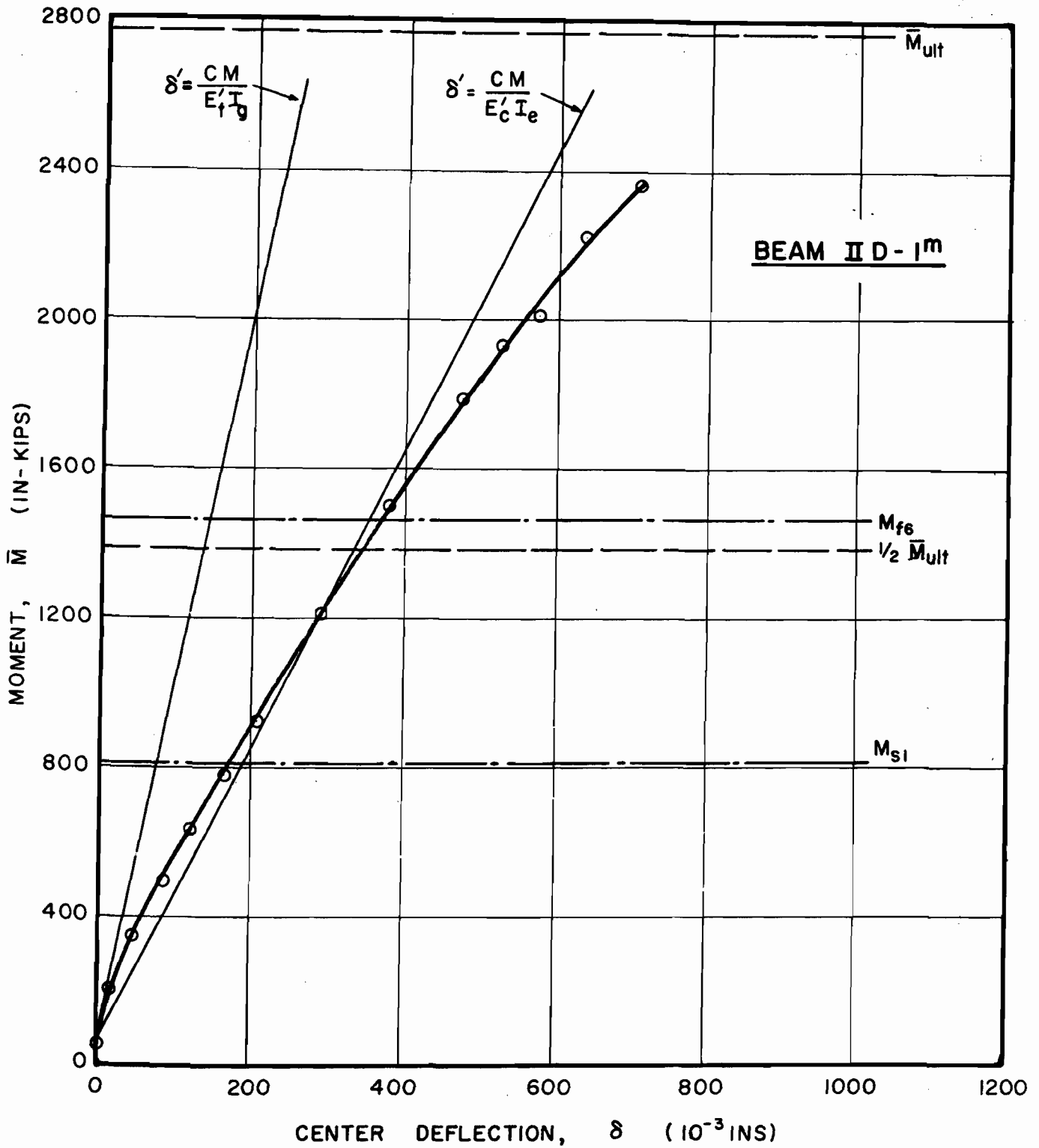


FIG. 12a TYPICAL MOMENT-DEFLECTION CURVE FOR BEAMS WITH WEB REINFORCING WHICH FAILED IN FLEXURE

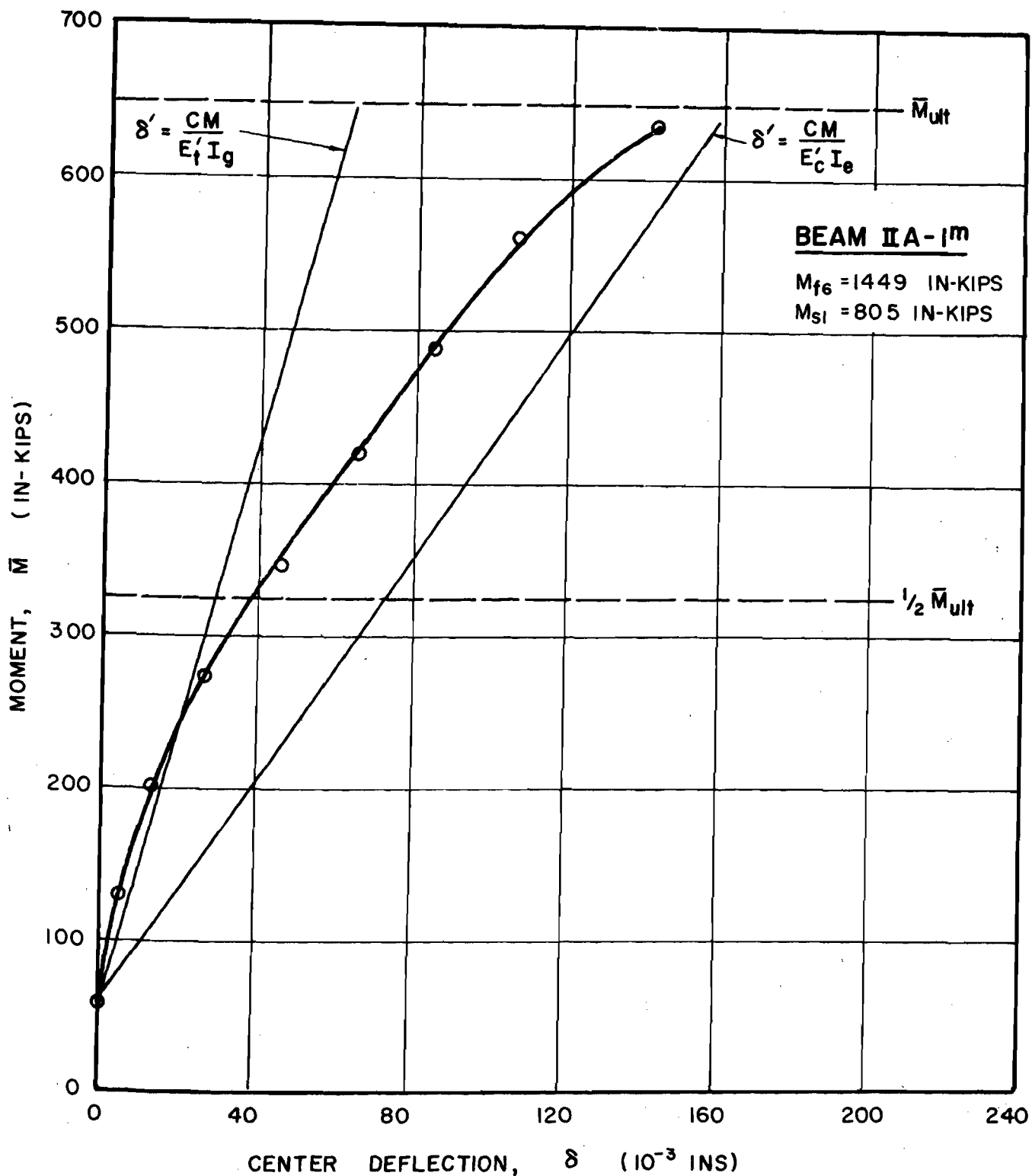


FIG. 12b TYPICAL MOMENT-DEFLECTION CURVE FOR BEAMS WITHOUT WEB REINFORCING WHICH FAILED IN SHEAR

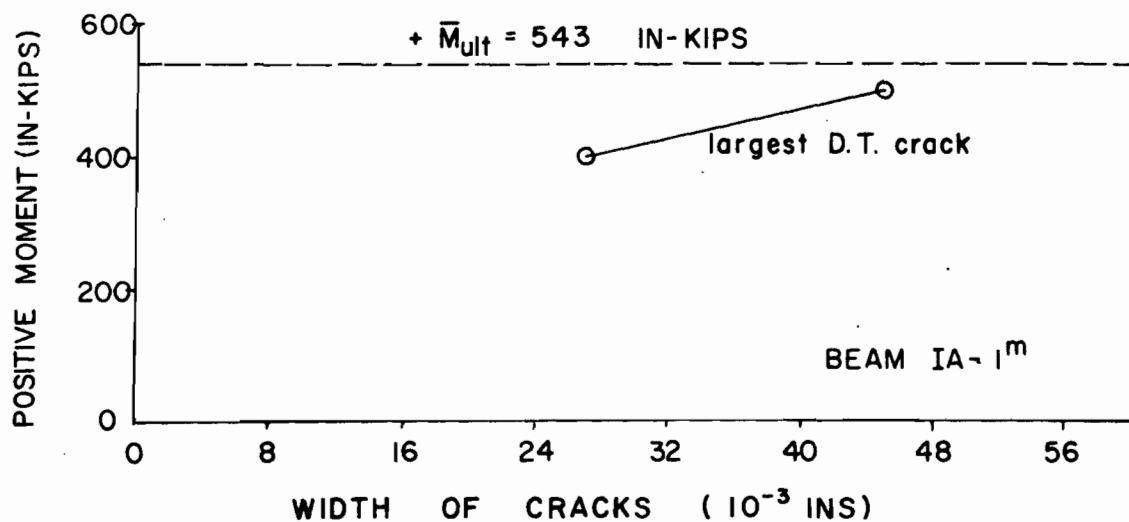
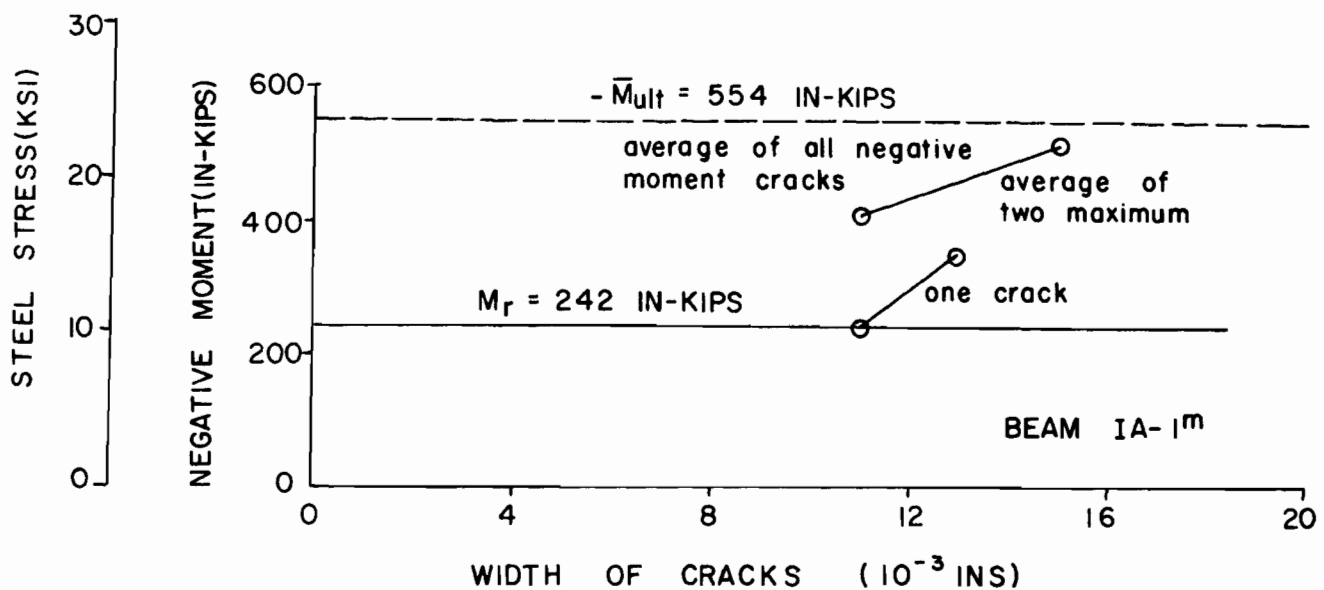
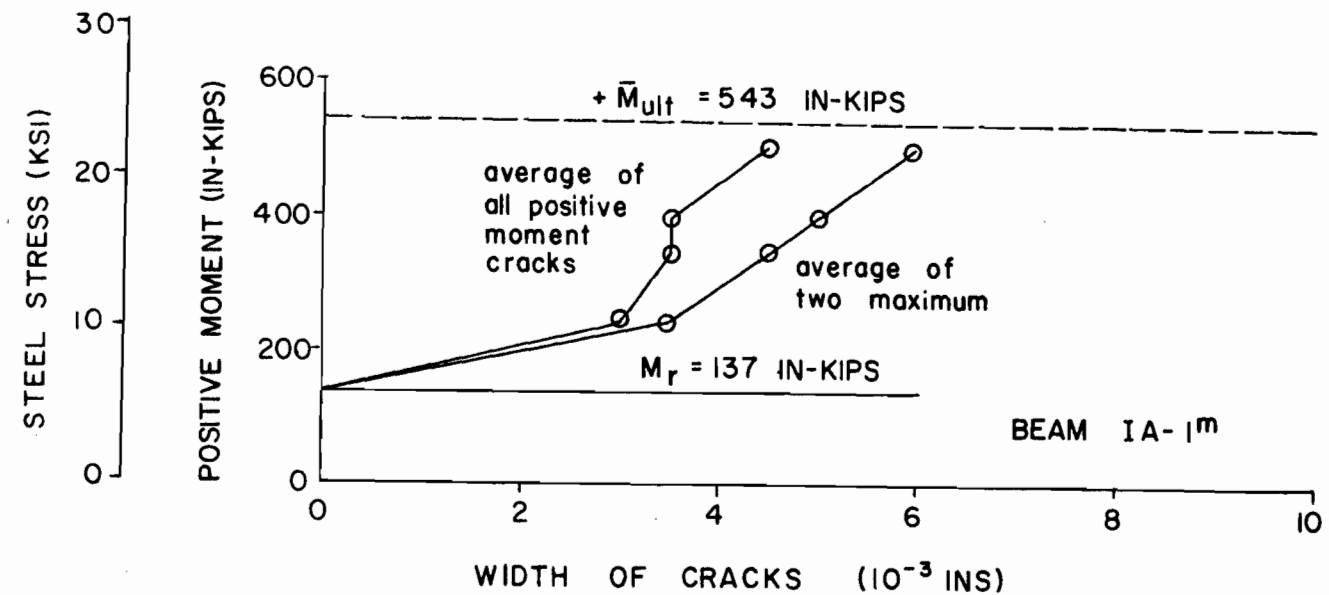


FIG. 13a TYPICAL CURVES FOR STEEL STRESS AND MOMENT
VERSUS CRACK WIDTHS FOR BEAMS WITHOUT
WEB REINFORCING

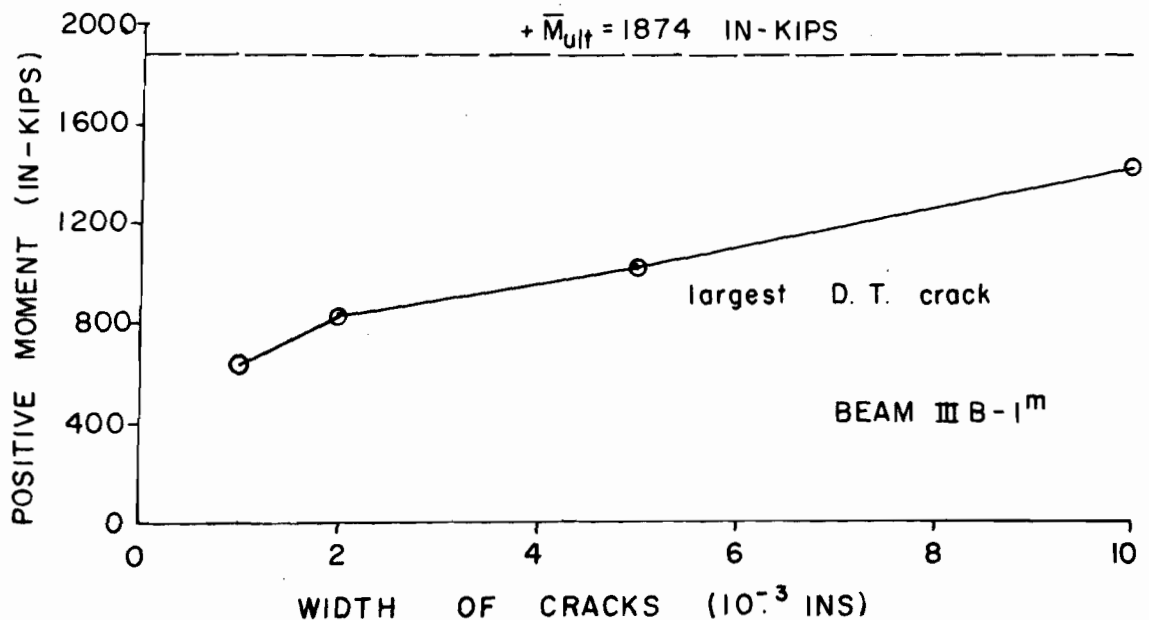
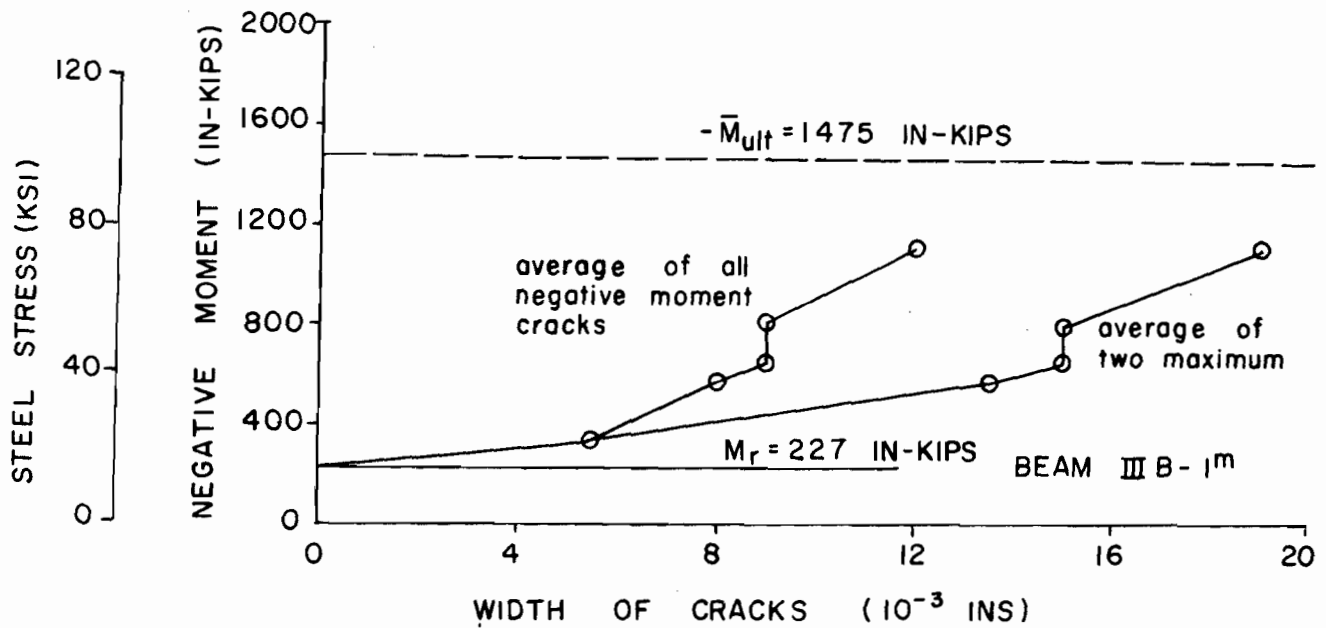
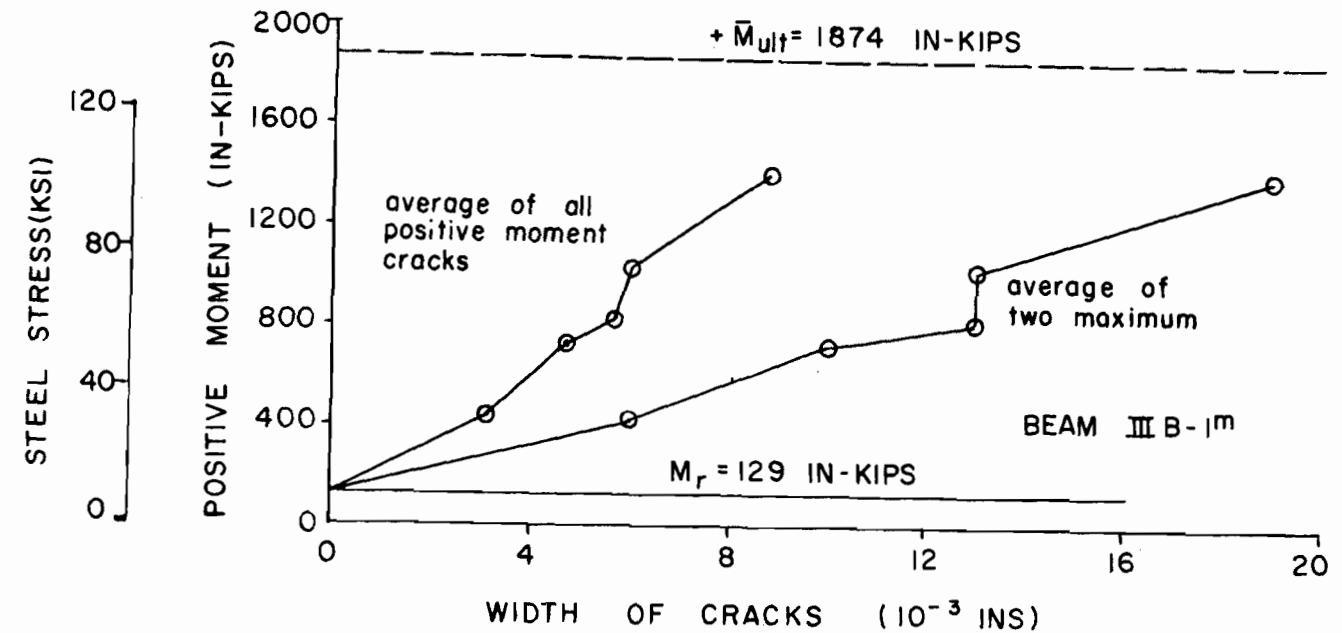


FIG.13b TYPICAL CURVES FOR STEEL STRESS AND MOMENT VERSUS CRACK WIDTHS FOR BEAMS WITH WEB REINFORCING

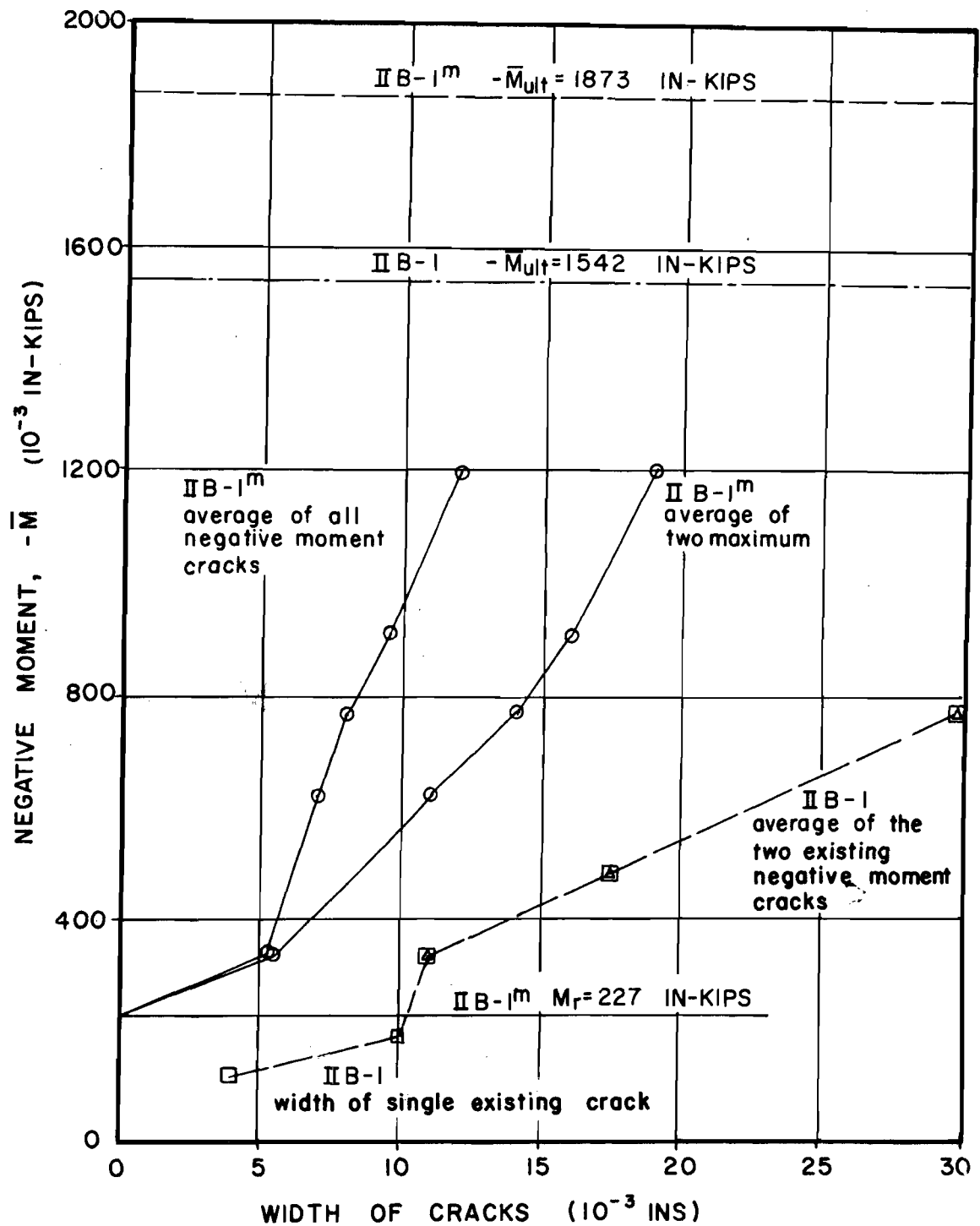


FIG.14a COMPARISON OF MOMENT VERSUS CRACK WIDTH
CURVES FOR BEAM IIB-I WITH "BUNCHED" AND
BEAM IIB-I^m WITH "DISTRIBUTED" NEGATIVE TEN-
SION REINFORCING

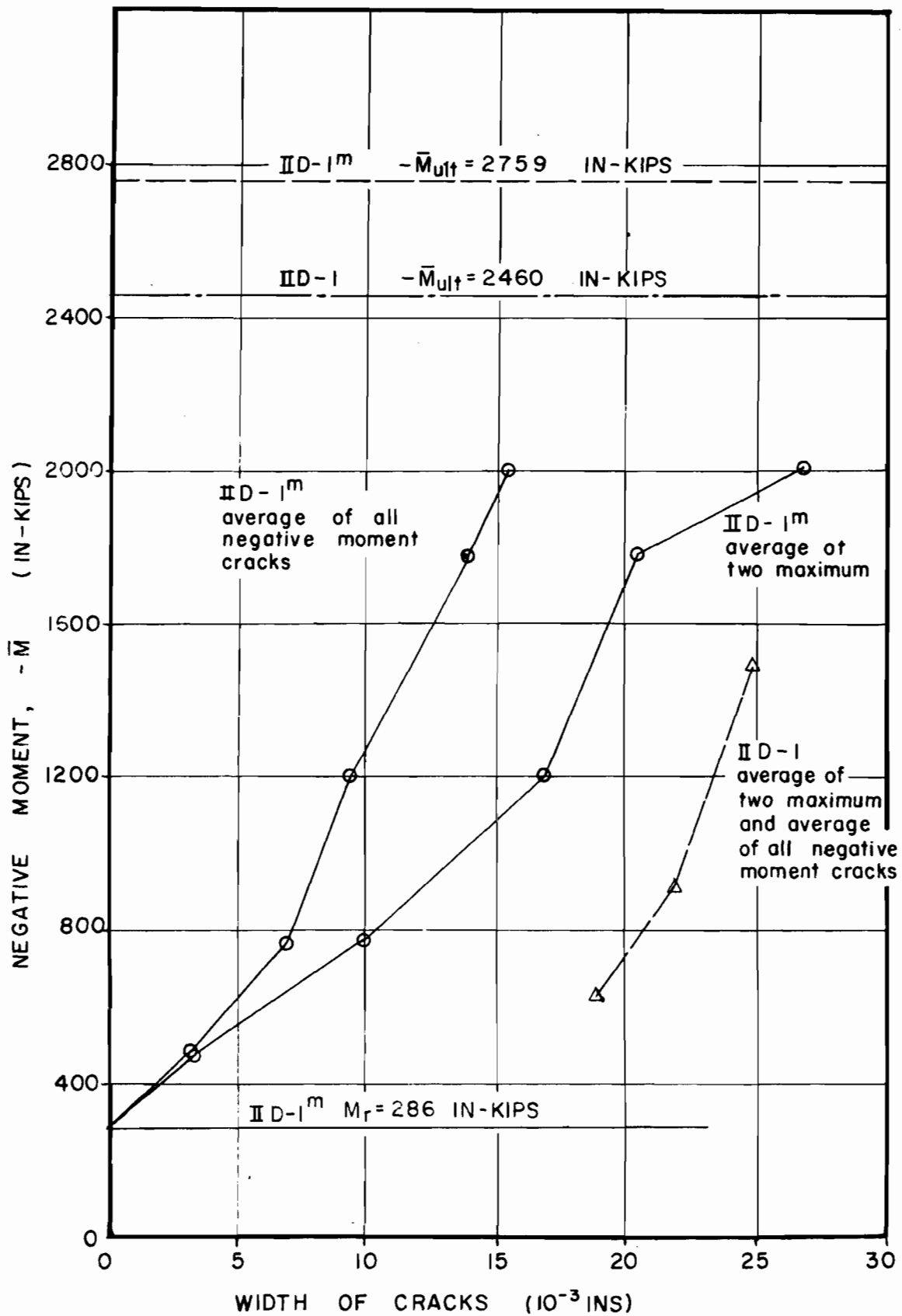


FIG.14b COMPARISON OF MOMENT VERSUS CRACK WIDTH
CURVES FOR BEAM II D-I WITH "BUNCHED" AND
BEAM II D-I^m WITH "DISTRIBUTED" NEGATIVE
TENSION REINFORCING

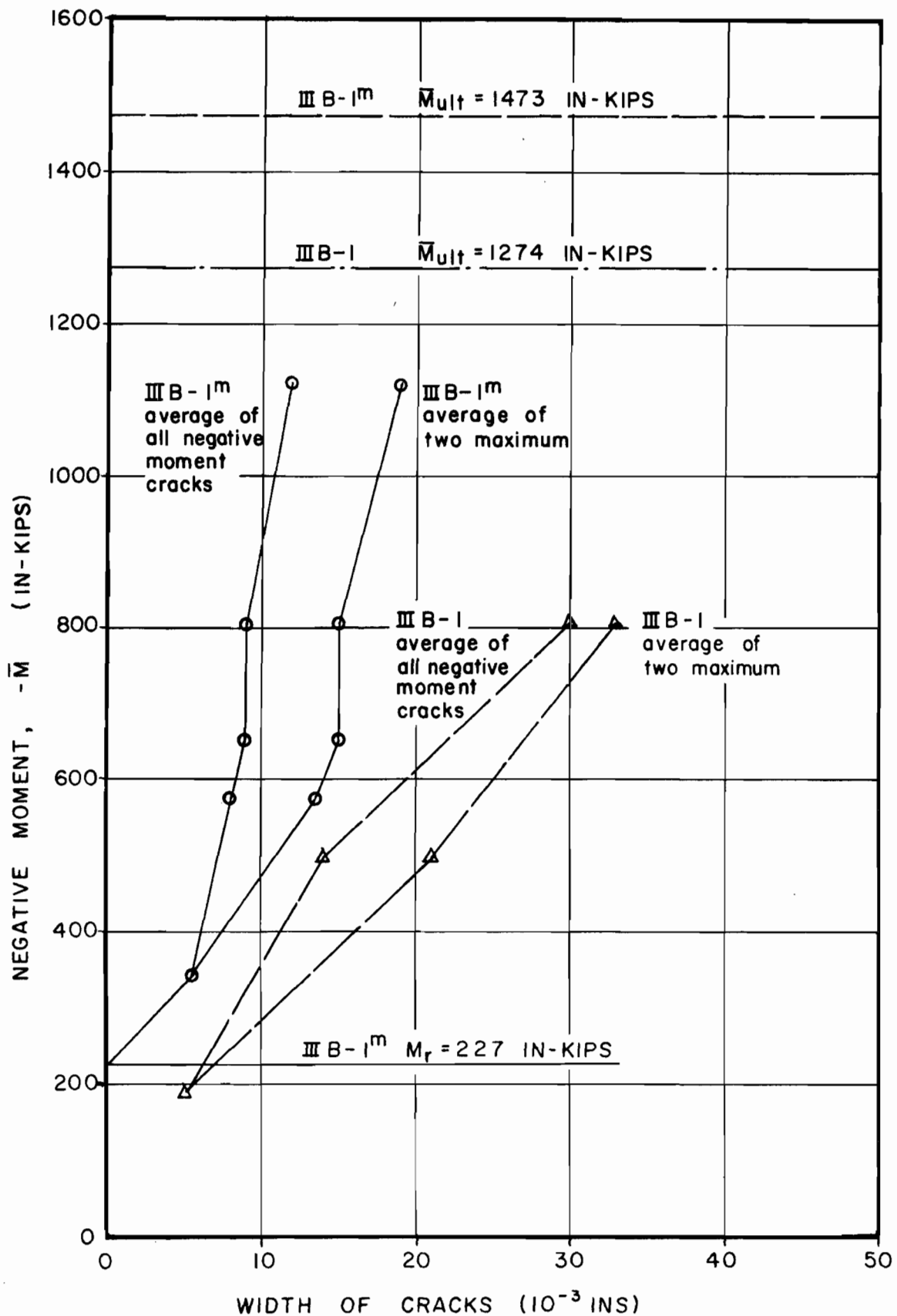


FIG.14c COMPARISON OF MOMENT VERSUS CRACK WIDTH CURVES FOR BEAM IIIB-I WITH "BUNCHED" AND BEAM IIIB-I^m WITH "DISTRIBUTED" NEGATIVE TENSION REINFORCING

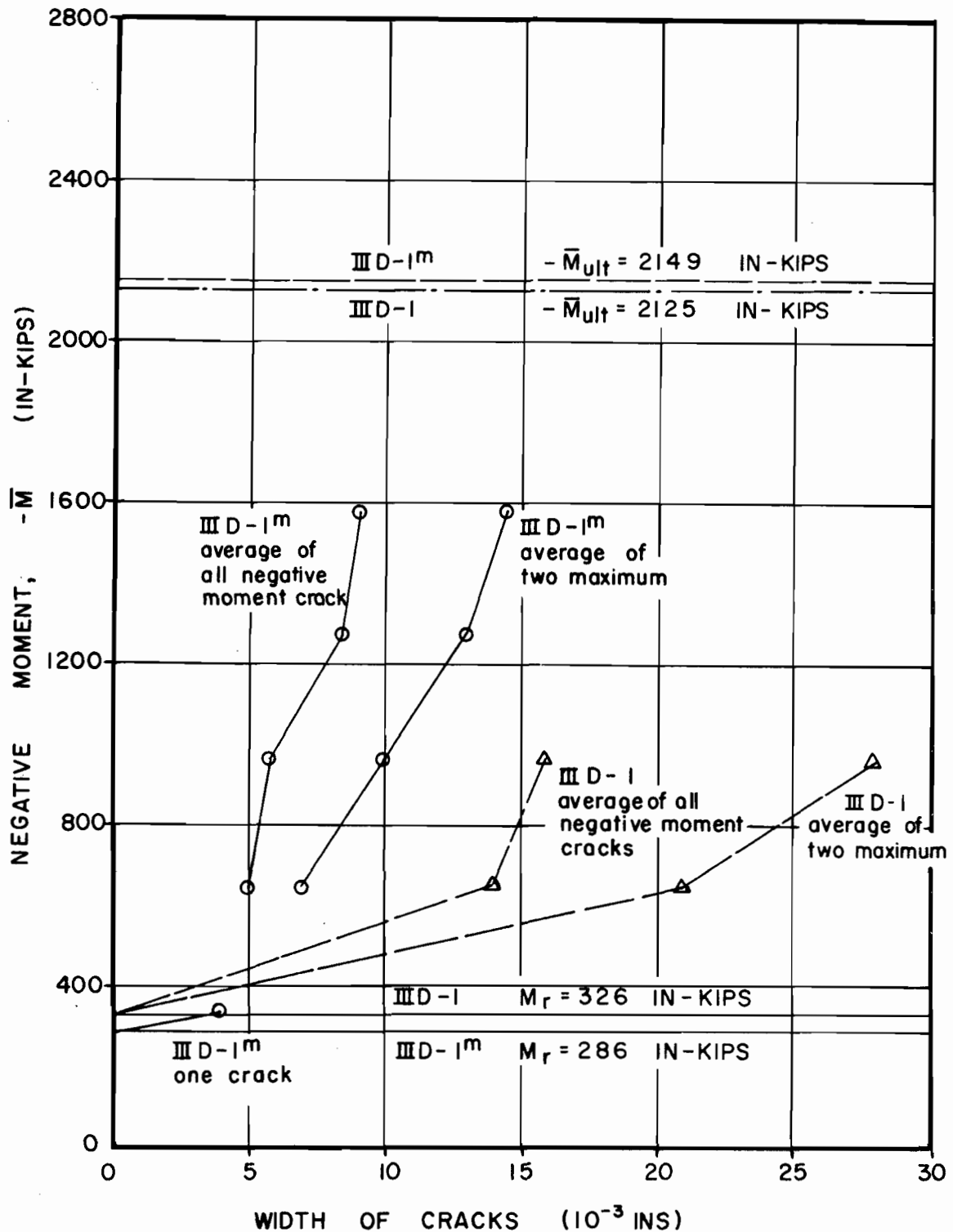


FIG.14 d COMPARISON OF MOMENT VERSUS CRACK WIDTH CURVES FOR BEAM III D-I WITH "BUNCHED" AND BEAM III D-I^m WITH "DISTRIBUTED" NEGATIVE TENSION REINFORCING

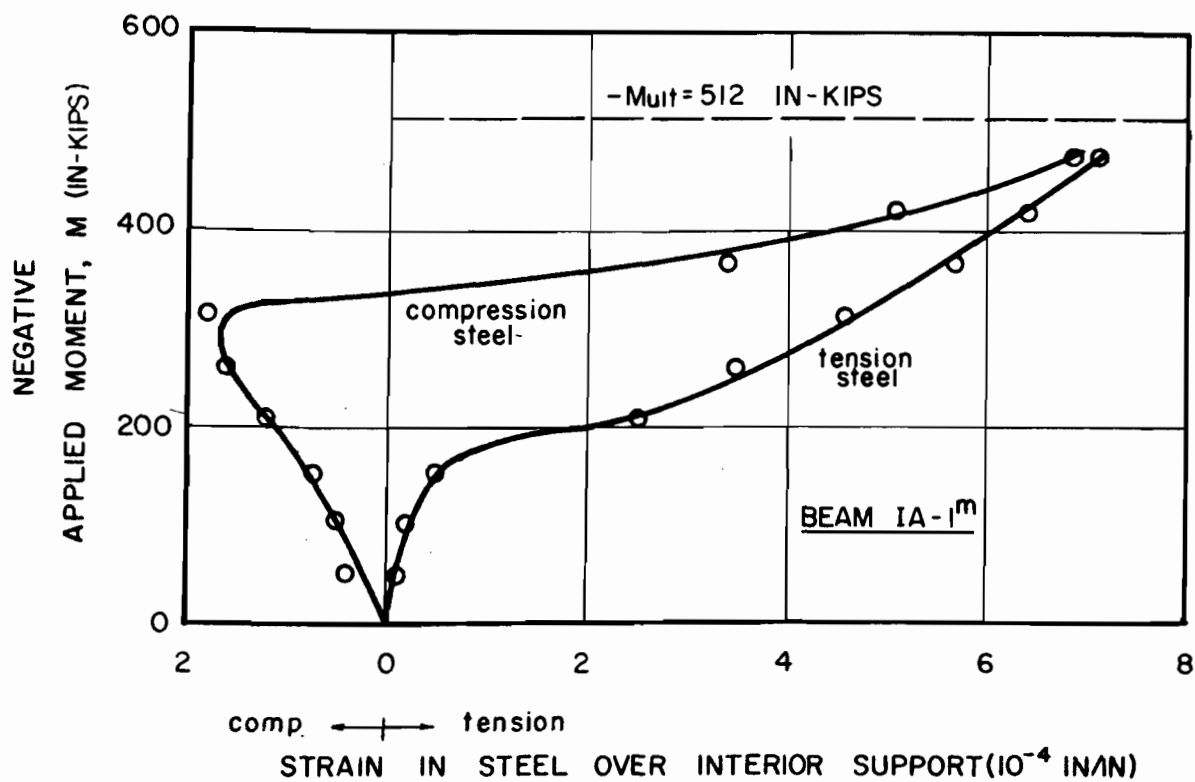
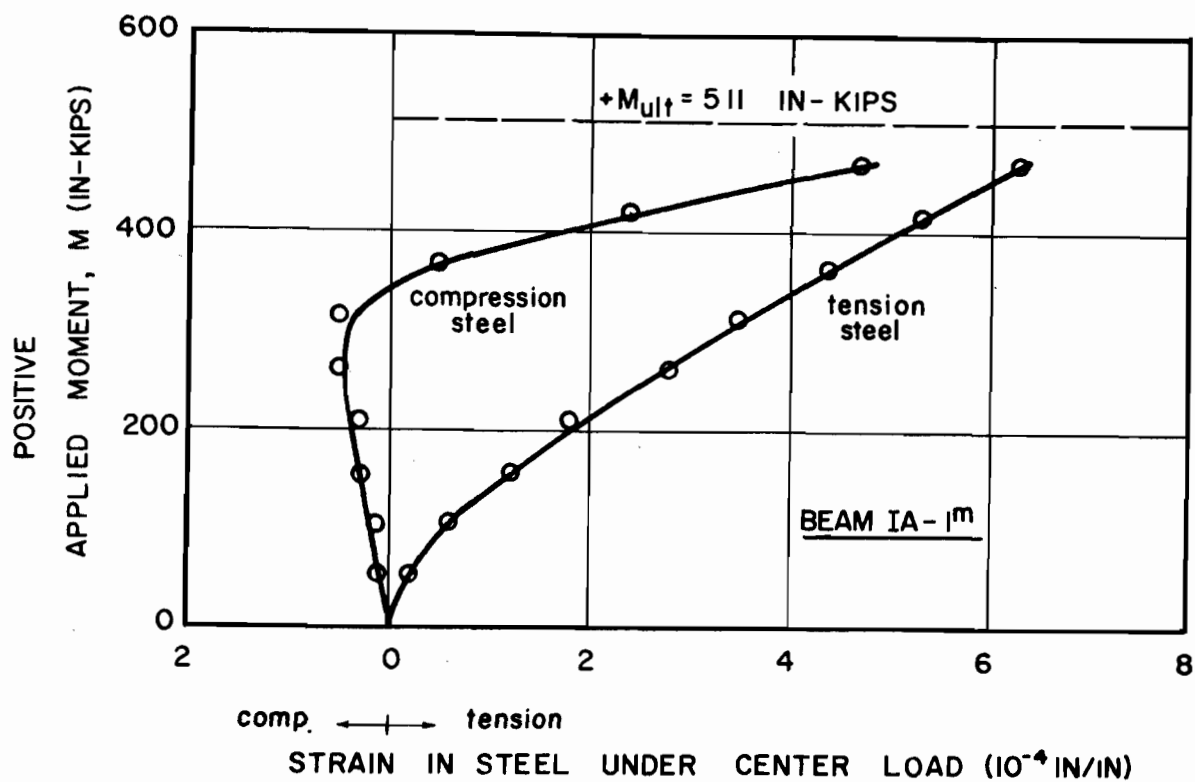


FIG. 15a TYPICAL APPLIED MOMENT-LONGITUDINAL STEEL STRAIN CURVES FOR BEAMS WITHOUT WEB REINFORCING WHICH FAILED IN DIAGONAL TENSION

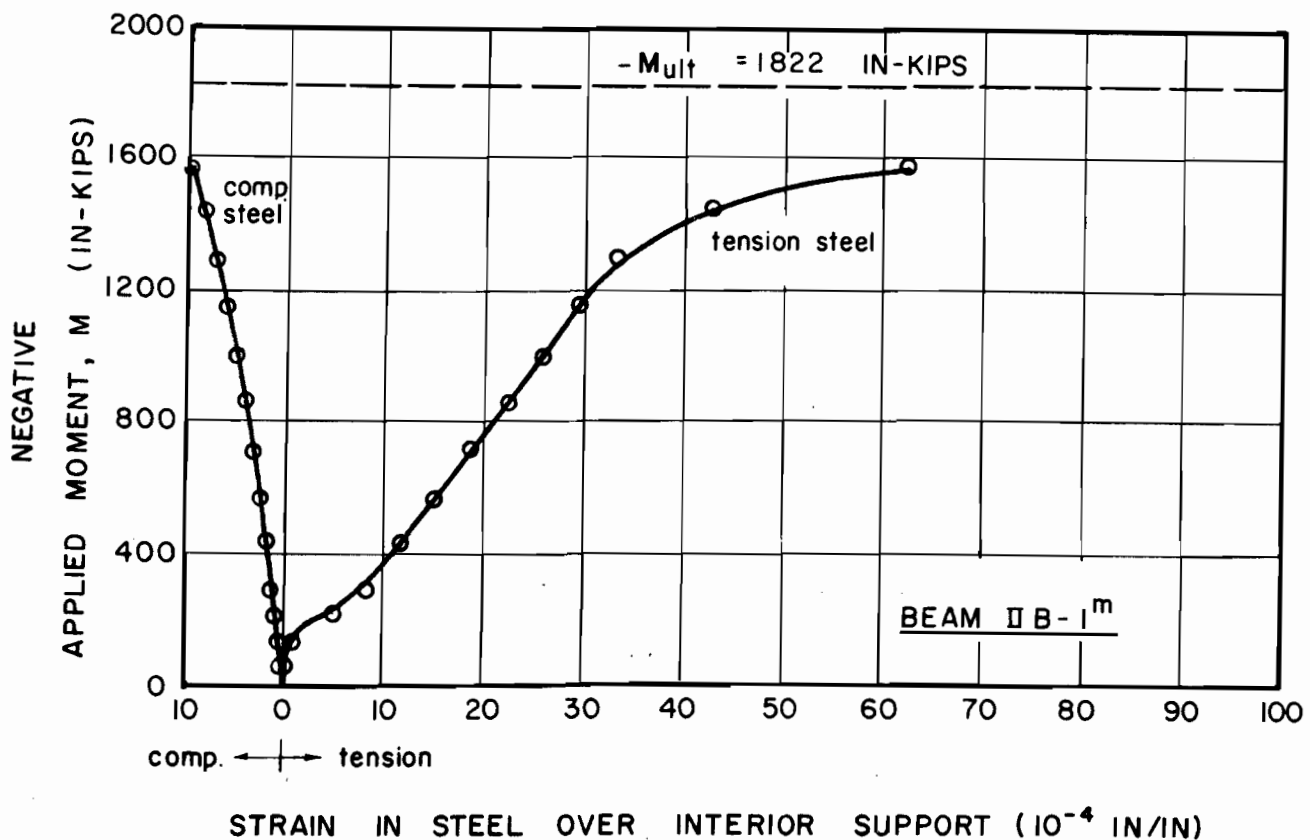
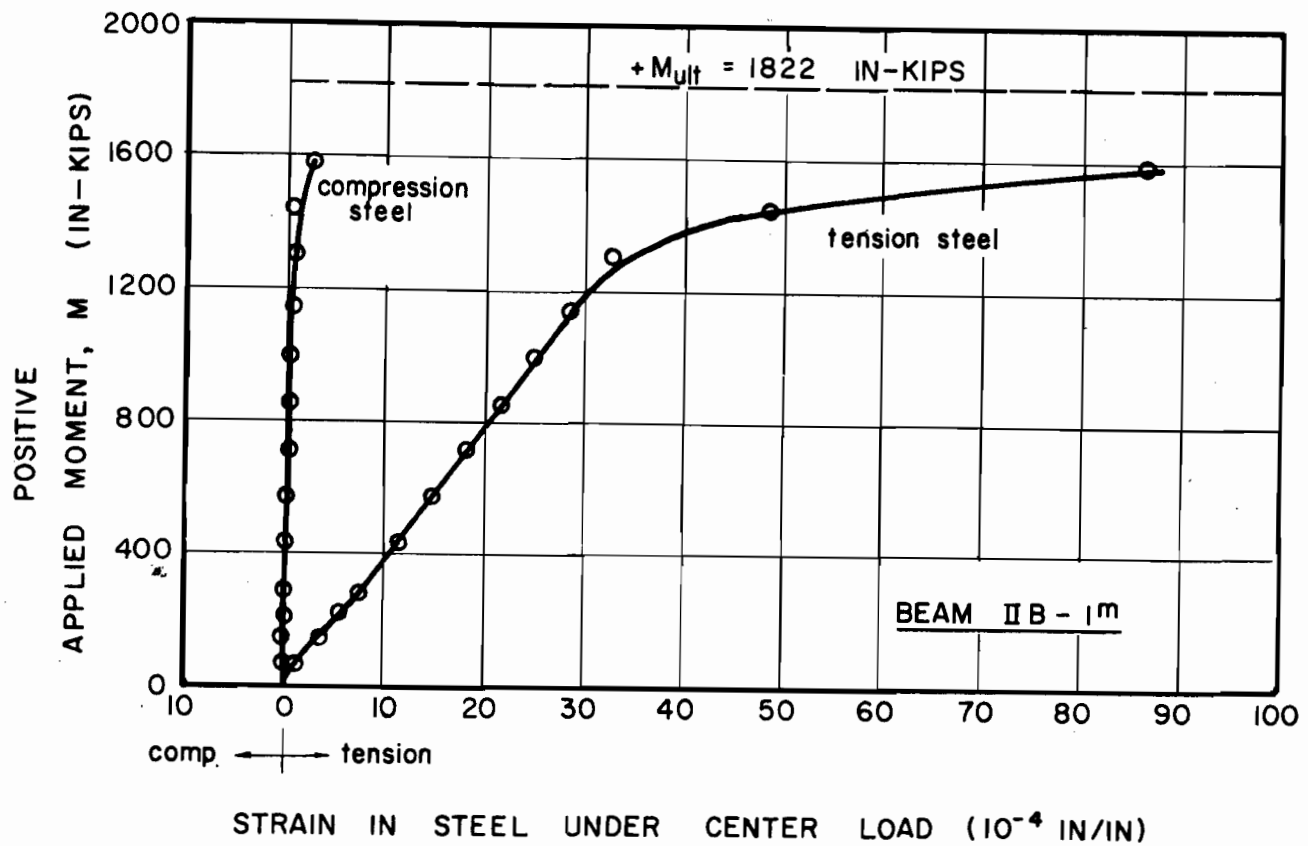


FIG. 15b TYPICAL APPLIED MOMENT-LONGITUDINAL STEEL STRAIN CURVES FOR BEAMS WITH WEB REINFORCING WHICH FAILED IN FLEXURE

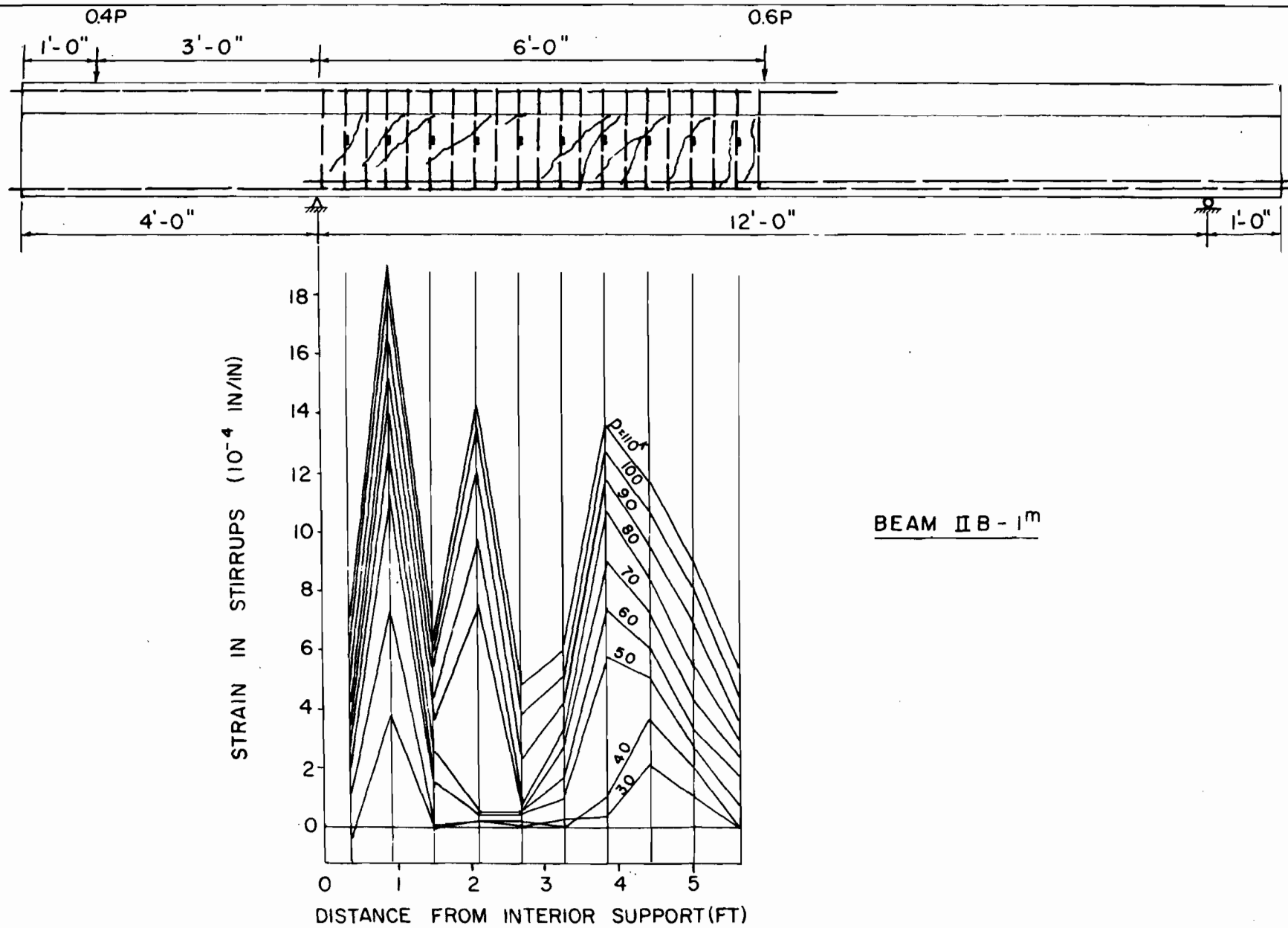


FIG. 16a STIRRUP STRAIN DISTRIBUTION AT EACH STAGE OF APPLIED LOAD

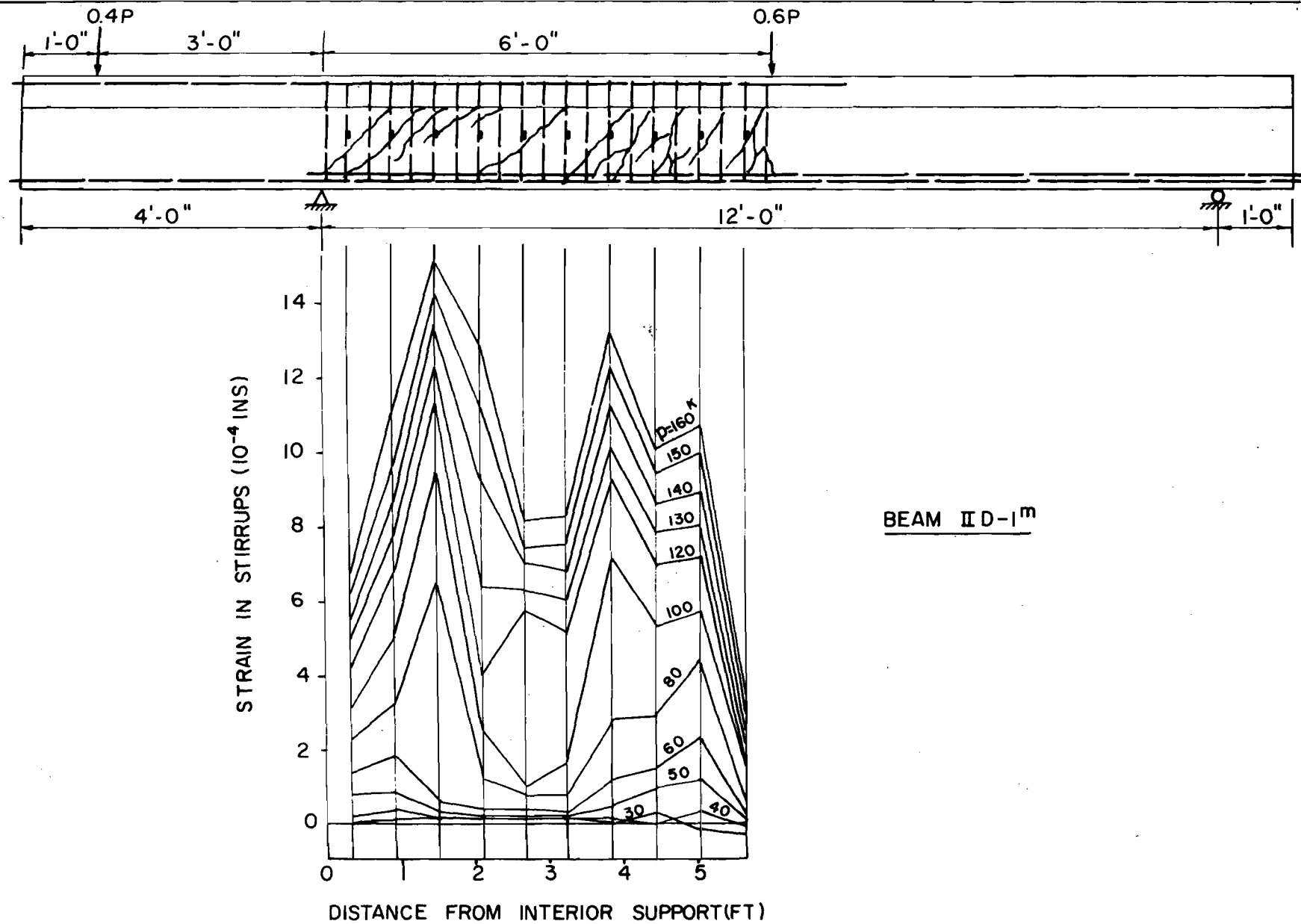
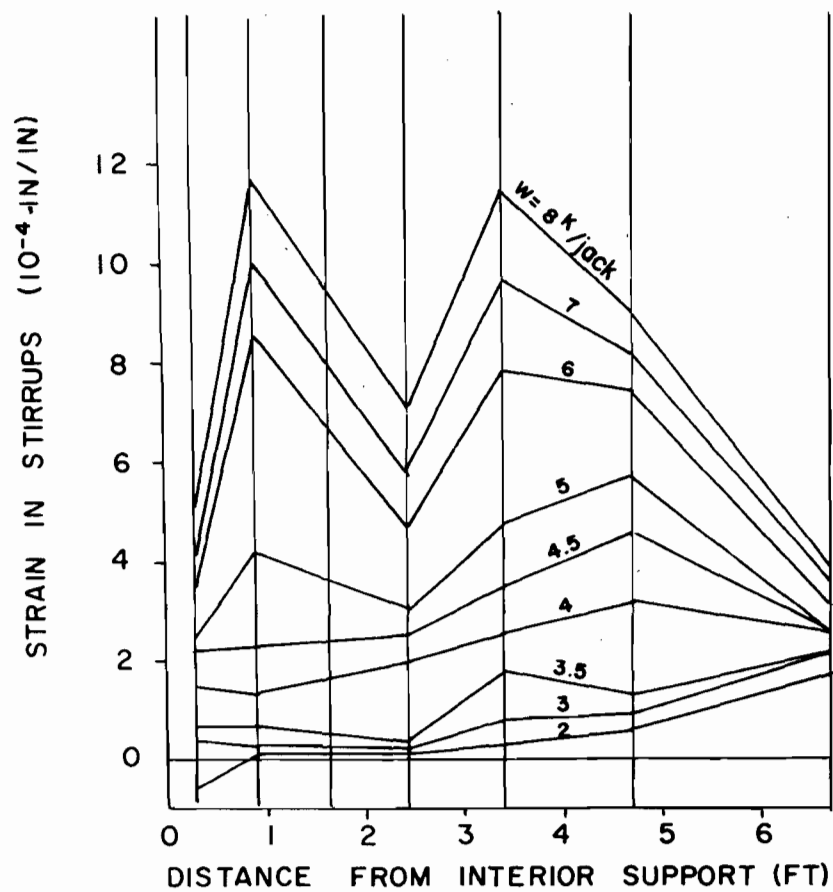
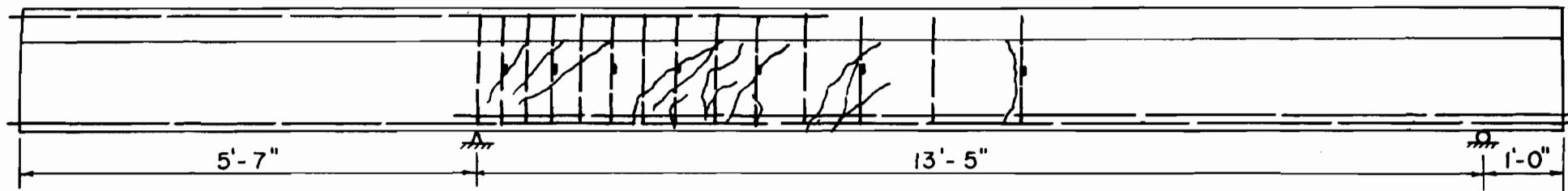
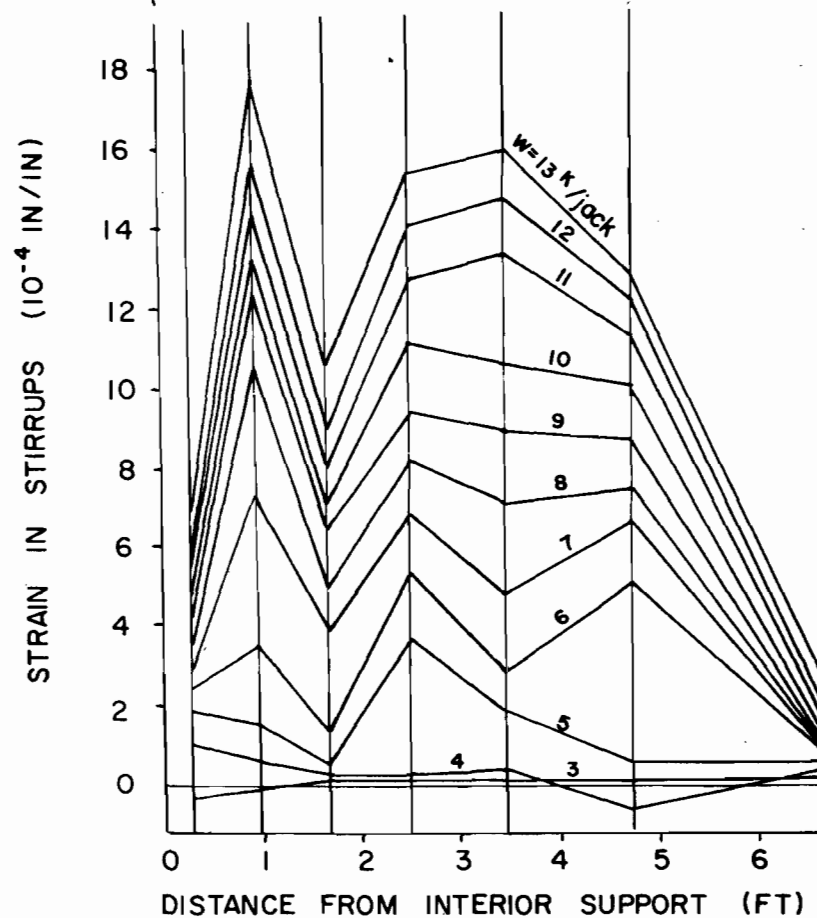
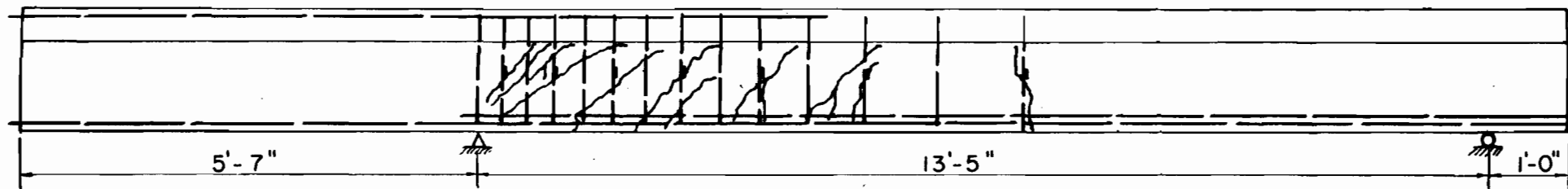


FIG. 16b STIRRUP STRAIN DISTRIBUTION AT EACH STAGE OF APPLIED LOAD



BEAM III B-1^m

FIG. 16c STIRRUP STRAIN DISTRIBUTION AT EACH STAGE OF APPLIED LOAD



BEAM IID-1^m

FIG. 16d STIRRUP STRAIN DISTRIBUTION AT EACH STAGE OF APPLIED LOAD

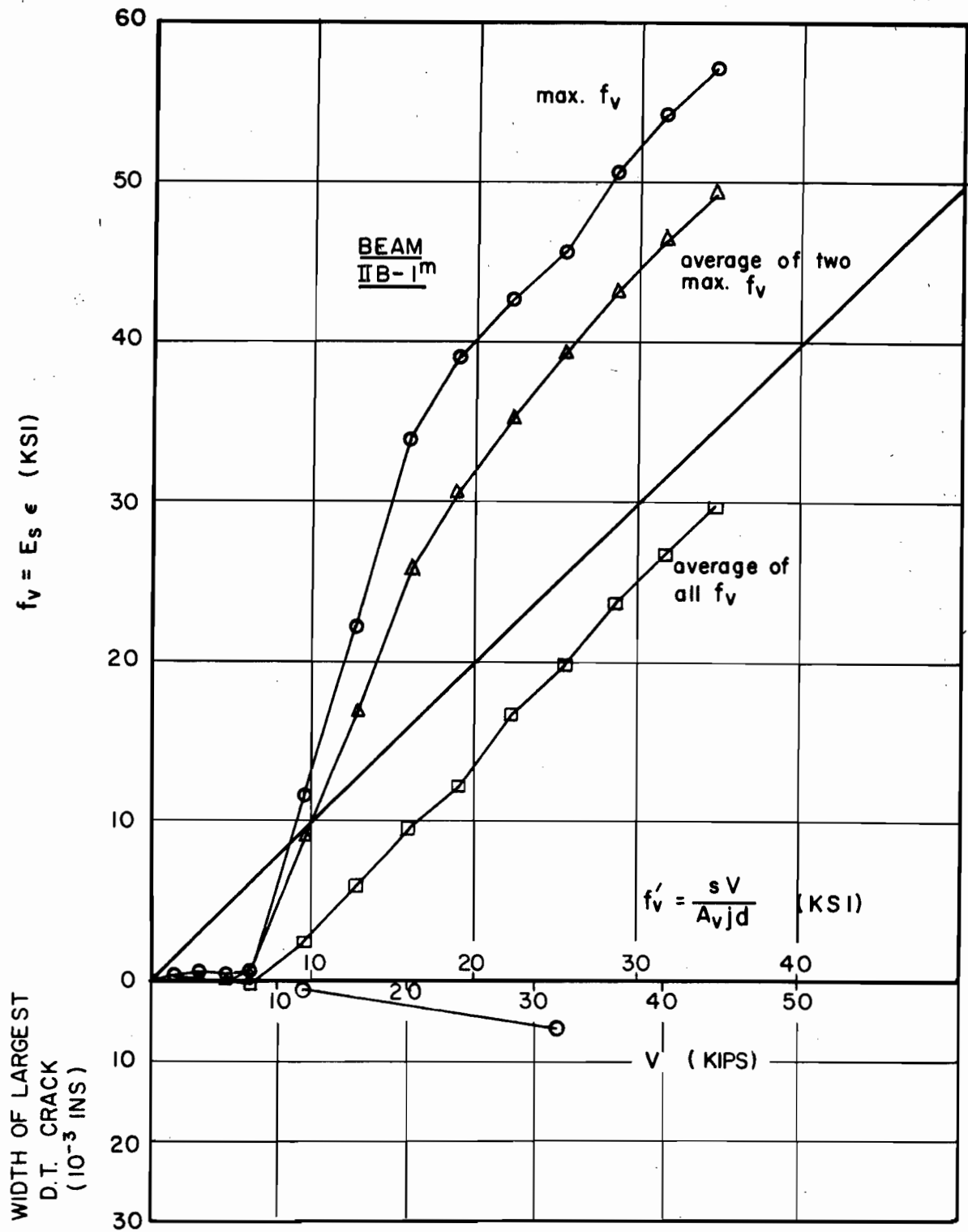


FIG. 17a MEASURED STIRRUP STRESS VERSUS COM-
PUTED STIRRUP STRESS CURVES

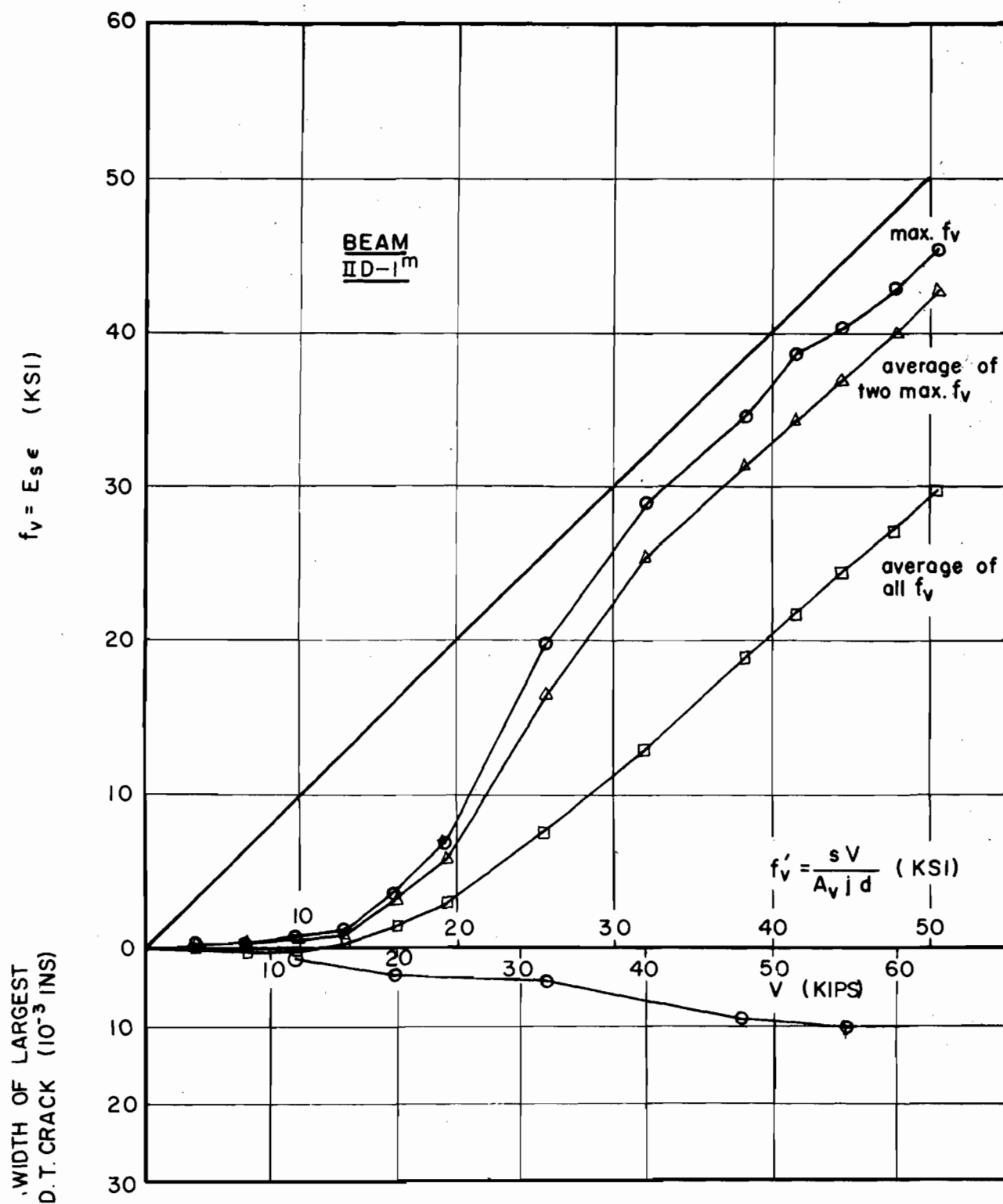
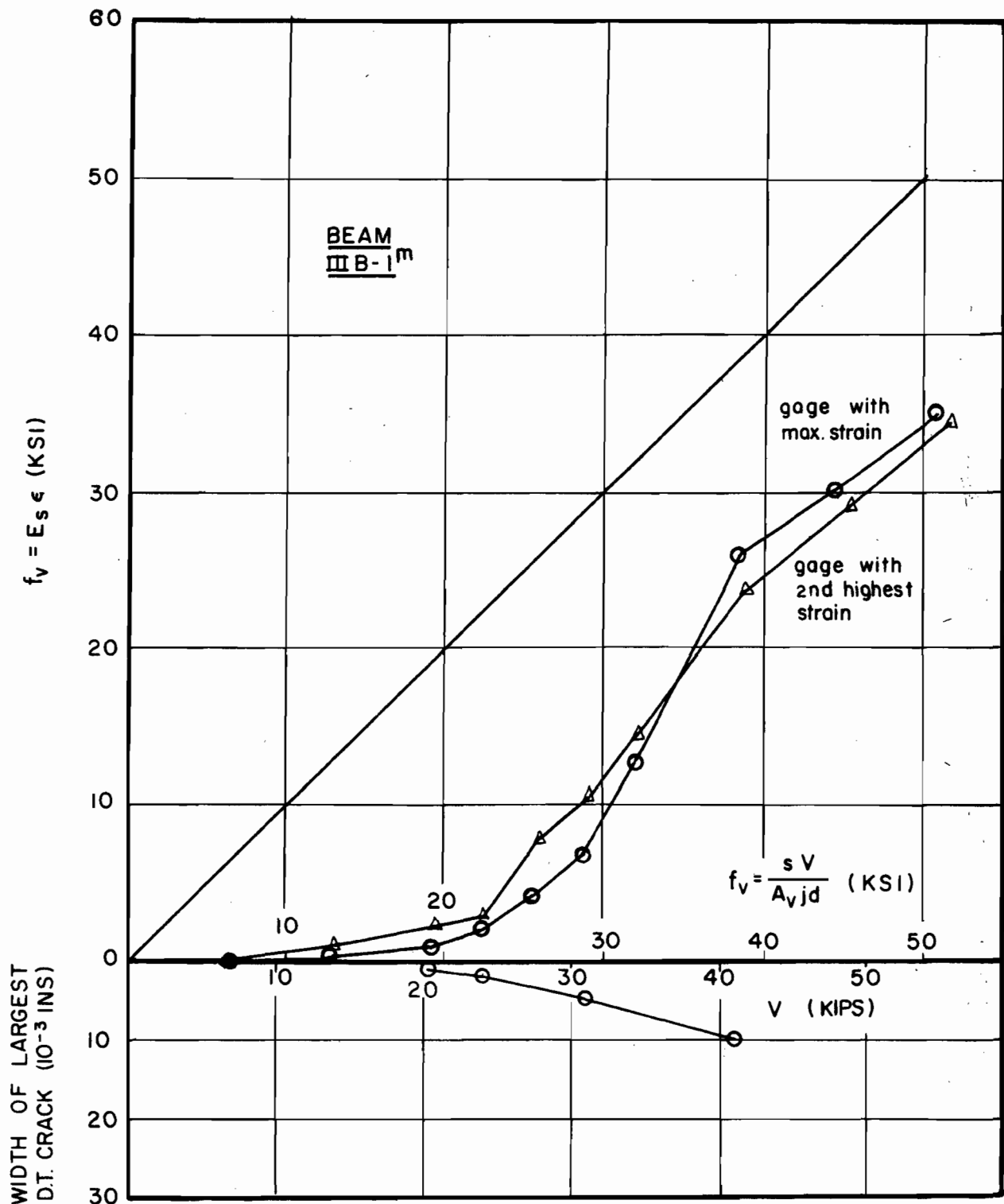
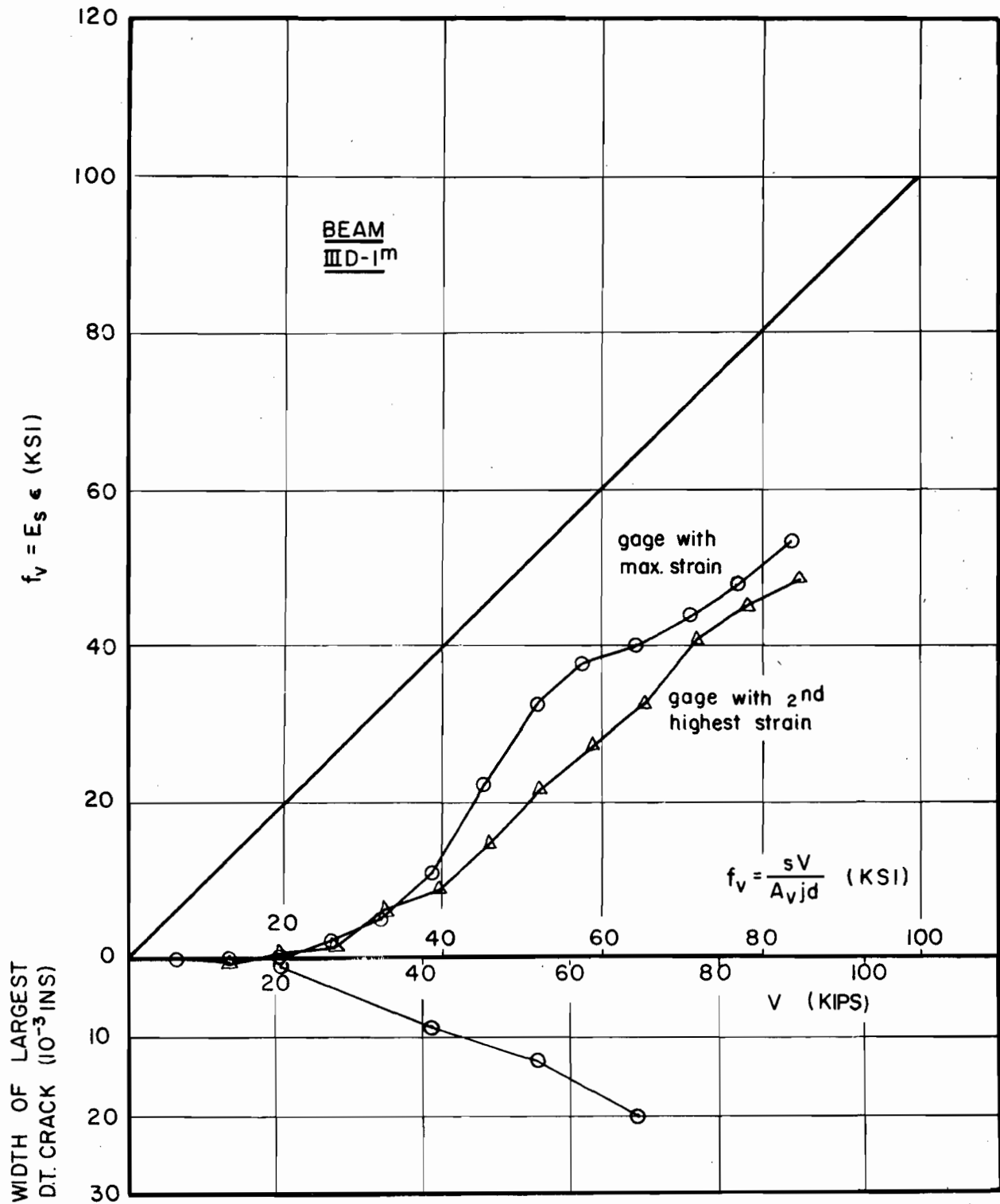


FIG.17b MEASURED STIRRUP STRESS VERSUS COMPUTED
STIRRUP STRESS CURVES



NOTE: HORIZONTAL SCALE FOR SHEAR, V, RELATES ONLY TO STIRRUP HAVING MAXIMUM STRAIN

FIG.17c MEASURED STIRRUP STRESS VERSUS COMPUTED STIRRUP STRESS CURVES



NOTE: HORIZONTAL SCALE FOR SHEAR, V, RELATES ONLY TO STIRRUP HAVING MAXIMUM STRAIN

FIG.17d MEASURED STIRRUP STRESS VERSUS COMPUTED STIRRUP STRESS CURVES

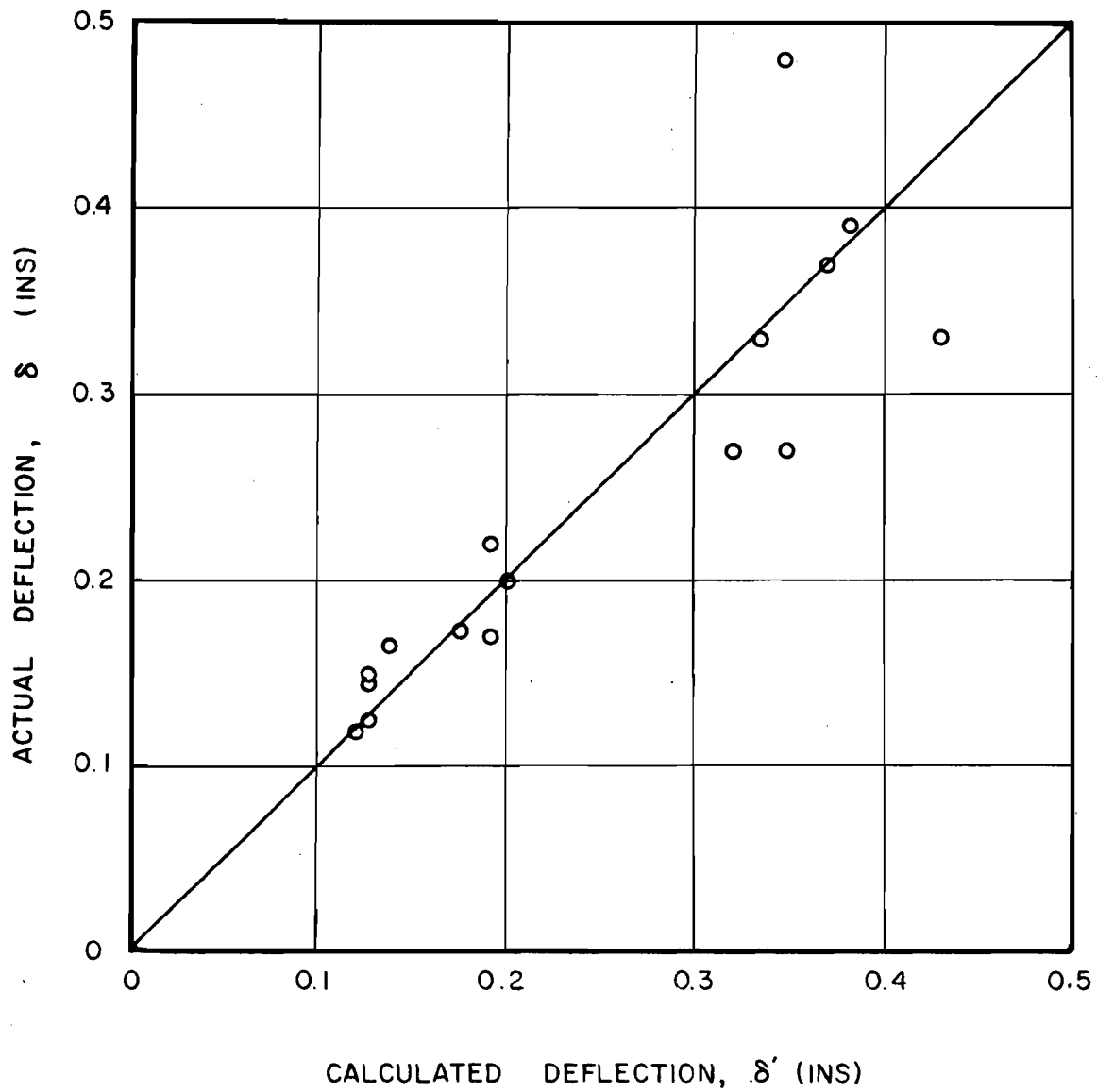


FIG.18 COMPARISON OF ACTUAL DEFLECTION WITH
CALCULATED VALUES FOR ALL BEAMS FAIL-
ING IN FLEXURE

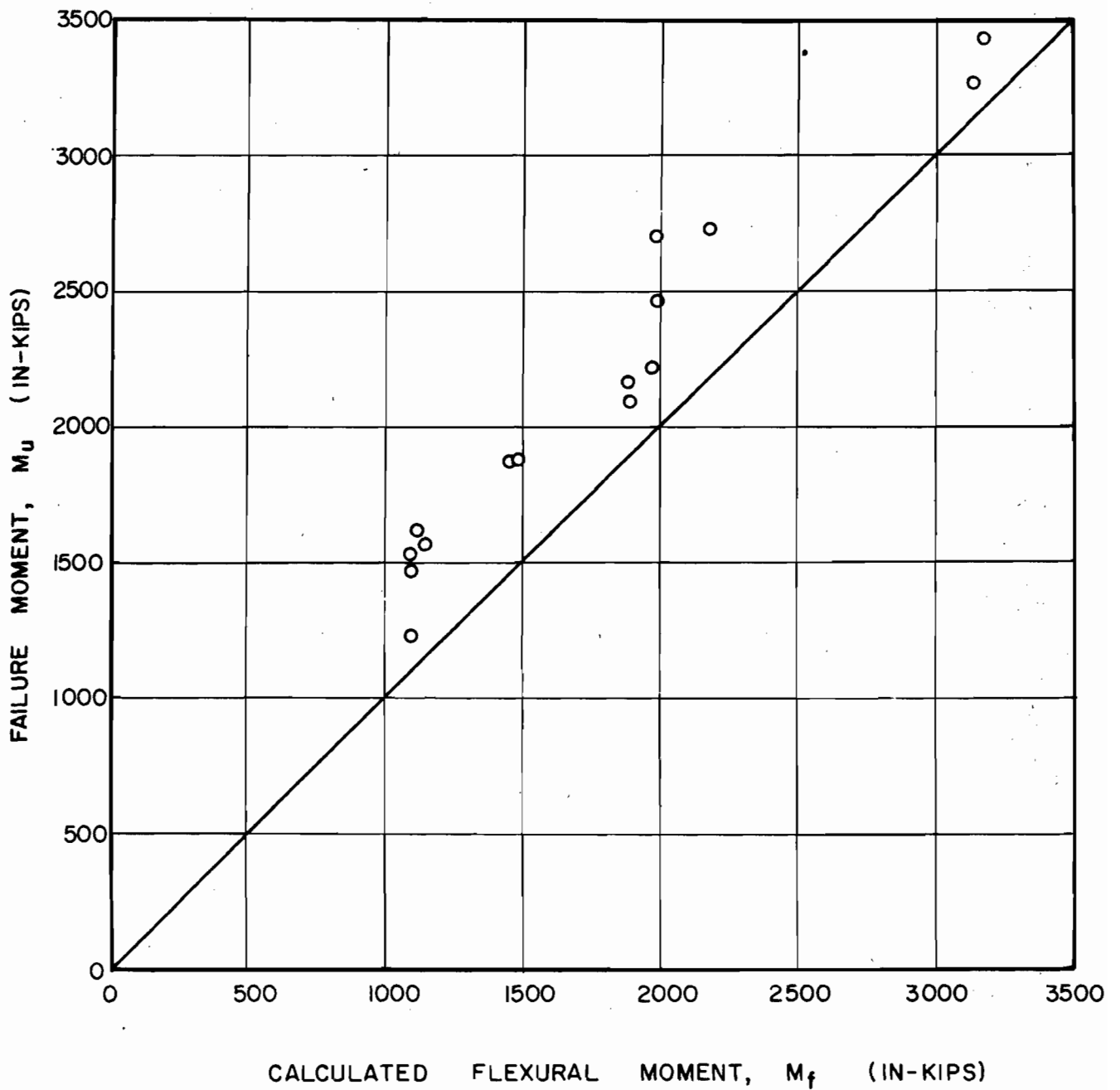


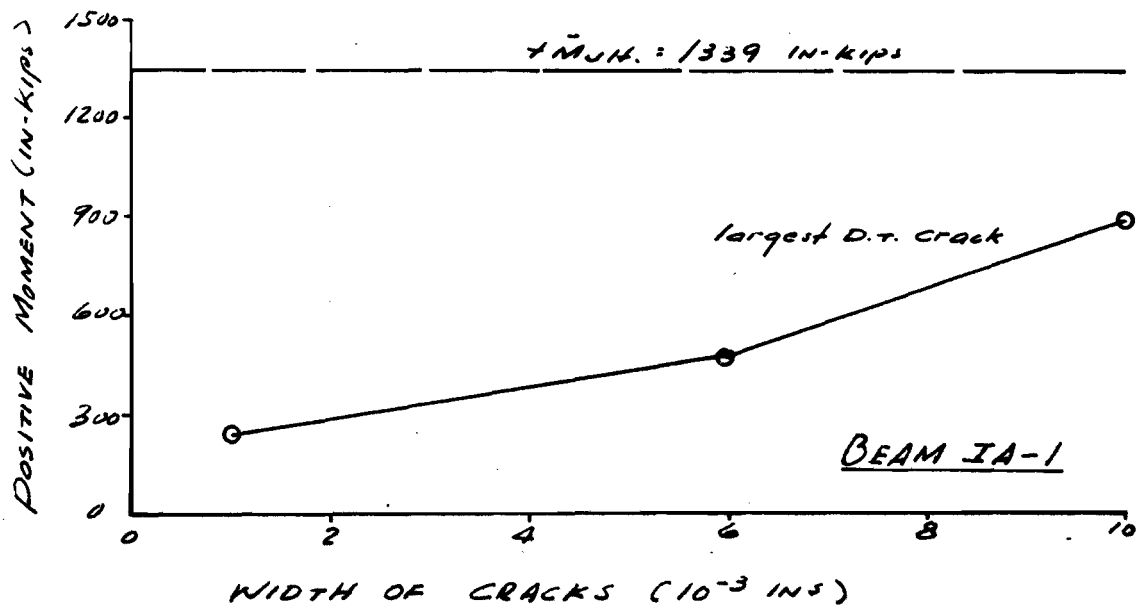
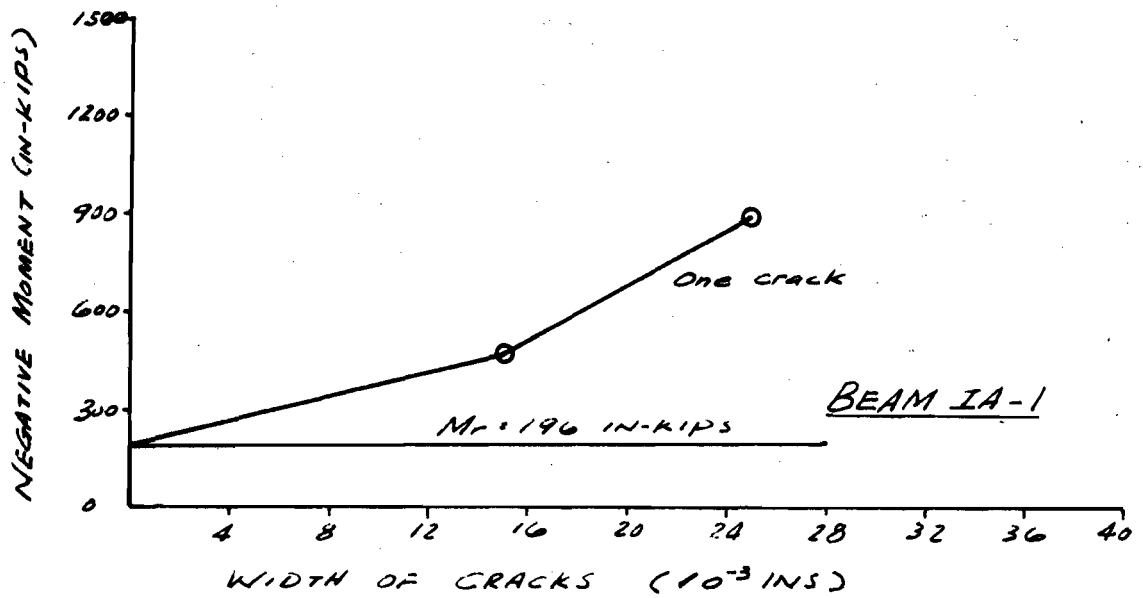
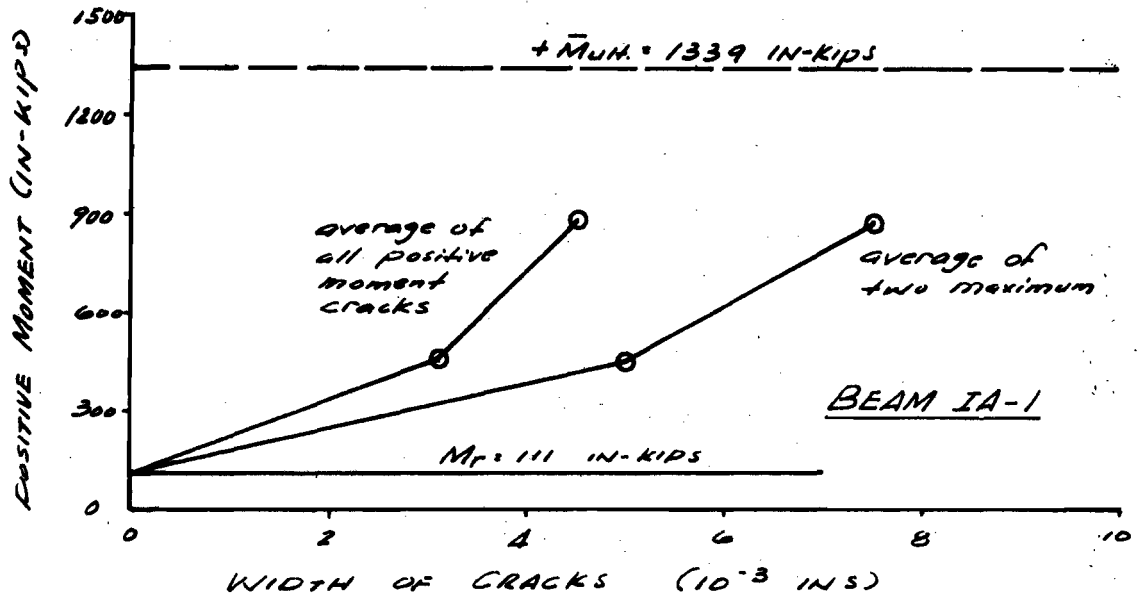
FIG. 19 COMPARISON OF FAILURE MOMENT WITH CALCULATED
ULTIMATE FLEXURAL MOMENT

A P P E N D I X
C R A C K W I D T H D A T A

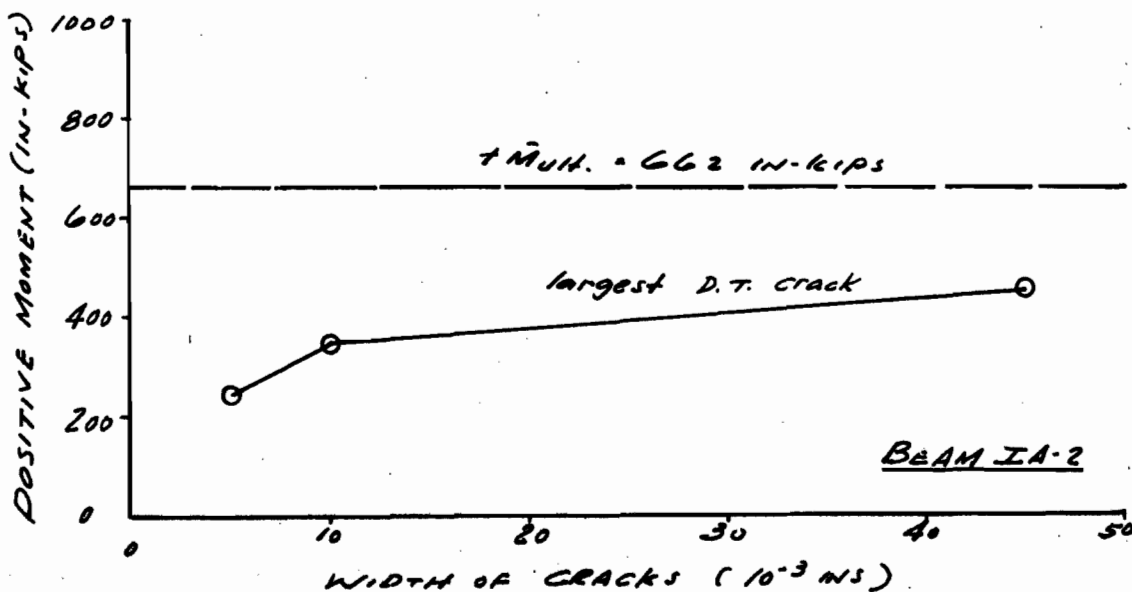
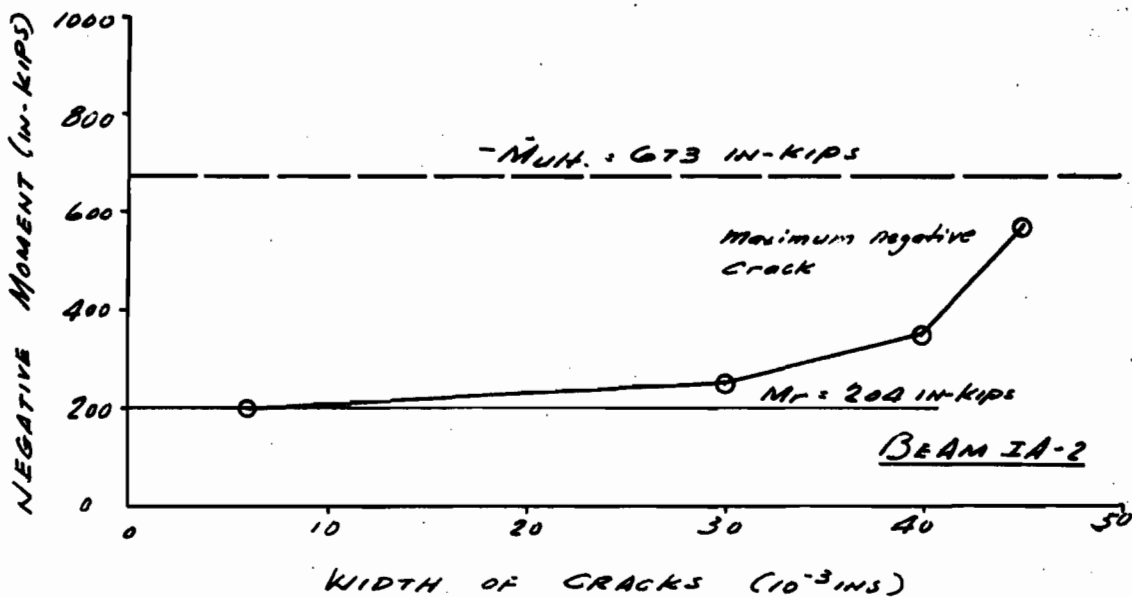
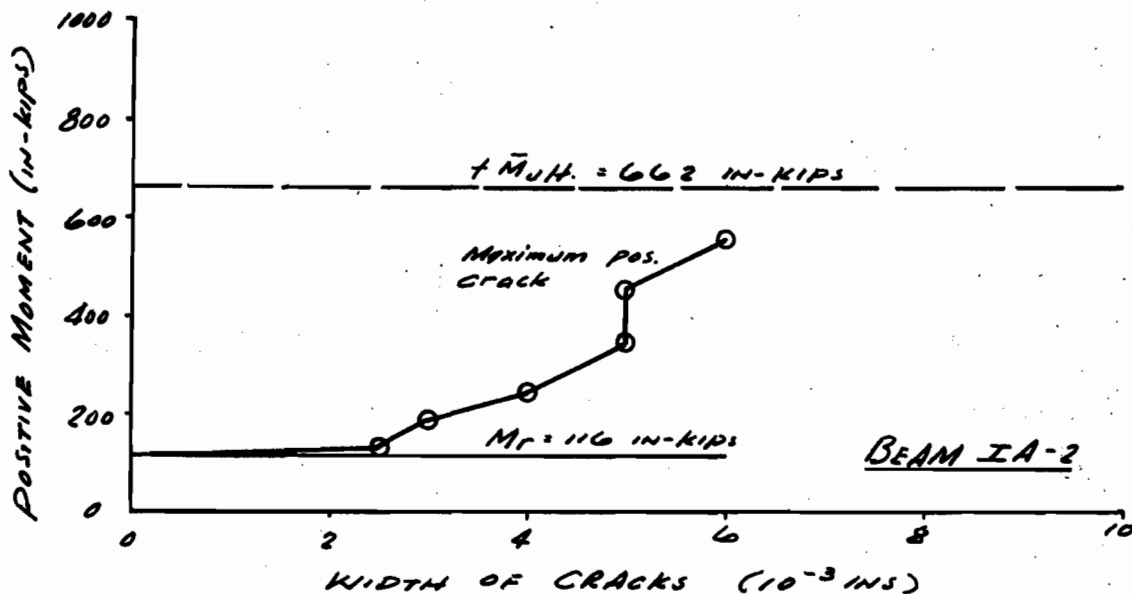
The figures which follow contain detailed information on crack development for all beams of both parts of this investigation, except for the eight "re-test" beams IA-1R to ID-2^R. The limited cracking which had occurred in these specimens when first tested as restrained beams distorted the crack pattern obtained later when they were re-tested as simple beams, resulting in atypical crack performance.

For each beam there is plotted, against bending moment, (a) for positive moment cracks, the average width of all cracks and the average width of the two widest cracks; (b) for negative moment cracks, the average width of all cracks and the average width of the two widest cracks, (where only one or two negative cracks formed, this is so noted); (c) for diagonal tension cracks, the width of the widest crack.

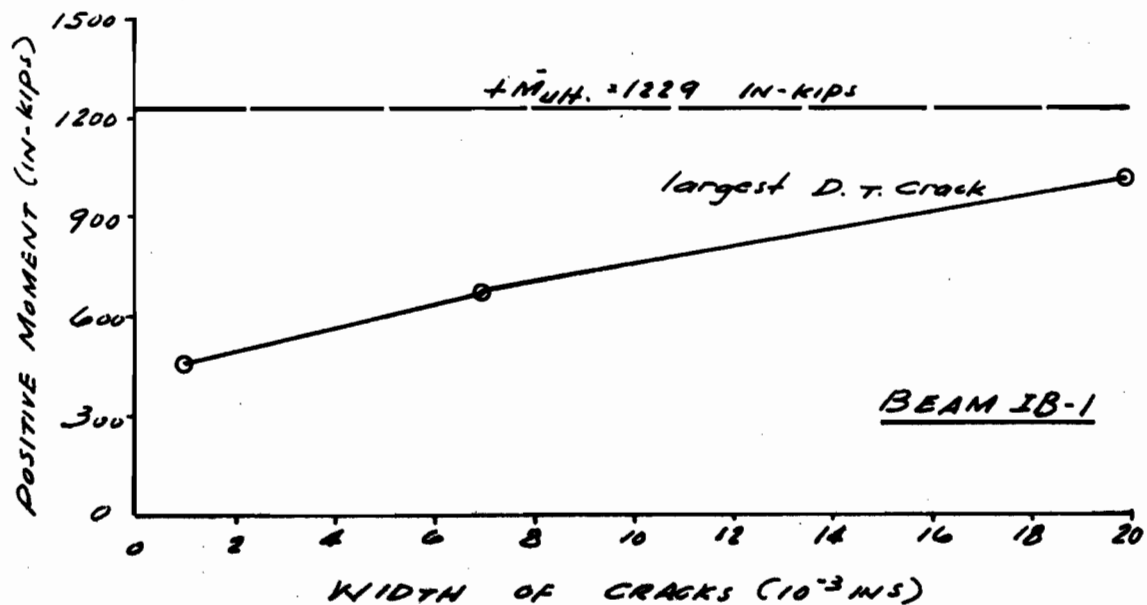
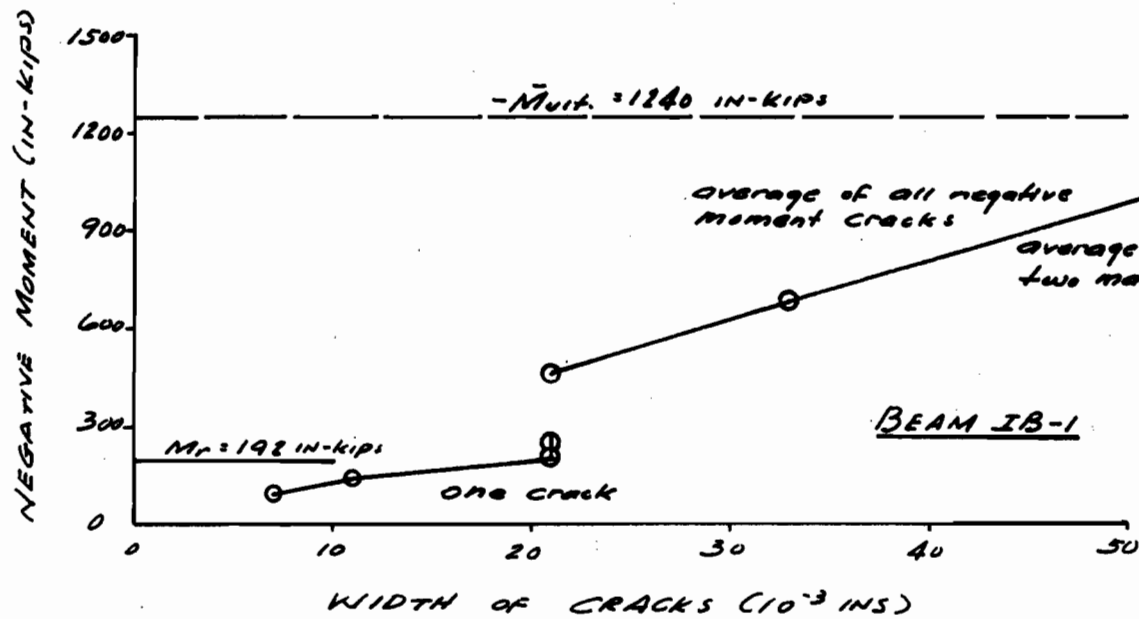
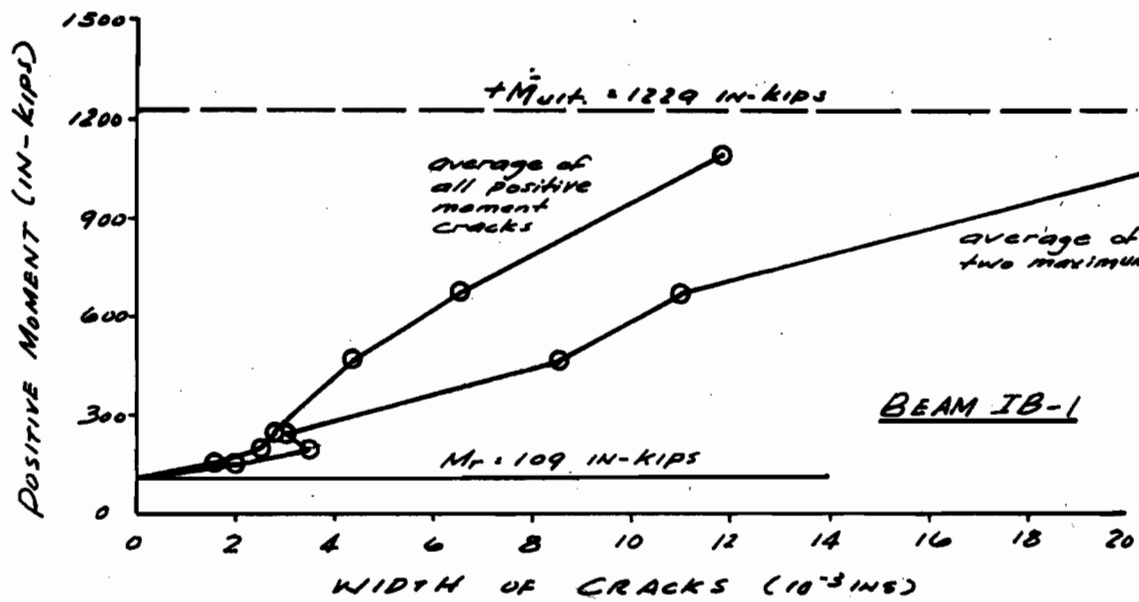
A-1



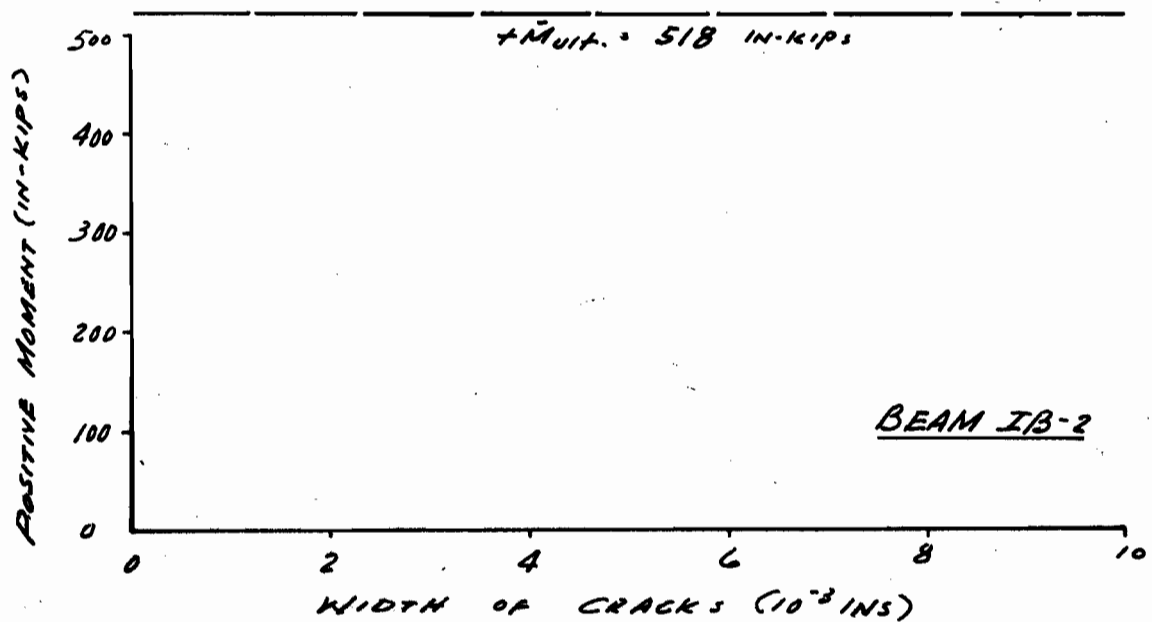
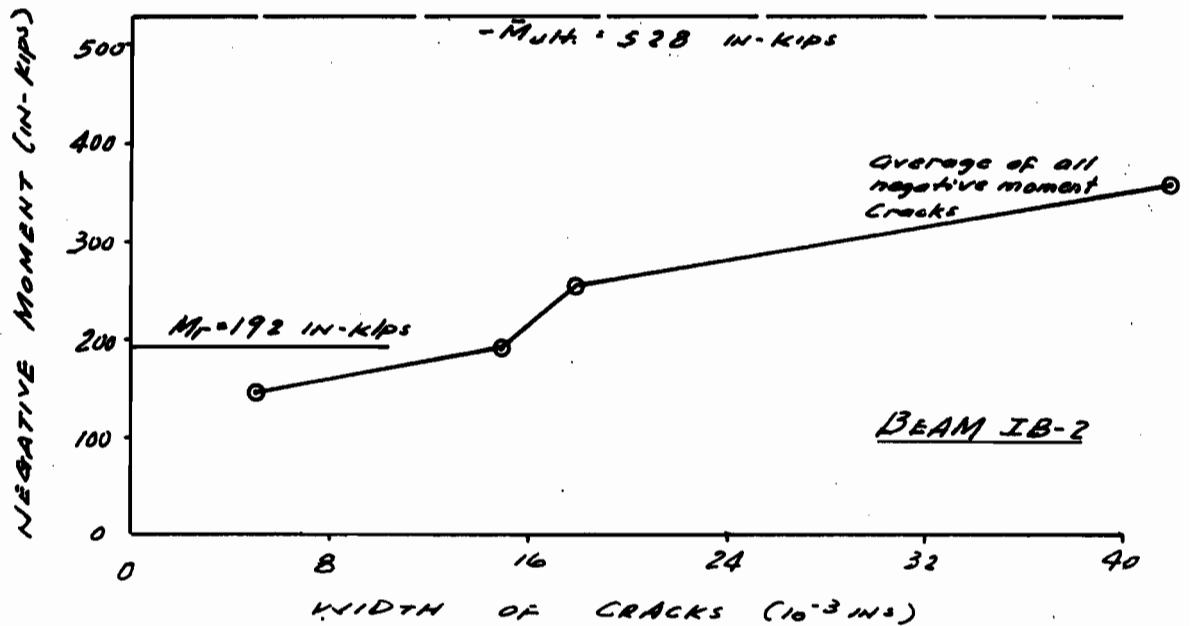
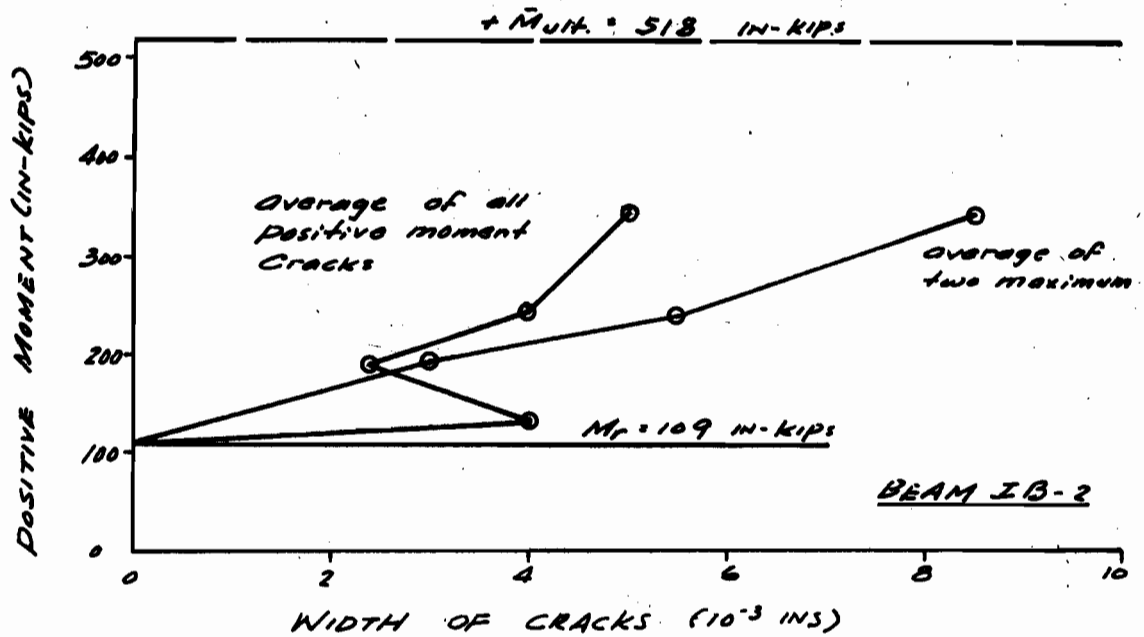
A-2



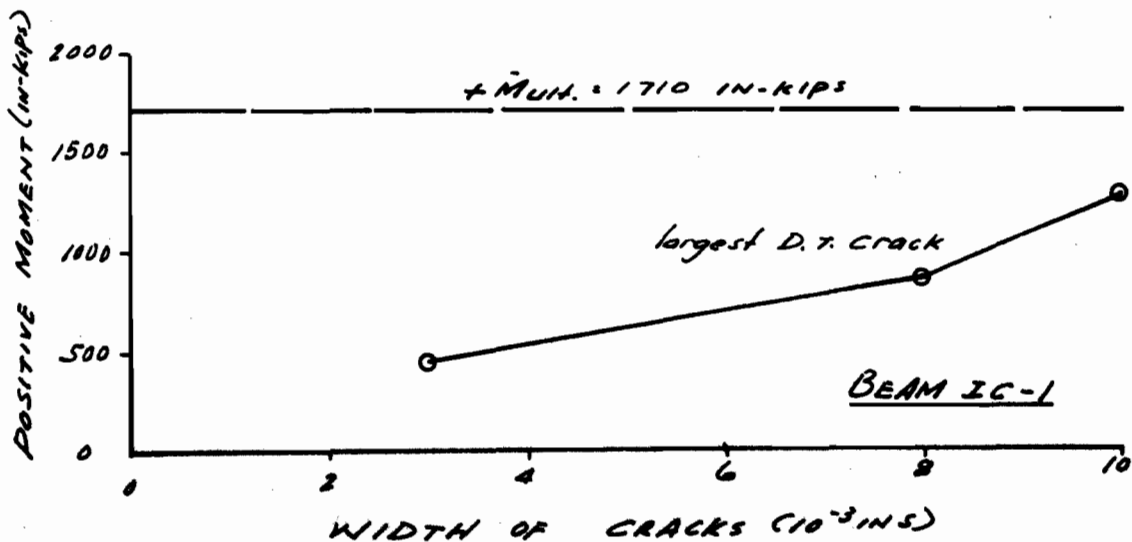
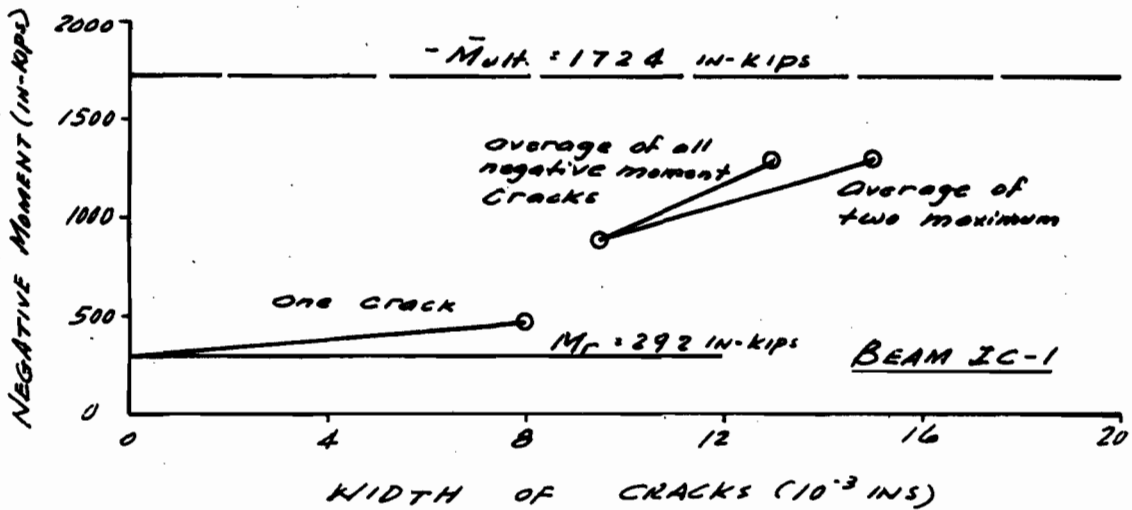
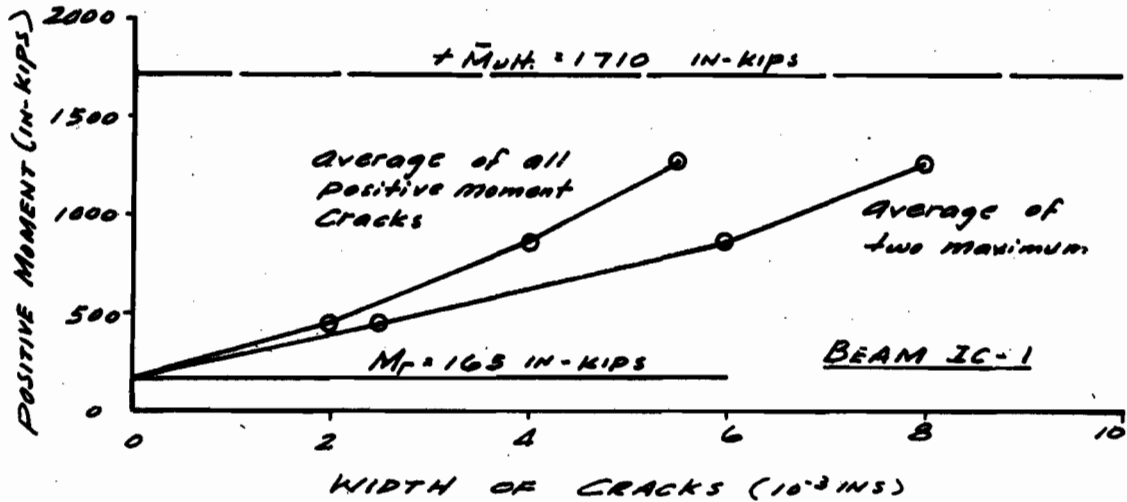
A-3



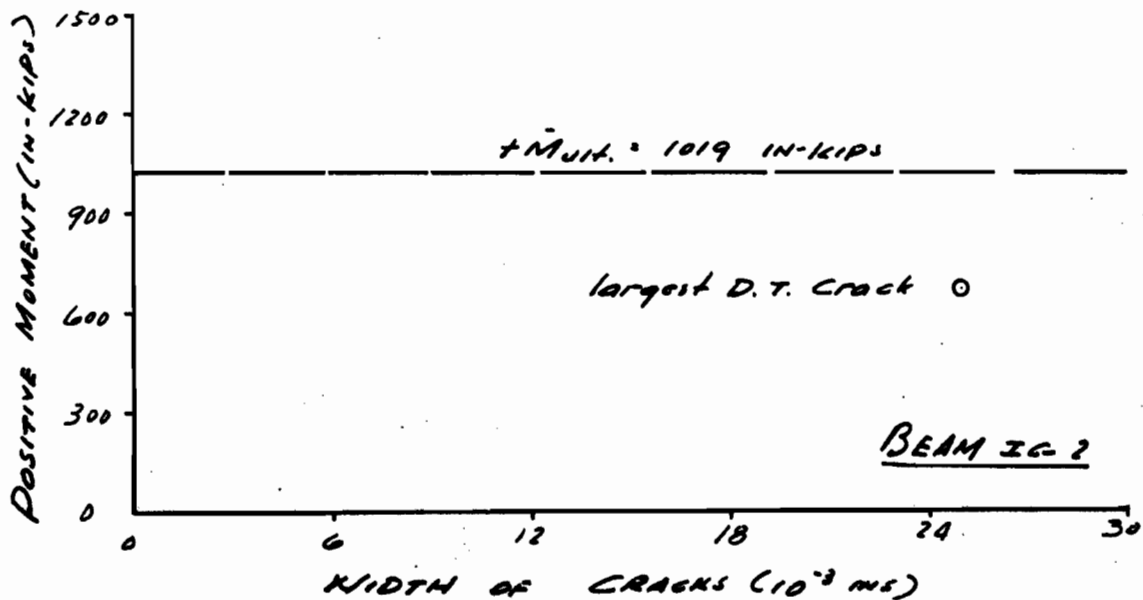
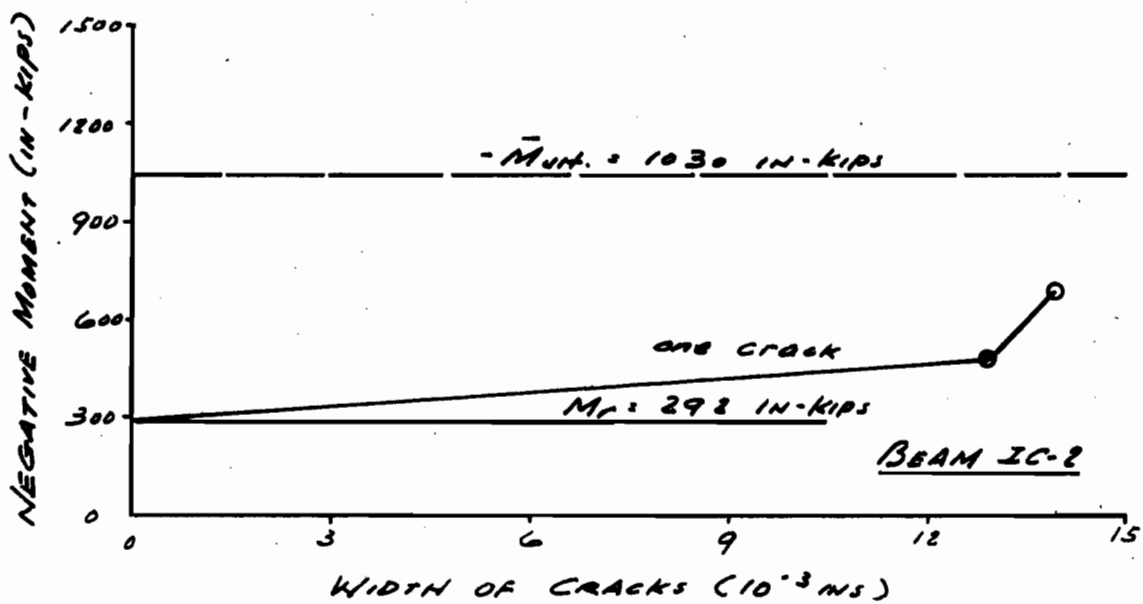
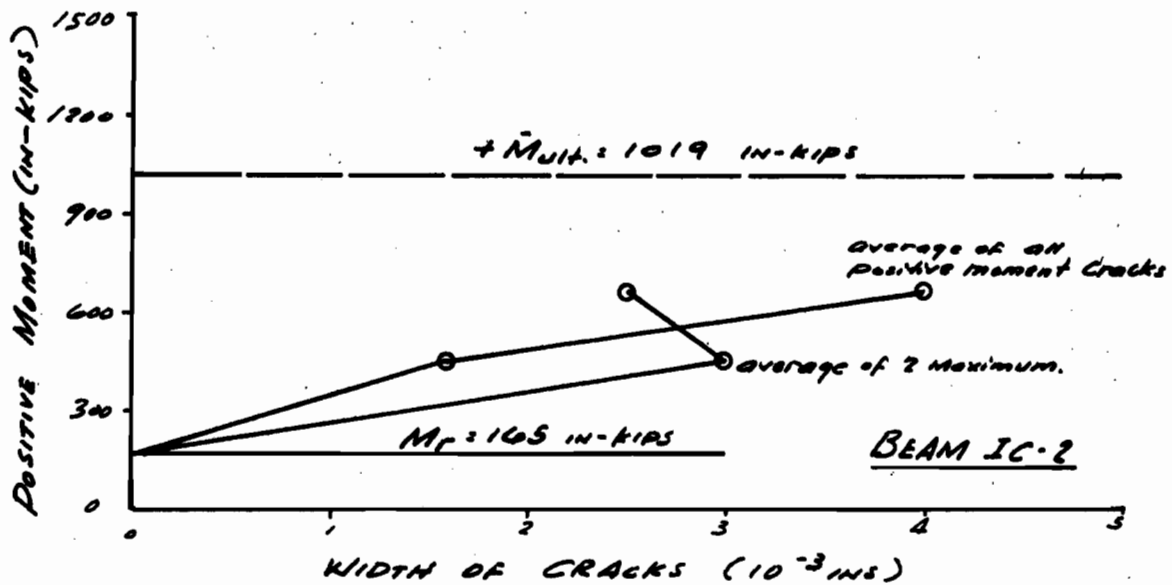
A-4



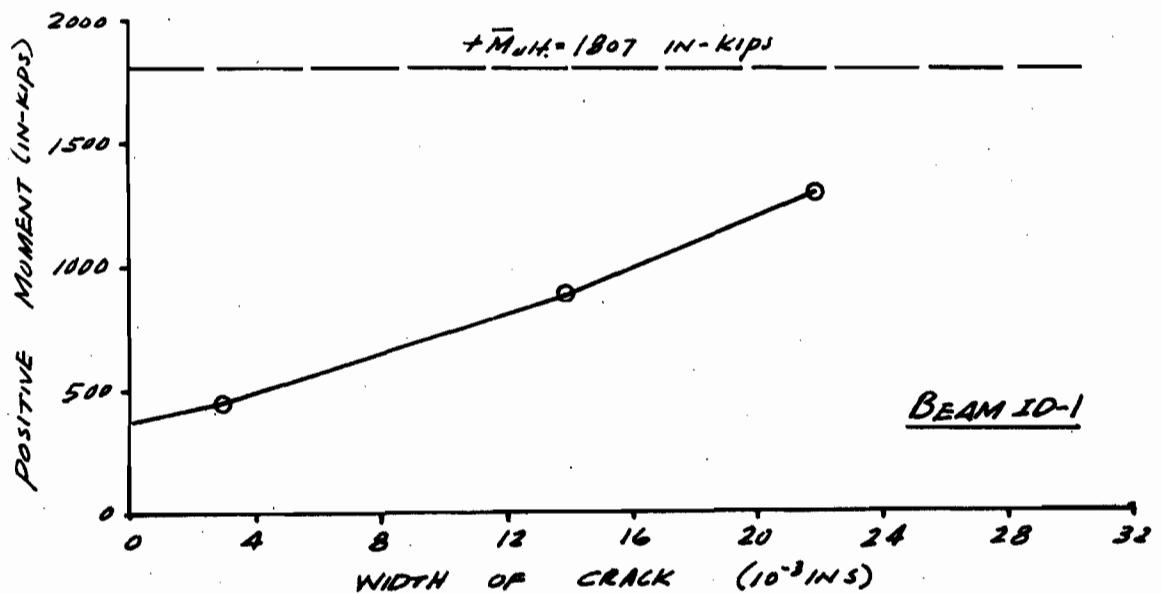
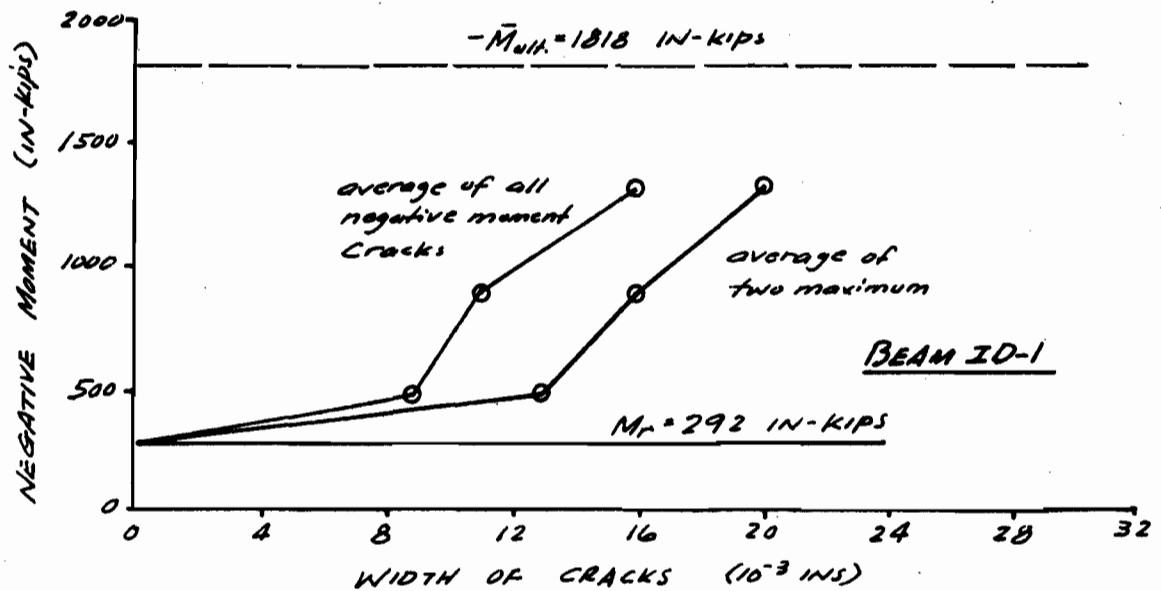
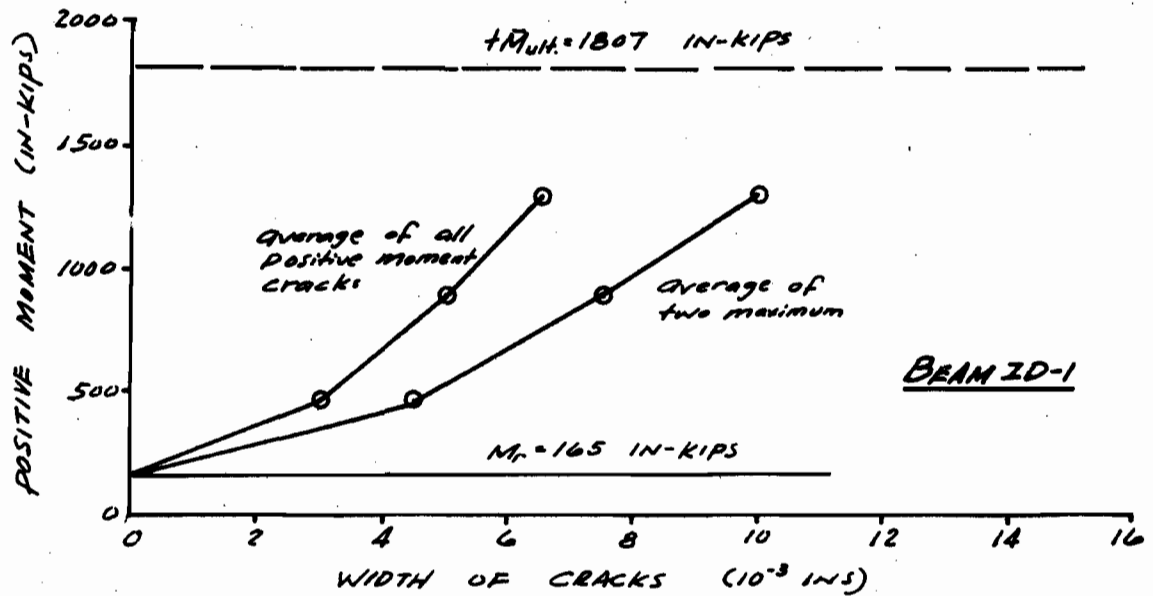
A-5



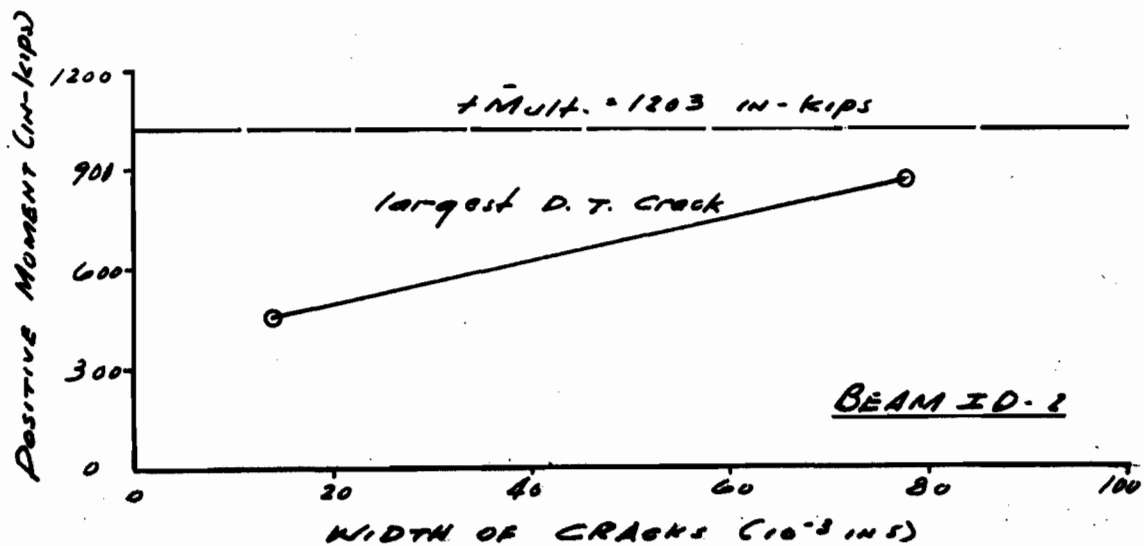
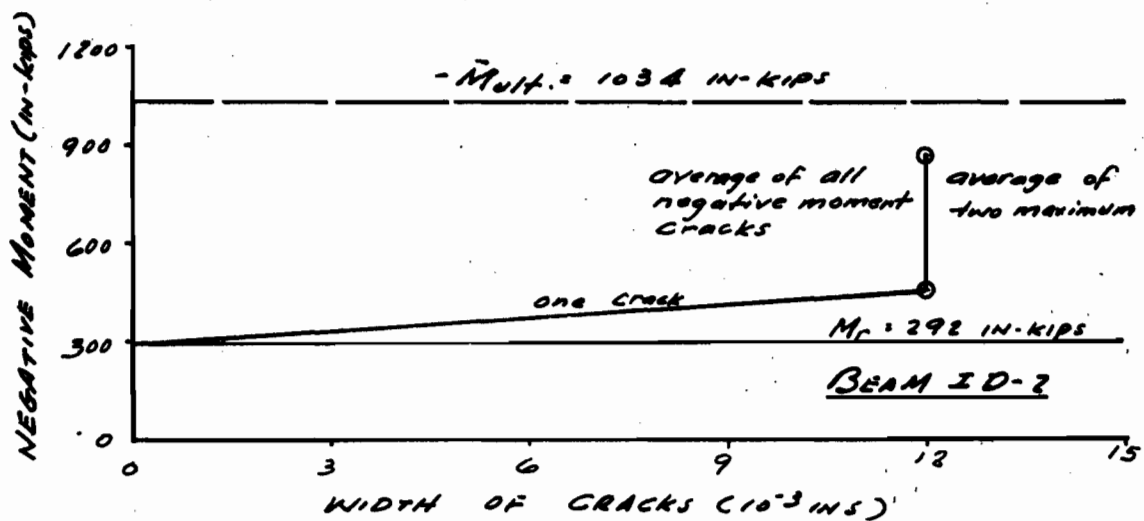
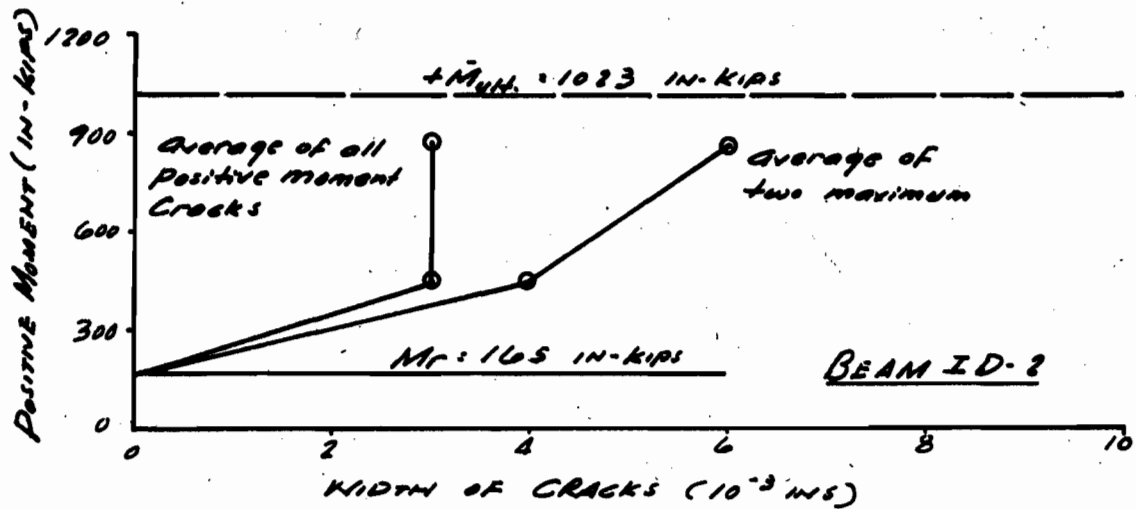
A-6



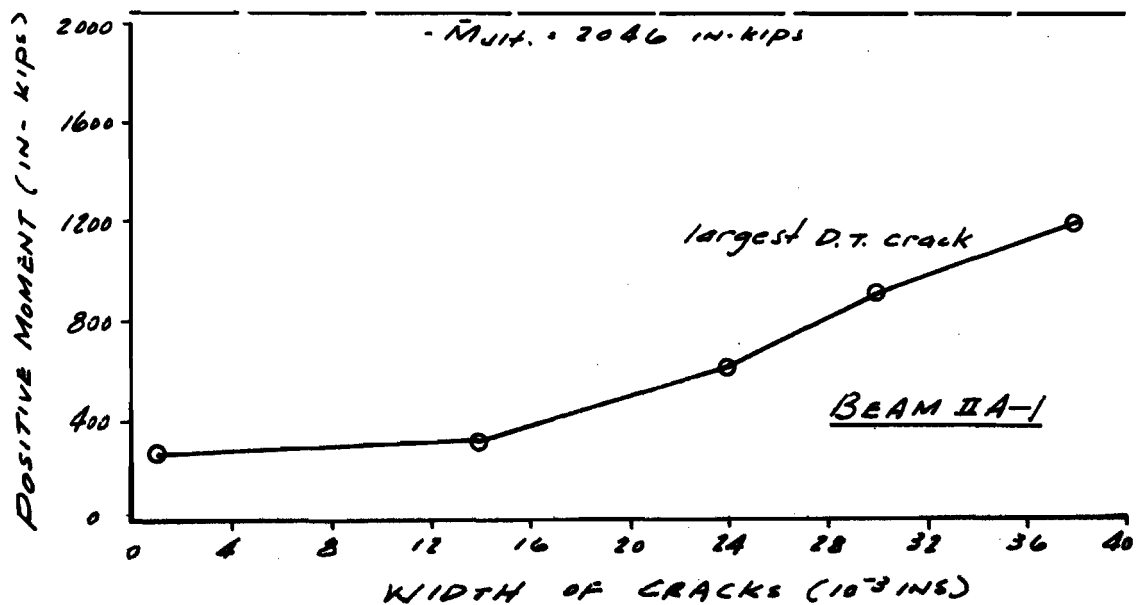
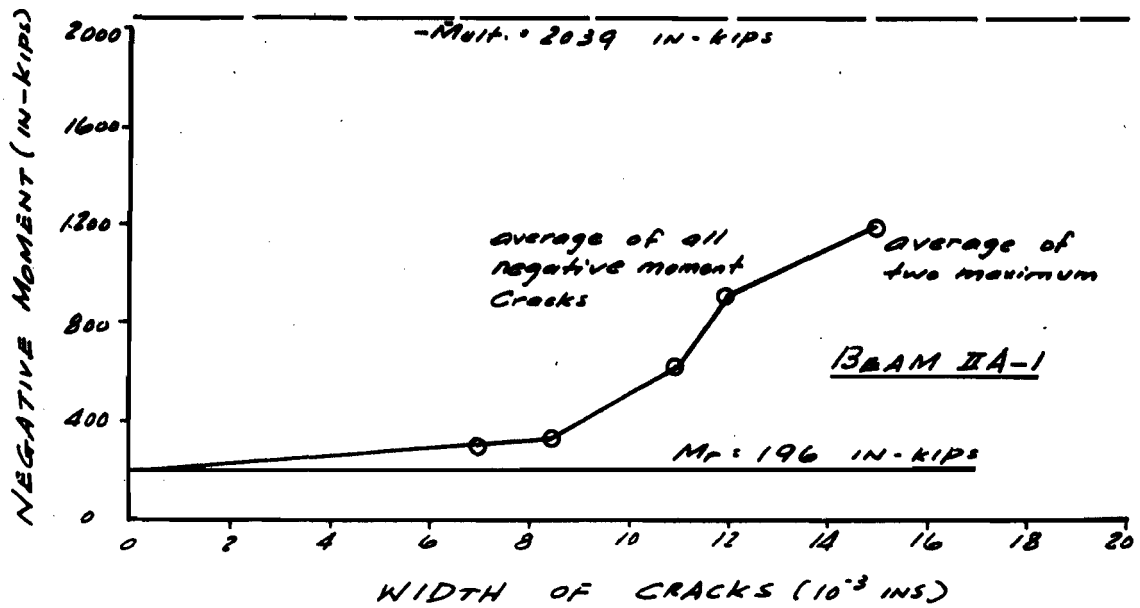
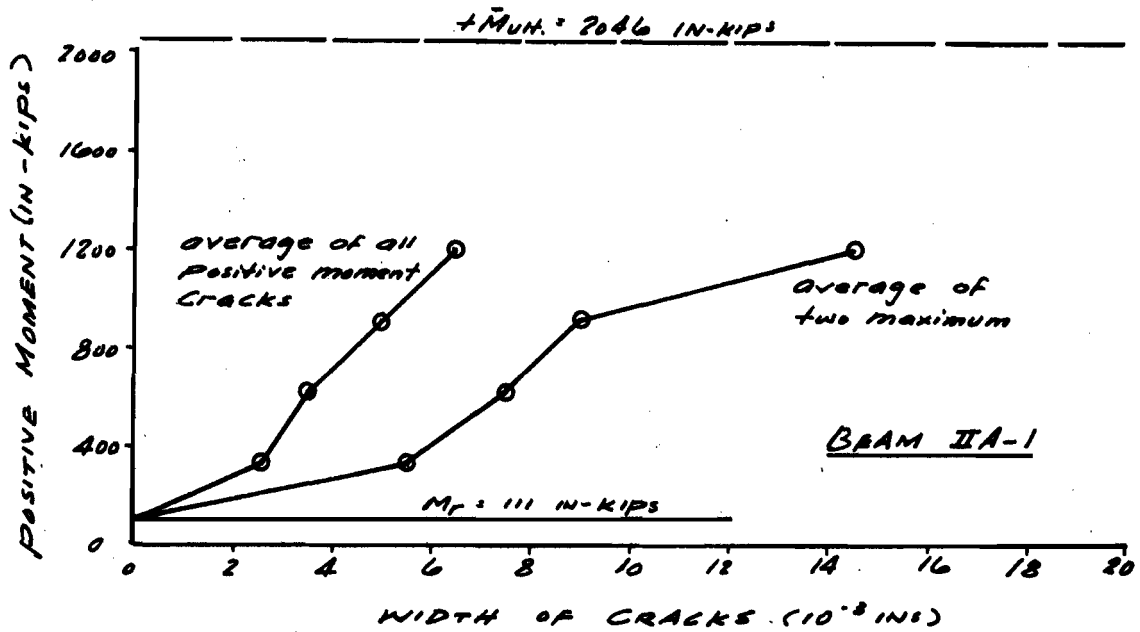
A-7



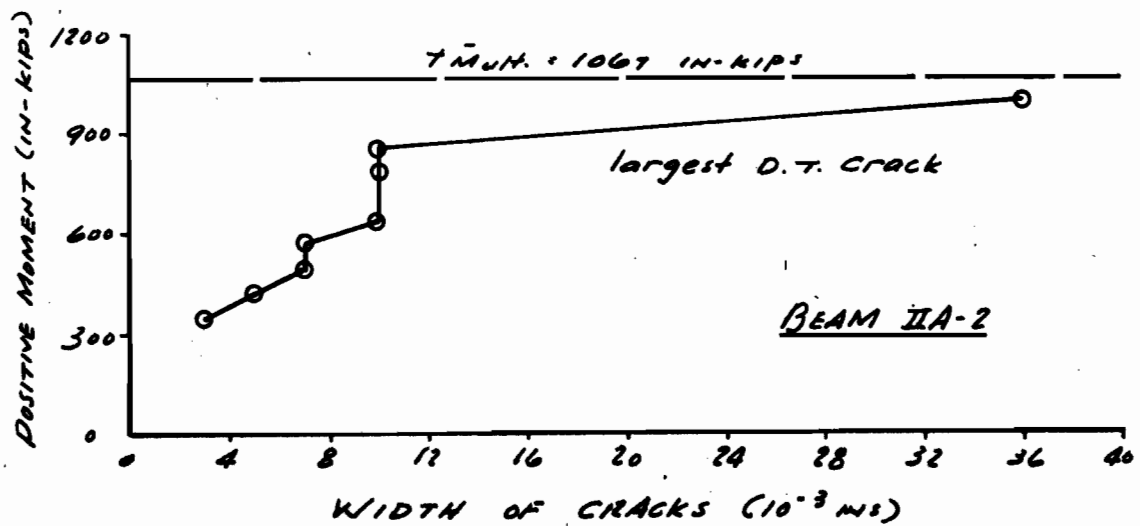
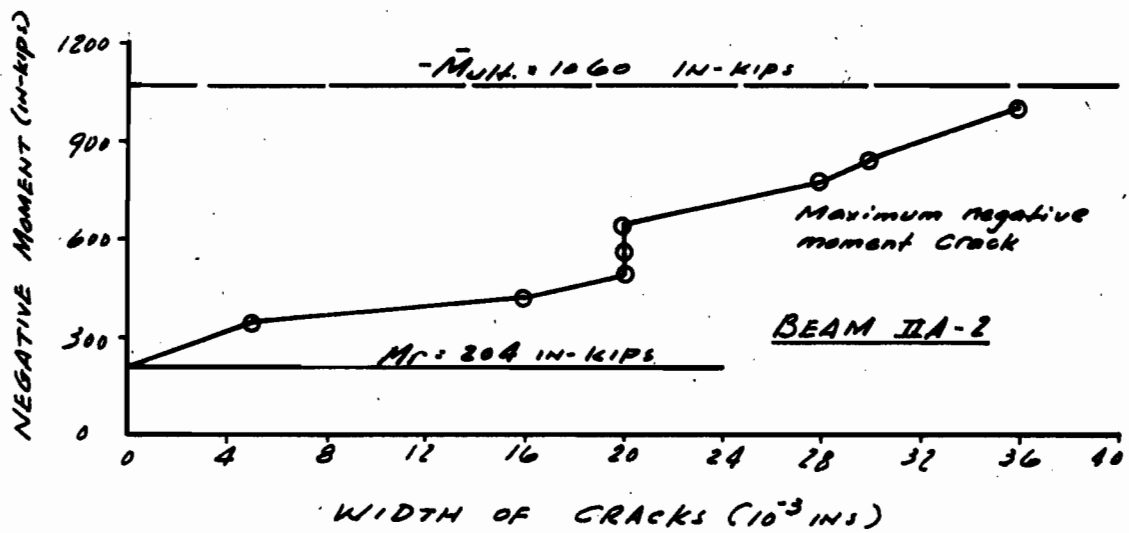
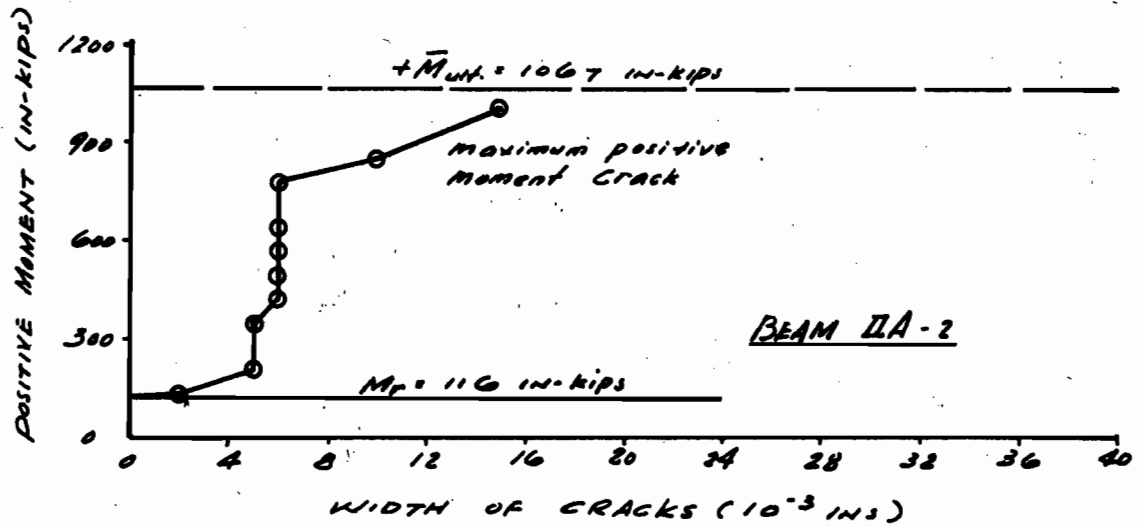
A-8



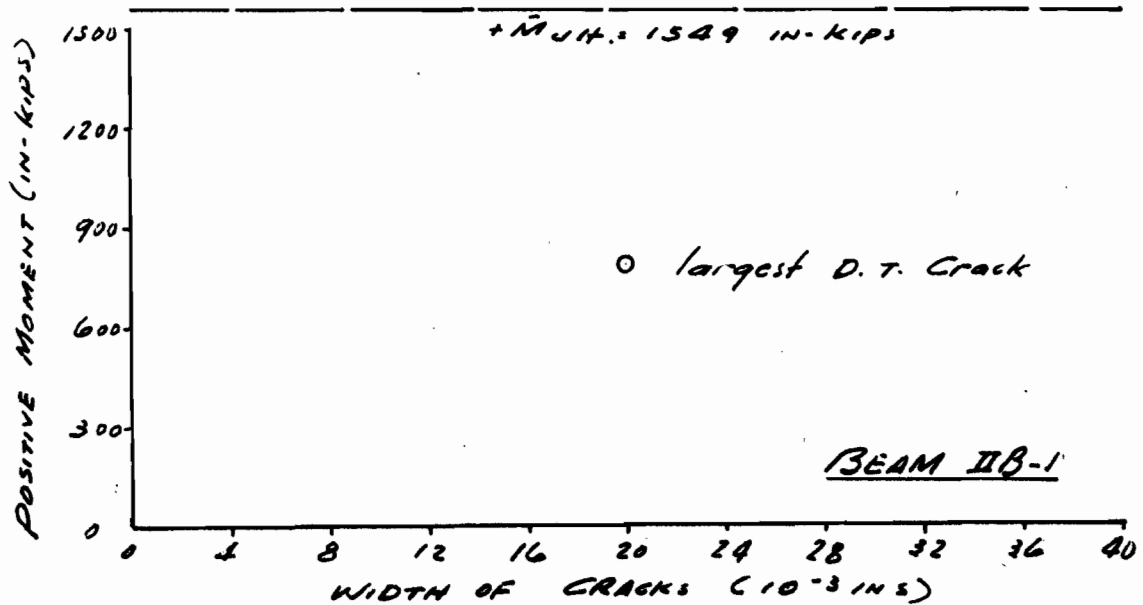
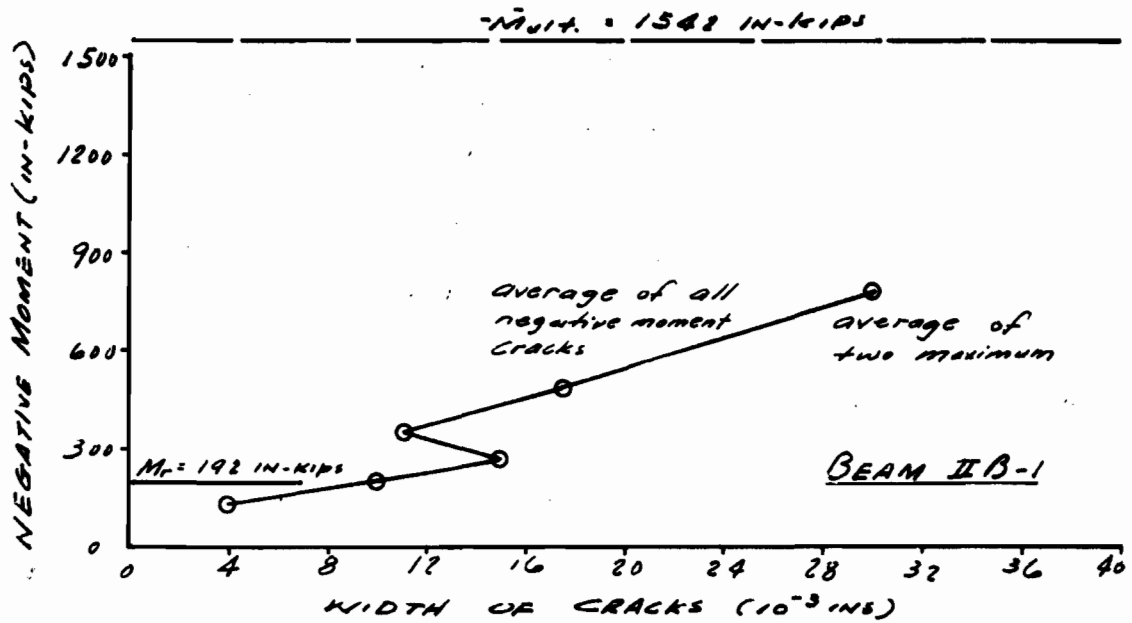
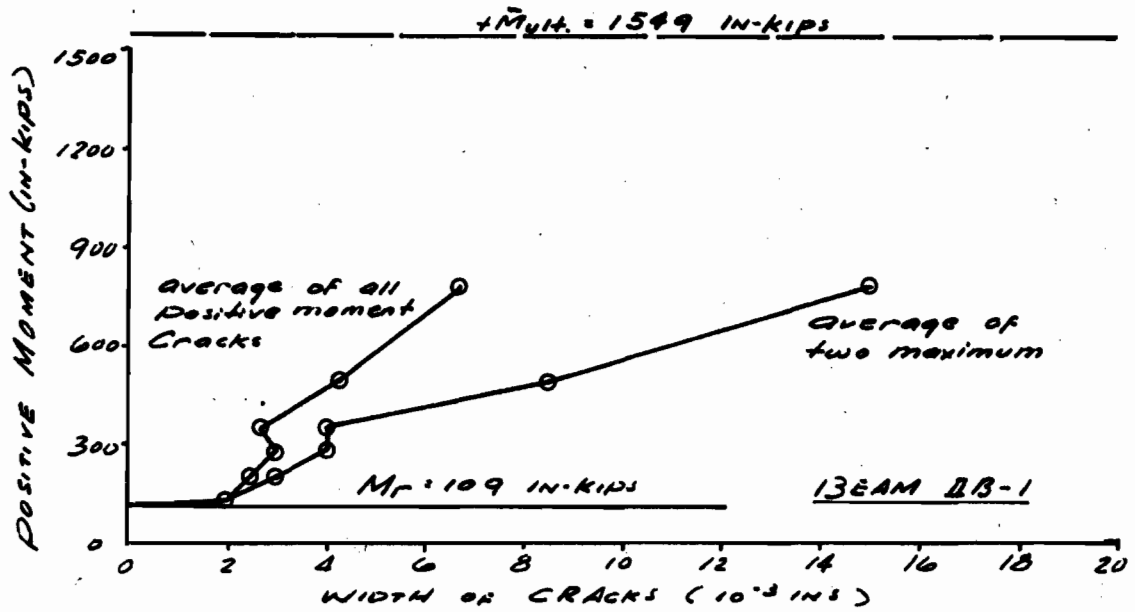
A-9



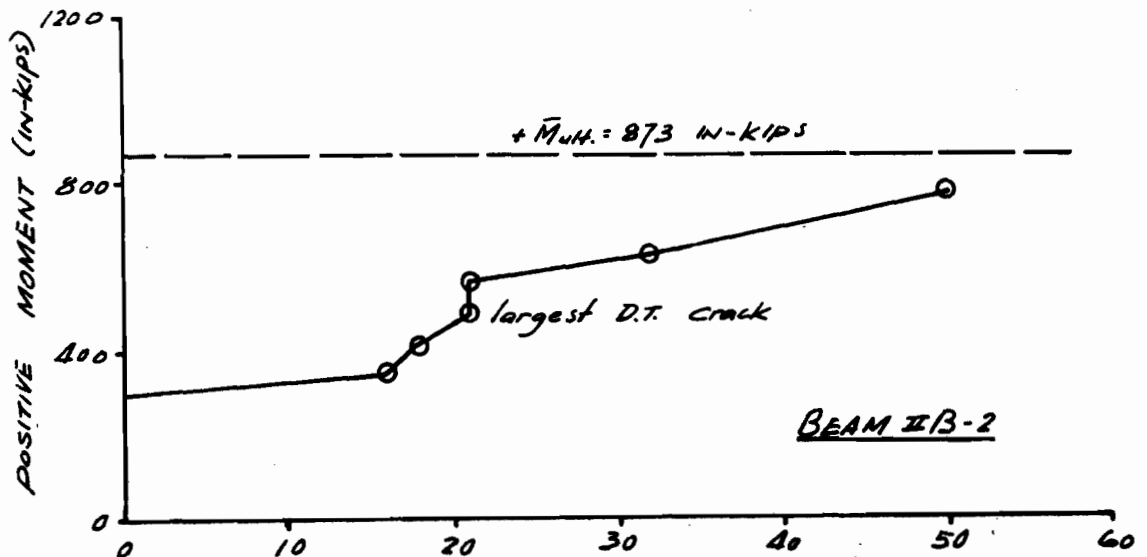
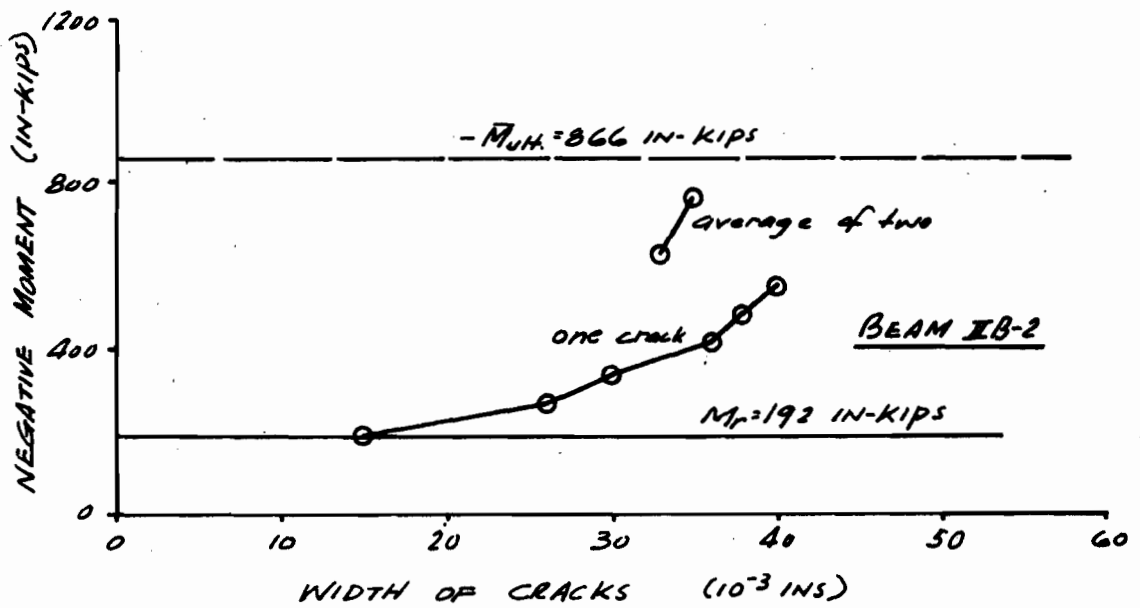
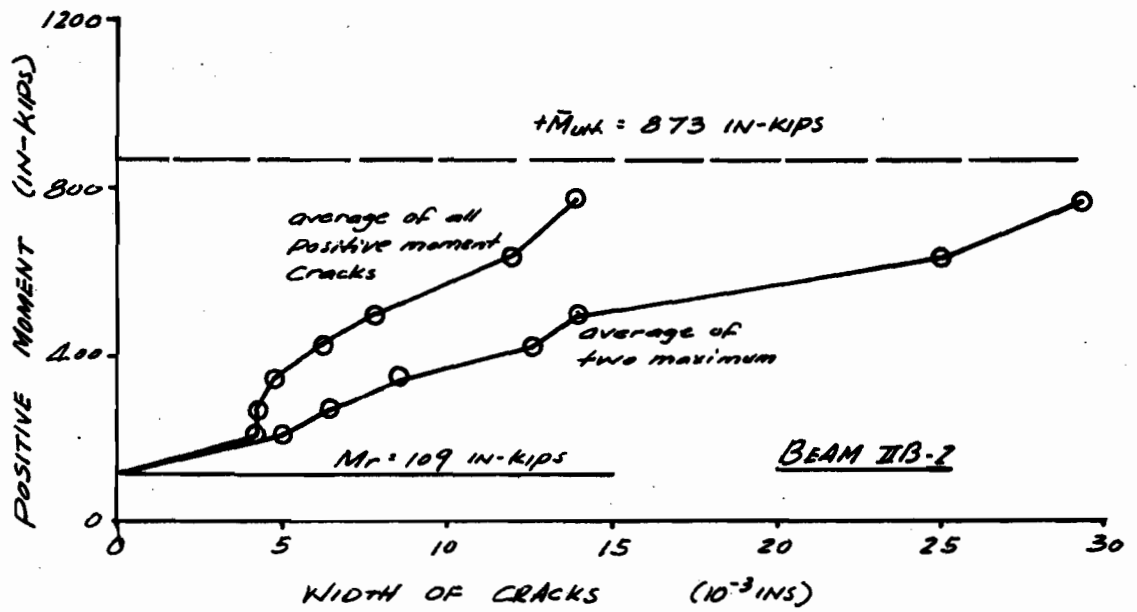
A-10



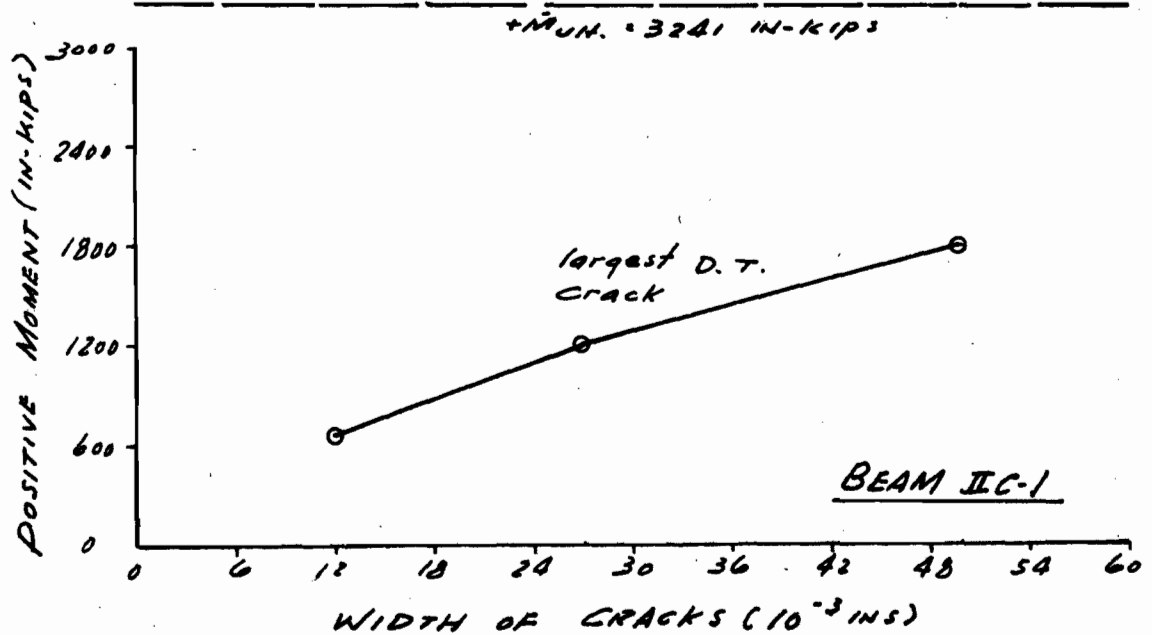
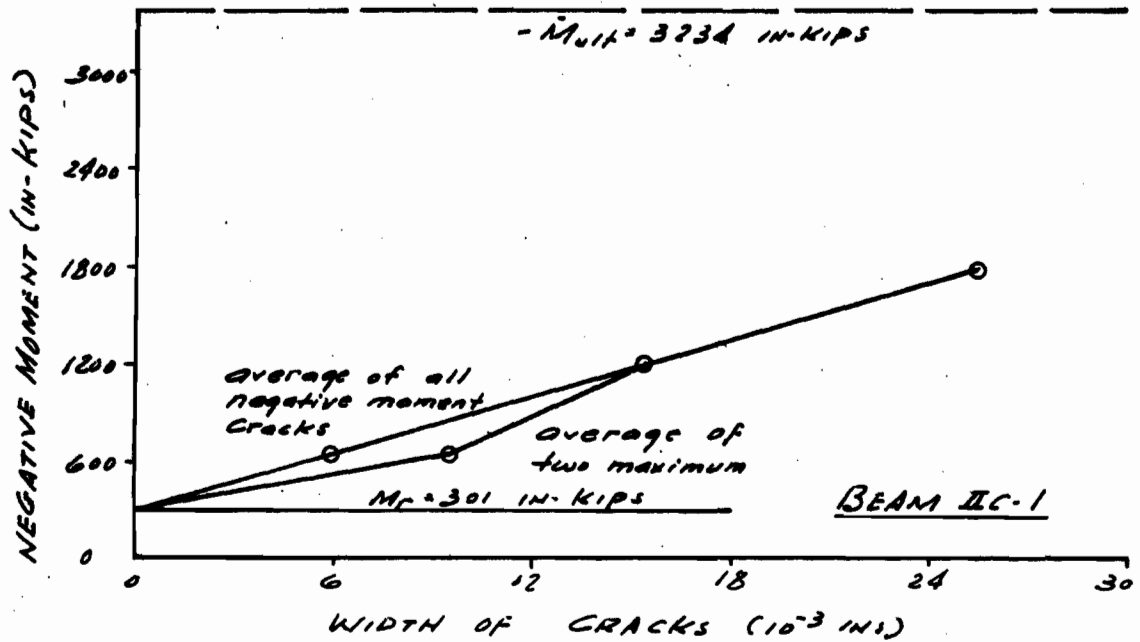
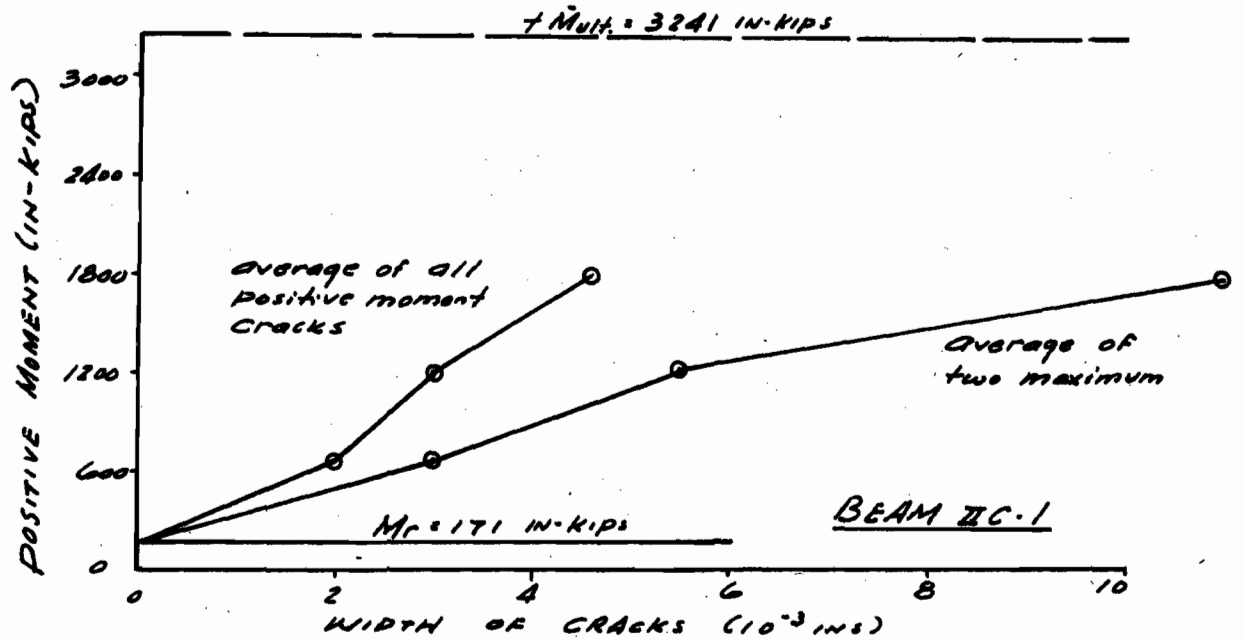
A-11



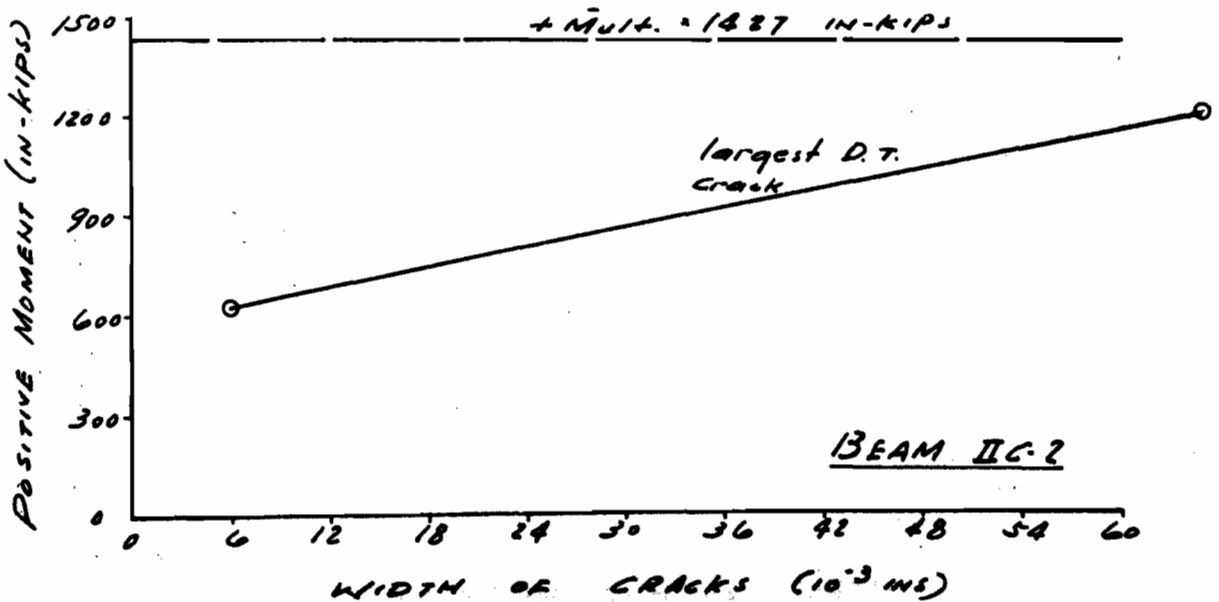
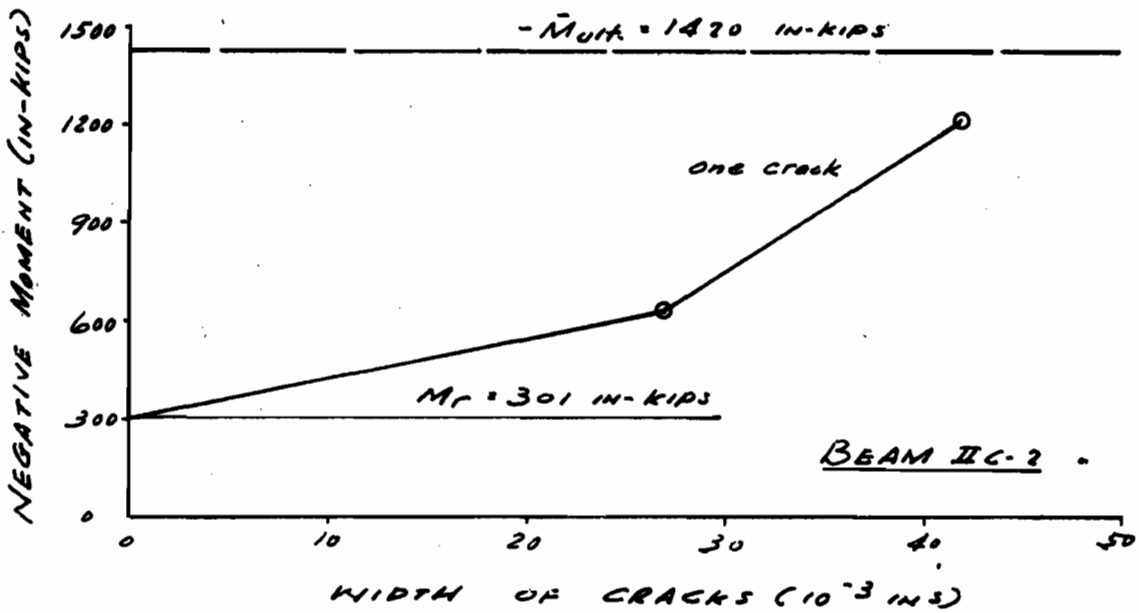
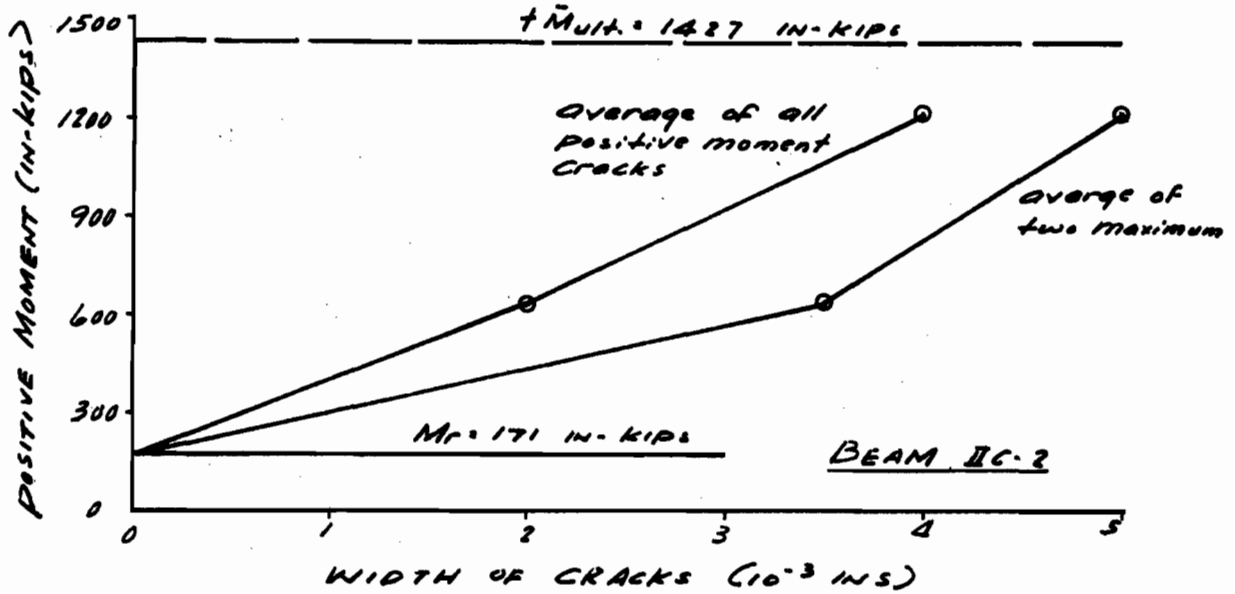
A-12



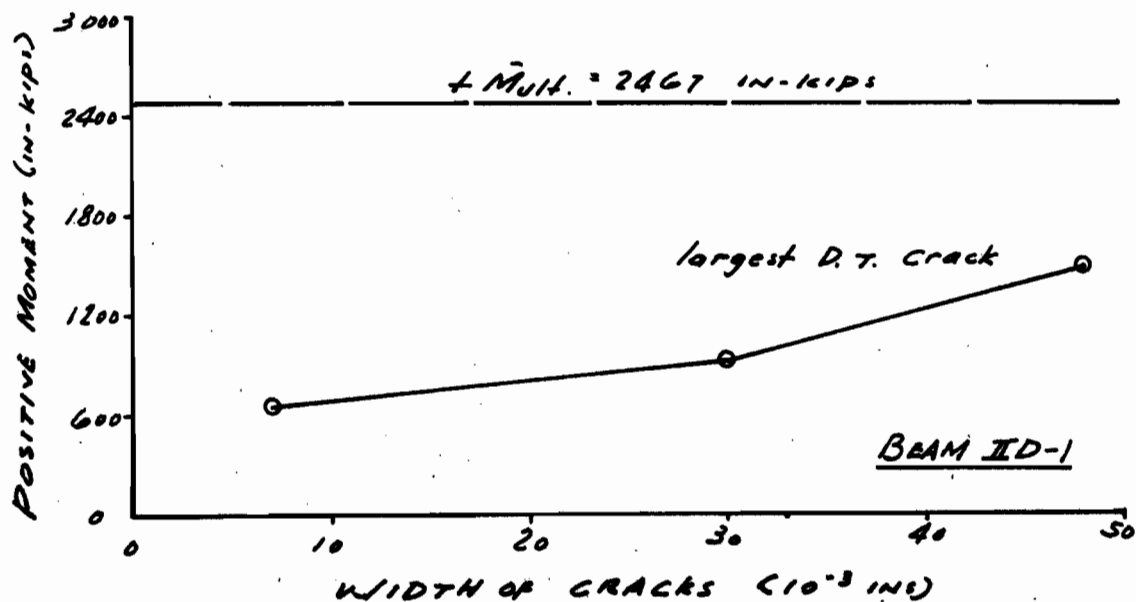
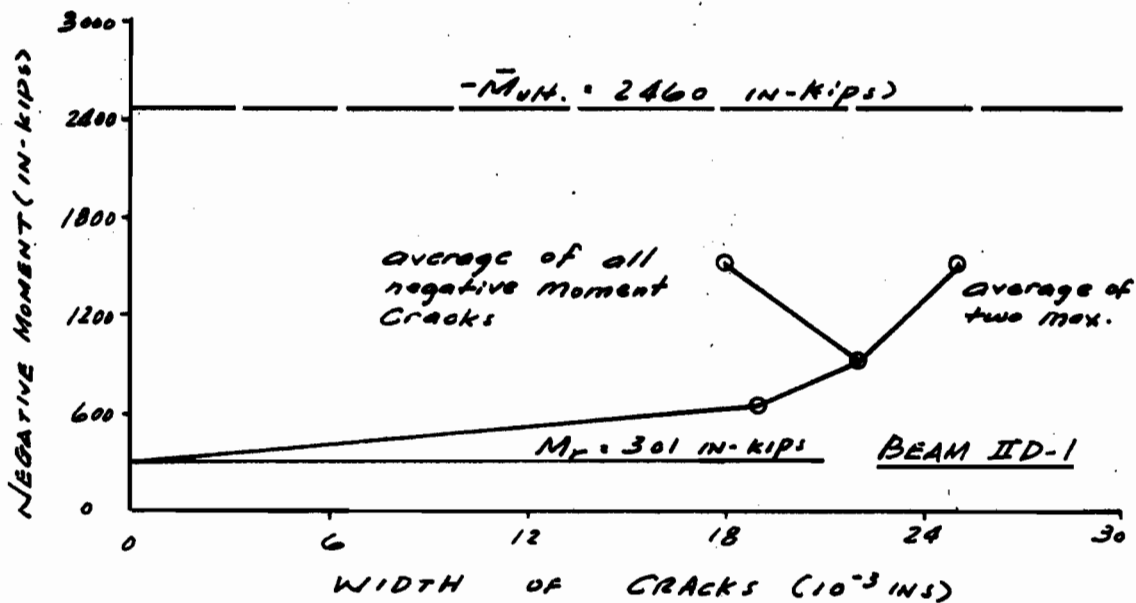
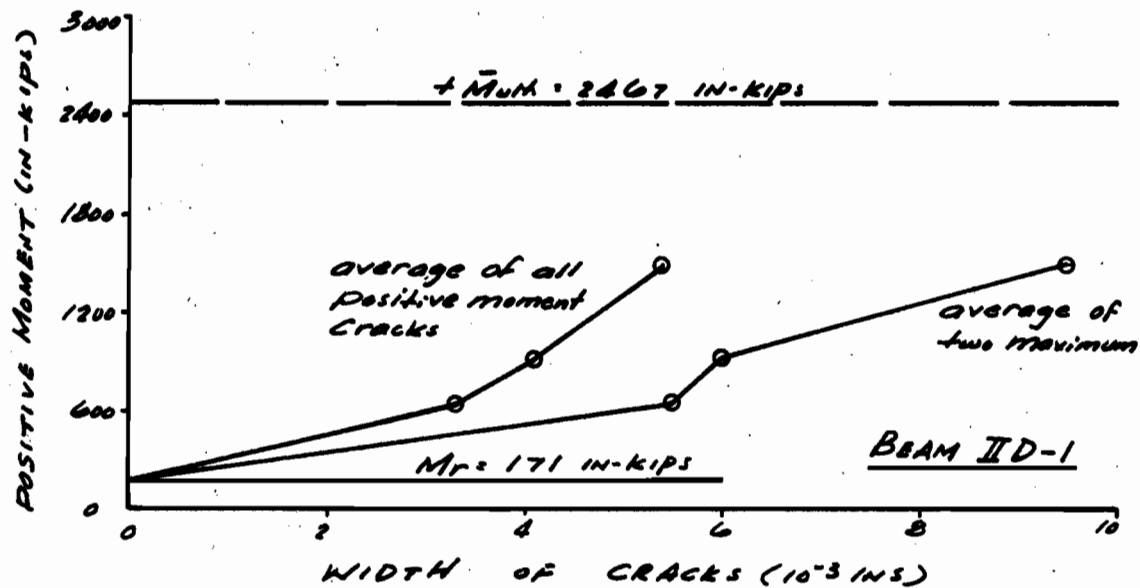
A-13



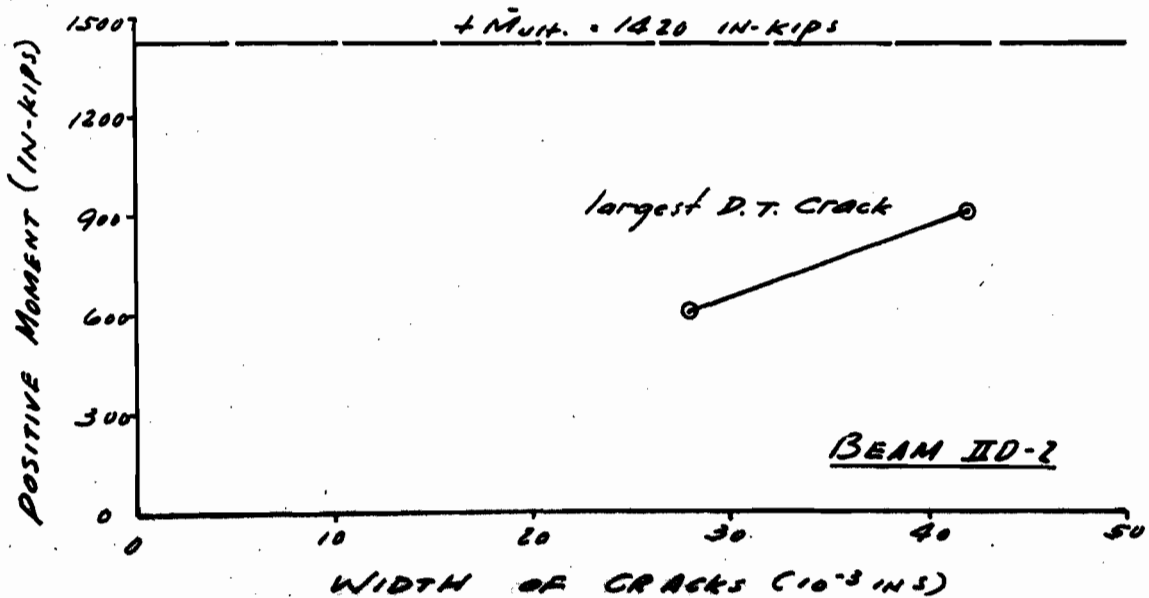
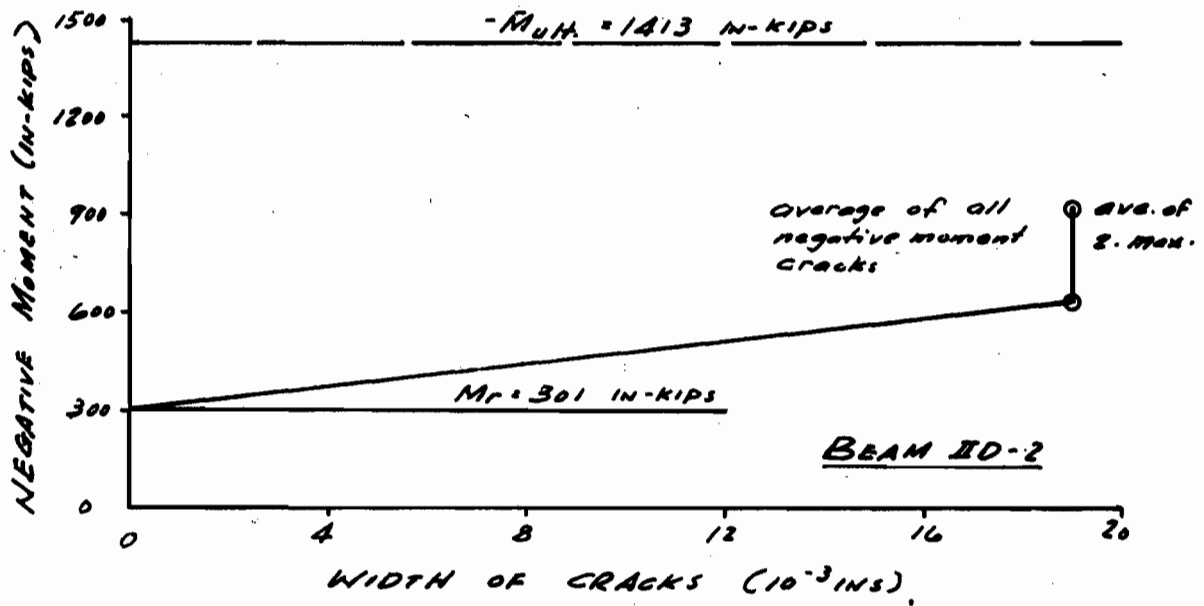
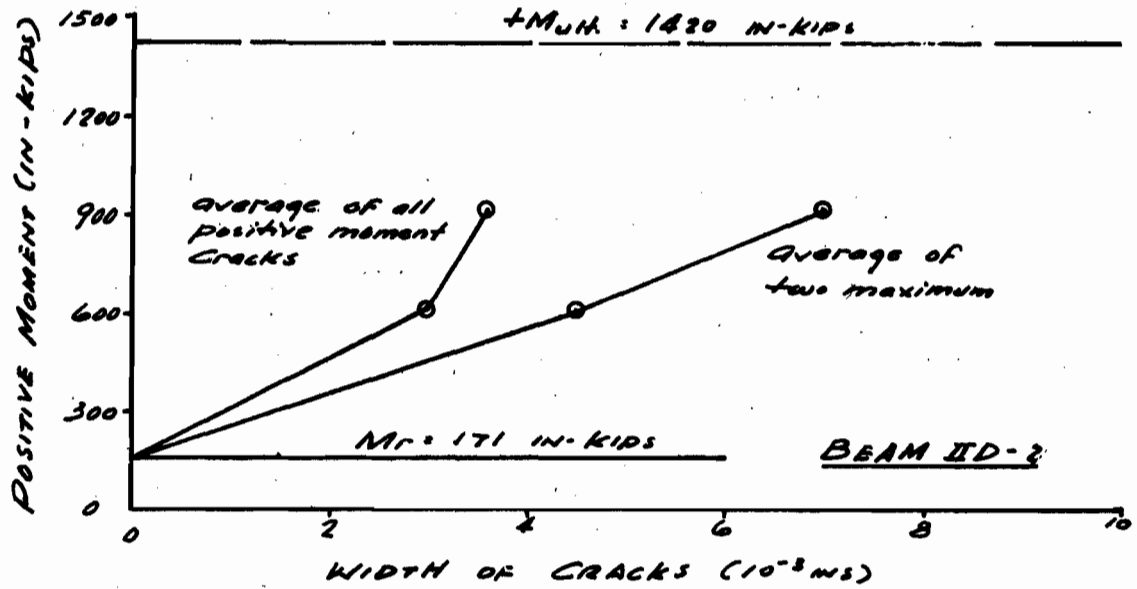
A-14



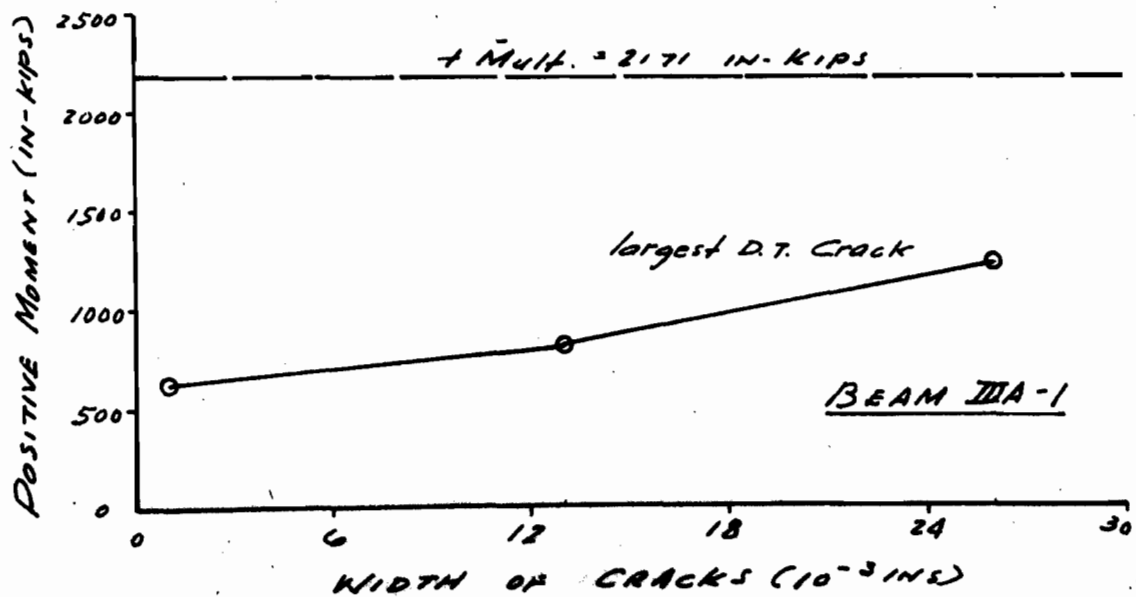
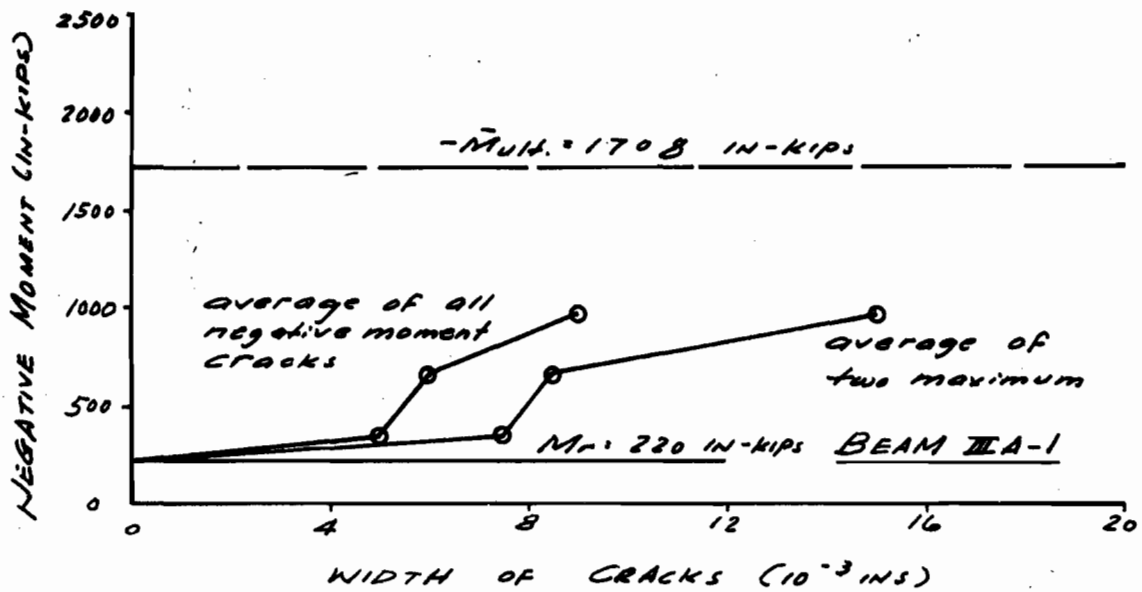
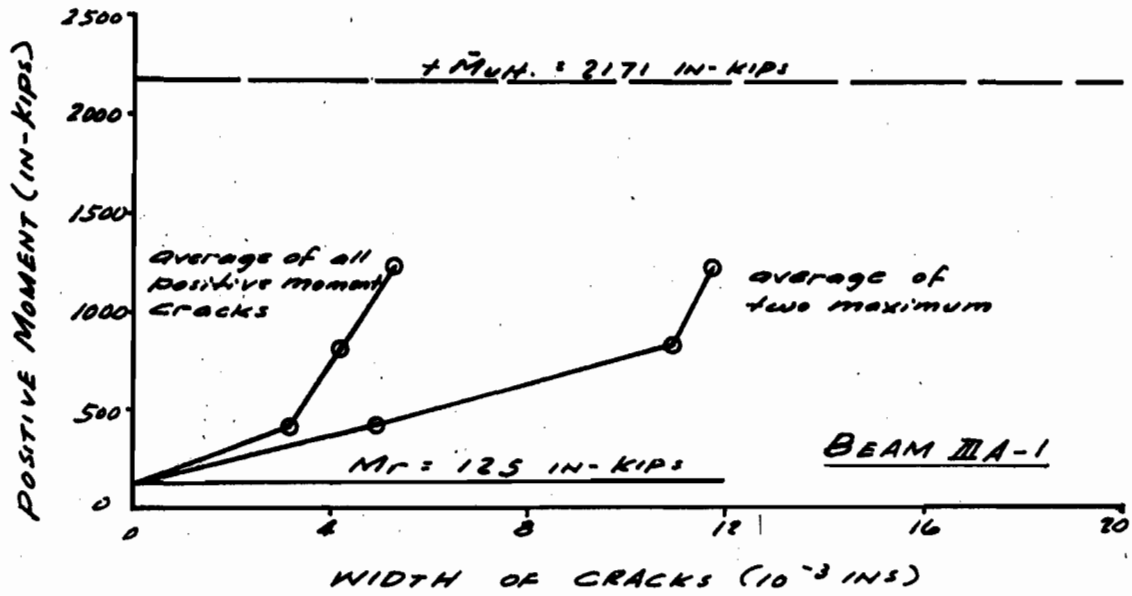
A-15



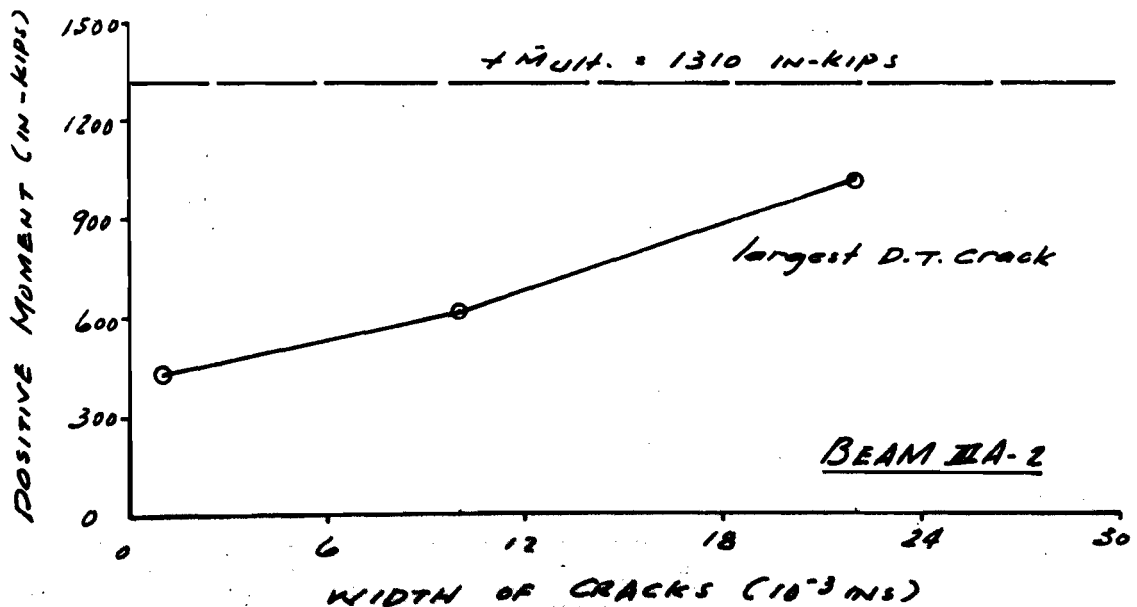
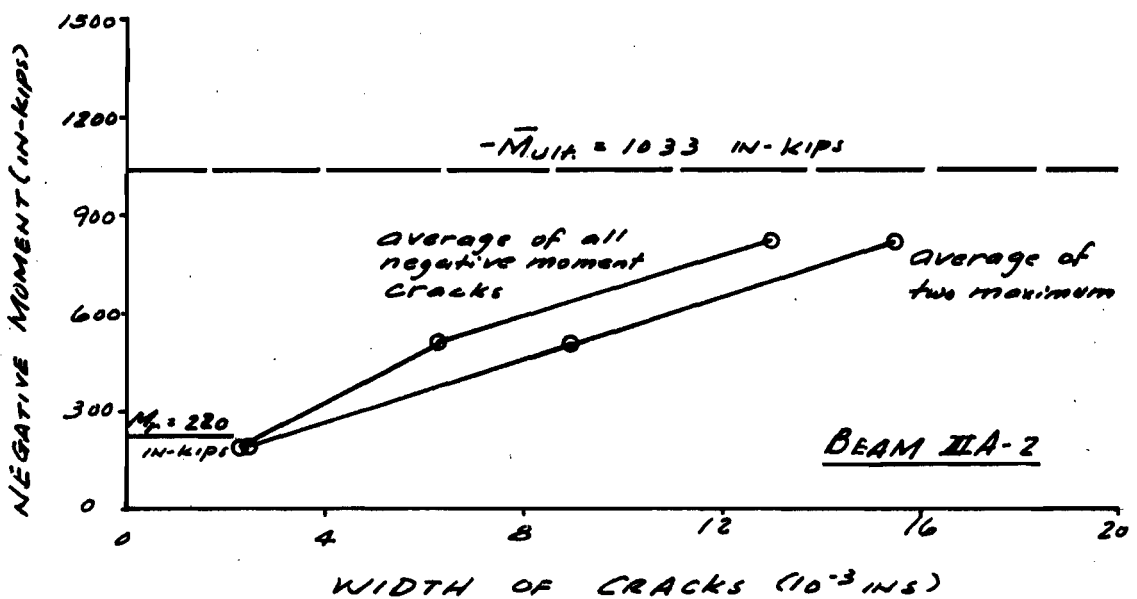
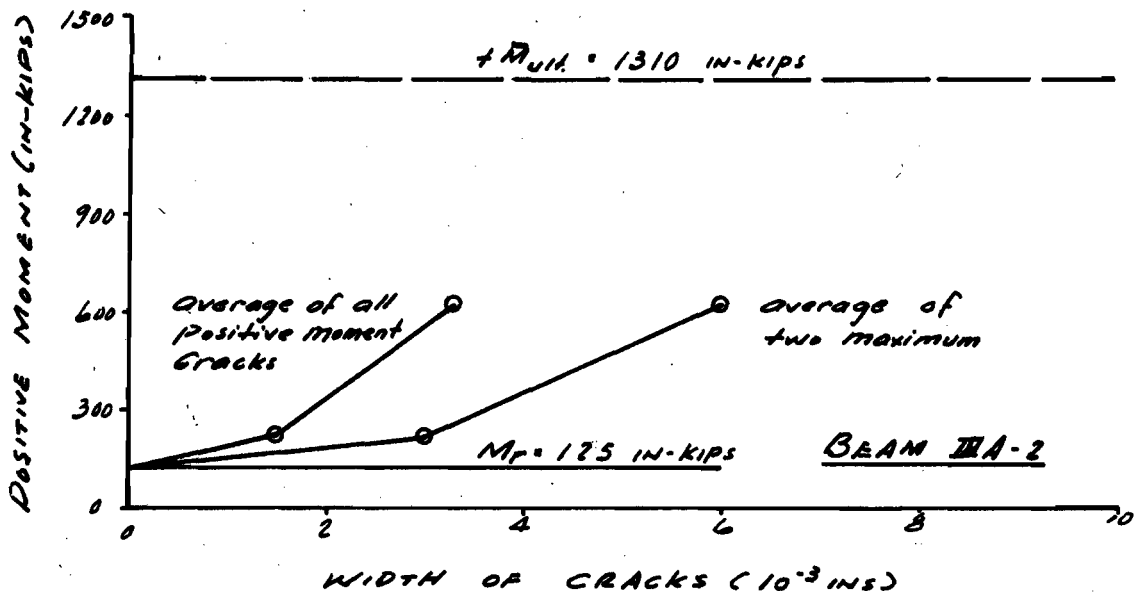
A-16



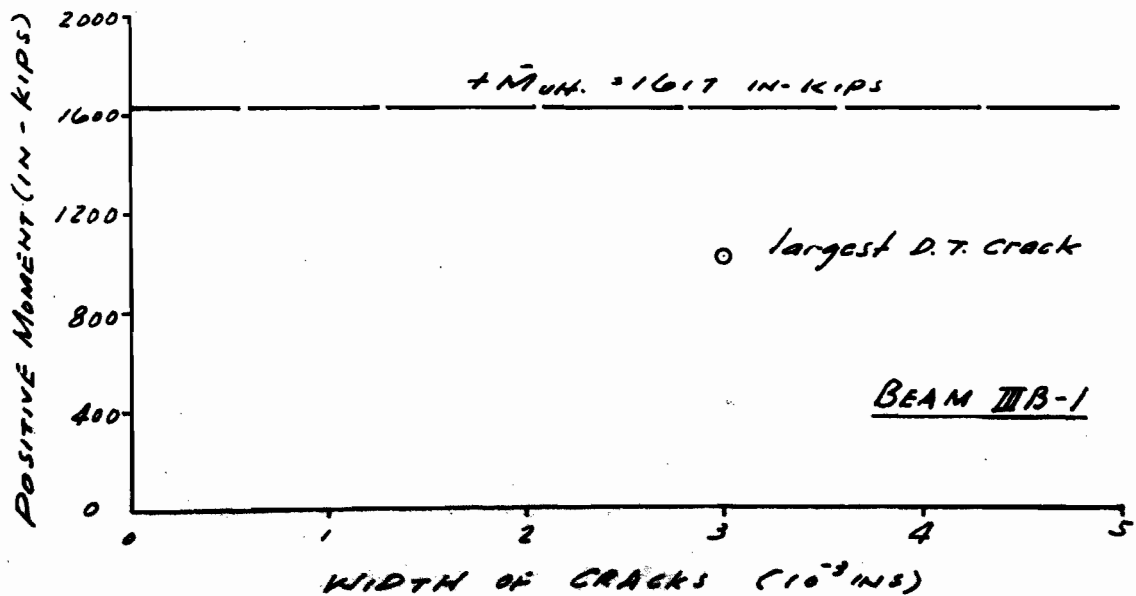
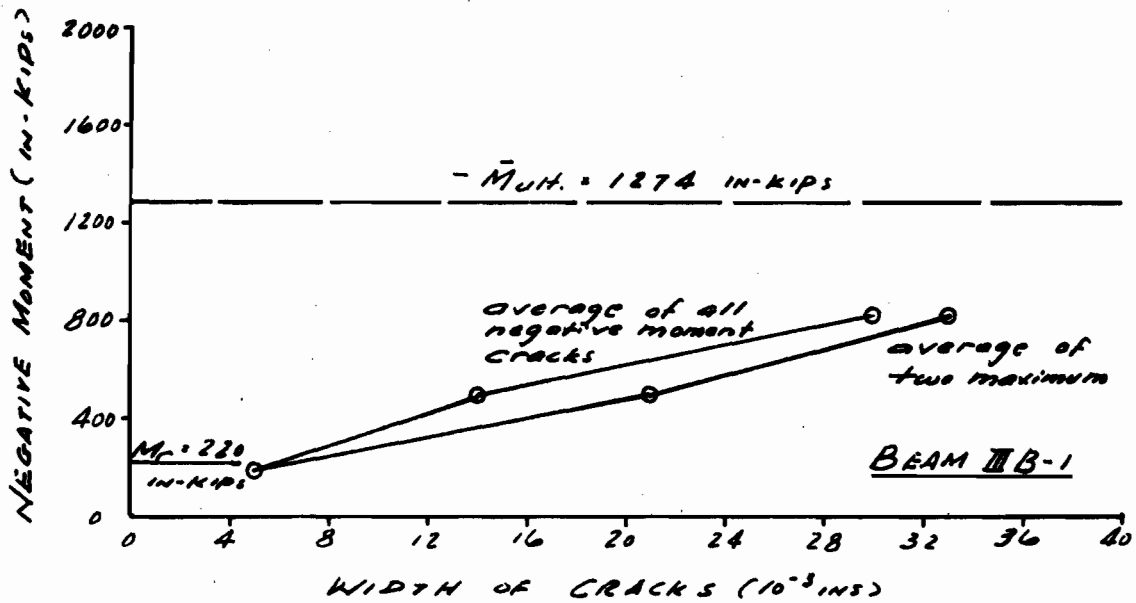
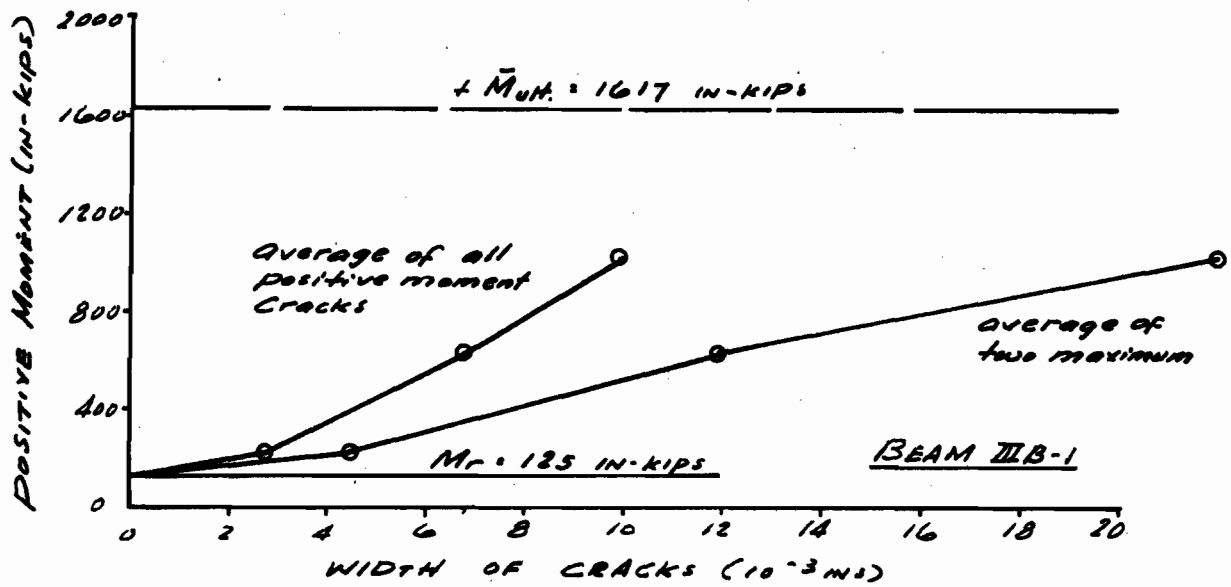
A-17



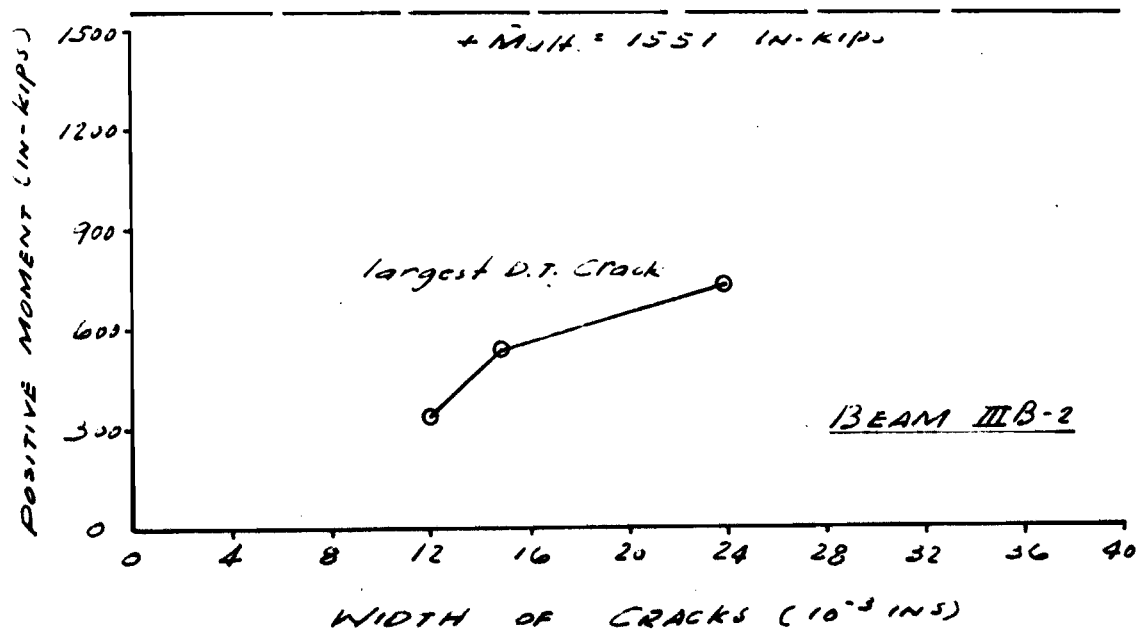
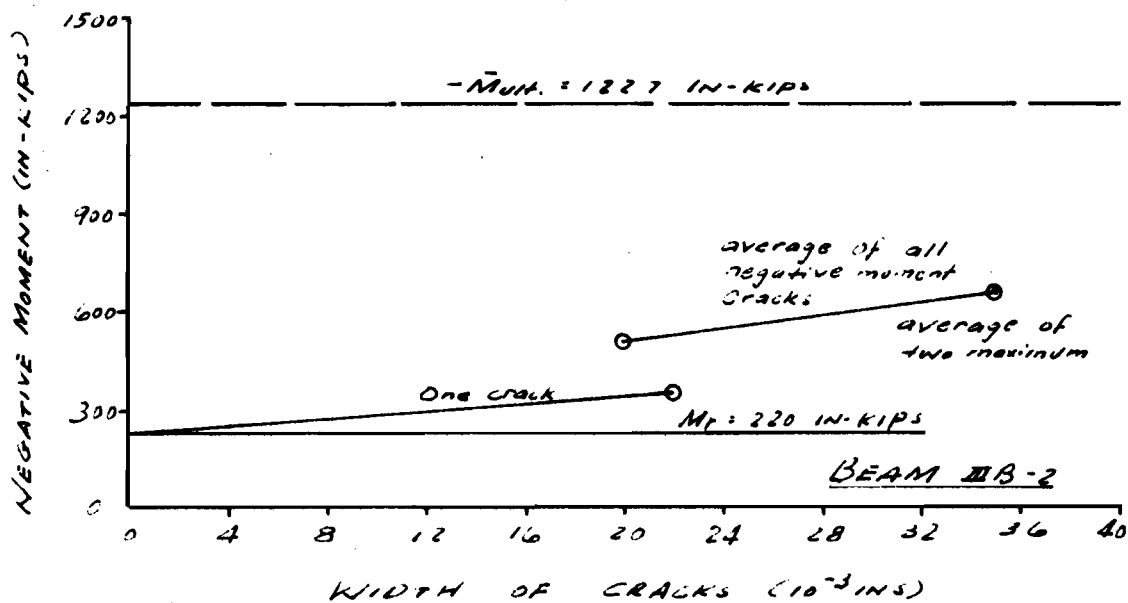
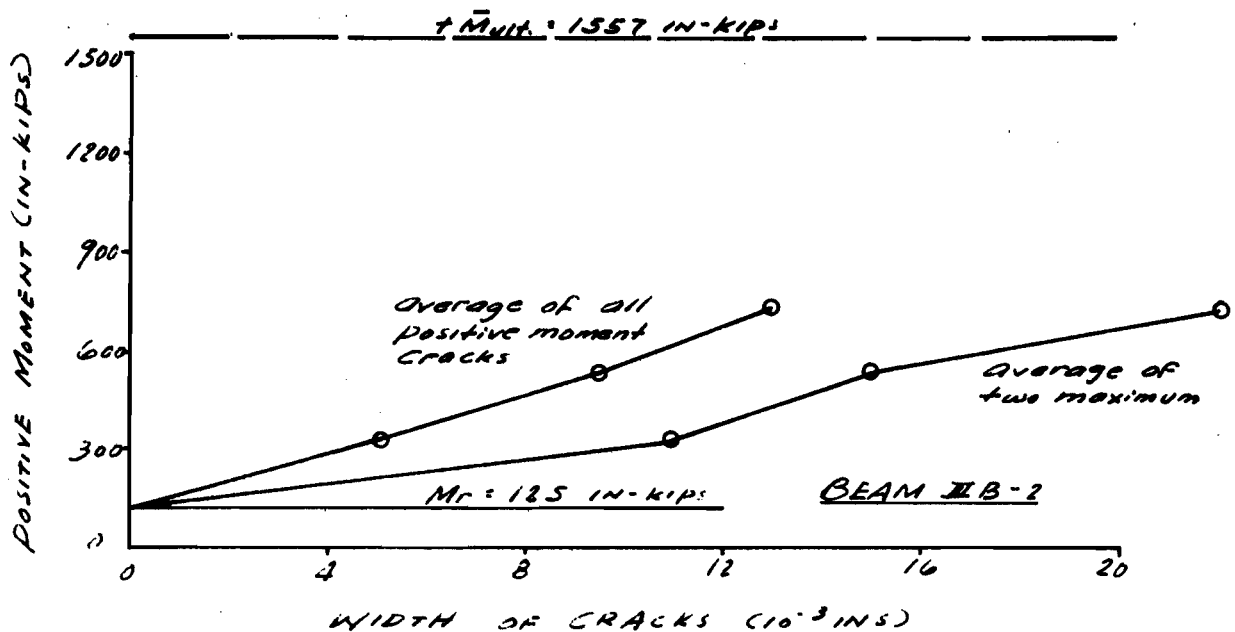
A-18

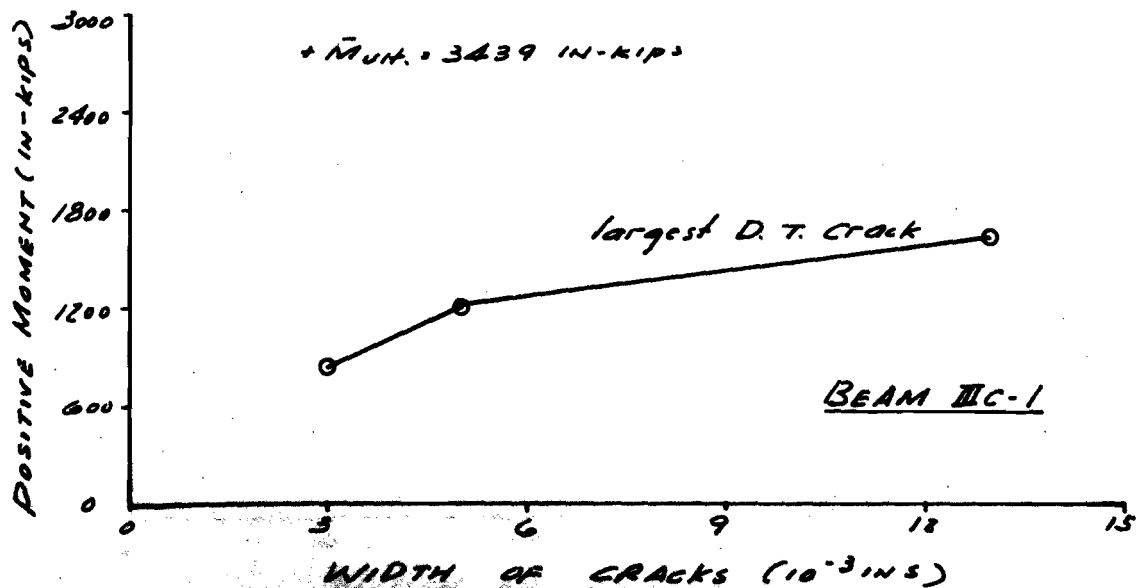
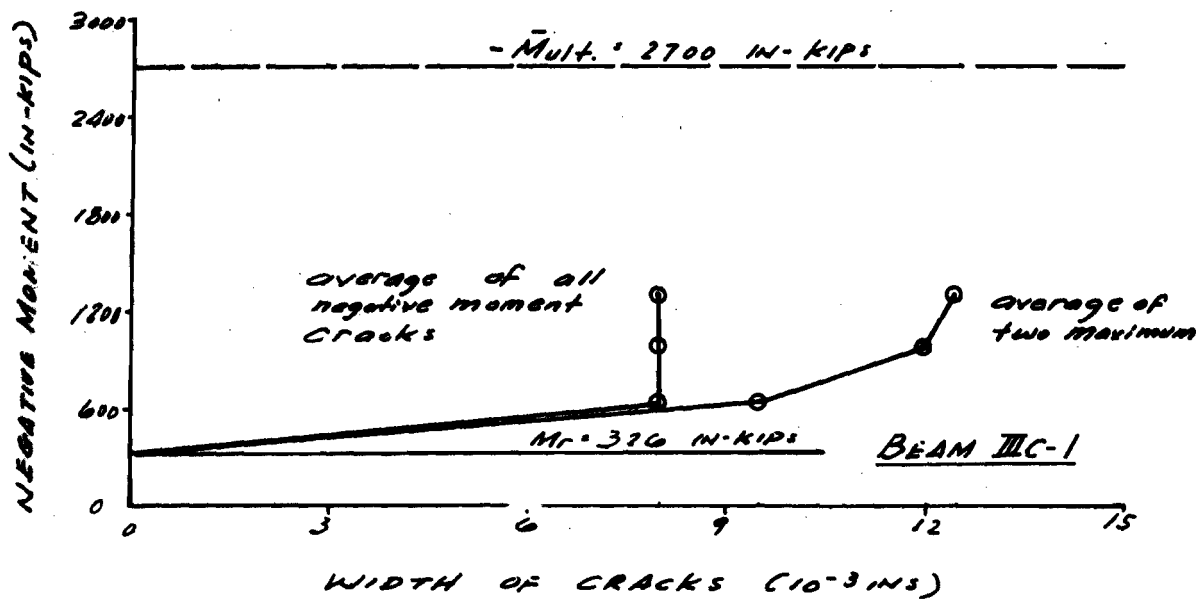
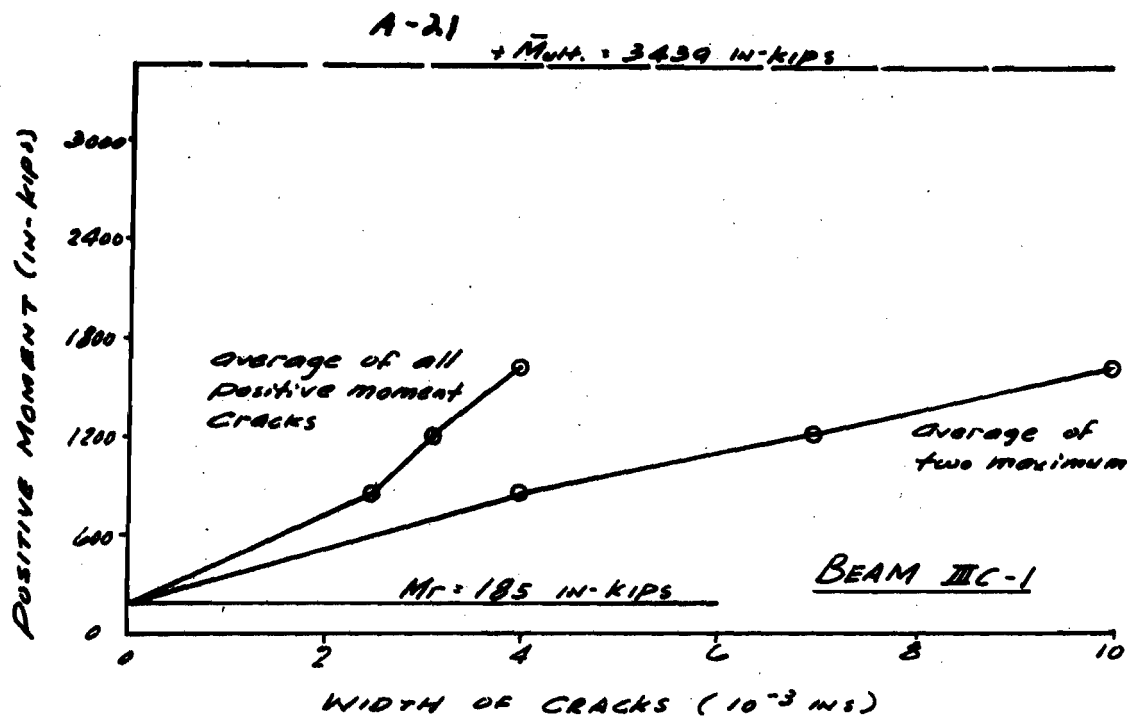


A-19

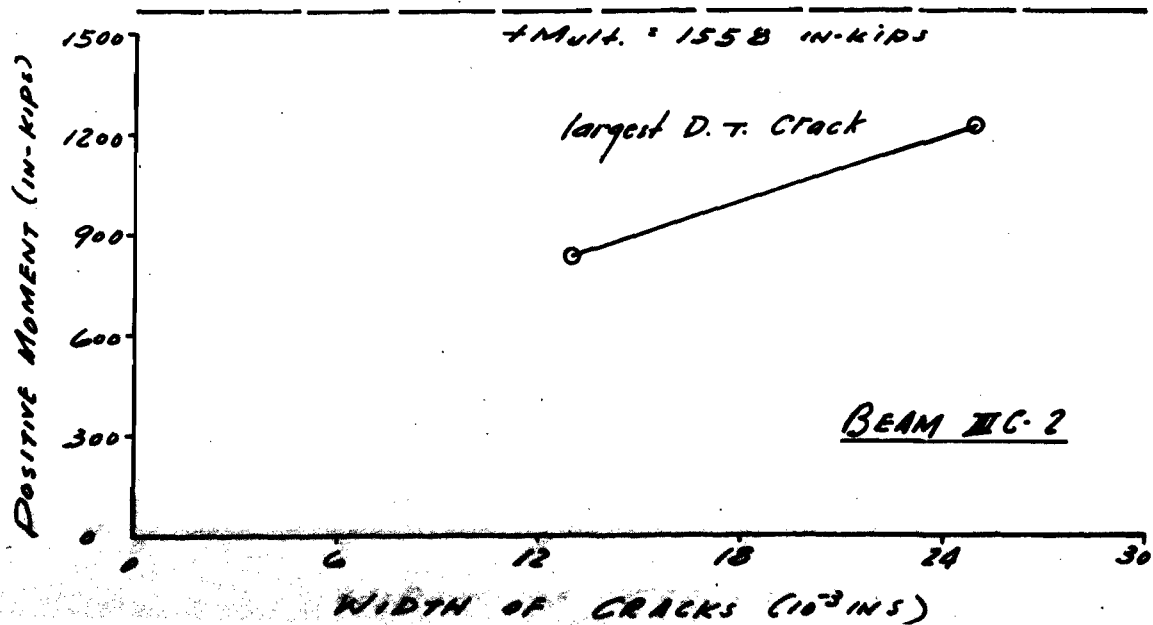
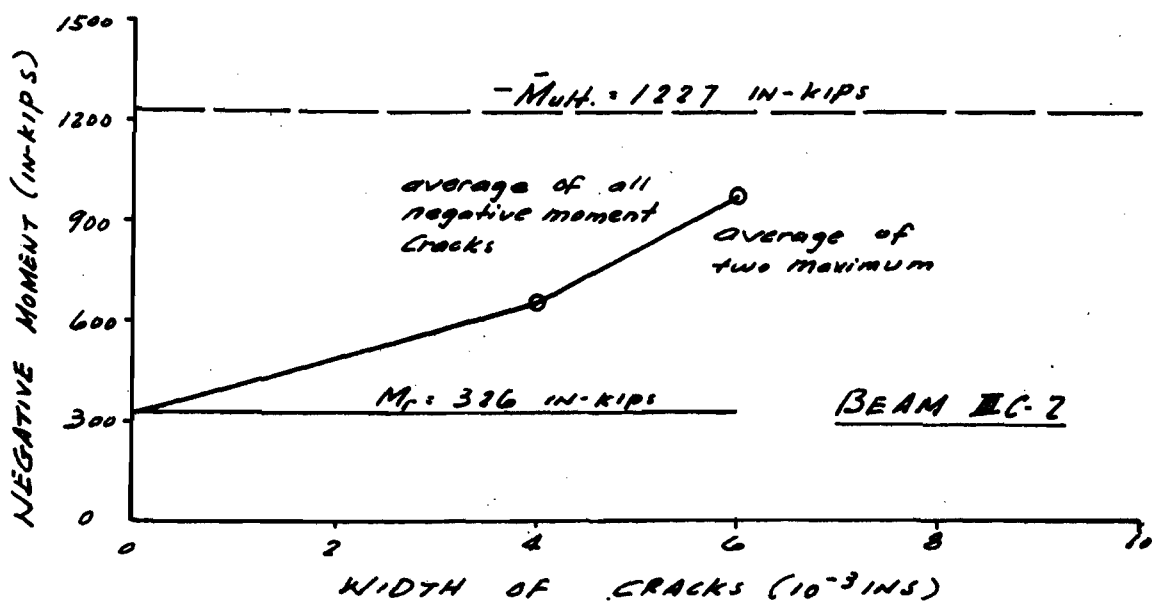
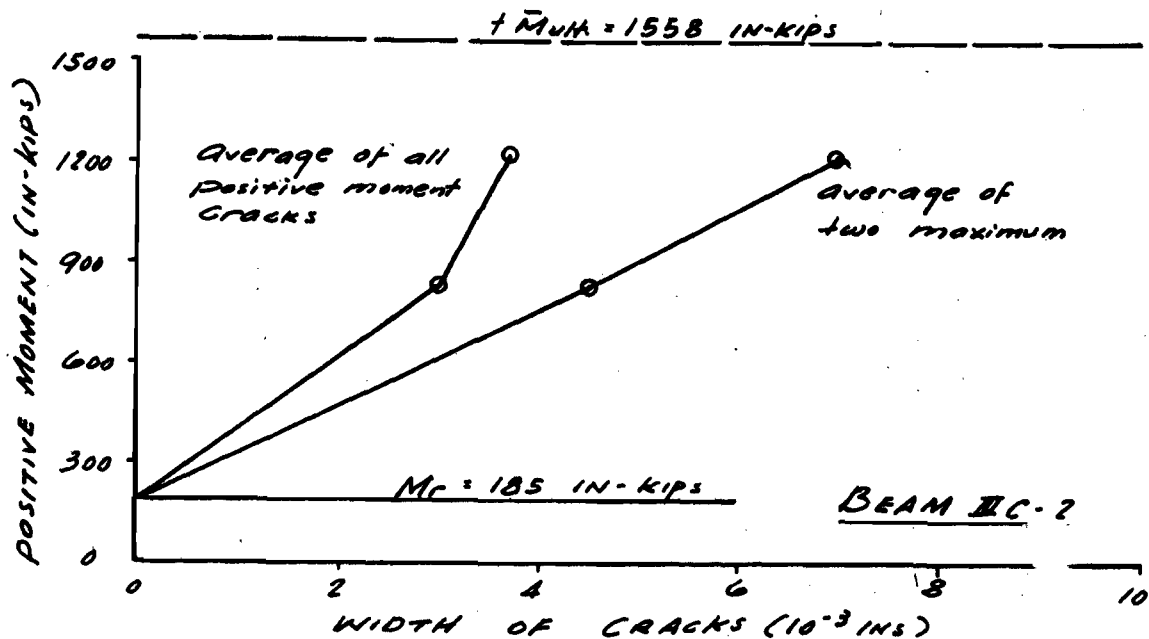


A-20

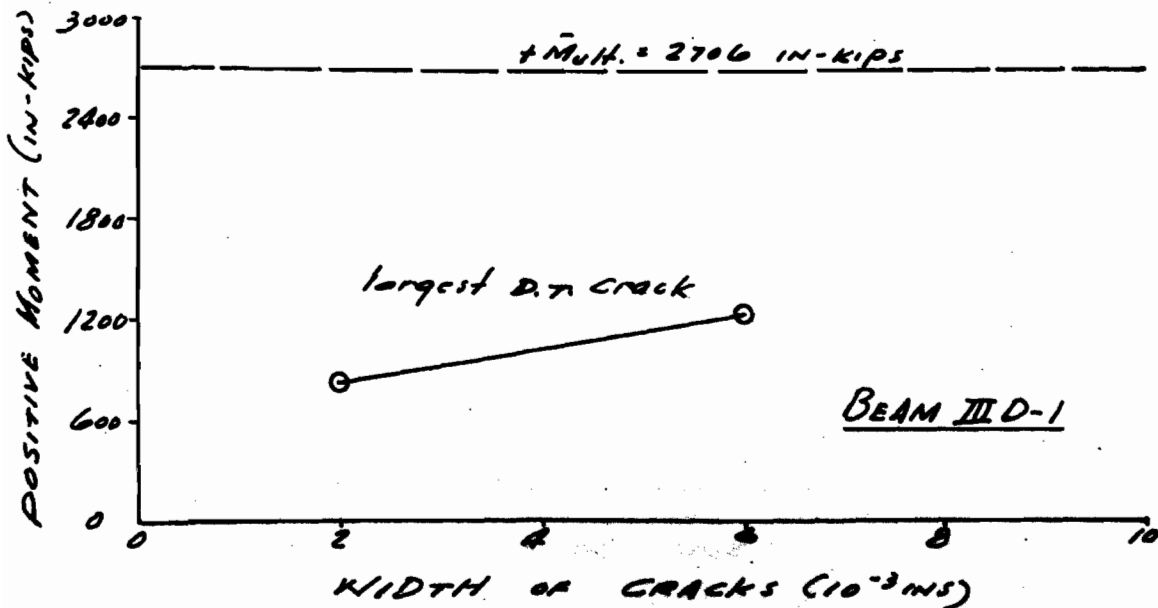
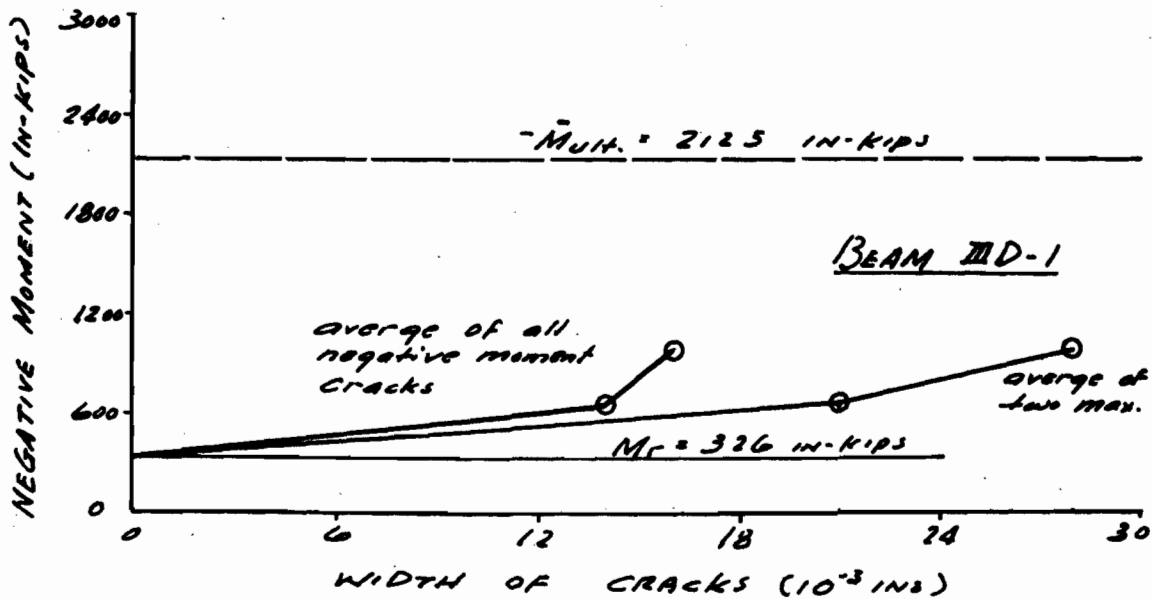
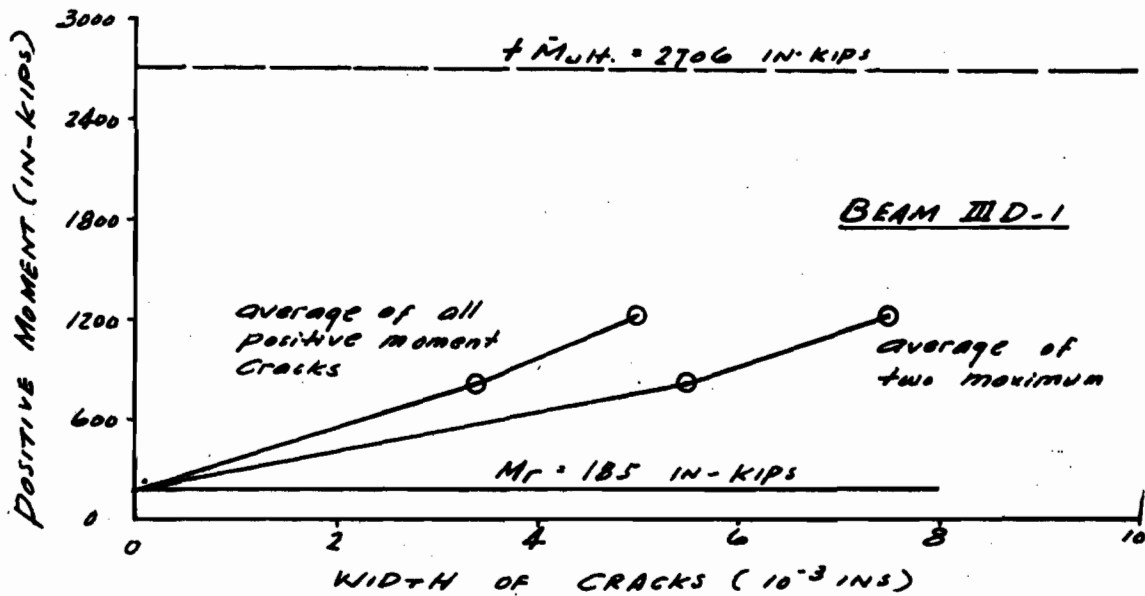




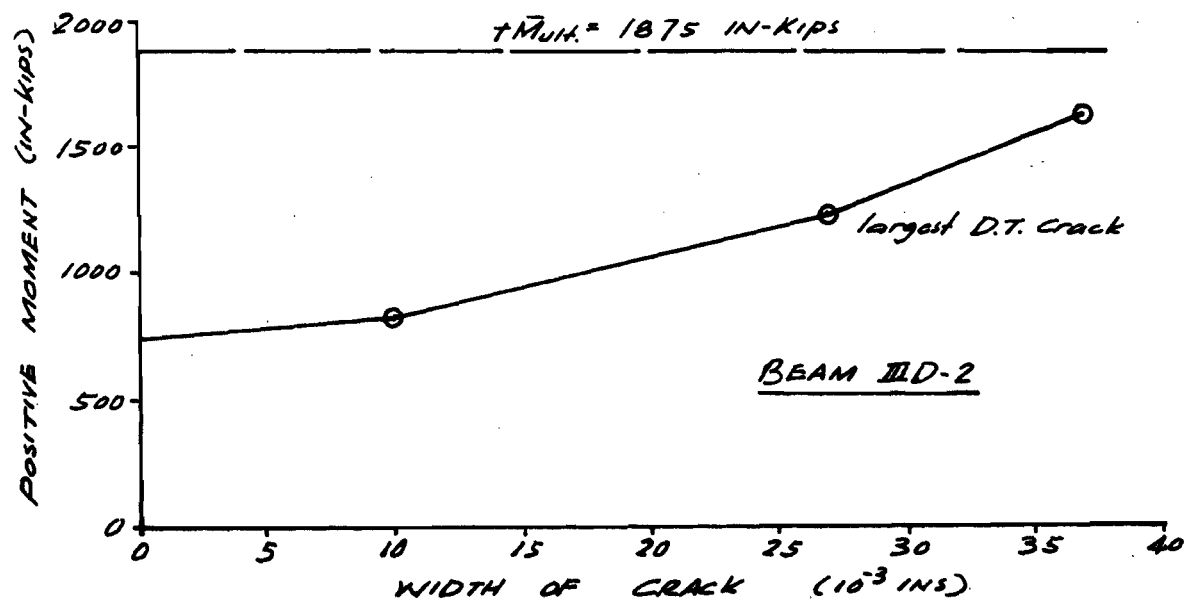
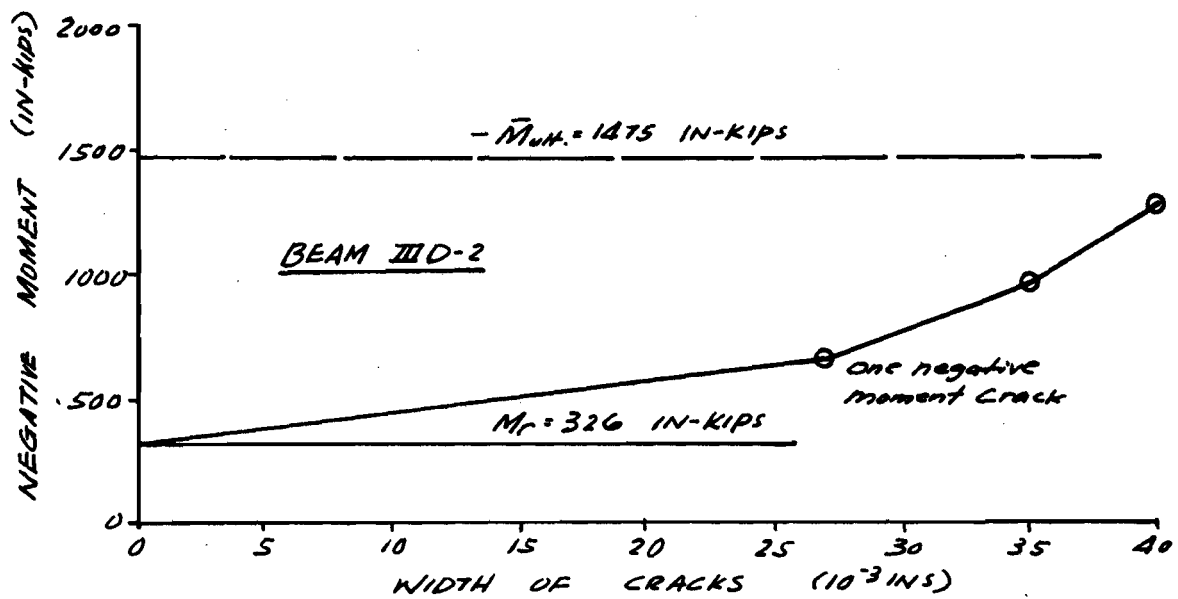
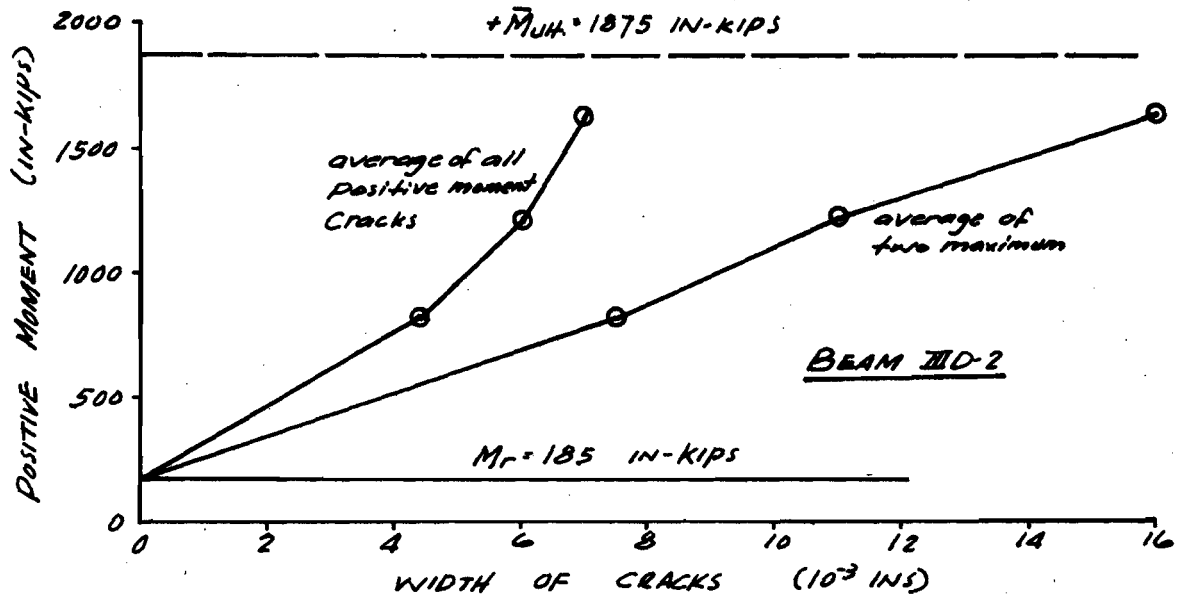
A-22



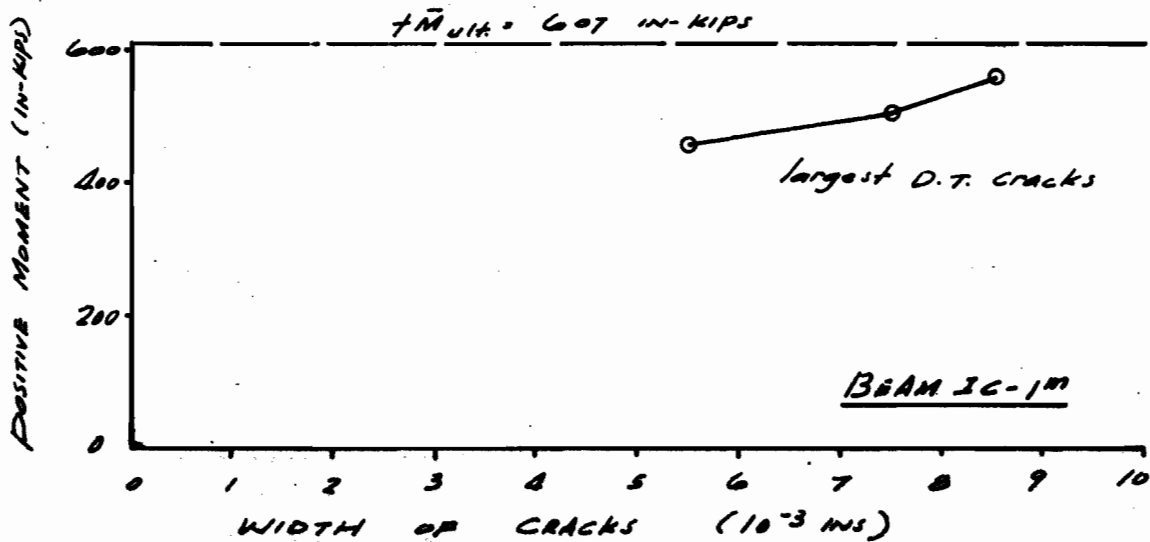
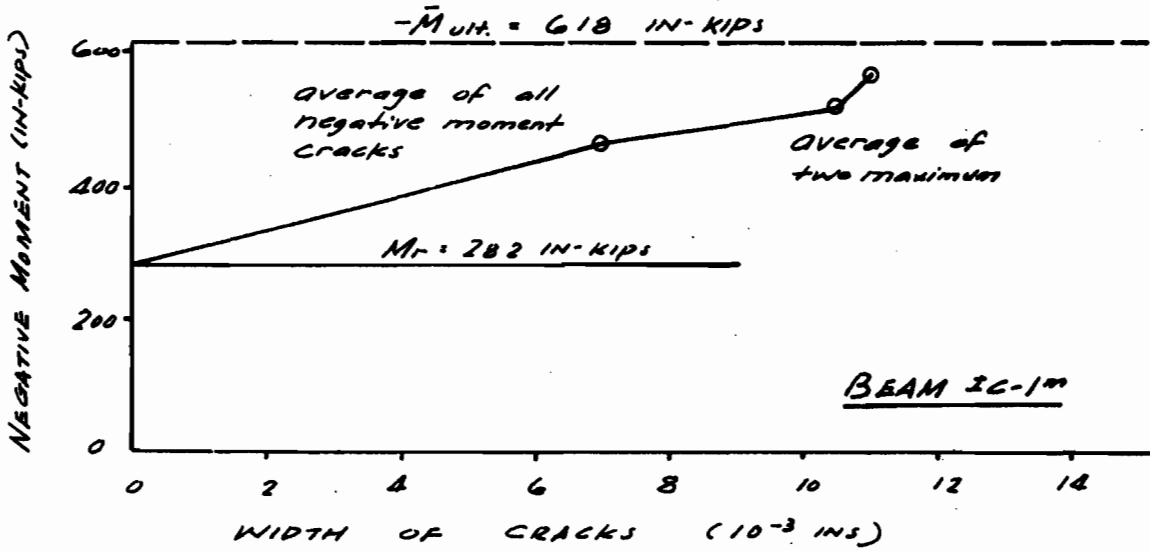
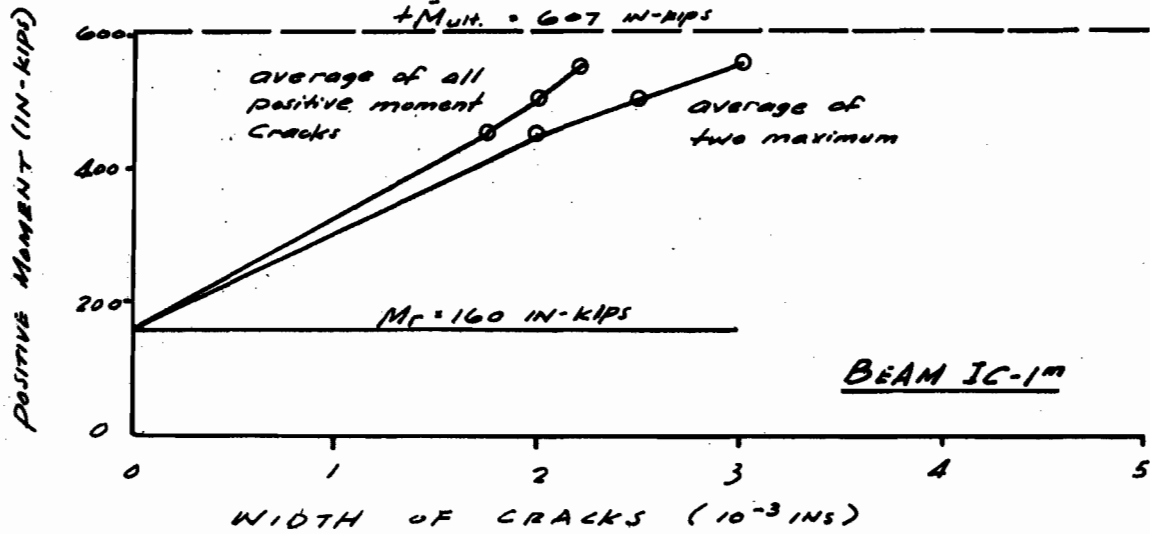
A-23



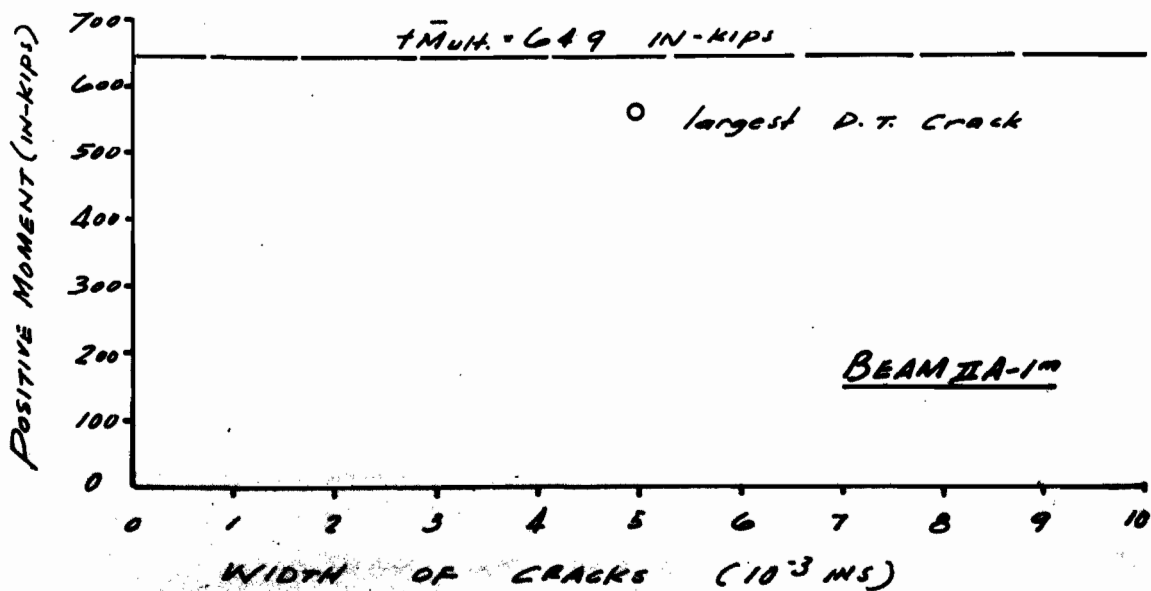
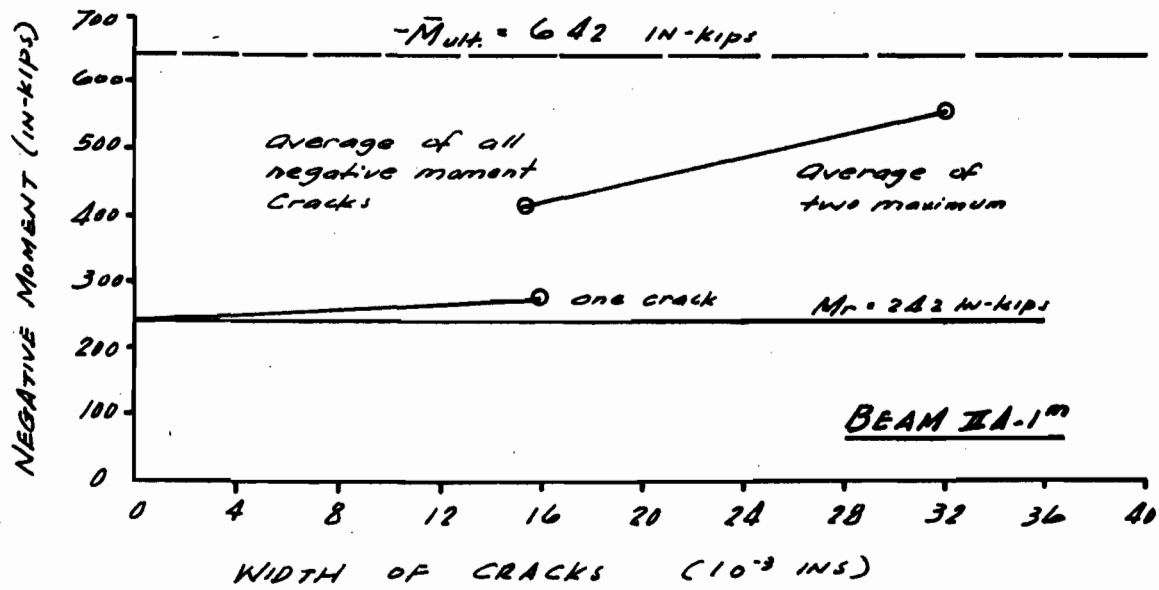
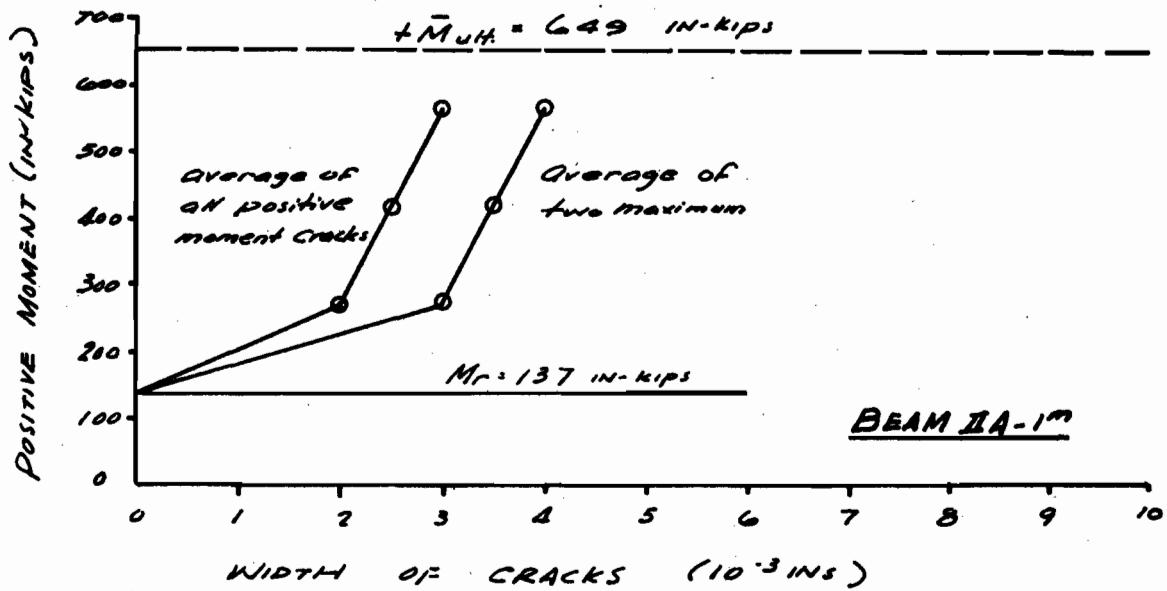
A-24



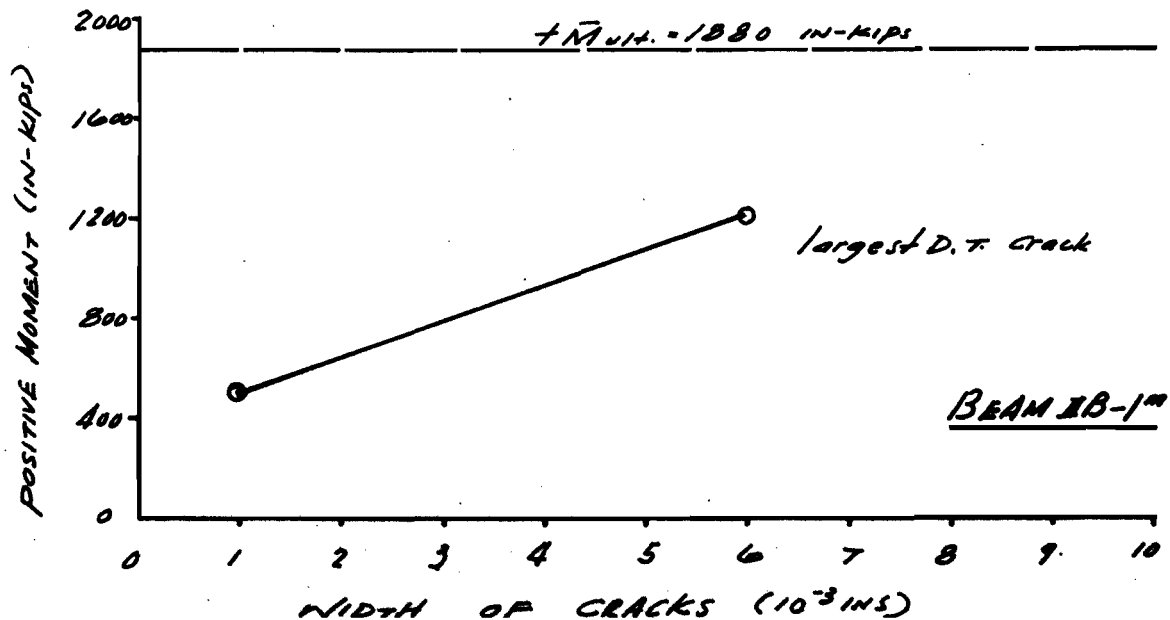
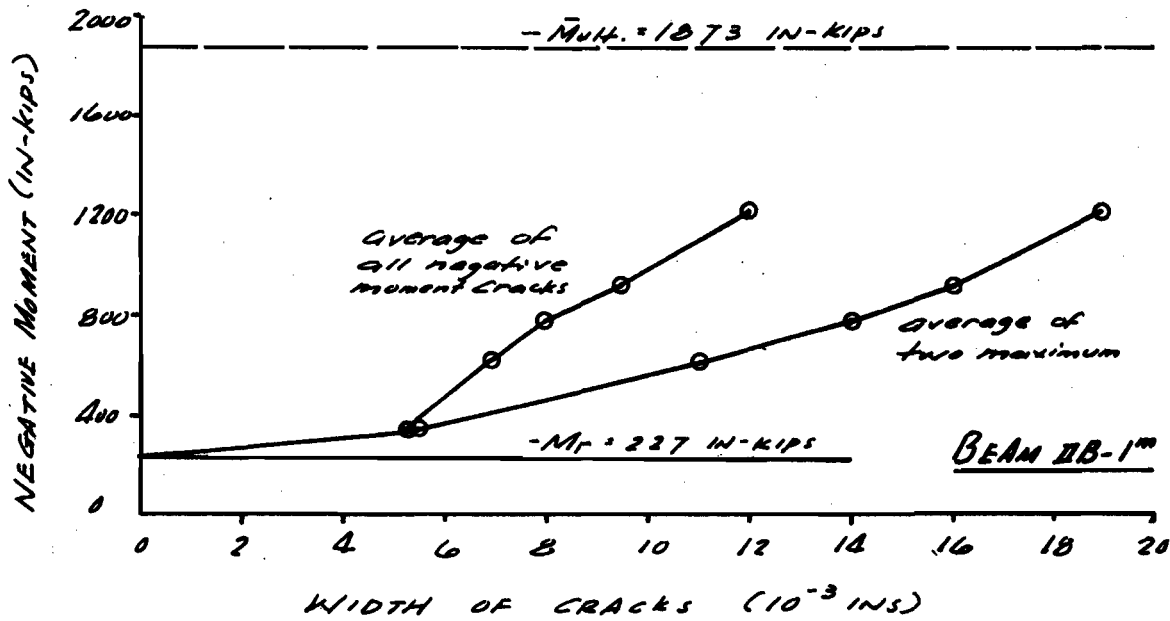
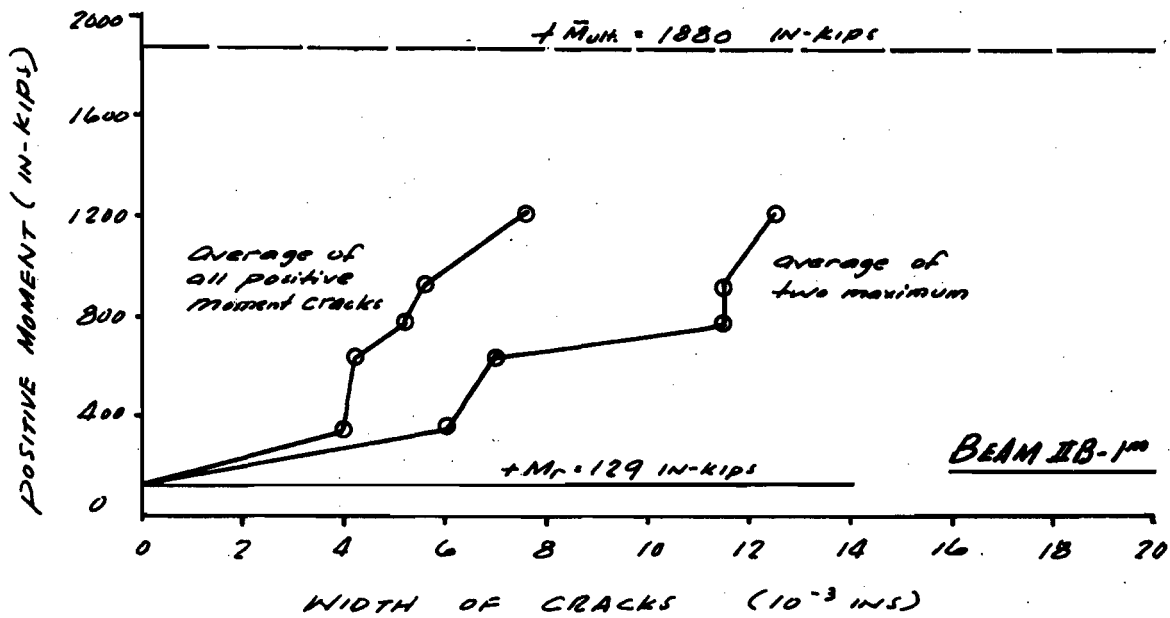
A-25



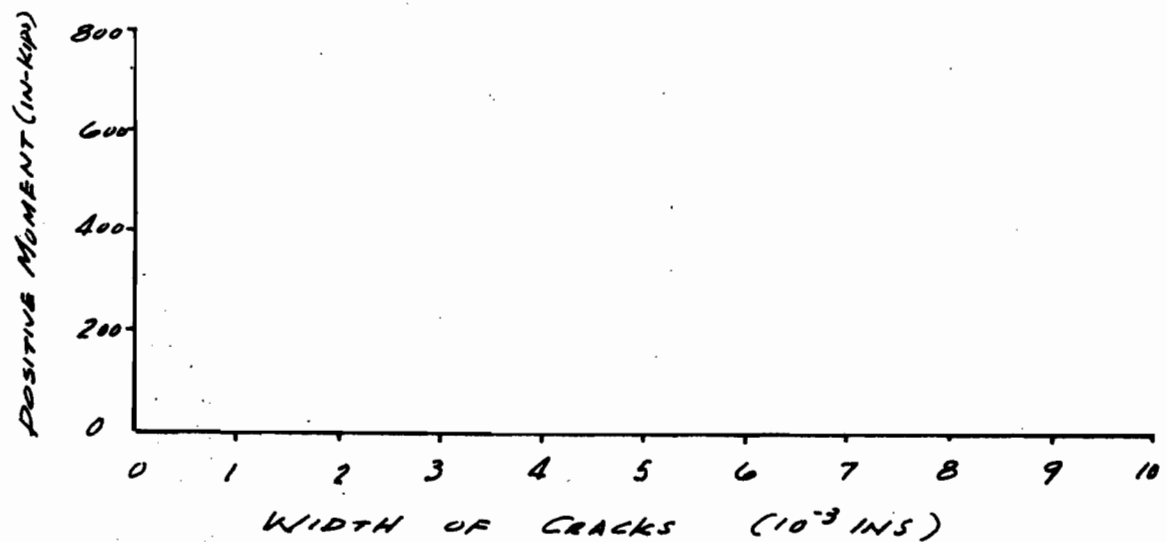
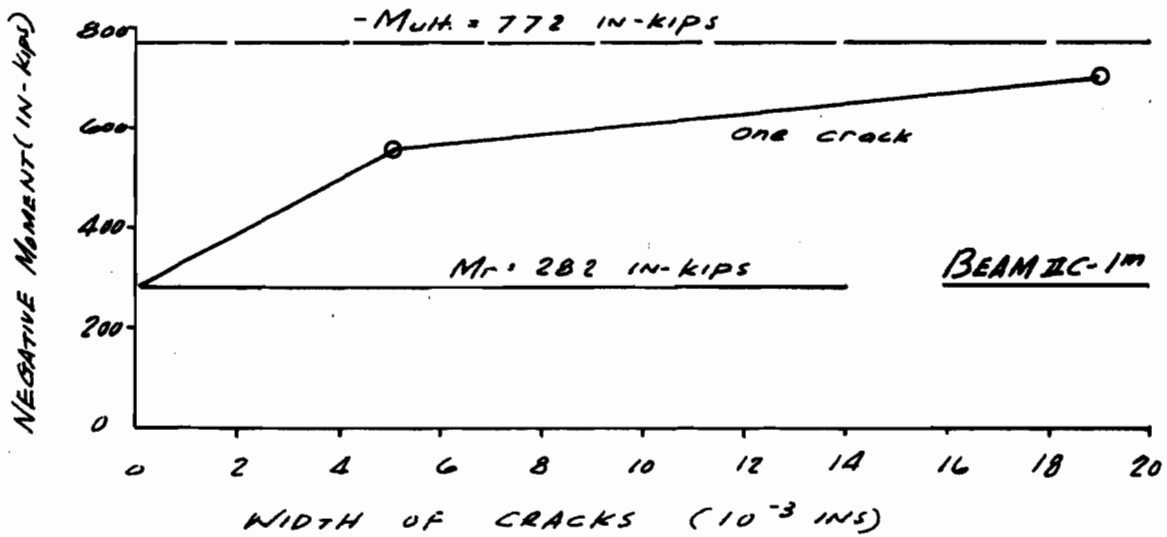
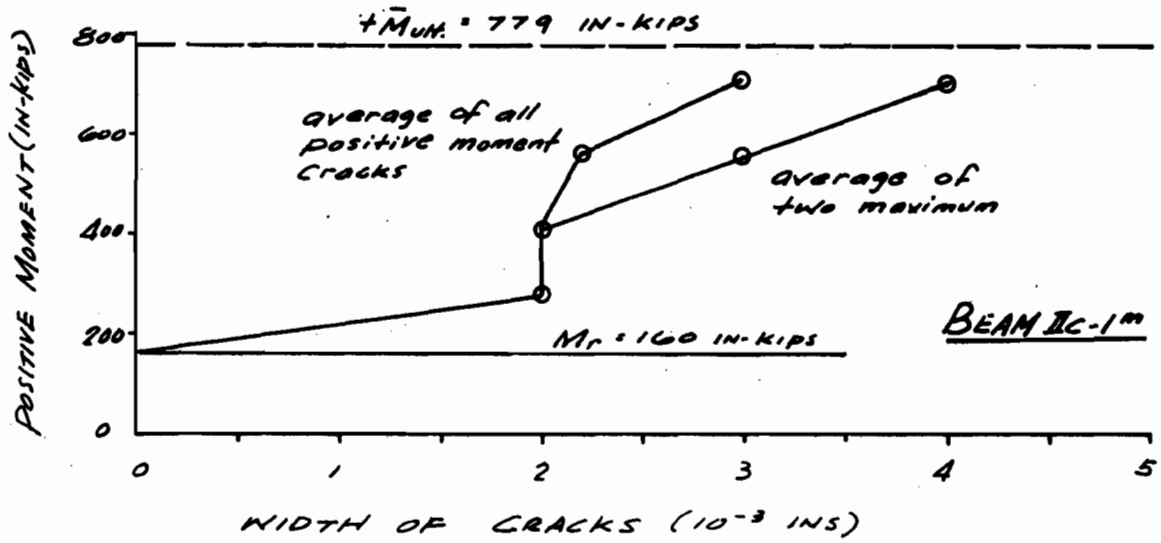
A-26



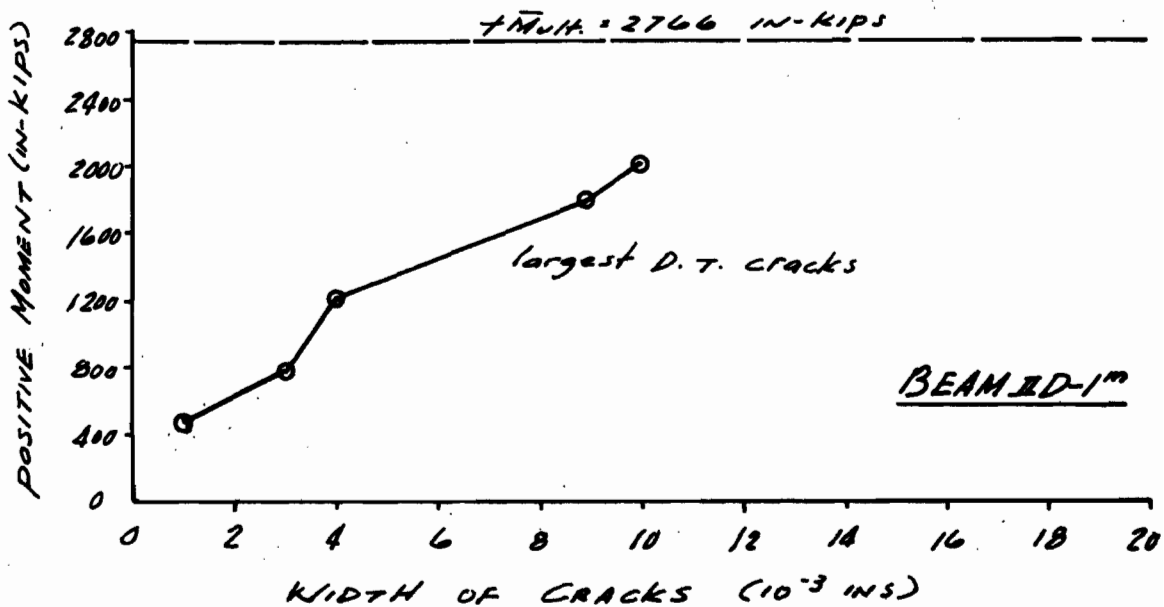
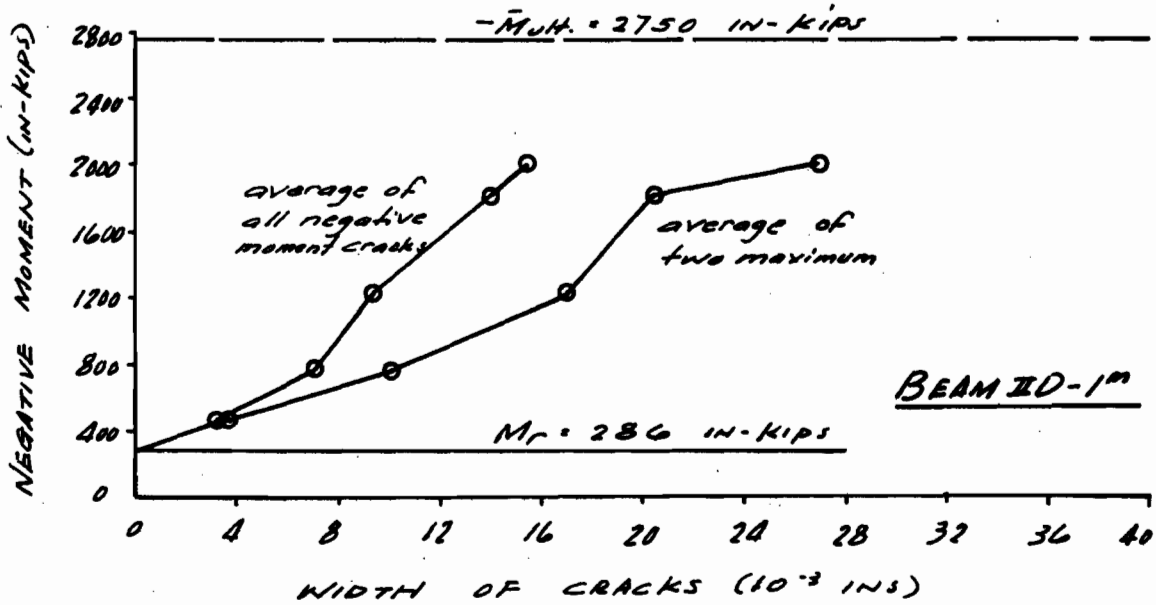
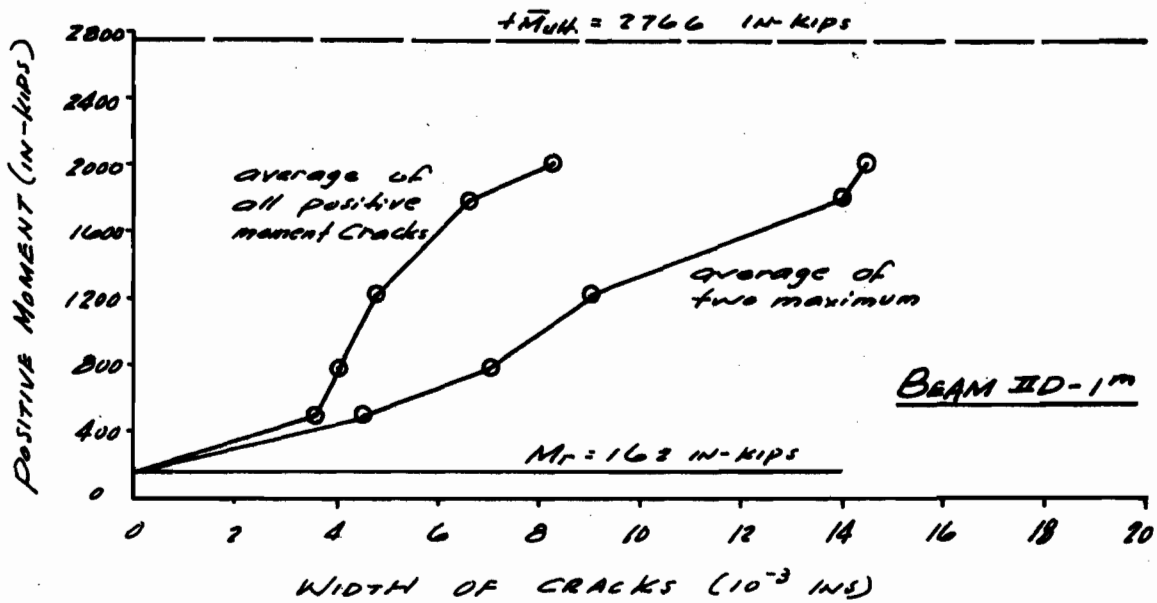
A-27



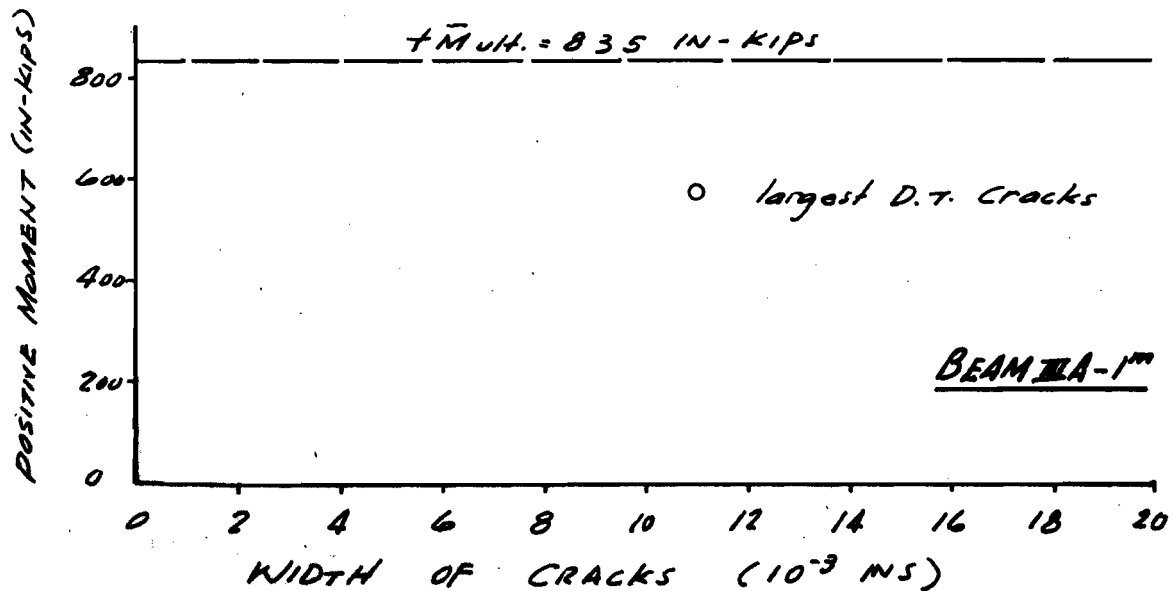
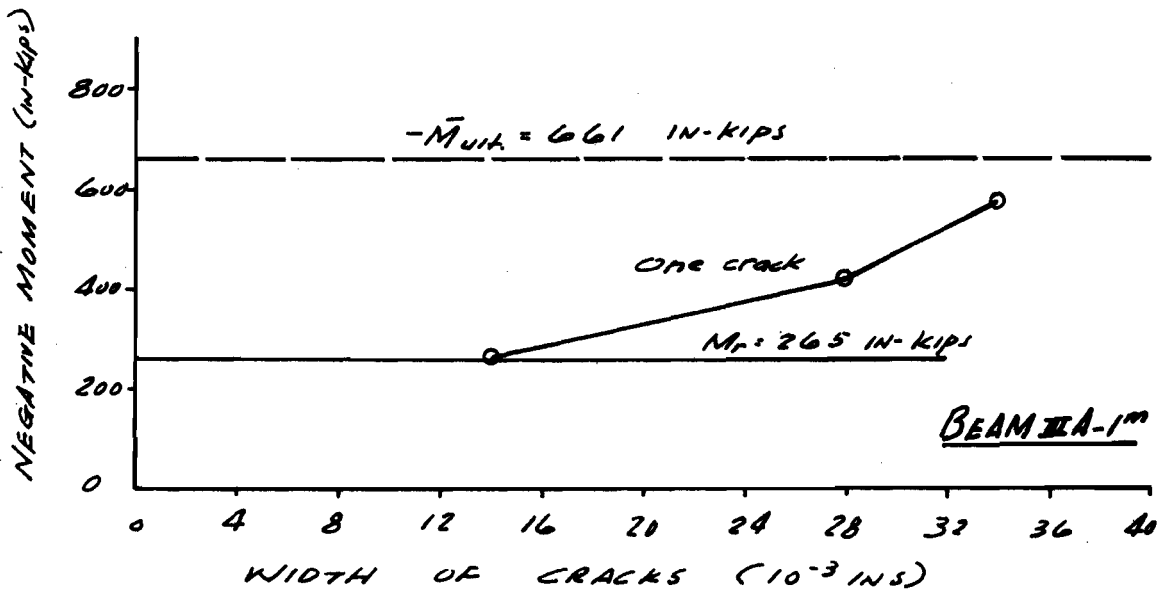
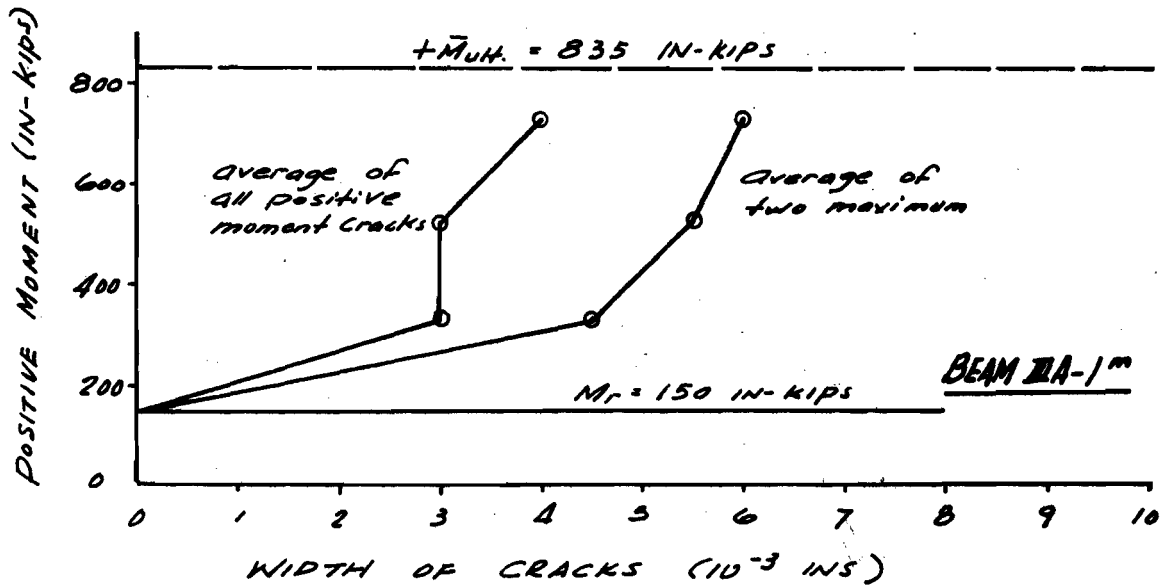
A-28



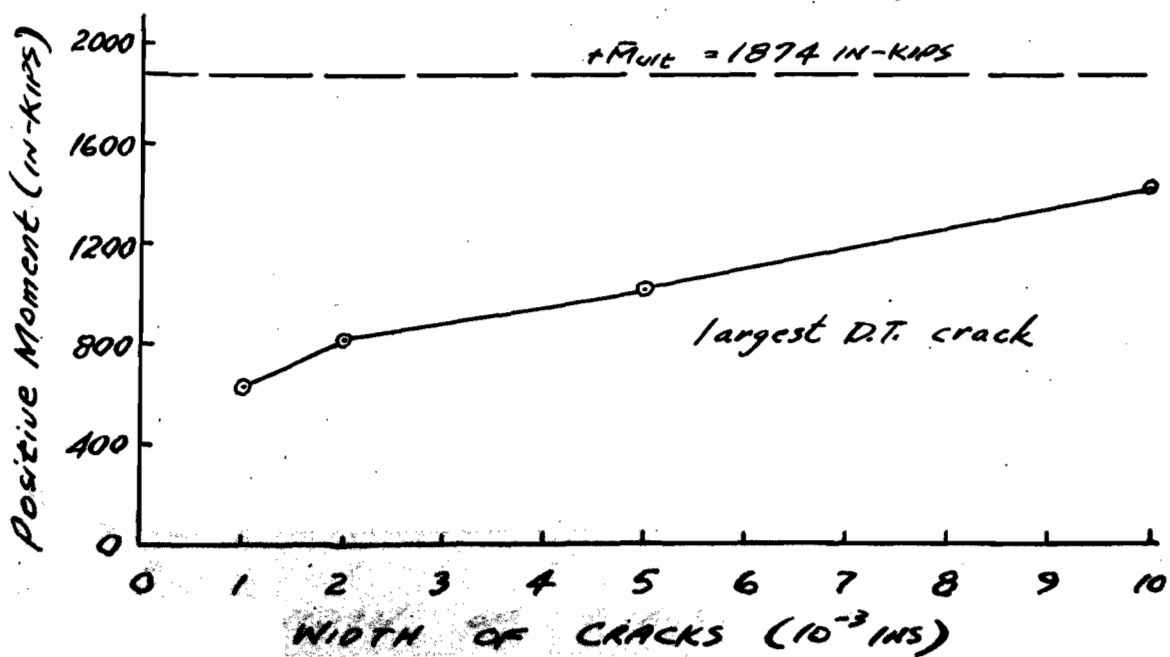
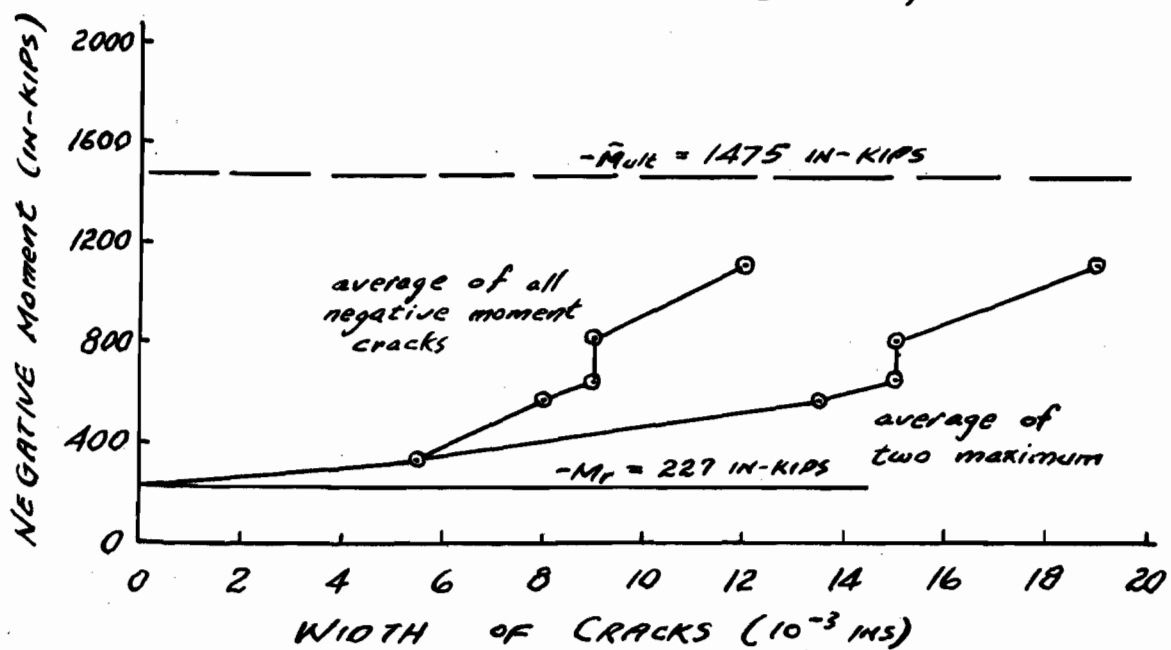
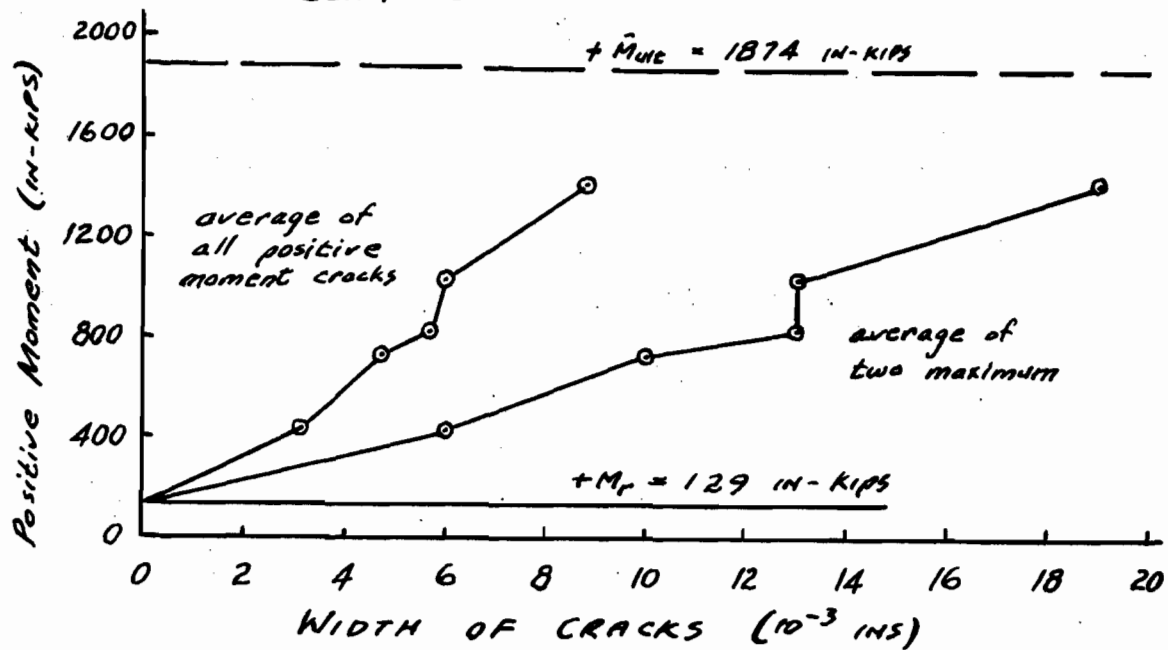
A-29



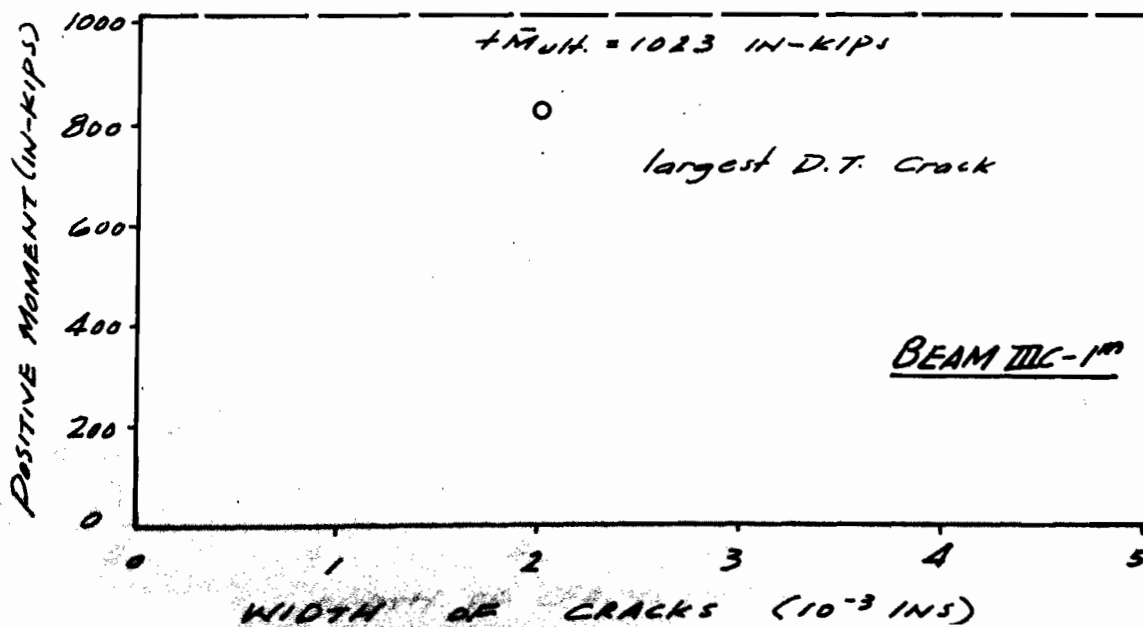
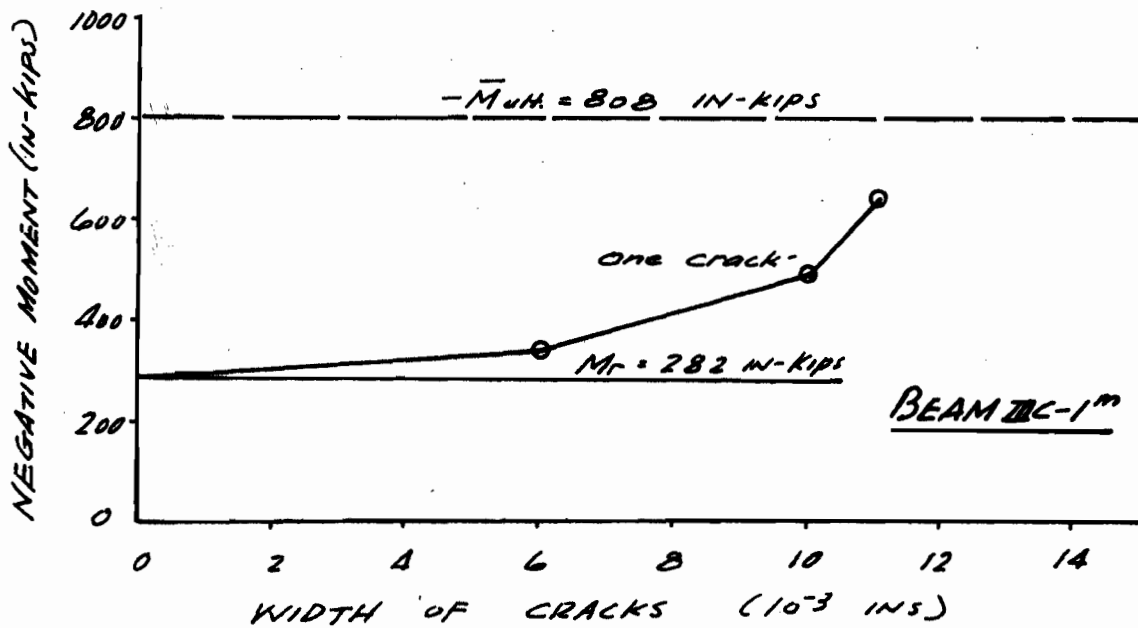
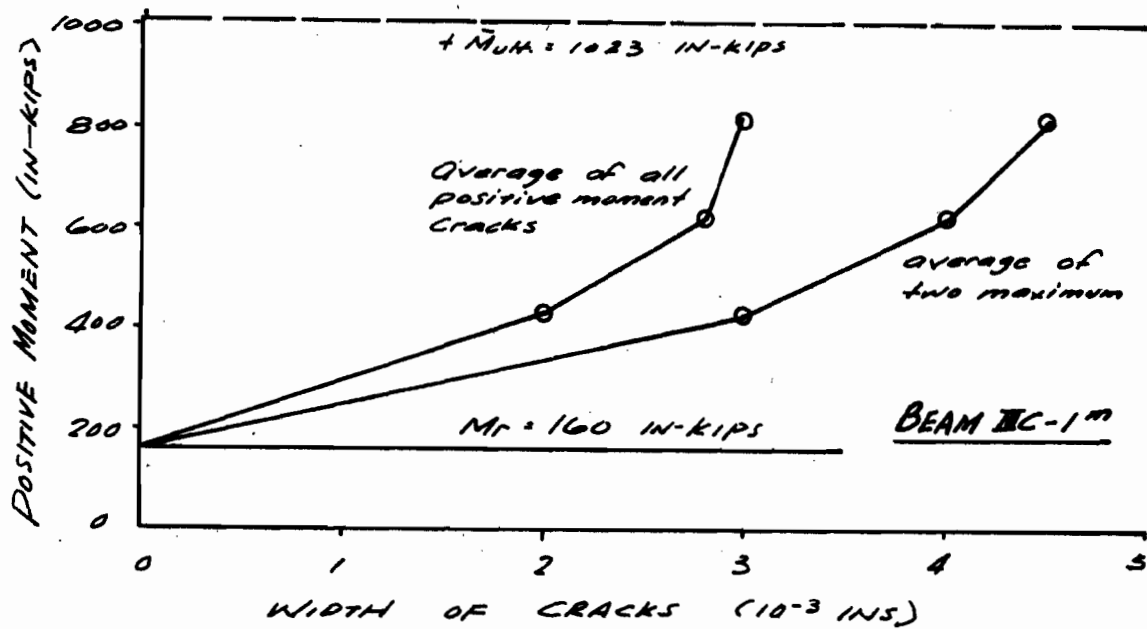
A-30



A-31
BEAM IIB-1^m



A-32



A-33

